Aquaporin Expression, Regulation and Function in the Intervertebral Disc

Joseph William Snuggs

A thesis submitted in partial fulfilment of the requirements of

Sheffield Hallam University for the degree of Doctor of Philosophy

February 2019

Candidate Declaration

I hereby declare that:

1. I have not been enrolled for another award of the University, or other academic or professional organisation, whilst undertaking my research degree.

2. None of the material contained in the thesis has been used in any other submission for an academic award.

3. I am aware of and understand the University's policy on plagiarism and certify that this thesis is my own work. The use of all published or other sources of material consulted have been properly and fully acknowledged.

4. The work undertaken towards the thesis has been conducted in accordance with the SHU Principles of Integrity in Research and the SHU Research Ethics Policy.

5. The word count of this thesis is 39,850.

Name	Joseph William Snuggs
Date	February 2019
Award	PhD
Faculty	Health and Wellbeing
Director of Studies	Professor Christine Le Maitre

Abstract

Intervertebral disc degeneration-associated low back pain is a debilitating condition with no current treatments directed towards halting or reversing the degenerative cascade at a cellular level. The lack of such treatments is in part due to an incomplete knowledge of the molecular mechanisms that govern IVD function in health and degeneration. Due to the unique location and role of the IVD within the spine, many factors contribute to the microenvironment that cells reside within. The survival and function of cells has been irrefutably linked to their ability to adapt to the microenvironment in which they live. However, it is not completely understood how IVD cells have been able to survive and adapt to their environment.

The intervertebral disc is a highly hydrated tissue; the rich proteoglycan matrix imbibes water, enabling the disc to withstand compressive loads. During ageing and degeneration increased matrix degradation leads to dehydration and loss of function. Aquaporins are a family of transmembrane channel proteins that selectively allow the passage of water in and out of cells and are responsible for maintaining water homeostasis in many tissues; hence many AQPs are potentially expressed by cells within the intervertebral disc to enable their adaptation to this highly hydrated tissue.

The aim of this thesis was to investigate the expression, regulation and function of AQP transmembrane water channels within the IVD and how they potentially contribute to the adaptation of cells to their environment. Results have highlighted NP cells express many AQP water channels *in vivo*, whose expression may be altered between disc development and degeneration. AQP1 and 5 were found to be upregulated by TonEBP in hyperosmotic conditions, a transcription factor controlling osmotic adaptation and matrix expression, which may implicate them in the adaptation of NP cells to their environment, which becomes unachievable when AQP1 and 5 are decreased during degeneration. AQP4 and TRPV4 function in NP cells was required for fundamental cellular processes such as cell volume regulation and water permeability, enabling adaptation to their osmotically fluxing environment. Finally, it was identified that other microenvironmental factors also contribute to AQP expression in NP cells, indicating the regulation and function of these water channels is potentially very complex.

Together, investigations presented in this thesis have demonstrated many AQPs are expressed by the intervertebral disc and enable NP cells to respond and adapt to their environment, ultimately contributing to the overall function of the tissue. Their regulation by multiple environmental factors may signify that AQPs have diverse roles within the IVD, which remain to be elucidated. Importantly, this body of work has contributed novel findings, increased knowledge and opened new avenues of research in the field of IVD and spine biology.

Contents

Figure List

Table List

Equation List

Appendix List

Abbreviations

ACAN	Aggrecan
ADAMTS	A disintegrin and metalloproteinase with thrombospondin motifs
AF	Annulus fibrosus
AKAP13 (Brx)	A-kinase anchoring protein 13
AP-1	Activator protein 1
AQP	Aquaporin
AQPi	Aquaporin inhibition
AR	Aldose reductase
AVP	Arginine vasopressin
Bapx1	Bagpipe homeobox homolog 1
BCA	Bicinchoninic acid
BGT1	Betaine-γ-amino butyric acid transporter
CA (III, XII)	Carbonic anhydrase (III, XII)
Calcein-AM	Calcein-acetoxymethyl
cAM	Calmodulin
cAMP	Cyclic adenosine monophosphate
CD	Chondrodystrophic
CD24	Cluster of differentiation 24
cDNA	Complementary deoxyribonucleic acid
CEP	Cartilaginous endplate
CFSE	Carboxyfluorescein succinimidyl ester
CRE	cAMP-response element
CREB	cAMP-response element-binding protein
CTR	Control
ECM	Extracellular matrix
ERK 1/2	Extracellular signal-regulated kinases 1/2
F_1/F_0	Relative fluorescence

FSC	Forward scatter
GAG	Glycosaminoglycan
GlcAT-1	β1,3-glucoronosyl transferase 1
GLUT-1	Glucose transporter 1
GPCR	G protein-coupled receptor
HA	Hyaluronic acid
HIF-1α	Hypoxia-inducible factor 1α
ICC	Immunocytochemistry
IF	Immunofluorescence
IHC	Immunohistochemistry
IL-1	Interleukin-1
IL-1Ra	Interleukin-1 receptor antagonist
IL-1RI	Interleukin-1 Receptor I
IL-1RII	Interleukin-1 Receptor II
IL-1β	Interleukin-1β
IL-6	Interleukin-6
IMS	Industrial methylated spirits
IP_3	Inositol triphosphate
IVD	Intervertebral disc
Jnk	c-Jun N-terminal kinase
LBP	Low back pain
MCP-1	Monocyte chemoattractant protein 1
MMP	Matrix metalloproteinase
MPa	Mega Pascal
MSC	Mesenchymal stem cell
NC	Notochordal
NCD	Non-chondrodystrophic
NFAT	Nuclear factor of activated T cells
NFDM	Non-fat dried milk
NF-κB	Nuclear factor κ-light-chain-enhancer of activated B cells

NP	Nucleus pulposus
NPA	Asparagine-proline-alanine
p38 MAPK	p38 mitogen-activated protein kinase
PAX (1, 9)	Paired box protein (1, 9)
PKA	Protein kinase A
PKC	Protein kinase C
PM	Post-mortem
PVDF	Polyvinylidene fluoride
qRT-PCR	Quantitative real-time-polymerase chain reaction
RIPA	Radioimmunoprecipitation
rRNA	Ribosomal RNA
RT	Room temperature
Runx2	Runt-related transcription factor 2
SHH	Sonic hedgehog
siRNA	Small interfering RNA
SMIT	Sodium myo-inositol transporter
Sox (5, 6, 9)	Sex determining region box (5, 6, 9)
T	Brachyury
TauT	Taurine transporter
TG	Thompson grade
TNF-α	Tumour necrosis factor α
TonE	Tonicity response element
TonEBP	Tonicity enhancer binding-protein
TRP	Transient receptor potential
TRPV	Transient receptor potential vanilloid
TRPVi	TRPV inhibition
V2R	Vasopressin receptor 2
VB	Vertebral body
WT	Wildtype

Dissemination

Scientific publications

Johnson ZI, Doolittle AC, **Snuggs JW**, Shapiro IM, Le Maitre CL, Risbud MV. TNF-α promotes nuclear enrichment of the transcription factor TonEBP/NFAT5 to selectively control inflammatory but not osmoregulatory responses in nucleus pulposus cells. The Journal of Biological Chemistry. 2017, Oct 20; 292(42):17561-17575.

Bach FC, de Rooij KM, **Snuggs JW**, de Jong WAM, Zhang Y, Creemers LB, Chan D, Le Maitre C, Tryfonidou MA. IHH and PTHrP are implicated in degeneration of the intervertebral disc. Oncotarget - accepted subject to minor revisions.

Snuggs JW, Day RE, FC Bach, Conner MT, Bunning RAD, Tryfonidou MA, Le Maitre CL. Aquaporin expression in the human and canine intervertebral disc during maturation and degeneration. JOR Spine - accepted subject to minor revisions.

Conference abstracts

Oral presentations

November 2016, Society for Back Pain Research, Preston, UK: Aquaporin expression in the human intervertebral disc. **Snuggs JW**, Day RE, Chiverton N, Cole A, Michael R, Bunning R, Conner M, Le Maitre C.

November 2016, Society for Back Pain Research, Preston UK: Regulation of aquaporin gene expression in human nucleus pulposus cells. **Snuggs JW**, Chiverton N, Cole A, Michael R, Bunning R, Conner M, Le Maitre C.

November 2017, Society for Back Pain Research, Northampton, UK: Aquaporin expression in the human and canine intervertebral disc/hyperosmotic regulation of AQP and 5. **Snuggs JW**, Day RE, Chiverton N, Cole A, Michael R, Bunning R, Conner M, Tryfonidou MA, Risbud RV, Le Maitre C.

March 2018, Britspine, Leeds, UK: Molecular mechanisms regulating aquaporin expression and activity in the intervertebral disc. **Snuggs JW**, Conner MT, Bunning RAD, Le Maitre C.

October 2018, European Orthopaedic Research Society, Galway, IE: Osmoregulation of aquaporin 1 and 5 in the intervertebral disc. **Snuggs JW**, Conner MT, Bunning RAD, Risbud MV, Le Maitre C.

November 2018, Society for Back Pain Research, Groningen, NL: Water permeability of human nucleus pulposus cells in response to extracellular osmolality. **Snuggs JW**, Chiverton N, Cole A, Michael R, Bunning R, Conner M, Le Maitre C.

Poster presentations

September 2015, DISCS Charity, London, UK: Aquaporin expression and regulation in the human intervertebral disc. **Snuggs JW**, Day RE, Chiverton N, Cole A, Michael R, Bunning R, Conner M, Le Maitre C.

November 2015, Philadelphia Spine Research Symposium, Philadelphia, PA, US: Aquaporin expression and regulation in the human intervertebral disc. **Snuggs JW**, Day RE, Chiverton N, Cole A, Michael R, Bunning R, Conner M, Le Maitre C.

March 2017, Orthopaedic Research Society, San Diego, CA, US: Aquaporin expression in the human and canine intervertebral disc. **Snuggs JW**, Day RE, Chiverton N, Cole A, Michael R, Bunning R, Conner M, Tryfonidou MA, Le Maitre C.

March 2017, Orthopaedic Research Society, San Diego, CA, US: Regulation of aquaporin gene expression in human nucleus pulposus cells. **Snuggs JW**, Chiverton N, Cole A, Michael R, Bunning R, Conner M, Le Maitre C.

November 2017, Philadelphia Spine Research Symposium, Philadelphia, PA, US: Osmoregulation of aquaporin 1 and 5 in the intervertebral disc. **Snuggs JW**, Conner MT, Bunning RAD, Risbud MV, Le Maitre C.

November 2018, Society for Back Pain Research, Groningen, NL: Water permeability of human nucleus pulposus cells in response to extracellular osmolality. **Snuggs JW**, Chiverton N, Cole A, Michael R, Bunning R, Conner M, Le Maitre C.

February 2019, Orthopaedic Research Society, Austin, TX, US: Osmoregulation of aquaporin 1 and 5 in the intervertebral disc. **Snuggs JW**, Conner MT, Bunning RAD, Risbud MV, Le Maitre C.

February 2019, Orthopaedic Research Society, Austin, TX, US: Water permeability of human nucleus pulposus cells in response to extracellular osmolality. **Snuggs JW**, Chiverton N, Cole A, Michael R, Bunning R, Conner M, Le Maitre C.

Chapter 1: Introduction

1.1 The Spine

The vertebral column consists of 24 articulating vertebrae, separated by 23 intervertebral discs (IVD), and 10 fused vertebrae. This is the main structural element of the spine which functions to provide support to the human body and allows rotation and bending with the contiguous IVDs, whilst also encasing and protecting the spinal cord within the vertebral foramen. The vertebral column is divided into 5 anatomical regions from superior to inferior (Figure 1.1).

The cervical spine contains the topmost 7 vertebrae (C1-C7). C1 and C2 (atlas and axis) enable the attachment and movement of the skull. The 12 thoracic vertebrae (T1-T12) are larger than the cervical vertebrae, contain large spinous processes and enable attachment and movement of the ribs to protect the lungs and heart. The 5 lumbar vertebrae (L1-L5) are the largest and increase in size and robustness from L1 to L5. The lumbar spine has an inward curve which forms the characteristic concavity of the lower back. The lumber vertebrae allow considerably more movement than the thoracic vertebrae; permitting a range of movements such as flexion and extension whilst also supporting weight bearing activities. The sacrum is attached inferiorly to the lumbar vertebrae at L5 by an IVD and contains 5 (S1-S5) fused vertebrae that integrate the two halves of the pelvis. The coccyx is the most inferior part of the spine and contains 3-5 fused bones. IVDs are not present between the fused bones of the sacrum or coccyx (Figure 1.1).

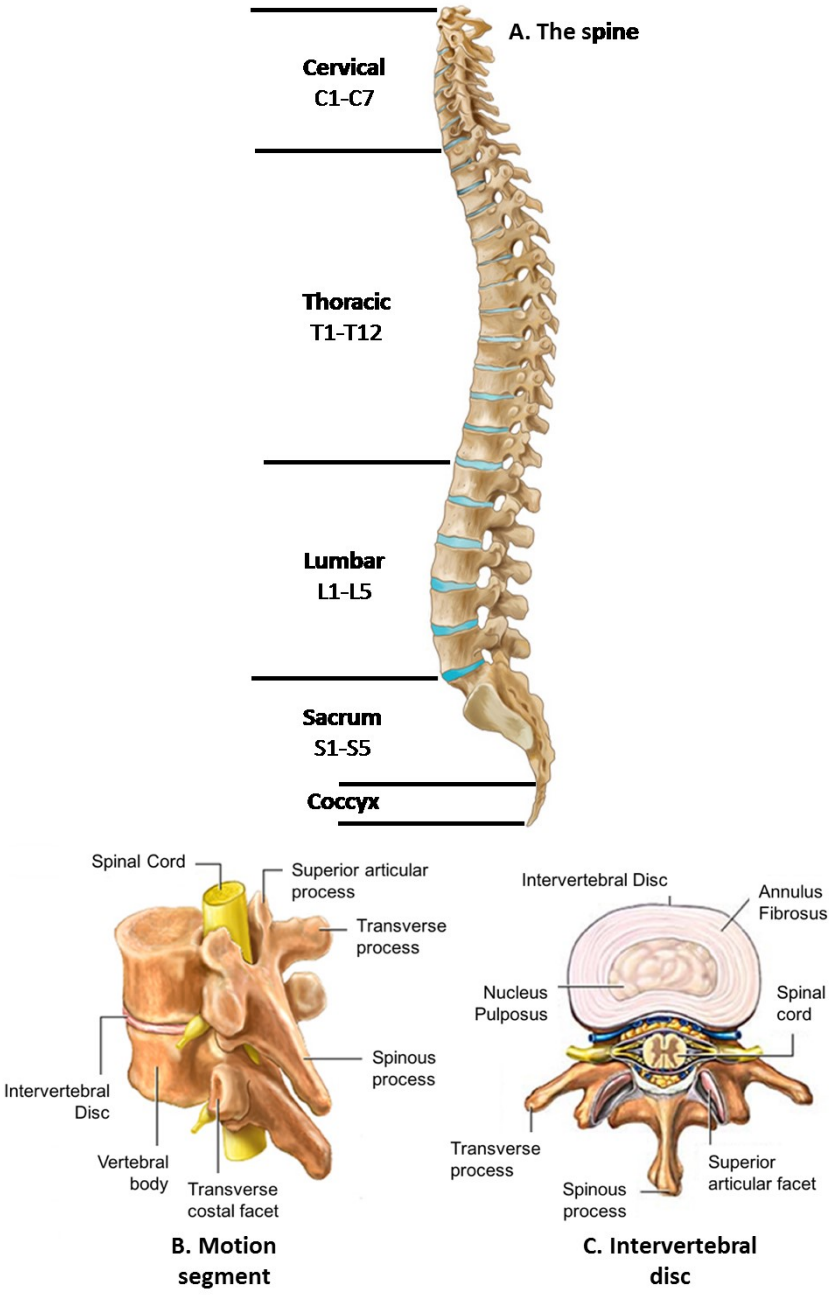

Figure 1.1. Anatomy of the human spine. (A) The spine contains a total of 34 vertebrae, 24 separated by IVDs and 8-10 fused. (B) A motion segment comprised of 2 adjacent vertebrae separated by an IVD. (B) The IVD is composed of the outer annulus fibrosus with lamellar fibrocartilaginous structure and the inner gelatinous nucleus pulposus. IVDs are attached to adjacent vertebrae via cartilaginous endplates. B and C show the posterior spinous processes and the spinal cord which travels protected through the vertebral foramen. Adapted from (*Medline*, 2018)

1.2 The intervertebral disc

The IVD is a fibrocartilaginous structure positioned between each of the 24 movable vertebrae. The main function of the IVD is mechanical; it enables the movement of the head and spine and accommodates the applied loading of the body. The IVD is comprised of 3 distinct regions; cartilaginous endplates (CEP), annulus fibrosus (AF) and nucleus pulposus (NP) (Figure 1.1). These regions within the IVD all work in unison to withstand mechanical loading and disperse energy evenly throughout the spine.

1.2.1 Cartilaginous endplates

Both the superior and inferior ends of the IVD are covered by a thin layer of hyaline cartilage. The cartilaginous endplate (CEP) has maximal thickness at birth which thins during aging, in adults it is approximately 0.5 – 1mm in width. They act as an interface between the internal IVD structures and the vertebral bone and prevent pressure being applied directly between both. Chondrocytes reside within the CEP embedded into an aggrecan and collagen type II rich matrix, which gives the CEP a structure similar to articular cartilage. The central region of the CEP contains the highest density of cells throughout the IVD, with approximately 18 x 10^6 cells/cm^3 in the young adult, these cells do not undergo osteochondral differentiation (Johnson *et al.*, 2006; Liebscher *et al.*, 2011). The CEP transitions into bone through a layer of calcified cartilage. The CEP is permeable to small molecules and thus also plays a role in the viability and metabolism of cells within the IVD, as it facilitates the diffusion of

nutrients and oxygen between the subchondral vertebral bone and the internal structures of the IVD which are avascular, except for the outer AF. The mechanical properties of the CEP may be altered due to weakening or mineralisation of the cartilage, which can lead to fractures and cause NP tissue to be exuded into the bone (Wu, Morrison and Schweitzer, 2006). These phenomena are called Schmorl's nodes.

1.2.2 Annulus fibrosus

The AF can be divided into 2 regions; the outer and inner AF. The outer AF is composed of bundled collagen type I fibres that are orientated into long parallel lamellae. The collagen fibres within each lamella run in parallel at a 65° angle to the adjacent lamellae. The fibres of the outer AF are anchored to the vertebral bone (Figure 1.2). This structural formation provides the outer AF with the ability to resist tensile forces from bending and twisting of the spine. The inner AF serves as a transition zone between the highly ordered outer AF and the disorganised NP, and characteristics of both tissues are observed. Aggrecan is found in both AF regions, whereas decorin and biglycan are mainly found within the outer AF. The inner AF contains collagens types I and II whilst the outer AF contains mainly collagen type I. Elastin accounts for 2% of the dry weight of the entire AF and forms inter-lamellar bridges. There are also cellular differences between the AF regions; outer AF cells are fibroblast-like; elongated and fusiform, whereas inner AF cells are spherical in shape and resemble the morphology of NP cells and chondrocytes. The cell density of mature AF tissue is approximately 9×10^6 cells/cm^3 (Roughley, 2004). The inner AF is also attached to the CEP, whilst the OAF is attached to vertebral bone.

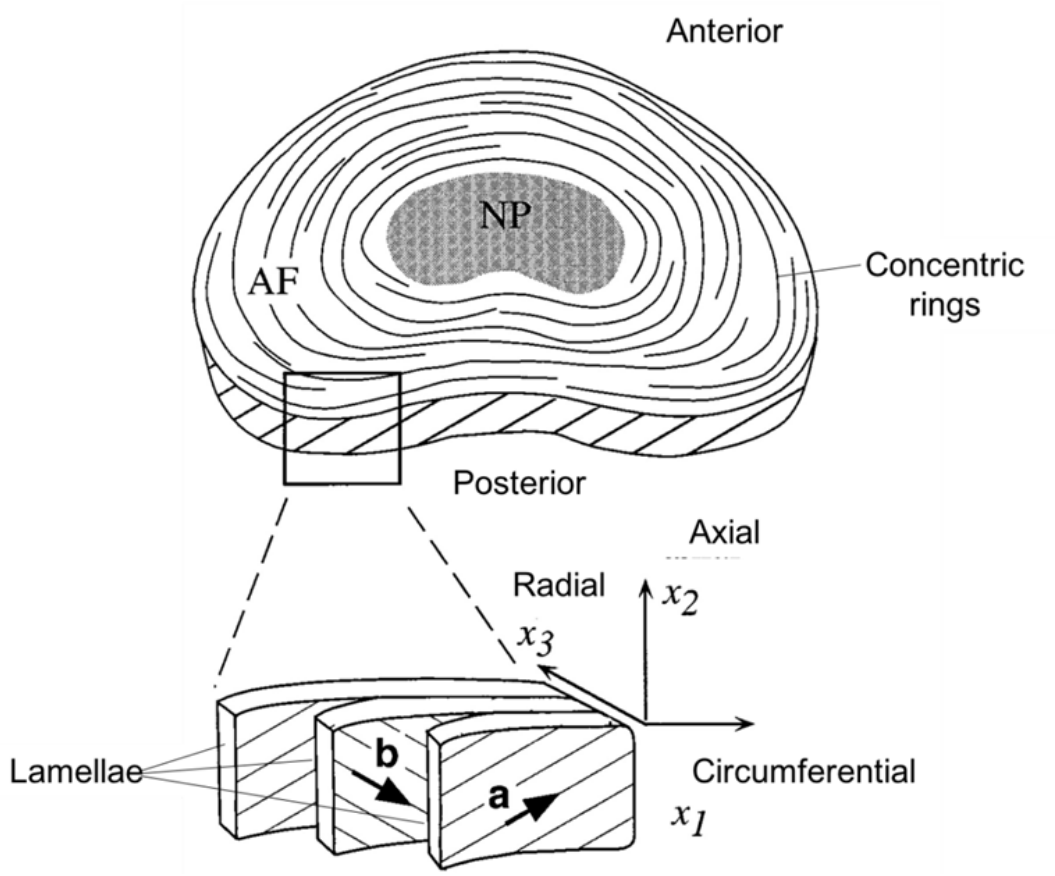

Figure 1.2. Schematic of the organisation of concentric AF lamellae. The direction of collagen fibres alternates at a 65° angle between adjacent lamellae. Adapted from (Elliott and Setton, 2000).

1.2.3 Nucleus pulposus

The NP is composed of mainly water (70 – 80%), randomly arranged collagen type II fibres (Figure 1.3), radially arranged elastin and small amounts of collagen types VI, IX and XI; collagen type X has also been observed within the NP during IVD degeneration and is linked to calcification (Grant *et al.*, 2016). These components are all embedded within a matrix rich in proteoglycans, which make up to 30 -50% of the dry weight of the tissue (Figure 1.3). The main proteoglycan matrix component is aggrecan which links to hyaluronan tethering it to the tissue (Figure 1.3); other proteoglycans such as versican, perlecan, lubricin and small leucine-rich repeat proteoglycans are also present within the NP(Inkinen *et al.*, 1998; Roughley, 2004). Crosslinked collagen within the NP confers tensile strength, which is reduced during ageing and degeneration as crosslinks between collagen fibrils decreases (Antoniou *et al.*, 1996). Proteoglycans and their negatively charged glycosaminoglycans (GAG) side chains, such as chondroitin sulphate and keratan sulphate, draw in water and cations via osmosis, meaning the NP exhibits high osmotic and hydrostatic pressure (Figure 1.3). This provides the NP with viscoelasticity and resistance to compression (Doege *et al.*, 1991; Dolan and Adams, 2001). As the NP has no blood supply, the oxygen tension is very low, prompting NP cells to rely on the glycolytic pathway for energy metabolism (Agrawal *et al.*, 2007).

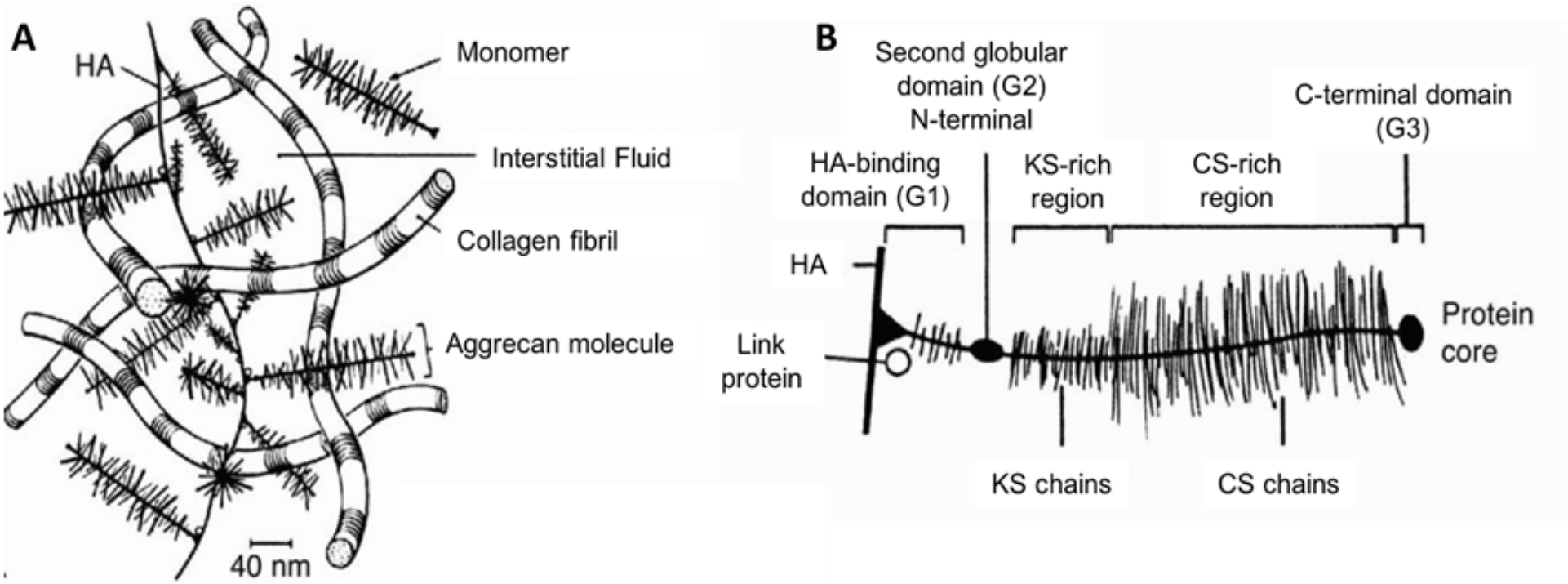

Figure 1.3. NP matrix composition. (A) A disorganised network of collage II fibrils intertwines with proteoglycans to produce a matrix that exhibits high hydrostatic pressure and enables resistance to compression. (B) Aggrecan consists of chondroitin sulphate (CS) and keratan sulphate (KS) GAG sidechains attached to a protein core, which is linked to hyaluronan (HA), tethering it to the matrix. Adapted from Ulrich-Vinther *et al.*, 2003.

The NP is derived from the notochord and during development the NP is highly cellular. During development and at birth the NP contains clusters of large cells with vacuolated (25 - 85µm) morphology, called notochordal cells (Figure 1.4). During aging the population of notochordal cells (and the total cell number in general) decreases and is replaced by smaller, spherical, non-vacuolated, chondrocyte-like cells (NP cells) (Figure 1.4). However, it has been shown that the proteoglycan to collagen ratio in the NP of healthy young adults (15 – 25 years) is much higher (27:1) when compared to articular cartilage (2:1), indicating phenotypic differences between NP cells and chondrocytes (Mwale, Roughley and Antoniou, 2004). In the mature NP, single cells encased within pericellular matrix lacunae are present, along with cell clusters that share a single lacuna (Johnson *et al.*, 2006). The cell density is approximately 4 x 10^6 cells/cm^3 (Roughley, 2004; Chen, Yan and Setton, 2006).

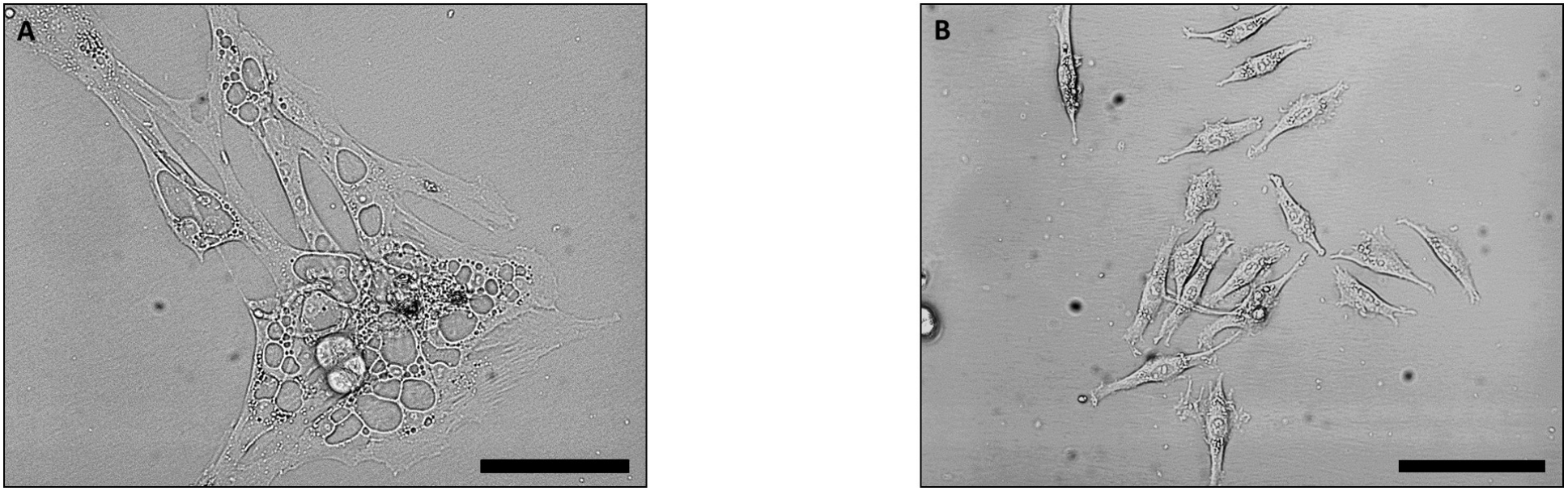

Figure 1.4. Cell types within the NP. (A) Clusters of large, vacuolated notochordal cells, similar to those present during human development, are present during *in vitro* culture 24hr after extraction from murine NP tissue, smaller chondrocyte-like cells are also present. (B) After ~10d *in vitro* culture, rat notochordal cells are completely replaced by/differentiate into smaller, non-vacuolated, mature NP cells, similar to those in the mature human. *In vivo,* the morphology of NC and NP cells is spherical. Scale bar 20µm.

It has been determined that during maturation notochordal cells undergo differentiation into the smaller chondrocyte-like NP cells found in the adult IVD (Choi, Cohn and Harfe, 2008; Minogue *et al.*, 2010b, 2010a; McCann *et al.*, 2012; Séguin *et al.*, 2018). Yet, there is also evidence that potentially notochordal cells die and are replaced by cells migrating from adjacent tissues as the IVD matures (Kim *et al.*, 2009; Yang *et al.*, 2009; Séguin *et al.*, 2018). Therefore, considerable work has been done to elucidate the NP phenotype and identify genetic markers to distinguish NP cells from AF cells and chondrocytes. Many markers have been proposed; genes involved during the development of the notochord such as sonic hedgehog (SHH) (Choi, Lee and Harfe, 2012) and brachyury (T) (Minogue *et al.*, 2010b), proteins linked to the physiology of NP cells such as (HIF-1α) (Risbud *et al.*, 2006), glucose transporter 1 (GLUT-1) (Rajpurohit *et al.*, 2002), carbonic anhydrase III and XII (CAIII (Silagi *et al.*, 2018)and CAXII) (van den Akker *et al.*, 2014), and other proteins like the intermediate filaments cytokeratin 18 and 19 (Sakai *et al.*, 2009; Rodrigues-Pinto *et al.*, 2016) and cell surface marker cluster of differentiation 24 (CD24) (Rutges *et al.*, 2010; Rodrigues-Pinto *et al.*, 2016). A consensus paper, authored by many groups, was published that recommended using a panel of these markers to determine the NP phenotype (Risbud *et al.*, 2015). However, since this publication other potential markers have been identified(Rodrigues-Pinto *et al.*, 2016; Silagi *et al.*, 2018), indicating that a true phenotypic marker differentiating NP cells remains to be discovered. Also, the panel of markers recommended by Risbud *et al.,* 2015 was focussed on determining the young, healthy NP cell phenotype, yet Thorpe *et al.,*

2016 identified different markers that distinguished mature, aging NP cells from AF cells and chondrocytes, indicating that factors such as NP maturity and the state of degeneration must also be considered when attempting to phenotypically characterise this elusive cell type.

1.3 Development of the intervertebral disc

The IVDs are derived from two embryonic structures called the notochord and the sclerotome (Peacock, 1951; Paavola, Wilson and Center, 1980). The central NP region is derived from the notochord (Peacock, 1951; Smits and Lefebvre, 2003) and the surrounding AF and CEP from the sclerotome (Peacock, 1951; Rodrigo *et al.*, 2003) (Figure 1.5). The notochord is a continuous rod-like structure positioned centrally, forming the axis of the embryo and is one of the defining structures of chordates (McCann and Séguin, 2016) (Figure 1.5). In mammals, an acellular sheath containing proteoglycans, collagens and laminins surrounds the notochord (Götz, Osmers and Herken, 1995). During embryonic development the notochord acts as a primitive support system and signalling centre, directing the development and differentiation of surrounding tissues and structures, including the neural tube (Yamada *et al.*, 1991) and sclerotome (Fan and Tessier-Lavigne, 1994), by secreting growth factors and morphogens (Christ, Huang and Scaal, 2004; Nimmagadda *et al.*, 2007; Christ and Scaal, 2008) (Figure 1.6).

The sclerotome is derived from the somites, transient structures adjacent to the notochord and neural tube during vertebrate development (Wilting *et al.*, 1994).

In response to Wnt signalling from the notochord and neural tube floor plate, and SHH signalling from the ectoderm, the somites undergo compartmentalisation (Christ and Scaal, 2008; McCann and Séguin, 2016). The development of the sclerotome is characterised by the formation of the ventral, lateral and dorsal sub-compartments from the somites (Monsoro-Burq *et al.*, 1994; Peters *et al.*, 1999). The dorsal sub-compartment differentiates and forms the dermomyotome, which generates the connective tissues of the axial skeleton (Capdevila, Tabin and Johnson, 1998). The ventral sub-compartment differentiates into the sclerotome, consisting of PAX-1-expressing cells, and produces the vertebral bodies, AF and CEP of IVDs (Peters *et al.*, 1999). In addition, each sclerotomal segment demonstrates rostral to caudal polarity; anterior vertebral structures are formed from the caudal sclerotome, whereas posterior vertebral structures are formed from the rostral sclerotome (Christ and Scaal, 2008).

As the vertebrae, AF and CEP form, the notochord contracts from the vertebral bodies, notochordal cells are expelled from vertebral regions and are limited to the centre of the forming IVD, which then expand to produce NP regions (Alkhatib *et al.*, 2018). The notochordal sheath contains and directs the retreating notochord and its internal hydrostatic pressure, which is essential for notochordal expansion and the subsequent formation of the NP (Adams, Keller and Koehl, 1990; Alkhatib *et al.*, 2018).

In humans, the number of notochordal cells within the notochord and subsequent NP starts to decline during maturation, even during embryonic

development (Peacock, 1951). The amount of notochordal cells continues to decline until they are virtually absent within the NP after the first decade of life (Risbud, Schaer and Shapiro, 2010). However, it has been observed in other species, such as rats and mice, that notochordal cells are still present beyond the point of skeletal maturity (Hunter, Matyas and Duncan, 2003a, 2004a). Curiously, chondrodystrophic (CD) dogs (long bodies, short legs) lose notochordal cell populations very early in life and suffer frequent, early-onset IVD degeneration, whereas non-chondrodystrophic (NCD) dogs (bodies and limbs in proportion) retain notochordal cell populations into adulthood and suffer infrequent, later-onset IVD degeneration (Bergknut *et al.*, 2013; Smolders *et al.*, 2013). This has led to canine studies determining a link between the decline of notochordal cells and IVD degeneration (Hunter, Matyas and Duncan, 2003, 2004). The exact underlying mechanisms responsible for the differentiation of notochordal cells into mature NP cells has not yet been elucidated, yet progressive alterations to the mechanical loading of the IVD (and the changes to the microenvironment thereafter) during development and growth are likely to influence the phenotype of notochordal and NP cells (Navaro *et al.*, 2015; Palacio-Mancheno *et al.*, 2018). It has also been shown that notochordal cells require very specific culture conditions to retain their phenotype *in vitro* (Spillekom *et al.*, 2014).

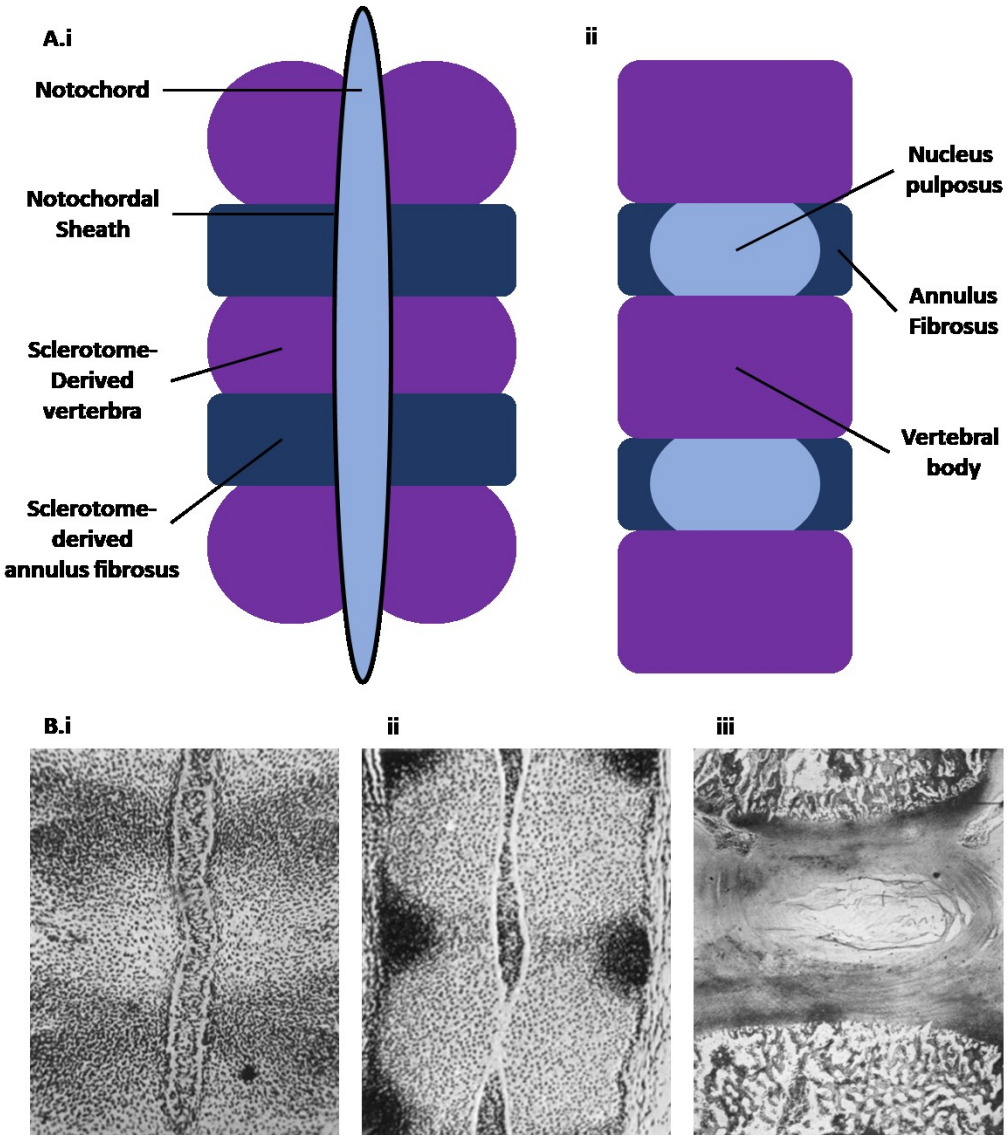

Figure 1.5. IVD development. (A.i) During embryonic development, the notochord directs the differentiation and segmentation of the sclerotome. (A.ii) At birth, the notochord forms the NP, whilst the sclerotome differentiates into the surrounding AF, CEP and vertebral bodies. (B) Haematoxylin and eosin staining (black and white) of the developing human spine. (B.i) Coronal section of a human 10mm (~7 weeks) embryo showing the intact notochord spanning the sclerotome, x415 magnification. (B.ii) Sagittal section of a 21mm (~10 weeks) human embryo showing the notochord contract towards the future NP and the segmentation of the sclerotome into the AF and vertebral bodies, x60 magnification. (B.iii) Sagittal section of a full-term human foetus (~40 weeks) showing the completely formed IVD; the concentric lamellae of the AF encapsulate the NP, which now contains fewer notochordal cells and 'abundant mucoid substance', x50 magnification. Adapted from (Peacock, 1951).

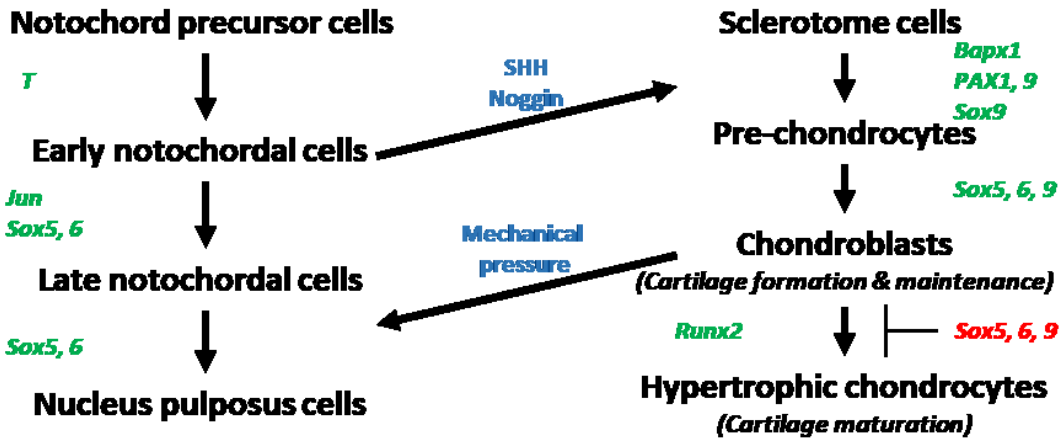

Figure 1.6. Transcriptional regulation of IVD development. The fate of cells during IVD development is governed by many transcription factors (green and red), secreted proteins and environmental factors (blue). Differentiation of early notochordal cells is mediated by T; Sox5, 6 and Jun are required for notochordal cell survival. SHH and Noggin are secreted by notochordal cells, and along with downstream signalling by Bapx1, PAX1, 9 and Sox9, induce the differentiation of sclerotome cells into pre-chondrocytes. Sox5 and 6 promote expression of matrix genes that form the notochordal sheath and cartilage. Mechanical pressure forces the relocation of notochordal cells into the centre of the IVD. Sox5 and 6 promote NP cell differentiation whilst also preventing the differentiation of chondroblasts into hypertrophic chondrocytes. Runx2 may promote hypertrophic chondrocyte maturation in vertebrae. Adapted from (Smits and Lefebvre, 2003).

1.4 The microenvironment of the intervertebral disc

Due to the unique development and positioning of the IVD within the human body, many environmental factors contribute to the physiology of the tissue and influence cellular behaviour.

1.4.1 Biomechanics

The function of the IVD is to enable movement and withstand the compressive forces of the spine; hence the IVD has a loaded environment subjected to a number of physical stresses. The biomechanics of the IVD is determined by

interactions of loading patterns between all the structures of the IVD. The IVD can withstand axial compression, torsion, flexion/extension, lateral bending and disperse mechanical energy evenly throughout the spine (Setton and Chen, 2004).

Due to the high level of hydration and gelatinous consistency the NP is considered a viscoelastic material, demonstrating both fluid and solid-like behaviours (Iatridis *et al.*, 1999). Internal stresses and strains exist within the NP, even in the unloaded IVD, which arise from the water content resulting in a high hydrostatic pressure with a baseline of 0.1 – 0.2MPa when supine, approximately 0.5MPa when standing and increasing up to 3 – 4MPa during extreme physical activity (Wilke *et al.*, 1999). Due to the variation of physical activity and posture during day and night the NP undergoes a diurnal change in intradiscal pressure (Chan *et al.*, 2011). Under increased load, during load-bearing and vertical posture, the IVD deforms which causes an increase in hydrostatic pressure and fluid is slowly expelled from the NP (Chan *et al.*, 2011). When in the supine position, the reduced load causes a release in intradiscal pressure and fluid is re-imbibed into the NP (McMillan, Garbutt and Adams, 1996; Malko, Hutton and Fajman, 2002). During compression the increase in NP pressure is constrained by the lamellae of the AF which produces longitudinal and circumferential AF tension (Galante, 1967). Therefore, the predominant mechanical stimuli acting on AF cells are tensile strain and shear (Galante, 1967). Whereas the predominant mechanical stimuli acting on NP cells are compressive and shear stresses, alongside hydrostatic pressure due to the water content and swelling properties of the NP (Setton and Chen, 2006).

As IVD cells are exposed to mechanical stimuli, it has been determined that the type, magnitude, frequency and duration of applied loading are crucial in determining cellular responses (Maclean *et al.*, 2004; Wang, Jiang and Dai, 2007; Wuertz *et al.*, 2009; Walter *et al.*, 2011). IVD cells respond to mechanical stimuli by activating mechanotransduction signalling pathways. The loss of aggrecan expression by NP cells due to a decrease in hydrostatic pressure was inhibited by pre-treatment with RGD blocking peptides (Le Maitre *et al.*, 2009). However, this was only observed in NP cells derived from healthy IVD tissue, not NP cells derived from degenerate IVD tissue (Le Maitre *et al.*, 2009). This suggests not only that NP cells respond to pressure via RGD domains and integrin signalling, but also that mechanotransduction pathways are altered during IVD degeneration (Le Maitre *et al.*, 2009). Healthy physiological loading, such as dynamic low pressure loads (0.1 – 1.0MPa), induces matrix synthesis and is essential for matrix production and IVD homeostasis (Wuertz *et al.*, 2007; Neidlinger-Wilke *et al.*, 2012). In contrast, overloading (1 – 4MPa) has been demonstrated to evoke degenerative changes, increasing catabolic gene expression, leading to the destruction of matrix (Iatridis *et al.*, 1999; Korecki, MacLean and Iatridis, 2008). Thus, indicating that the IVD has adapted to its function of withstanding the compressive forces of the spine and that IVD cell biology is finely tuned by the biomechanical forces exerted upon them.

1.4.2 Osmolality

The extracellular matrix (ECM) of the IVD enables its mechanical function. Proteoglycans and their negatively charged side chains draw water and ions into the

NP, increasing the hydrostatic pressure, so the IVD can withstand compression (Chan *et al.*, 2011). These actions simultaneously increase the fixed charge density and osmotic pressure within the NP, increasing the intradiscal osmolality when compared to most other tissues (400 – 500mOsm/kg H_2O) (Urban and McMullin, 1985; McMillan, Garbutt and Adams, 1996). Similar to responses to mechanical loading, culturing NP cells in physiological conditions mimicking the osmolality of the healthy IVD increases the expression of matrix genes (Wuertz *et al.*, 2007; Neidlinger-Wilke *et al.*, 2012; O'Connell, Newman and Carapezza, 2014) via osmotically regulated signalling pathways (Tsai *et al.*, 2006; Hiyama *et al.*, 2009; Johnson, Shapiro and Risbud, 2014b). However, these signalling pathways may become altered when the osmolality decreases, mimicking the degenerate IVD (~300mOsm/kg H_2O) when proteoglycan content decreased (Ishihara *et al.*, 1997). Which may lead to the production of catabolic genes in preference over matrix genes (Johnson, Shapiro and Risbud, 2014b; Johnson *et al.*, 2017), indicating that NP function is controlled by the osmotic environment bestowed upon the IVD by proteoglycans and mechanical loading. There are numerous signalling pathways, transcription factors and transmembrane channel proteins expressed in NP cells that are implicated in their adaptation to the hyperosmotic environment of the IVD, yet how NP cells sense and respond to this stimulus has not been fully elucidated (Johnson, Shapiro and Risbud, 2014b; Sadowska *et al.*, 2018).

1.4.3 Nutrition, pH and oxygen tension

The IVD is the largest avascular tissue in the human body (Urban, 2002). In healthy IVDs, blood vessels only penetrate into the periphery of the outer AF and NP cells are 6 – 8mm away from the nearest blood supply. Therefore, the transport of nutrients and waste products occurs via diffusion (Urban, 2002). Small amounts of diffusion take place via the blood vessels at the AF periphery, but the majority of transport occurs from blood vessels within the vertebral bodies and across the CEP (Roberts *et al.*, 1996).

Nutrient transport through the IVD occurs almost exclusively by diffusion facilitated by load-induced water transport. This results in steep concentration gradients of glucose, oxygen and lactic acid across the IVD (Roberts *et al.*, 1996; Urban, 2002; Bibby *et al.*, 2005). As the concentration of glucose and oxygen progressively decreases towards the centre of the IVD, the concentration of lactic acid increases (Ohshima and Urban, 1992). Therefore, the NP has a slightly acidic pH (pH6.9 – 7.2) and low oxygen microenvironment (8 – 10% at the IVD-vertebral interface decreasing to 0.3 – 0.5% in the NP) that cells are required to adapt to (Holm *et al.*, 1981; Urban, 2002). Oxygen concentration has been observed at 0.7% in degenerate human IVDs (Bartels *et al.*, 1998). Consequently, NP cells favour glycolytic metabolism (causing the increase of lactic acid) due to the lack of oxygen (Agrawal *et al.*, 2007) and have adapted to their acidic surroundings (Urban, 2002; Silagi *et al.*, 2018a; Silagi *et al.*, 2018b). Such adaptation is mediated by hypoxia-inducible factor-1α (HIF-1α), which has been shown to support the survival and function of NP cells

by driving glycolytic metabolism and ECM production, enabling adaptation to their hypoxic niche (Pfander *et al.*, 2003; Risbud *et al.*, 2006; Richardson *et al.*, 2008; Fujita *et al.*, 2012; Silagi *et al.*, 2018).

The nutrient supply into the IVD can be reduced by a number of factors such as CEP calcification (Roberts *et al.*, 1996), decreased blood flow to segmental arteries (Kauppila, 1997) or a decrease in the water content of the IVD (Horner and Urban, 2001). The decrease in nutrient supply has been linked to IVD degeneration due to an increase in cell death, caused by decreases in glucose concentration (< 0.5mmol/L) and pH (< 6.5) (Horner and Urban, 2001), and the production of catabolic enzymes that mediate the destruction of ECM (Urban and Roberts, 2003). However, it may also be possible that the nutrient supply can be increased during IVD degeneration, due to a possible increase in vascularisation (which may also cause pain due to associated nerve ingrowth) (Freemont *et al.*, 2002; Binch *et al.*, 2014) and the presence of fissures, allowing rapid nutrient diffusion (Melrose *et al.*, 2002; Stefanakis *et al.*, 2012; Binch *et al.*, 2015).

1.5 Degeneration of the intervertebral disc

Approximately 80% of the population will suffer from low back pain (LBP) during their lifetime (Hoy *et al.*, 2015), resulting in a global economic burden (UK ~£12 billion, US ~$85 billion) (Maniadakis and Gray, 2000; Martin *et al.*, 2008) 2008. Recently LBP was found to be one of the 5 top causes of disability worldwide (Vos *et al.*, 2017; James *et al.*, 2018). LBP is multifactorial, yet 40% of cases are attributed to

IVD degeneration (Luoma *et al.*, 2000). The aetiology of IVD degeneration itself is also multifactorial; aging (Gruber and Hanley, 1998), smoking (Battié *et al.*, 1991), genetic factors (Matsui *et al.*, 1998), decreased nutrient uptake and waste removal (Horner and Urban, 2001; Bibby *et al.*, 2005) and repetitive mechanical loading greater than tolerable limits (Adams *et al.*, 2000). IVD degeneration is characterised by progressive destruction of the ECM caused by altered cell metabolism and function, matrix synthesis and degradation of matrix components (Le Maitre *et al.*, 2007).

1.5.1 Cytokines

IVD cells produce a plethora of cytokines and chemokines (Le Maitre, Freemont and Hoyland, 2005; Hoyland, Le Maitre and Freemont, 2008; Phillips *et al.*, 2013, 2015), interleukin - 1β (IL-1β) and tumour necrosis factor – α (TNF-α) are the most studied and are clearly implicated in the pathogenesis of IVD degeneration. IL-1β, IL-1 receptor I (IL-1RI) and IL-1 receptor antagonist (IL-1Ra) are all expressed in healthy IVD cells, but the expression of IL-1β and IL-1RI (not IL-1Ra) is increased with increasing severity of degeneration (Le Maitre, Freemont and Hoyland, 2005)and has been shown to induce many catabolic events (Le Maitre, Freemont and Hoyland, 2005; Hoyland, Le Maitre and Freemont, 2008). TNF-α expression is also increased during IVD degeneration, but not to as high a level as IL-1β (Le Maitre, Hoyland and Freemont, 2007a). Also, as TNF receptor I (TNF-RI) was not increased in degenerate IVDs and TNF-α inhibition has no effect on matrix degradation, whereas IL-1β inhibition completely abrogated matrix degradation, this may highlight the prominent role of IL-1β, over TNF-α, during IVD degeneration (Hoyland, Le Maitre

and Freemont, 2008). The importance of IL-1β during degeneration has been strengthened by the observation of spontaneous IVD degeneration in a knockout mouse model of IL-1Ra, the natural inhibitor of IL-1β (Phillips *et al.*, 2013), and the presence of polymorphisms in the IL-1 gene cluster linked to an increased risk of IVD degeneration (Solovieva *et al.*, 2004, 2006; Karppinen *et al.*, 2009). Conversely, an increase in both TNF-α receptors (TNF-RI and TNF-RII) expression has been identified in herniated IVD tissue and showed a positive correlation with pain levels assessed by the visual analogue scale (Andrade *et al.*, 2011), indicating TNF-α also plays an important role during IVD degeneration and possibly in the manifestation of pain. Recently the overexpression of TNF-α in a transgenic mouse model showed the early onset of IVD herniation, yet no overt signs of degeneration (Gorth, Shapiro and Risbud, 2019), which supports that TNF-α is involved in IVD degeneration, but less so than the pivotal role played by IL-1β. These changes in cellular behaviour initiate IVD degeneration by leading to the increased production of more cytokines, vascularisation and innervation causing pain, and the increased expression of matrix degrading enzymes.

1.5.2 Degeneration of extracellular matrix

As IVD degeneration advances, collagen type II within the NP is gradually replaced by the more fibrous collagen type I (Roughley, 2004). The overall composition of proteoglycans is reduced and altered with decreased aggrecan expression and versican, decorin and biglycan expression is increased, thus reducing the capacity of the NP to imbibe water, resulting in decreased hydration and loss of

IVD height (Inkinen *et al.*, 1998; Cs-Szabo *et al.*, 2002). Concurrently, the increased cytokine production by IVD cells upregulate a variety of catabolic mediators including matrix metalloproteinases (MMP) -1, -2, -3, -13 and -14, and a disintegrin and metalloproteinase with thrombospondin motifs (ADAMTS) -1, -4 and -5 (Séguin *et al.*, 2006; Le Maitre *et al.*, 2007; Pockert *et al.*, 2009; Wang *et al.*, 2011; Tian *et al.*, 2013). MMPs and ADAMTSs are important mediators of matrix remodelling during healthy physiology, but their overexpression during degeneration (Roberts *et al.*, 2001; Le Maitre, Freemont and Hoyland, 2004; Pockert *et al.*, 2009) brings about the destruction of collagen and proteoglycans within the NP, which is exacerbated by the suppression of important matrix genes during these processes (Wang *et al.*, 2011; Tian *et al.*, 2013; Johnson *et al.*, 2017). The resulting compositional changes during degeneration cause alterations to the IVD microenvironment, such as decreased nutrition, pH and osmolality and excessive biomechanical loading (Section 1.4) (Figure 1.7). This consequently leads to adverse cellular changes, including apoptosis/necrosis (Gruber and Hanley, 1998; Ding, Shao and Xiong, 2013), senescence (Roberts *et al.*, 2006; Gruber *et al.*, 2007; Le Maitre, Freemont and Hoyland, 2007) and a decrease in the viability and number of remaining cells (Le Maitre, Freemont and Hoyland, 2007). As the IVD has developed a hostile microenvironment during degeneration, those cells still present are also more likely to develop a catabolic phenotype, continuing the degenerative cascade.

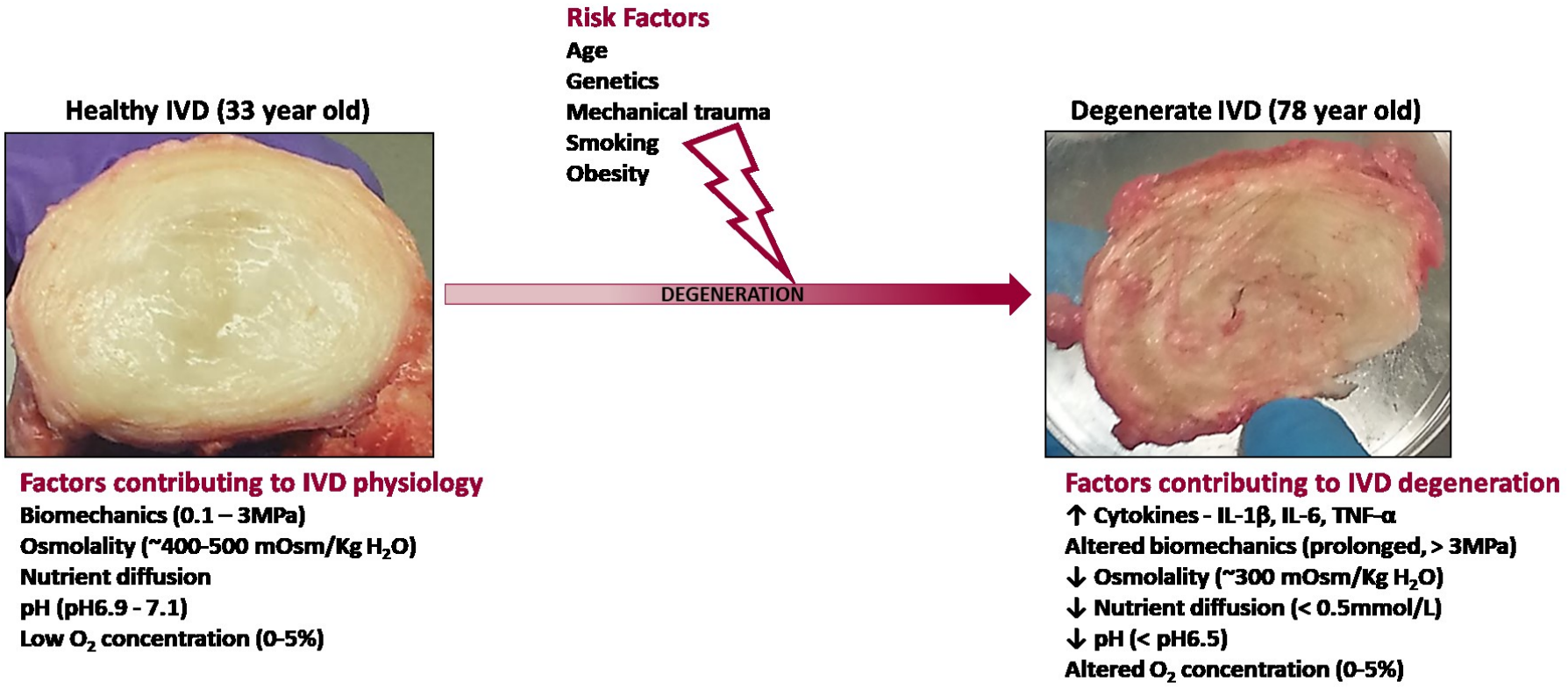

Figure 1.7. Microenvironmental factors within the IVD that dictate cellular function and how these factors are altered during degeneration.

1.5.3 Consequences of intervertebral disc degeneration

The imbalance between normal matrix synthesis and degradation results in a loss of the structural integrity of the NP due to a reduction in hydration, osmotic swelling pressure and IVD height (Urban and McMullin, 1988). These changes result in a diminished ability of the IVD to withstand and evenly distribute the compressive loading of the spine. This may ultimately lead to IVD injuries such as the formation of tears and fissures through the AF, due to the asymmetric distribution of compressive loading, and the eventual herniation and extrusion of the NP through such tears (Adams and Roughley, 2006) (Figure 1.8). IVD herniation may also be associated with the sensation of chronic pain as extruded NP material may impinge on spinal nerves (Risbud and Shapiro, 2014) (Figure 1.8), which may also act as an access route for the vascularisation and innervation of the IVD (Binch *et al.*, 2014).

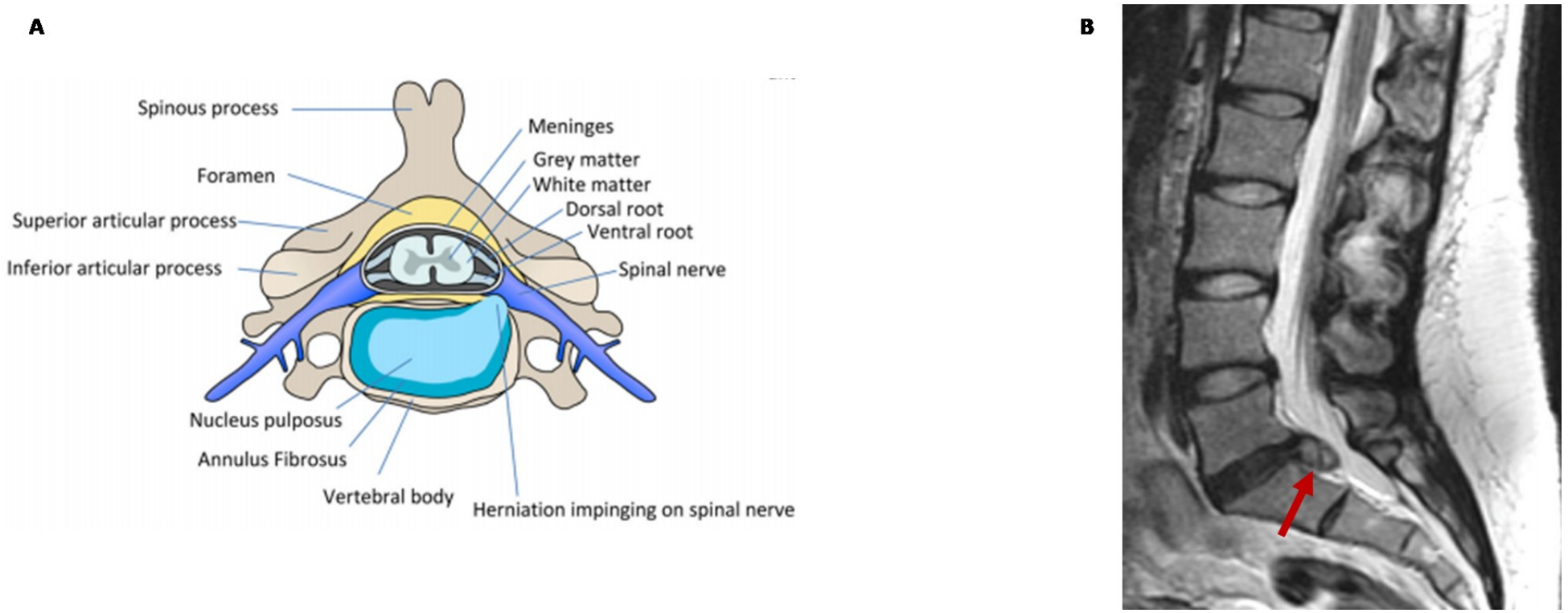

Figure 1.8. IVD herniation. (A) Schematic showing NP herniation through the AF and impingement on a spinal nerve. (B) A T2-weighted MRI image showing posterior L5-S1 IVD herniation (red arrow) in a patient with symptomatic IVD degeneration. Adapted from Risbud and Shapiro, 2014.

1.5.4 Current treatment

Most current practices for the treatment of LBP are directed towards alleviating and managing symptoms, including analgesic medication, physiotherapy, acupuncture and chiropractic treatment (Chou *et al.*, 2009). However, as these practices only be able to treat symptoms such as pain, they may only be successful in the short term (Carette *et al.*, 1997). Other options for patient treatment include surgical procedures to stabilise or remove damaged tissue. Microdiscectomy, the removal of herniated NP tissue, and spinal fusion, the removal of the degenerated IVD and vertebral fusion, can be offered to patients when conservative methods have been unsuccessful (Andrews and Lavyne, 1990). However, these treatments have been associated with alterations in spinal biomechanics and the potential degeneration of adjacent IVDs (Lund and Oxland, 2011). It has also been reported that approximately 23% of patients receiving microdiscectomy required repeat operations, due to recurrent IVD herniation (Parker *et al.*, 2015).

Emerging research has aimed to develop a biological approach to address the underlying pathophysiology of IVD degeneration. The use of growth factors and/or inhibitors has been investigated in attempts to promote anabolic processes, such as matrix synthesis, whilst also inhibiting catabolic processes, such as matrix degradation and inflammation (Tim Yoon *et al.*, 2003; Christine L Le Maitre, Hoyland and Freemont, 2007; Le Maitre, Freemont and Hoyland, 2009; Cao *et al.*, 2012; Gorth *et al.*, 2012; Feng *et al.*, 2017; Li *et al.*, 2017; Mern *et al.*, 2017). However, so far, the use of such modulating compounds/proteins has failed to substantially treat dysfunctional NP cells which continue to display a catabolic phenotype (Roberts *et al.*, 2006; Le Maitre, Hoyland and Freemont, 2007; Gruber *et al.*, 2007; Le Maitre, Freemont and Hoyland, 2007).

Therefore, further research has focussed on the use of regenerative cell sources, such as mesenchymal stem cells (MSCs), together with biomaterial scaffolds. With the aim of simultaneously repopulating the NP whilst also providing a microenvironment for the preferential differentiation into cells that regenerate the correct matrix and inhibit the degenerative cascade (Le Maitre *et al.*, 2015). To enable such treatments to become successful it is essential that the physiology of the IVD is understood with respect to the development and adaptation of NP cells to their multifaceted microenvironment (Thorpe *et al.*, 2018). The elucidation of these adaptations may be essential in determining how healthy NP cells function and how dysregulation may cause or occur during IVD degeneration. Thus, identifying vital physiological traits that must be protected and restored to ensure potential future treatments not only work but are performed on patients that will benefit from them.

1.6 Aquaporins

The movement of water throughout cells and tissues is essential for the maintenance of homeostasis in all organisms. In mammals, water can pass freely in and out of cells by diffusion through the plasma membrane as individual molecules, or passively co-transported with other ions and solutes such as Na^+ and glucose (Loo *et al.*, 1996). However, these modes of water transport cannot account for the rapid and highly selective water movement that has been shown to regulate many processes such as determining urine concentration in the kidneys (Marples *et al.*, 1995), the secretion of saliva (Krane *et al.*, 2001b) and the formation of a fluid-filled cavity alongside oocytes during folliculogenesis (McConnell *et al.*, 2002).

It was almost fifty years ago when the existence of water channels was hypothesised due to the drastic decrease in water permeability observed in cells when incubated with mercurial sulfhydryl reagents (Macey and Farmer, 1970). This hypothesis was confirmed with the discovery of the first aquaporin (AQP), AQP1, in erythrocytes and renal tubules (Denker *et al.*, 1988) and their characterisation as a selective water channel within cell membranes (Zeidel *et al.*, 1992; Agre *et al.*, 1993). Since their discovery, 13 members of the mammalian AQP family of membrane channel proteins have been identified (AQP0-12), which are expressed and have a variety of functions in a plethora of different tissues (Day *et al.*, 2014).

1.6.1 Structure

Despite the diverse expression and roles of AQPs throughout different tissues they contain a highly conserved structure relating to their specific function to transport water across cell membranes. Functional AQPs exist as ~28kDa homotetramers, with each monomer consisting of six α-helical transmembrane domains (1-6) linked through five alternating extracellular and intracellular loops (A-E), with both the C-terminus and N-terminus located on the cytosolic side of the cell membrane (Figure 1.9).

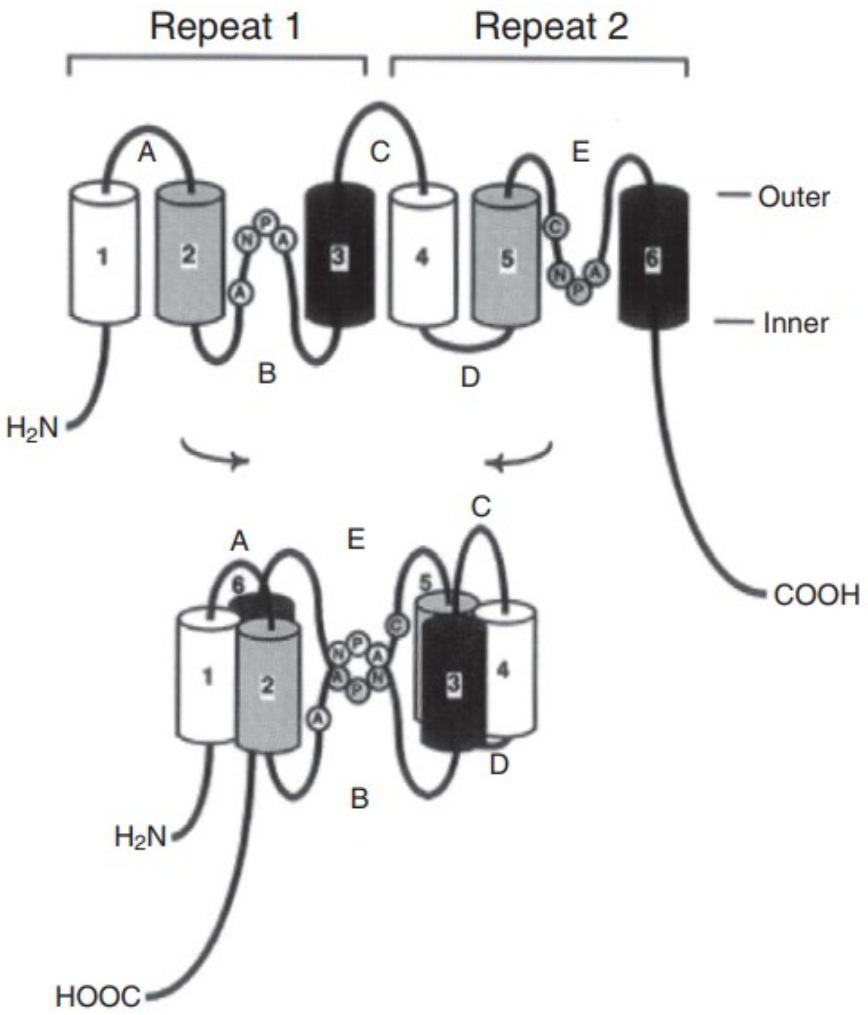

Figure 1.9. The structure of a single AQP channel monomer. The six transmembrane domains (1-6) form two tandem repeats and are attached by five loop regions (A-E). The transmembrane domains fold to form a central pore. Loops B and E fold inwards and line the pore opening. This produces the hourglass model of AQP monomer folding. Adapted from Spring, Robichaux and Hamlin, 2009.

Each monomer folds to form individual water-transporting pores, therefore each functional AQP homotetramer contains four pores and not one single, central pore (Figure 1.10). This structural information was first determined through electron-diffraction studies on AQP1 in erythrocytes (Murata *et al.*, 2000), followed by more high-resolution imagery determining similar structures for other human AQPs (Horsefield *et al.*, 2008; Ho *et al.*, 2009).

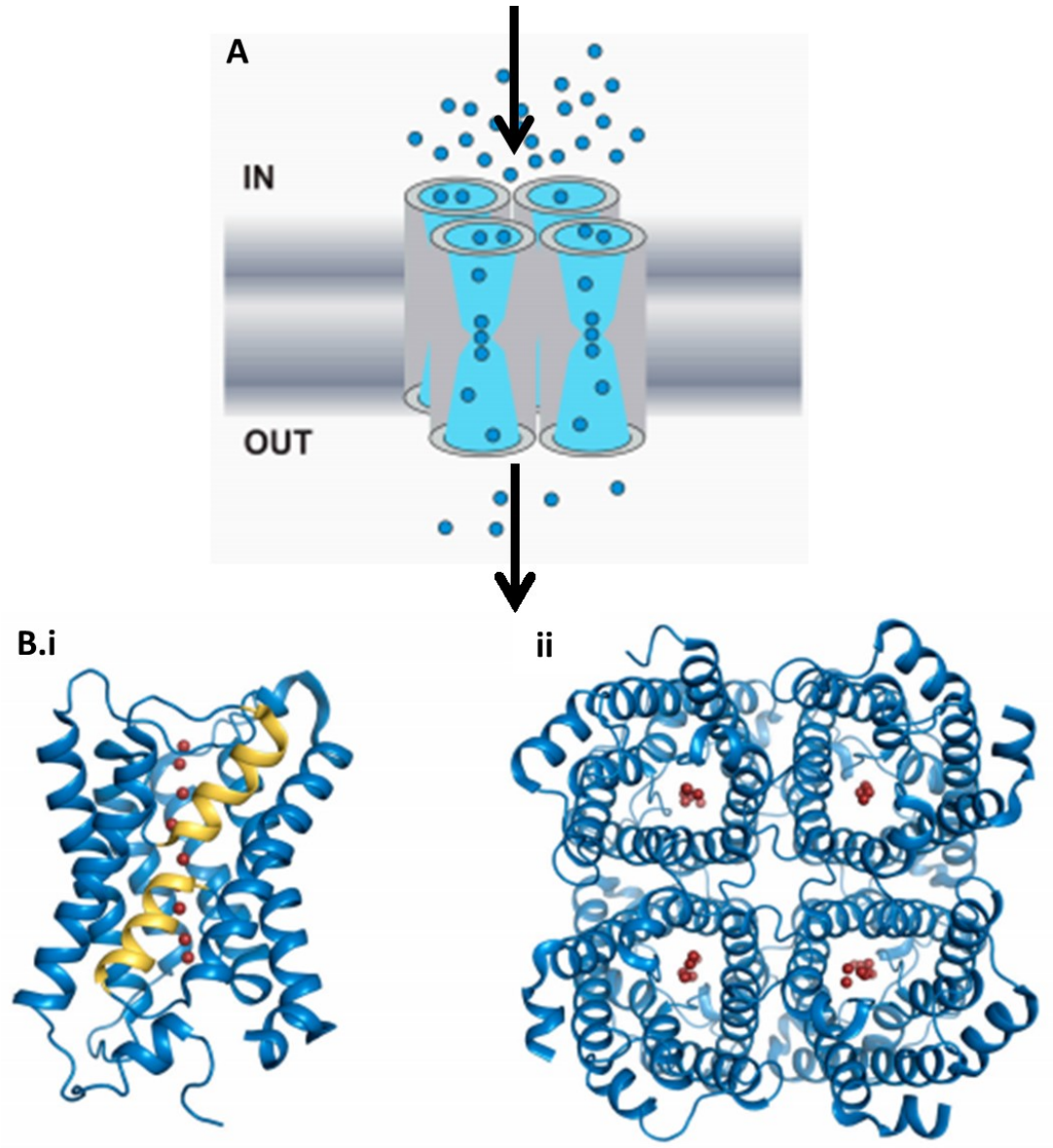

Figure 1.10. The structure of the AQP homotetramer. (A) AQP channels consist of four transmembrane monomers folded to produce one water-transporting pore each. Water (blue spheres) is transported across an osmotic gradient (arrows) adapted from Ozu *et al.*, 2018. (B.i) Side-view of the x-ray crystal structure of human AQP5 monomer. The half-helices B and E form the central pore (yellow) that permeates water (red spheres) in a single-file. (B.ii) Top-view of AQP tetrameric assembly, with each monomer forming a water-transporting pore. Adapted from Nesverova and Törnroth-Horsefield, 2019.

AQPs are highly specific in their roles as water channels as the structure of the pore itself determines the type of molecule that can pass through cell membranes via these channels. The majority of human AQPs (0, 1, 2, 4, 5 and 8) are selective for water molecules only, due to two selection stages within the pore. The first is due to the folding

of intracellular loop B and extracellular loop E into the pore, forming two half-helical regions, which both contain a conserved amino acid sequence of Asparagine-Proline-Alanine (NPA) (Sui *et al.*, 2001). Since α-helices have a natural dipole, both half-helices focus their positive dipole towards the centre of the channel which creates an electrostatic barrier to protons and cations whilst also aligning the dipole of water molecules as they pass the NPA signature motifs, when entering the AQP pore (de Groot and Grubmüller, 2005) (Figure 1.11).

The second stage of selectivity is due to a constriction region located on the extracellular side of the AQP pore, which contains another conserved amino acid motif. The aromatic/Arginine (ar/R) motif facilitates selectivity by re-positioning water molecules for their entry into the AQP pore and also contributes to the exclusion of protons (Wu *et al.*, 2009) (Figure 1.11). The remaining AQPs (3, 6, 7, 9, 10, 11 and 12) have the ability to transport other molecules as well as water (Section 1.6.2).

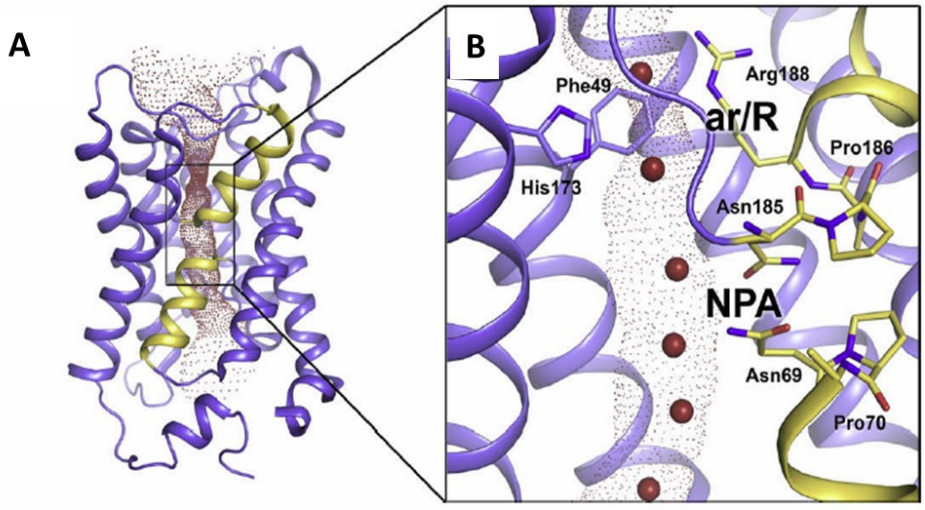

Figure 1.11. Structure of the AQP monomer indicating The NPA and ar/R selectivity motifs. (A) Overall structure of an AQP monomer. (B) Detail of the conserved NPA and ar/R motifs that confer the selective passage of water molecules (red spheres) through the pore. Structures have been drawn from the x-ray structure of human AQP5. Adapted from Törnroth-Horsefield *et al.*, 2010.

1.6.2 Function

The AQP family of membrane channel proteins have been identified to be highly selective in their transport of water across cell membranes; however, some are known to have the ability of transporting other small molecules in addition to water. AQP6 has been shown to be potentially permeable to ionic molecules as well as being highly permeable to water (Beitz *et al.*, 2006). Unlike other AQPs that are mainly located within the plasma membrane, AQP6 is localised to intracellular membranes in acid-secreting, intercalated cells of kidney collecting ducts. This exclusive localisation of AQP6 and its potential to transport ionic molecules suggests a role in renal acid-base regulation.

AQPs 3, 7, 9 and 10 have also been shown to transport other small molecules such as glycerol, urea and ammonia (Litman, Søgaard and Zeuthen, 2009). The so-called "aquaglyceroporins" additional function may be due to structural changes in the ar/R selectivity filter lining the water-transporting pore. When the diameter of the AQP pore at the ar/R restriction site is 2.8 Å in diameter this will only allow the passage of water molecules, whereas when point mutations were introduced at both the aromatic and arginine residues (F56A and R195V, respectively) the diameter of the pore was increased to >3.4 Å. This increase led to the conductance of not only water but also other small molecules such as glycerol in AQP1 (Beitz, Wu, *et al.*, 2006; Hub and de Groot, 2008).

Changes to the NPA motif have also been determined in other AQPs that have different functions other than as a selective water transport. The structure of this conserved motif in the "unorthodox" AQPs (11 and 12) has been demonstrated to be altered which may explain their as of yet, unknown role. Tchekneva *et al.*, 2008 highlighted that by substituting a single amino acid within the E-loop NPA box (C227S) in mice gave rise to a phenotype that resembled AQP11 knockout mice, thus suggesting a vital role for C227 in the function of the NPA motif in AQP11. AQP structure is related

to their function as selective water channels as highly conserved amino acid sequences within the AQP family allow for such a high specificity for the movement of water molecules through plasma membranes. Changes in these amino acid sequences have led to a number of these channels acquiring altered functions such as the ability to transport a number of different small molecules in addition to water.

1.6.3 Expression and physiological roles

Due to the unique and vital molecular function of AQP channels, they contribute to many physiological processes and are expressed almost ubiquitously throughout the human body (Figure 1.12). The expression of specific AQP isoforms within specific tissues also alludes to their potential roles. AQPs have been shown to regulate many processes such as cell volume regulation (Kitchen *et al.*, 2015); cell structure and adhesion (Varadaraj and Kumari, 2018); cell migration and proliferation (Papadopoulos, Saadoun and Verkman, 2008); water homeostasis in the kidney (Hasler *et al.*, 2008); blood-brain barrier function (Clément, Rodriguez-Grande and Badaut, 2018); lens function (Schey *et al.*, 2017); fluid secretion (Ramli *et al.*, 2019); sperm motility (Laforenza *et al.*, 2016; Fujii *et al.*, 2018); and glycerol metabolism (Méndez-Giménez *et al.*, 2018). As such, alteration to AQP expression and function has also been implicated in the pathophysiology of many disorders, including: renal water imbalance (Kortenoeven and Fenton, 2014); brain oedema (Clément, Rodriguez-Grande and Badaut, 2018); cataract formation (Biswas *et al.*, 2014); infertility (Kasimanickam *et al.*, 2017); and cancer metastasis (Marlar *et al.*, 2017) are all, in-part, due to the dysregulation of AQP expression and function. This indicates that aside from passive water transport, AQPs play active roles during the adaptation of many important physiological processes. Their function, however, relies on their integration into the

plasma membrane of cells in which their expression is not ubiquitous; the localisation of AQPs within cells is tightly regulated by a number of mechanisms.

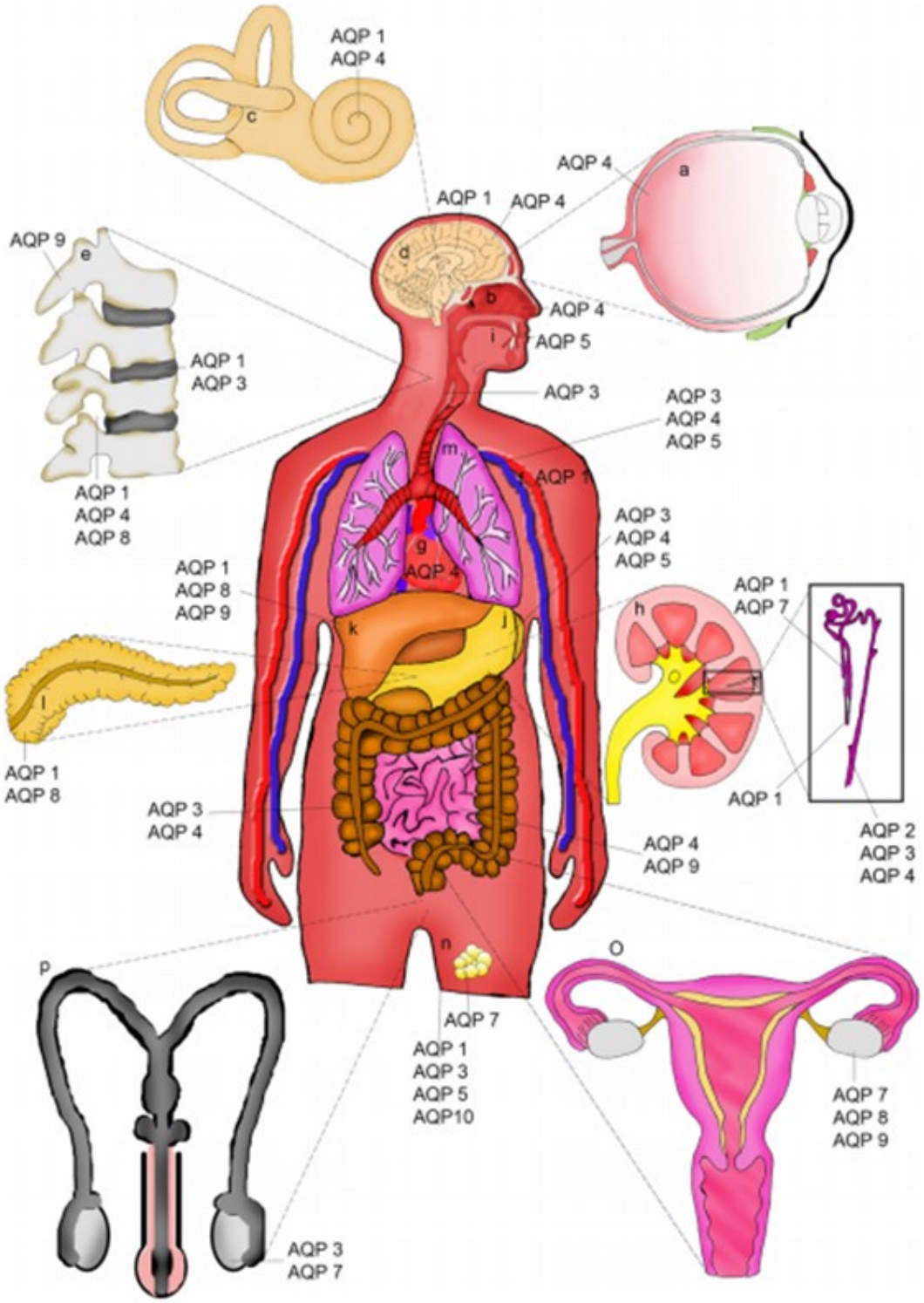

Figure 1.12. AQP expression in humans. The main AQP isoforms expressed in different tissues is indicated. (a) Retina, (b) Olfactory epithelium (c) The inner ear, (d) Brain, (e) Spinal cord, IVD, Osteoclasts, (f) Blood vessels, (g) Heart (h) Kidney (nephron in detail), (i) Salivary glands, (j) Gastrointestinal tract, (k) Liver, (l) Pancreas, (m) Lungs, (n) Fat (adipocytes), skin, (o) Female reproductive system, (p) Male reproductive system. Adapted from (Day *et al.*, 2014).

1.6.4 Aquaporin gating and channel inhibition

Gating mechanisms in AQPs have long been debated to regulate their function by changing structure of the pore to allow or halt the flow of water through cells. It is well documented that plant AQPs contain gating mechanisms that respond to a number of different stimuli including phosphorylation (Johansson *et al.*, 1998; Nyblom *et al.*, 2009), pH (Tournaire-Roux *et al.*, 2003), and divalent cations and protons (Verdoucq, Grondin and Maurel, 2008). Yeast AQP gating has also been documented using x-ray crystal structures determining the involvement of AQP N-termini (Fischer *et al.*, 2009).

Potential gating for mammalian AQPs still remains an elusive topic and is not a widely-accepted regulatory mechanism (Wang and Tajkhorshid, 2007). However, studies into mammalian AQP gating by Reichow *et al.*, 2013 and Janosi and Ceccarelli, 2013 have identified novel gating mechanisms in mammalian AQP0 and human AQP5 respectively, potentially indicating a more substantial role for gating mechanisms in mammalian AQPs (Figure 1.13)**.** There is also evidence that phosphorylation in response to many microenvironmental factors may also contribute to AQP gating (Nesverova and Törnroth-Horsefield, 2019) and recently mechanical stimuli has proposed as a potential gating mechanism (Hill and Shachar-Hill, 2015; Ozu *et al.*, 2018) (Figure 1.13).

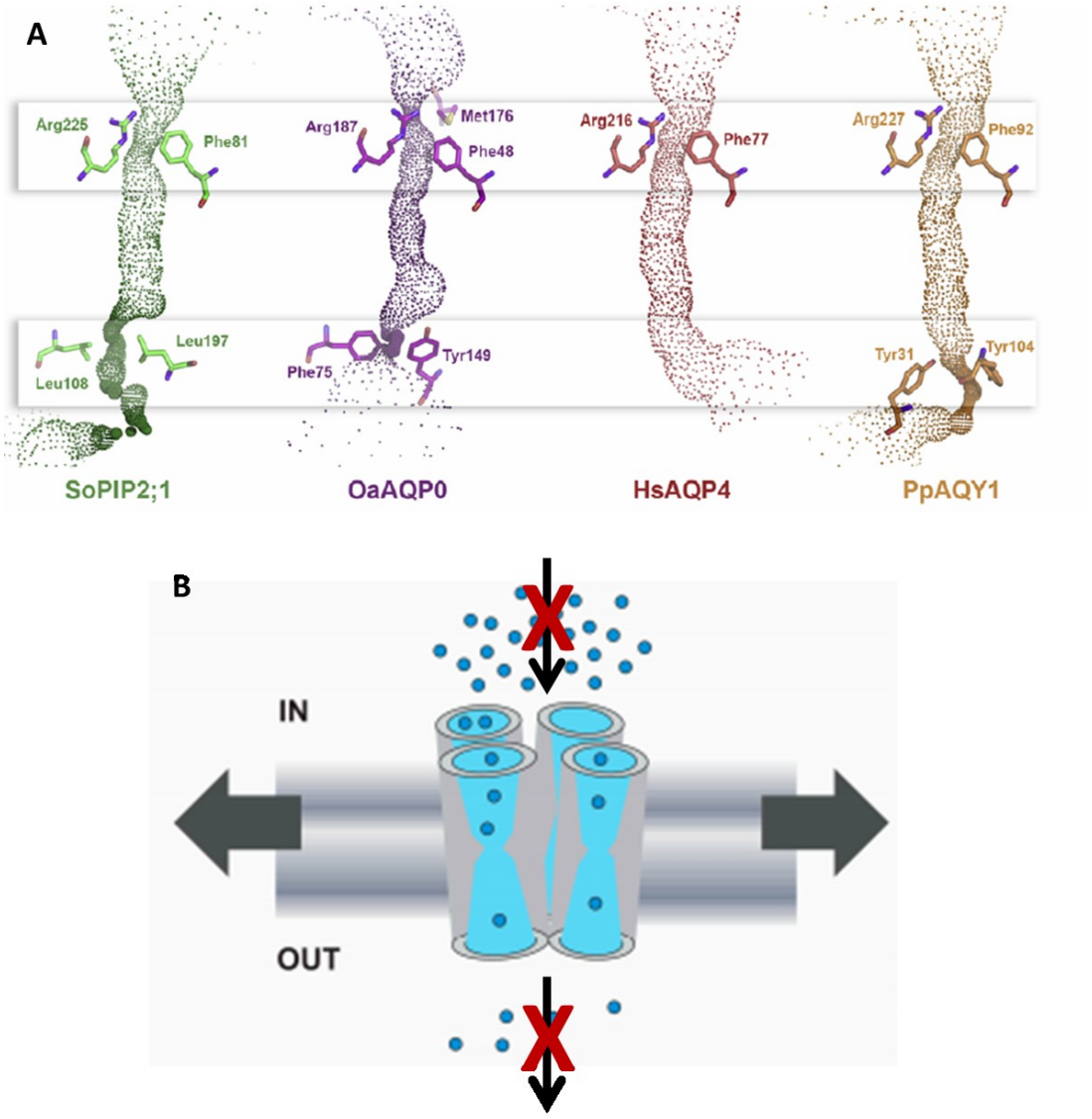

Figure 1.13. Comparison of the gating mechanisms in eukaryotic AQPs. (A) Plant SoPIP2;1 (green), sheep AQP0 (purple), human AQP4 (red) and yeast Aqy1 (orange). Structures show the pore of each AQP monomer with regulatory amino acid residues highlighted. All AQPs share the ar/R selectivity filter at the extracellular side of the pore. At the cytosolic side of the pore, residues are displayed that contribute to gating; plant and yeast mechanisms are well established and recently discovered in sheep. Adapted from Törnroth-Horsefield *et al.*, 2010. (B) Membrane stretch as a gating mechanism of AQP function. During osmotic stress, rapid water flux causes changes in cell volume and membrane tension (horizontal arrows). It is proposed that AQP structure may become distorted, halting water transport (vertical arrows), thereby controlling the osmotic response of cells. Adapted from Ozu *et al.*, 2018.

AQPs are also described as mercury-sensitive water channels due to the ability of mercury-containing compounds, such as $HgCl_2$, to inhibit water flow. Mercury containing compounds regulate the function of AQPs by binding to amino acid residues and occlude the pore. The specific residue is C183 which contains two mercury binding sites (Savage and Stroud, 2007). Such compounds could potentially be useful drugs to regulate AQPs in disease if it was not for the highly toxic mercury content.

1.6.5 G-Protein Coupled Receptors and Protein Kinases

One of the most well-established mechanisms of AQP regulation is the effect of vasopressin on the G-protein coupled receptor (GPCR) Vasopressin receptor 2 (V2R), to increase AQP2 expression and trafficking in the collecting ducts of the kidney. Upon vasopressin binding, the seven-transmembrane domain GPCR initiates adenylate cyclase through active Gs-protein (Roos *et al.*, 2012). This results in increased levels of intracellular cyclic adenosine monophosphate (cAMP) which in turn activates protein kinase A (PKA). PKA is a serine/threonine kinase that increases expression and trafficking of AQP2.

AQP2 expression is also increased as PKA phosphorylates and activates the nuclear import and binding of cAMP responsive element-binding protein (CREB) to the cAMP responsive binding element (CRE) transcription factor (Moeller and Fenton, 2012). CRE resides upstream and is responsible for the up-regulation of many genes, including AQP2.

PKA also has a more direct action in the regulation of AQP2 as phosphorylation of specific amino acid residues, C256, causes AQP2 trafficking to the plasma membrane; first investigated using site-directed mutagenesis of putative phosphorylation residues by Kuwahara *et al.*, 1995.

PKA is not the only serine/threonine kinase to play a role in AQP trafficking. The lipid-activated and C2 calcium binding domain containing kinase, protein kinase C (PKC), also activates AQP phosphorylation and trafficking (Conner *et al.*, 2012). Serine/threonine kinase phosphorylation of AQPs is a required action for movement; whether this corresponds to trafficking to the plasma membrane or internalisation into the cytoplasm. A number of different phosphorylation sites for many human AQPs have been determined (Figure 1.14).

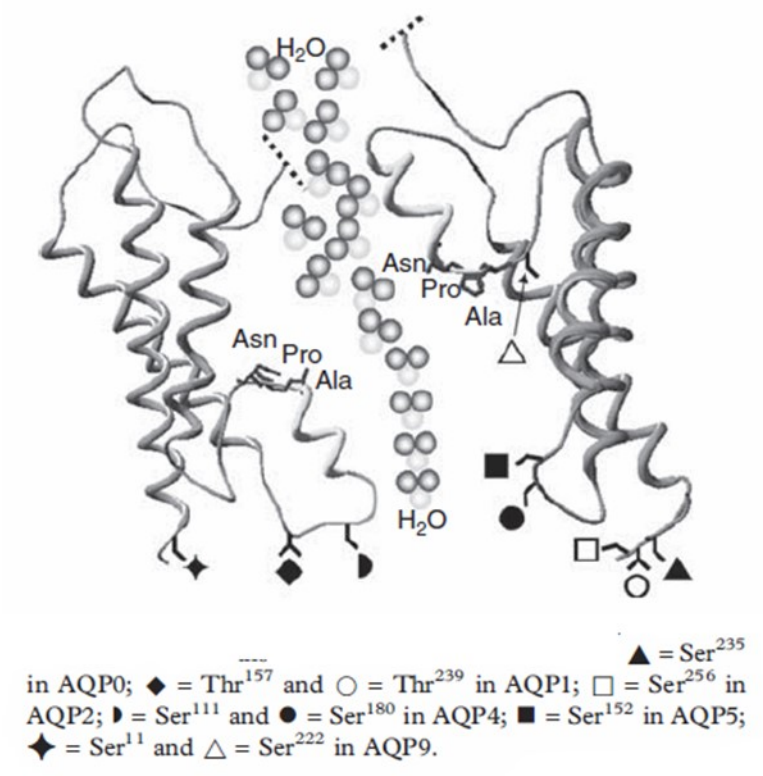

Figure 1.14. The phosphorylation sites of AQPs. NPA motifs on B and E-loops are shown that orientate and specifically allow the passage of water molecules (grey and white spheres) through the channel. The positions of serine/threonine kinase phosphorylation sites for individual AQPs are shown as symbols above. Adapted from (Conner, Bill and Conner, 2013).

1.6.6 Calcium

Calcium plays a role in numerous cell signalling pathways, including AQP regulation. Along with AQP phosphorylation by protein kinases, Ca^{2+} interactions with AQPs is essential for their trafficking (Conner *et al.*, 2012). Ca^{2+} ions interact via the calcium binding protein calmodulin (Yáñez, Gil-Longo and Campos-Toimil, 2012). The structure of calmodulin is comprised of four identical helix-loop-helix 'EF-hand' groups. Each EF-hand structure contains the binding site for a single Ca^{2+} ion (Grabarek, 2005). AQPs have been identified to share sequence homology with calmodulin (Fotiadis *et al.*, 2002) and calmodulin binding sites have been identified within the structure of AQP6 (Rabaud *et al.*, 2009). Ca^{2+} ions enter cells through numerous pathways including voltage-gated ion channels, G-protein coupled receptors (GPCR) and their associated second messenger pathways and the transient receptor potential (TRP) families of voltage-insensitive Ca^{2+} channels. These specialist calcium channels are sensitive to a number of stimuli such as mechanical stress, temperature and a change in osmolality, with an emphasis on the latter regulating AQP trafficking (Benfenati and Ferroni, 2010).

1.6.7 Cytoskeletal proteins

When not integrated into the membrane AQPs are stored within intracellular vesicles, upon calcium activation and phosphorylation, these AQP-containing vesicles are trafficked to the cell surface along microtubules using the motor proteins dynein and kinesin (Tietz *et al.*, 2006). There is also evidence that when AQP trafficking is activated the actin cytoskeleton is remodelled and relaxed to facilitate the movement of vesicles towards the membrane (Nicchia *et al.*, 2008). Figure 1.15 shows an overview of the mechanisms the govern AQP expression and function.

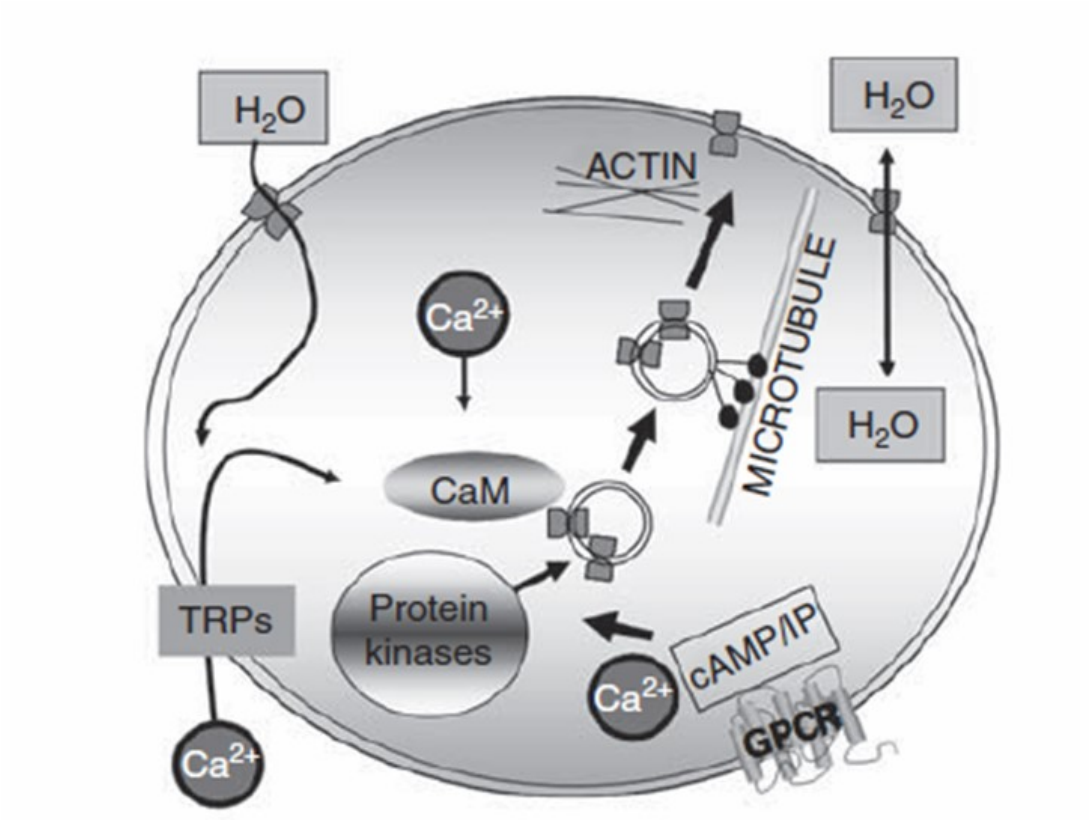

Figure 1.15. Mechanisms that regulate AQP translocation and function. Many cellular processes, such as calcium influx, phosphorylation and cytoskeletal rearrangement all contribute to the membrane expression, and therefore function, of AQPs. Transient potential receptor channels (TRPs); G-protein coupled receptor (GPCR); calmodulin (CaM); cyclic adenosine monophosphate (cAMP); inositol triphosphate (IP_3). Adapted from Conner, Bill and Conner, 2013.

1.7 Aims and objectives

The IVD is a unique tissue that is well-adapted to its role in enabling the movement of the spine and withstanding compressive forces applied by the human body. Due to its location and function, the microenvironment bestowed upon the IVD is complex. Resident cells of the IVD have adapted to their microenvironment, which enables their overall function to maintain the role of the IVD within the spine. However, it is not completely understood how IVD cells have been able to survive and adapt to their environment or how such adaptation is affected during IVD degeneration, when the microenvironment is permanently altered causing adverse cellular functions and the destruction of tissue.

The overall aim of this PhD was to test the hypothesis that because the function of NP cells is governed by many microenvironmental factors that are in-part controlled by the function of AQPs (particularly osmolality), many AQP isoforms are expressed and regulated in NP cells, contributing to their adaptation to the unique environment of the IVD, and possible dysregulation during degeneration.

1.7.1 Specific aims

1. Investigate the expression of all 13 (AQP0-12) AQP isoforms in non-degenerate and degenerate human NP tissue, to determine potential changes in expression during IVD degeneration. Investigate AQP expression in non-chondrodystrophic (NCD) and chondrodystrophic (CD) dogs to determine how the expression of AQPs is potentially altered between NC and NP cells during IVD development (Chapter 2).
2. Investigate the hyperosmotic regulation of AQP1 and 5 in human and rat NP cells and determine if TonEBP, a transcription factor essential for osmoadaptation and

matrix synthesis, is essential for the hyperosmotic regulation of AQP1 and 5 in NP cells and tissue (Chapter 3).

3. Determine how AQP4 and TRPV4 function contributes to the adaptation of human NP cells to healthy and degenerate osmotic conditions, with respect to fundamental cell functions such as the rate and change in cell volume, water permeability and calcium influx (Chapter 4).
4. Investigate how other microenvironmental factors attributed to IVD degeneration such as cytokines, pH, oxygen tension and combined 'healthy' and 'degenerate' treatments all regulate the gene expression of AQPs in human NP cells (Chapter 5).

Chapter 2: Aquaporin expression in the human and canine intervertebral disc during maturation and degeneration.

2.1 Introduction

The IVD, composed of the central gelatinous NP, surrounded by the AF and CEP, is a highly specialised tissue facilitating the biomechanical function of the spine (Urban *et al.*, 1977). Resident cells within the NP produce vast amounts of ECM that contain high concentrations of proteoglycans whose hydrophilic GAG side-chains promote water and cation retention (Ishihara *et al.*, 1997). This allows the disc to resist compressive loading and permits motion of the spine due to a high level of hydration (Maroudas, Muir and Wingham, 1969; Maroudas, 1970; Urban *et al.*, 1977; Urban, Holm and Maroudas, 1978; Kraemer, Kolditz and Gowin, 1985; Ishihara *et al.*, 1997). Therefore, in comparison to other tissues, the healthy IVD maintains a hyperosmolar environment (Ishihara *et al.*, 1997; Urban, 2002; van Dijk, Potier and Ito, 2011; Johnson, Shapiro and Risbud, 2014a). However, the hydration and osmolality of the disc is not constant (Urban and McMullin, 1985). With applied loading, between 18-25% of fluid is recycled during a diurnal cycle (McMillan, Garbutt and Adams, 1996; Urban, 2002). The increased physiological osmolality within the disc has been shown to increase matrix synthesis by NP cells compared to lower osmolalities (Neidlinger-Wilke *et al.*, 2012; O'Connell, Newman and Carapezza, 2014). This highlights that NP cells can respond to osmotic changes within the disc which may be via control of water transport (Gajghate *et al.*, 2009).

During human IVD development the NP contains populations of large, vacuolated notochordal (NC) cell clusters that are replaced by mature NP cells during ageing (Risbud, Schaer and Shapiro, 2010). Interestingly, there are differences in IVD development between different species and different groups within the same species. An example of this difference is highlighted in dogs; those classified as NCD retain NC

cells into adulthood, maintain a healthier IVD environment and suffer infrequent degeneration. Whereas CD dogs lose NC cells before adolescence and suffer early-onset IVD degeneration (Bergknut *et al.*, 2013; Smolders *et al.*, 2013). These differences in canine IVD biology enable research into how cell viability, function and differentiation are affected by the IVD environment and vice versa. To preserve their phenotype during culture, NC cells require a hyperosmolar environment (Spillekom *et al.*, 2014) and they have been shown to provide a protective and regenerative effect on NP cells when co-cultured together (de Vries *et al.*, 2016; Mehrkens *et al.*, 2017). This indicates that the behaviour of disc cells during development and maturation is, in some part, controlled by fluctuations in extracellular osmolality, and that responses may vary between NC cells and mature NP cells. IVD degeneration can also further disrupt the osmotic flux of the disc.

Around 40% of chronic LBP cases are attributed to IVD degeneration (Luoma *et al.*, 2000), which is characterised by altered biomechanical properties of the spine caused by an imbalance between anabolic and catabolic mechanisms leading to the destruction of the ECM (Freemont *et al.*, 2002; Haefeli *et al.*, 2006; Le Maitre *et al.*, 2007; Le Maitre, Freemont and Hoyland, 2007; Le Maitre *et al.*, 2015). The production of pro-inflammatory cytokines by NP cells are known to play a role in the degenerative cascade of IVD degeneration (Takahashi *et al.*, 1996; Burke *et al.*, 2002; Le Maitre, Freemont and Hoyland, 2005; Weiler *et al.*, 2005; Le Maitre, Hoyland and Freemont, 2007a; Studer *et al.*, 2011; Andrade *et al.*, 2013; Purmessur *et al.*, 2013; Risbud and Shapiro, 2014). Specifically, over-expression of cytokines leads to increased production of matrix degrading enzymes (Roberts *et al.*, 2000; Le Maitre, Freemont and Hoyland, 2004; Patel *et al.*, 2007; Hoyland, Le Maitre and Freemont, 2008; Pockert *et al.*, 2009; Zhao *et al.*,

2011), and the resulting loss of hydrophilic proteoglycans causes a decrease in IVD osmolality compared to normal physiological conditions. This could further contribute to degeneration, as under low osmolality MMP-3 expression is increased and aggrecan expression is decreased in NP cells (Wuertz *et al.*, 2007; Neidlinger-Wilke *et al.*, 2012). This further highlights the importance of regulating osmotic responses in the disc.

Aquaporins (AQPs) are a family of transmembrane channel proteins that function as selective water pores driven by osmotic gradients (Agre *et al.*, 2002). Aquaporin 1 (AQP1) was the first member to be discovered in erythrocytes and renal tubules (Denker *et al.*, 1988) and since then thirteen members have been discovered (AQP0-12). These channels are localised to tissues with roles relating to water homeostasis, cell volume regulation and structural function (Day *et al.*, 2014), and therefore may contribute towards the adaptation and responses of NC and NP cells when exposed to the fluctuating osmolality of the healthy and degenerate disc.

In human and murine discs, expression of AQP1, 2, 3 and 5 have been identified (Richardson, Knowles, Marples, *et al.*, 2008; Gajghate *et al.*, 2009; Wang and Zhu, 2011; Taş *et al.*, 2012; Johnson *et al.*, 2015; Palacio-Mancheno *et al.*, 2018). Studies have also demonstrated that expression of AQPs in NP and NCs can be regulated by physiological conditions. Hyperosmolality upregulates AQP 2 in murine NP cells (Gajghate *et al.*, 2009), and AQP3 in murine NC cells (Palacio-Mancheno *et al.*, 2018). Whilst the expression of AQP1 and AQP5 is maintained at basal levels by hypoxia-inducible factor 1 alpha (HIF-1α) in NP cells (Johnson *et al.*, 2015). Johnson *et al.*2015 also reported that AQP1 and AQP5 expression decreased in human IVDs with increasing degeneration. To date only AQP1, 2, 3 and 5 have been shown to be expressed by NP cells (Richardson, Knowles, Marples, *et al.*, 2008; Wang and Zhu, 2011; Taş *et al.*, 2012; Johnson *et al.*,

2015) and AQP1, 2 and 3 by NC cells (Gajghate *et al.*, 2009; Palacio-Mancheno *et al.*, 2018). However, no studies have investigated expression of the remaining AQP family members, and few have investigated expression in NC and NP cells and determined whether expression alters during maturation or degeneration. Hence, this study aimed to identify the expression of all thirteen AQP family members in human and canine NP tissues. Discs from NCD and CD canines were used as a model to investigate changes in AQP expression during NC to NP cell transition in IVD maturation, and adult human discs were used to investigate changes in AQP expression in NP cells during IVD degeneration.

2.2 Materials and Methods

2.2.1 Experimental Design

As only a few AQP family members have been identified in the human NP, within this study firstly qRT-PCR was utilised to identify the gene expression of all 13 AQP family members. IHC was then used to determine protein expression of AQPs that were expressed at gene level. Human NP samples used were graded histologically from non-degenerate to severely degenerate which enabled this study to identify changes in AQP expression in mature human tissue as IVD degeneration progresses. This study also aimed to determine the expression of AQPs during IVD maturation which was achieved via AQP protein expression using immunohistochemistry (IHC) in NCD and CD canine NP samples. The differences in physiology between NCD and CD canine IVD samples enables changes in AQP expression to be identified as NC cells transition into NP cells during IVD maturation. The isolation of NP cells and NC cells from human and canine IVD samples, and subsequent ICC/IF experiments enabled the localisation of AQPs within IVD cells to be investigated. The experimental design is summarised in Figure 2.1.

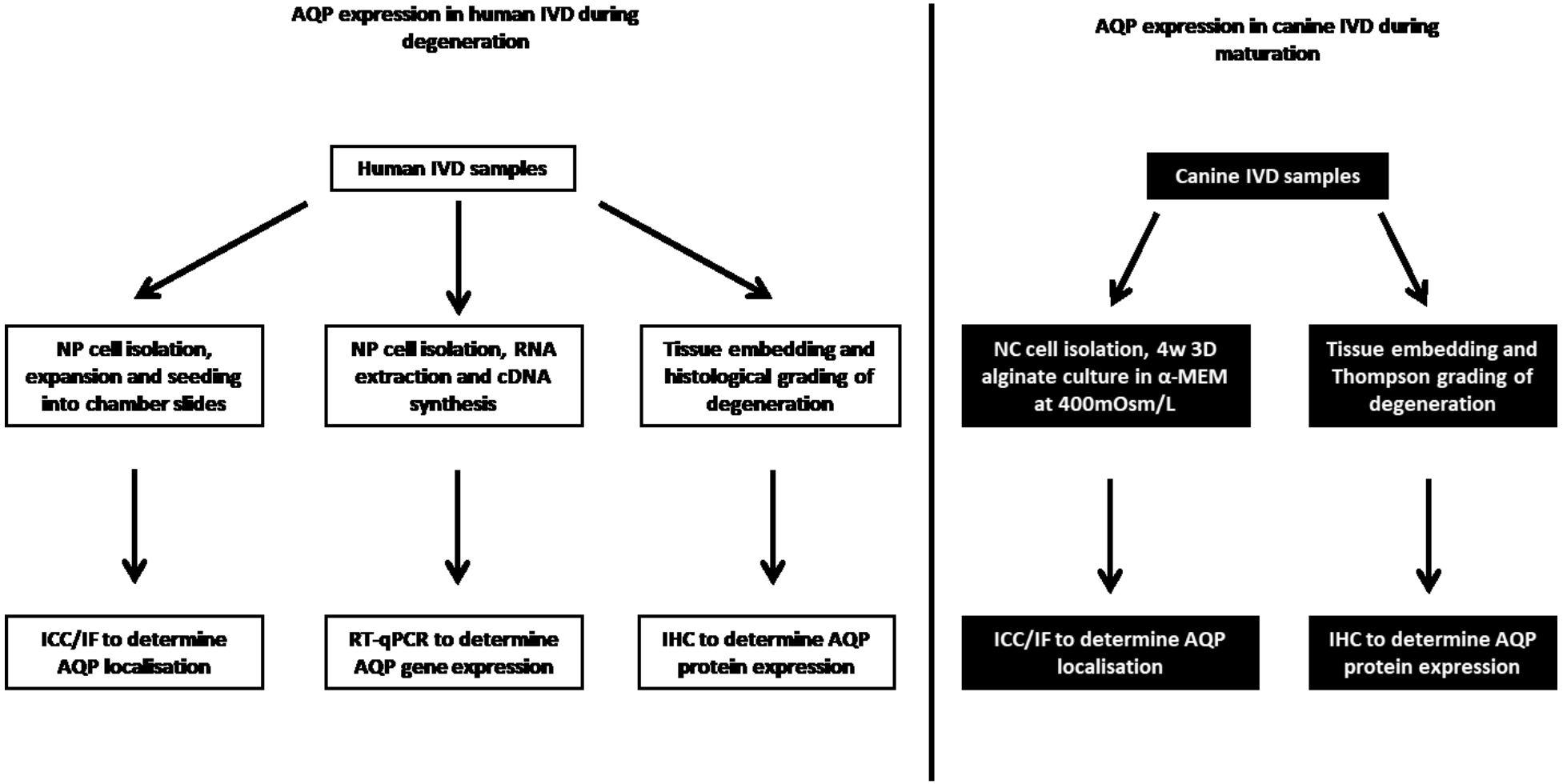

Figure 2.1. Experimental design to investigate AQP expression during IVD maturation and degeneration.

2.2.2 Human Tissue

Human IVD tissue was obtained from patients undergoing microdiscectomy surgery for the treatment of nerve root compression as a result of IVD herniation or post-mortem (PM) examination with informed consent of the patients or relatives (Sheffield Research Ethics Committee (09/H1308/70) approval form Appendix I). This study utilised 97 surgical samples from 97 individuals and 5 PM samples from 3 individuals (Appendix II).

2.2.3 Canine Tissue

Canine IVD samples (n=35) were obtained from 19 NCD and CD dogs (Thompson grade 1-5) euthanized for unrelated experiments with approval from the Ethics Committee of Animal Experiments of Utrecht University (Appendix III). The gross morphology of canine discs was categorised using a modified Thompson grading scheme (TG), specifically developed for canine IVDs, and each sample given a grade (1-5) to determine the state of disc degeneration (Bergknut *et al.*, 2013). Canine IVD samples were sent to Sheffield Hallam University after tissue processing (Section 2.2.4).

2.2.4 Tissue Processing

Human tissue was fixed in 10% (v/v) neutral buffered formalin (Leica Microsystems, Milton Keynes, UK) for 48h and embedded into paraffin wax. Following embedding, 4µm sections were cut and human IVDs histologically graded by performing haematoxylin and eosin staining. Paraffin was removed from sections using sub-X (Leica Microsystems) 3 x 5min washes. Sections were then rehydrated in IMS 3 x 5min before 1min staining with Mayer's Haematoxylin (Leica Microsystems). Sections were left to 'blue' in running tap water for 5min before subsequent staining with alcoholic eosin

(Leica Microsystems) for 1min. Sections were then dehydrated in IMS 3 x 5min and cleared in sub-X (Leica Microsystems) 3 x 5min. Sections were finally mounted with pertex (Leica Microsystems). Microscopic tissue morphology was assessed to determine the grade of degeneration for each sample based on four distinct changes to IVD morphology during degeneration: demarcation of NP tissue, presence of fissures, cell clustering and reduction of eosin staining adjacent to NP cells. Each morphological feature was scored between 0-3 (higher score is more degenerate) and added together for each sample, to give a final grade of 0-12. Samples were separated into cohorts depending on grade: non-degenerate (grade 0-4); moderately degenerate (grade 4.1-6.9) and severely degenerate (grade 7-12).

Canine lumbar spinal segment (IVD and adjacent ½ vertebral bodies) extraction was performed by Bach *et al.*, 2018. Canine vertebral columns (T11-S1) were harvested using an electric multipurpose saw (Bosch). Vertebrae were transversely transected using a band saw (EXAKT tape saw) and spinal segments were sagitally transected using a diamond band saw (EXAKT 312). Lumbar spinal segments were fixed in 4% (v/v) neutral buffered formaldehyde (Klinipath, Duiven, the Netherlands) for 14d and decalcified in PBS with 0.5M EDTA for 2 months. Spinal segments were then paraffin embedded and 5µm sections were cut (Bach *et al.*, 2018). The grade of IVD degeneration was determined using the modified TG (grade 1-5) developed by Bergknut *et al.*, 2013.

2.2.5 Investigation of AQP gene expression in directly extracted human NP cells

NP tissue from surgical and PM IVD tissue was separated from surrounding AF and CEP tissue and NP cells were isolated using 2mg/mL collagenase type I (Sigma) in DMEM for 4h at 37°C. Cells were then passed through a 40µm cell strainer (Sigma) to remove tissue debris. Following extraction, NP cells were either used for direct RNA

extraction or cell culture. RNA was extracted by adding trizol (Life Technologies) for 10min at RT before chloroform (Sigma) was added, samples vortexed and allowed to stand for 10min at RT before centrifugation at 12,000g for 15min at 4°C. After separation of RNA, DNA and protein layers, the upper, clear, aqueous RNA layer was collected and 500µL molecular grade isopropanol added (Sigma) for ≥1 hour at -80°C to precipitate RNA. Subsequently, RNA was eluted and DNase removed using RNeasy® mini clean-up kit (74204, Qiagen, Manchester, UK) as per the manufacturer's instructions. RNA samples were incubated at 60°C for 5 minutes prior to adding 36µL reverse transcriptase mastermix per 14µL RNA sample (Table 2.1).

Component	Amount per reaction (µL)
dNTPs	1.5
Random hexamers	1.0
Bioscript 5x RT buffer	5.0
Bioscript RT enzyme	0.5
RNase free H_2O	28.0

Table 2.3. Reverse transcriptase master mix. Per 14µL RNA sample, 36µL complete mastermix is added. dNTPs, Bioscript 5x RT buffer and Bioscript RT enzyme all purchased from Bioline. Random hexamers and RNase free H_2O purchased from Life Technologies.

Samples were incubated at 42°C for 1 hour, to synthesise cDNA, followed by 10 minutes at 80°C to denature the MMLV reverse transcriptase in Bioscript RT enzyme (Bioline). Expression of target genes: AQP0-12 together with housekeeping genes: glyceraldehyde-3-phosphate dehydrogenase (GAPDH) and 18S rRNA (18S), was investigated using quantitative real-time polymerase chain reaction (qRT-PCR) employing pre-designed Taqman™ gene expression assays (Life Technologies). A volume

of 2µL cDNA sample, per well, was added in duplicate into 96-well FAST PCR plates (Life Technologies), qRT-PCR mastermix was prepared (Table 2.2), and 8µL was added per well.

Component	Amount (µL)
Taqman™ gene expression assay	0.5
2x Taqman™ fast mastermix	5.0
Sterile deionised H_2O	2.5

Table 4.2. qRT-PCR mastermix. 8µL of complete mastermix were added to 2µL cDNA samples. Both Taqman™ gene expression assays and 2x Taqman™ fast mastermix were purchased from Life Technologies.

Plates were sealed with MicroAmp™ optical adhesive film (Life Technologies). Expression of target genes was determined using a QuantStudio 3 real time PCR machine (Life Technologies). Fast programme was used where the temperature was first ramped up to 95°C for 10min, to activate Taq polymerase, followed by 50 cycles of denaturing at 95°C for 1sec and subsequent annealing and extension at 60°C for 20sec. qRT-PCR was conducted on 19 non-degenerate samples (grade ≤4), 13 moderately degenerate samples (grade 4.1-6.9), 38 severely degenerate samples (grade 7-12) and 32 samples with evidence of cell infiltration identified histologically (Appendix II). Results were analysed using the $2^{-\Delta Ct}$ method (Livak and Schmittgen, 2001) and presented as relative gene expression normalised to the average C_T of GAPDH and 18S. Both housekeeping genes used in this study have been previously shown to be stably expressed, using geNorm algorithm, in human IVD samples across all grades of degeneration (Phillips *et al.*, 2015).

2.2.6 Isolation and culture of NCs from Canine discs

NC cells were isolated from spines of six mongrel dogs (mean age 1.4 years; mean weight 23kg), performed by Spillekom *et al.*, 2014, euthanized for unrelated experiments and made available for other research, which is the policy of the Animal Welfare and Ethics Committee of Utrecht University. NP material was collected from IVDs within 6h PM. NP tissue from each dog was pooled and digested in 0.1% (w/v) pronase (Sigma-Aldrich) for 45min and 0.1% (w/v) collagenase II (Sigma-Aldrich) overnight. NC cells were then collected by filtering through a 40µm cell strainer, which NC cells cannot pass through and remain on the filter. Cell strainers were then reverse rinsed with DMEM/F12 (Invitrogen) containing 10% (v/v) FCS (PAA Laboratories) and 1% (v/v) P/S (PAA Laboratories) to collect NC cells. After centrifugation at 300g for 5min, NC cell pellets were resuspended in 100% FCS (PAA Laboratories); 24.4 ± 0.9 x 10^6 (mean ± SD) live NC cells were recovered per dog (Spillekom *et al.*, 2014). Cells were encapsulated in 2.4% (w/v) sterilised alginate solution (Sigma-Aldrich) with a final cell density of 3 x 10^6 cells/mL. The alginate/cell suspension was gently pressed through a 26-gauge needle into 102mM $CaCl_2$ (Sigma-Aldrich) and 10mM HEPES (Sigma-Aldrich) to form solid, cell-encapsulated, beads. Alginate beads were cultured in 24-well plates (~6 beads/well). Beads were cultured in 1mL α-MEM (Invitrogen) supplemented with 10% (v/v) FCS (PAA Laboratories) and 1% (v/v) P/S (PAA Laboratories) for 28d at 37°C, 5% (v/v) CO_2. Media osmolarity was raised to 400mOsm/L by adding 1% (w/v) 5M NaCl (Merck) and 1% (w/v) 0.4M KCl (Sigma-Aldrich), before the start of culture. Media was replaced every 3d. These culture conditions were used as they allow the retention of the NC cell phenotype in culture (Spillekom *et al.*, 2014). After culture duration beads were fixed in 10% (v/v) neutral buffered formalin (Leica Microsystems) and embedded into paraffin wax. NC cell extraction, encapsulation into alginate beads, cell culture, fixation

and paraffin embedding were all performed by Spillekom *et al.*, 2014. Four µm sections were cut and used in immunofluorescence experiments (section 2.2.8).

2.2.7 Immunohistochemistry

After identifying which AQPs were expressed at gene level in directly extracted human NP cells, investigations into AQP protein expression in human and canine NP tissue were performed. Thirty human tissue samples were selected that contained both NP and AF tissue and which had been histologically graded; non-degenerate tissue (grade 0-4) (n=10), moderately degenerate tissue (grade 4.1-6.9) (n=10) and severely degenerate tissue (grade 7-12) (n=10) (Appendix II). Thirty-five canine tissue samples were selected to represent TG 1-5; TG 1 (n=8), TG2 (n=7), TG 3 (n=8), TG4 (n=6) and TG5 (n=6) (Appendix III). IHC was conducted to investigate the protein expression of AQP0, 2, 3, 4, 6, 7 and 9 in human and AQP0-7 and 9 in canine IVD tissues. Tissue sections were dewaxed in sub-X (Leica Microsystems) 3 x 5min and rehydrated in IMS 3 x 5min. Endogenous peroxidases were blocked in IMS containing 3% (v/v) H_2O_2 (Sigma-Aldrich) for 30min at RT. Samples were washed 1 x 5min in H_2O and then 2 x 5min in 1x tris-buffered saline (TBS) which was diluted 1:10 with H_2O from 10x TBS stock (Table 2.3).

Component	Concentration (mM)
Tris	200
NaCl	1500
pH 7.5	-

Table 2.3. 10x TBS composition. Diluted 1:10 with H_2O to produce 1x TBS working solution. All reagents purchased from Sigma-Aldrich.

Antigen retrieval methods were then performed. During heat antigen retrieval, slides were immersed in heat antigen retrieval buffer (50mM Tris, pH9.5, pre-heated to 60°C), irradiated for 5min at 40% power in an 800W microwave oven (Sanyo), left to stand at RT for 1min, before being irradiated at 20% power for 5min. Slides were then cooled at RT for 15min. If enzyme antigen retrieval was required, slides were immersed in 300mL enzyme antigen retrieval buffer (Table 2.5) for 30min at 37°C.

Component	Concentration
TBS (all other components diluted in)	1x
$CaCl_2$	0.1% (w/v)
α-chymotrypsin	0.01% (w/v)
pre-heated to 37°C	-

Table 2.4. Enzyme antigen retrieval buffer composition. $CaCl_2$ and α-chymotrypsin purchased from Sigma-Aldrich.

Slides were washed in 1x TBS 3 x 5min and then non-specific antibody-protein interactions were blocked in 1% (w/v) BSA (Sigma, UK) in 1x TBS with either 25% (w/v) rabbit or goat serum (Abcam) (matched to the host species of the secondary antibody) to neutralise secondary antibody-host interactions (Human samples Table 2.6, canine

samples Table 2.7). Blocking was performed in a humidified box for 1h at RT. Excess blocking solution was removed and slides were incubated with primary antibodies diluted in 1% (w/v) BSA in 1x TBS (Human samples Table 2.6, canine samples Table 2.7). IgG controls (Abcam) were used in place of primary antibodies at an equal protein concentration.

Target antibody	Clonality	Optimal dilution	Antigen retrieval	Secondary antibody	Serum block
AQP0 (ab134695)	Rabbit polyclonal	1/200	Enzyme	Goat anti rabbit	Goat
AQP2 (ab85876)	Rabbit polyclonal	1/400	None	Goat anti rabbit	Goat
AQP3 (ab125219)	Rabbit polyclonal	1/1600	Enzyme	Goat anti rabbit	Goat
AQP4 (ab9512)	Mouse monoclonal	1/200	Enzyme	Rabbit anti mouse	Rabbit
AQP6 (ab191061)	Rabbit polyclonal	1/200	Enzyme	Goat anti rabbit	Goat
AQP7 (ab85907)	Rabbit polyclonal	1/100	Enzyme	Goat anti rabbit	Goat
AQP9 (ab85910)	Rabbit polyclonal	1/400	Enzyme	Goat anti rabbit	Goat

Table 2.5. Antibody and blocking information used for IHC on human IVD tissue. All antibodies diluted in 1% (w/v) BSA in 1x TBS. All antibodies and serum purchased from Abcam. ab6720 (goat anti rabbit) and ab7074 (rabbit anti mouse) secondary antibodies at 1/500 dilution were used.

Target antibody	Clonality	Optimal dilution	Antigen retrieval	Secondary antibody	Serum block
AQP0 (ab134695)	Rabbit polyclonal	1/100	Enzyme	Goat anti rabbit	Goat
AQP1 (ab15080	Rabbit polyclonal	1/400	None	Goat anti rabbit	Goat
AQP2 (ab85876)	Rabbit polyclonal	1/400	Enzyme	Goat anti rabbit	Goat
AQP3 (ab125219)	Rabbit polyclonal	1/400	Enzyme	Goat anti rabbit	Goat
AQP4 (ab9512)	Mouse monoclonal	1/100	Heat	Rabbit anti mouse	Mouse
AQP5 (ab92320)	Rabbit monoclonal	1/100	Heat	Goat anti rabbit	Goat
AQP6 (ab191061)	Rabbit polyclonal	1/100	Enzyme	Goat anti rabbit	Goat
AQP7 (ab85907)	Rabbit polyclonal	1/100	Enzyme	Goat anti rabbit	Goat
AQP9 (ab85910)	Rabbit polyclonal	1/200	None	Goat anti rabbit	Goat

Table 2.6. Antibody and blocking information used for IHC on canine IVD tissue. All antibodies diluted in 1% (w/v) BSA in 1x TBS. All antibodies and serum purchased from Abcam. ab6720 (goat anti rabbit) and ab7074 (rabbit anti mouse) secondary antibodies at 1/500 dilution were used.

After washing in 1x TBS 3 x 5min, slides were incubated with 1:500 dilution of biotinylated secondary antibody (Abcam), diluted in 1% (w/v) BSA in 1x TBS, for 30min at RT. Slides were washed with 1x TBS 3 x 5min and secondary antibody binding was detected by adding ABC elite reagent (Vector Laboratories, UK) for 30min at RT. After washing with 1x TBS 3 x 5min, slides were incubated with 0.08% (v/v) H_2O_2 and 0.65mg/mL 3,3'-diaminobenzidine tetrahydrochloride (DAB) (Sigma-Aldrich) in 1x TBS for 20min at RT. Slides were washed in H_2O for 5min and counterstained with Mayer's haematoxylin (Leica Microsystems) for 1min before submersion into running tap water for 5min to 'blue' slides. Following, slides were dehydrated with IMS 3 x 5min, cleared with sub-X (Leica Microsystems) 3 x 5min, and finally mounted with pertex (Leica Microsystems).

2.2.8 Immunofluorescence

Following extraction, human NP cells were expanded in monolayer in DMEM (Life Technologies) supplemented with 10% v/v heat inactivated FBS, 1% (v/v) P/S, 2mM glutamine (all Life Technologies), 50µg/mL amphotericin B and 50µg/mL ascorbic acid (Sigma) and maintained at 37°C in a humidified atmosphere containing 5% (v/v) CO_2. Human NP cells, at passage 2, were seeded into chamber slides (Life Technologies) at a density of $1x10^4$ cells/well and allowed to adhere overnight. Media was aspirated and cells washed with PBS before fixing with 10% (v/v) neutral buffered formalin (Leica Microsystems) for 5min at RT. Sectioned canine NC cells in alginate were dewaxed in Sub-X 3 x 5min and rehydrated in IMS 3 x 5min. Fixed human NP cells and canine alginate sections were washed in PBS for 3 x 5min and human NP cells permeabilised in PBS 1% (v/v) Triton-X100 (Sigma-Aldrich) for 5min at RT. For both human NP cells and canine samples, non-specific binding sites were blocked for 1h at RT in 1% (w/v) BSA (Sigma-

Aldrich) in PBS with either 25% (w/v) rabbit or goat serum (Abcam) (Table 2.7). Samples were incubated overnight at 4°C with either mouse monoclonal or rabbit polyclonal primary antibodies in blocking solution (Table 2.7). Mouse or rabbit IgG controls (Abcam) were used in place of primary antibodies at an equal protein concentration. After washing in 0.1% (v/v) Tween 20 (Sigma-Aldrich) in PBS (PBST), samples were incubated with a 1:500 dilution of fluorescent-conjugated secondary antibody for 1h at room temperature (Table 2.7). After 3 x 5min washes in PBST slides were mounted with diamond antifade mountant with DAPI (Life Technologies).

Target antibody/Dye	Clonality	Optimal dilution	Secondary antibody	Serum block
AQP0 (ab134695)	Rabbit polyclonal	1/100	Invitrogen A11008	Goat
AQP1 (ab15080)	Rabbit polyclonal	1/100	Invitrogen A11008	Goat
AQP2 (ab85876)	Rabbit polyclonal	1/400	Invitrogen A11008	Goat
AQP3 (ab125219)	Rabbit polyclonal	1/200	Invitrogen A11008	Goat
AQP4 (ab9512)	Mouse monoclonal	1/200	Abcam ab150117	Rabbit
AQP5 (ab92320)	Rabbit polyclonal	1/100	Invitrogen A11008	Goat
AQP6 (ab191061)	Rabbit polyclonal	1/200	Invitrogen A11008	Goat
AQP7 (ab85907)	Rabbit polyclonal	1/100	Invitrogen A11008	Goat
AQP9 (ab85910)	Rabbit polyclonal	1/400	Invitrogen A11008	Goat
β-tubulin (ab206369)	Rabbit polyclonal	1/200	n/a	n/a
Alexa Fluor™ 488 Phalloidin A12379	n/a	1/1000	n/a	n/a

Table 2.7. Antibody and blocking information used in human and canine immunofluorescence experiments. All secondary antibodies were use at 1/500 dilution. Alexa Fluor™ 488 Phalloidin was purchased from Invitrogen.

2.2.9 Image Capture and Statistical Analysis

Slides were visualised with an Olympus BX60 microscope and images captured using software programme CellSens (Olympus, Southend, UK) and MicroCapture v5.0 RTV digital camera (Q Imaging, Buckinghamshire, UK). IHC staining was represented as percentage immunopostivity following analysis of 200 NP cells per sample. Canine analysis was restricted to morphologically distinct NP tissue and the presence of NC cells was identified by positive brachyury staining and morphological features (clusters of large, vacuolated cells) within the NP on consecutive sections. Data was shown to be non-parametric, therefore proportionality tests were performed to identify differences between the proportions of samples expressing mRNA for AQPs in directly extracted cohorts ($p \leq 0.05$). Kruskall-Wallis with Dwass-Steel-Critchlow-Fligner post hoc analysis test was used to identify significant differences in immunopositivity between grades of degeneration in human and canine cohorts ($p \leq 0.05$). To determine significant differences in the AQP immunopositivity of NC cells versus NP cells in pair matched canine samples, Wilcoxon's signed ranks test was performed ($p \leq 0.05$).

2.3 Results

2.3.1 Identification of aquaporin gene expression in human NP cells

The native gene expression of all mammalian AQP family members in directly extracted NP cells was investigated using qRT-PCR, of which AQPs 0-7 and 9 were identified within human IVD tissue (Figure 2.2). AQP8 was only expressed in 4 out of 97 samples, with no trends seen across grades of degeneration (data not shown) and AQPs 10, 11 and 12 were not identified in any sample. Whilst the levels of AQP 0-7 and 9 expression did not alter significantly between grades of degeneration, significant differences were seen in terms of the proportion of samples expressing AQPs between grades of degeneration (Figure 2.2). Proportions of samples expressing AQP0, 1 and 2 were increased in moderately or severely degenerate samples compared to non-degenerate samples ($p \leq 0.05$), whilst AQP3 was decreased in moderately degenerate samples compared to severely degenerate samples ($p \leq 0.05$) (Figure 2.2). In contrast AQP9 was decreased in degenerate and infiltrated samples compared to non-degenerate samples and AQP2 and 7 in degenerate compared to moderately degenerate samples ($p \leq 0.05$) (Figure 2.2). The proportions of samples expressing AQP4, 5 and 6 did not change significantly across grades of degeneration (Figure 2.2).

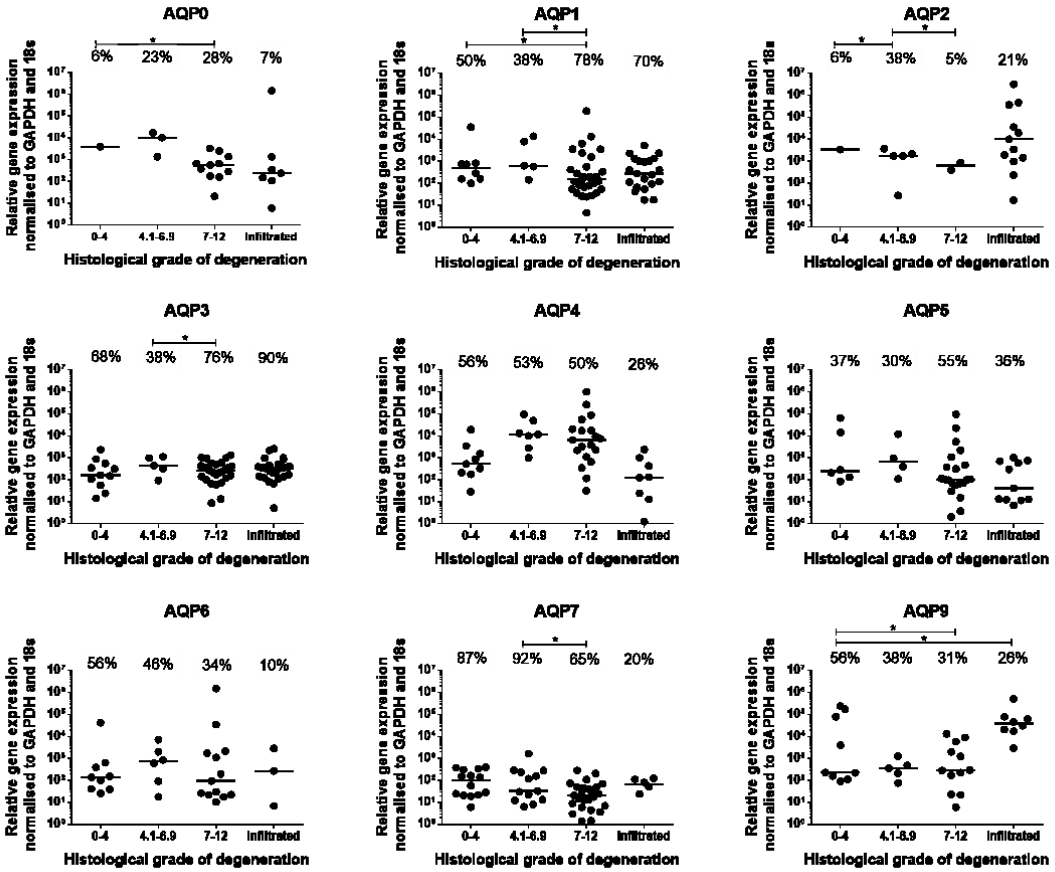

Figure 2.2. Gene expression of aquaporin family members within directly extracted human NP cells. The number of disc samples in each cohort expressing target genes is represented as percentage expression; the median value is shown by the bars. Target gene expression is separated into cohorts determined by histological grade of degeneration and evidence of infiltrating cells - grade 0-4 (non-degenerate n=16), grade 4.1-6.9 (moderately degenerate n=13), grade 7-12 (severely degenerate n=38), infiltrated *(n=30)*, total number of samples n=97. Statistical analysis was performed on proportions expressed $p \leq 0.05$.

2.3.2 Immunodetection of aquaporin proteins in human IVD tissue

The research group has previously identified AQP1 and 5 in human IVD tissues at protein levels (Johnson *et al.*, 2015), therefore AQPs 0, 2, 3, 4, 6, 7 and 9 were investigated here for their presence in human NP tissue in different histological grades of degeneration. Protein expression of all 7 AQP isoforms investigated was identified in the NP cells of human IVD tissues. However, the percentage immunopositivity for AQP0 and 3 was not significantly altered between grades of degeneration (Figure 2.3).

The percentage immunopositivity for AQP4 in human NP tissue significantly decreased in moderately and severely-degenerate discs compared to non-degenerate discs ($p \leq 0.05$) (Figure 2.4). Conversely, immunopositivity of AQP7 in severely-degenerate human NP tissue was significantly increased when compared to moderately and non-degenerate tissue ($p \leq 0.05$) (Figure 2.4). The immunopositivity of AQP6 and 9 was not significantly altered between grades of degeneration (Figure 2.4) (IgG controls, Appendix IV).

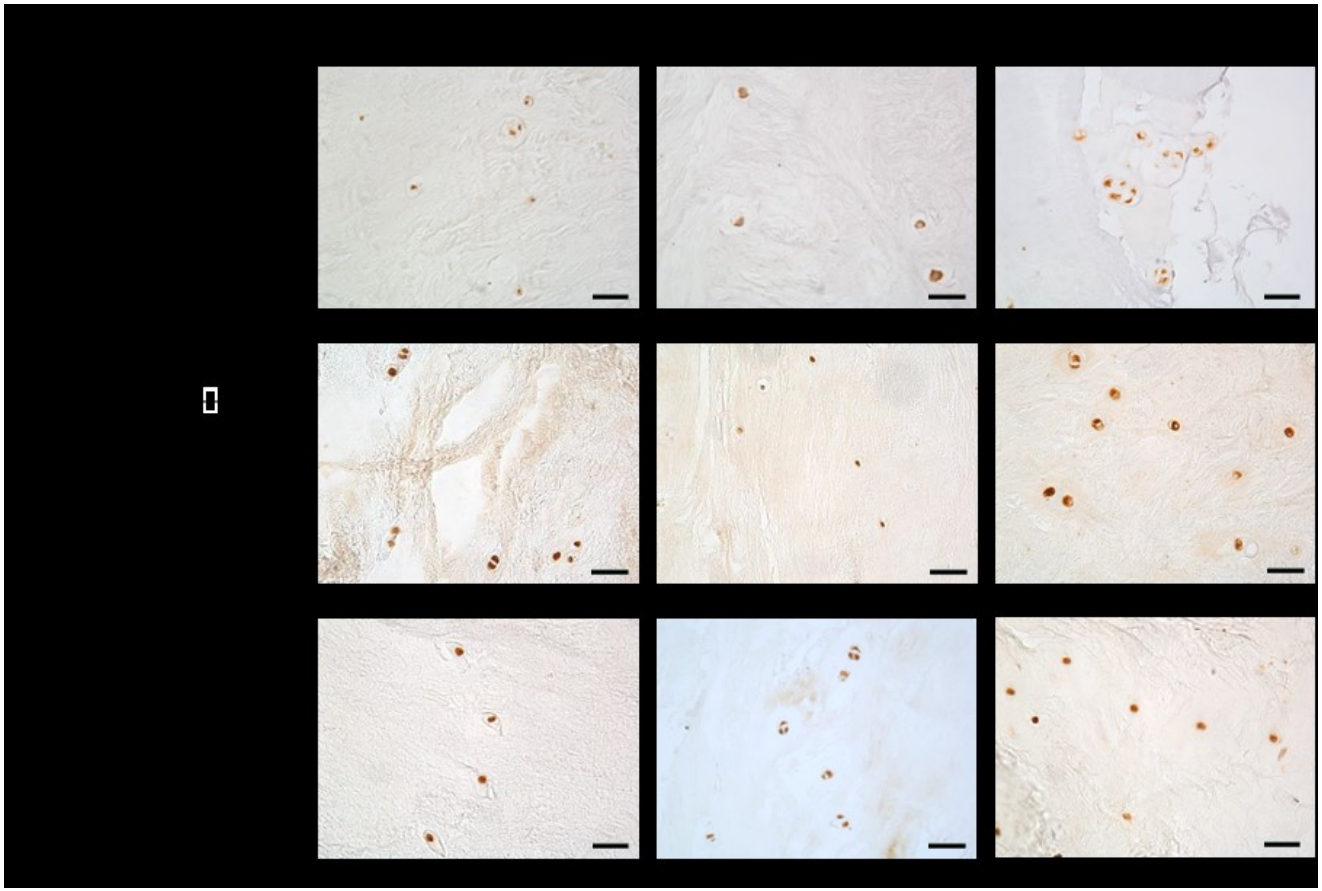

Figure 2.3. Immunopositivity of AQP0, 2 and 3 within human NP tissue. Three cohorts were investigated for the expression of AQP family members in human IVD; non-degenerate (grade 0-4, n=10), moderately degenerate (grade 4.1-6.9, n=10), severely degenerate (grade 7-12, n=10). Immunopositive cells were expressed as a percentage of total count; the median value is represented by the bars. Statistical significances in % immunopositivity determined using Kruskal-Wallis test * = $p \leq 0.05$. Scale bar 50µm.

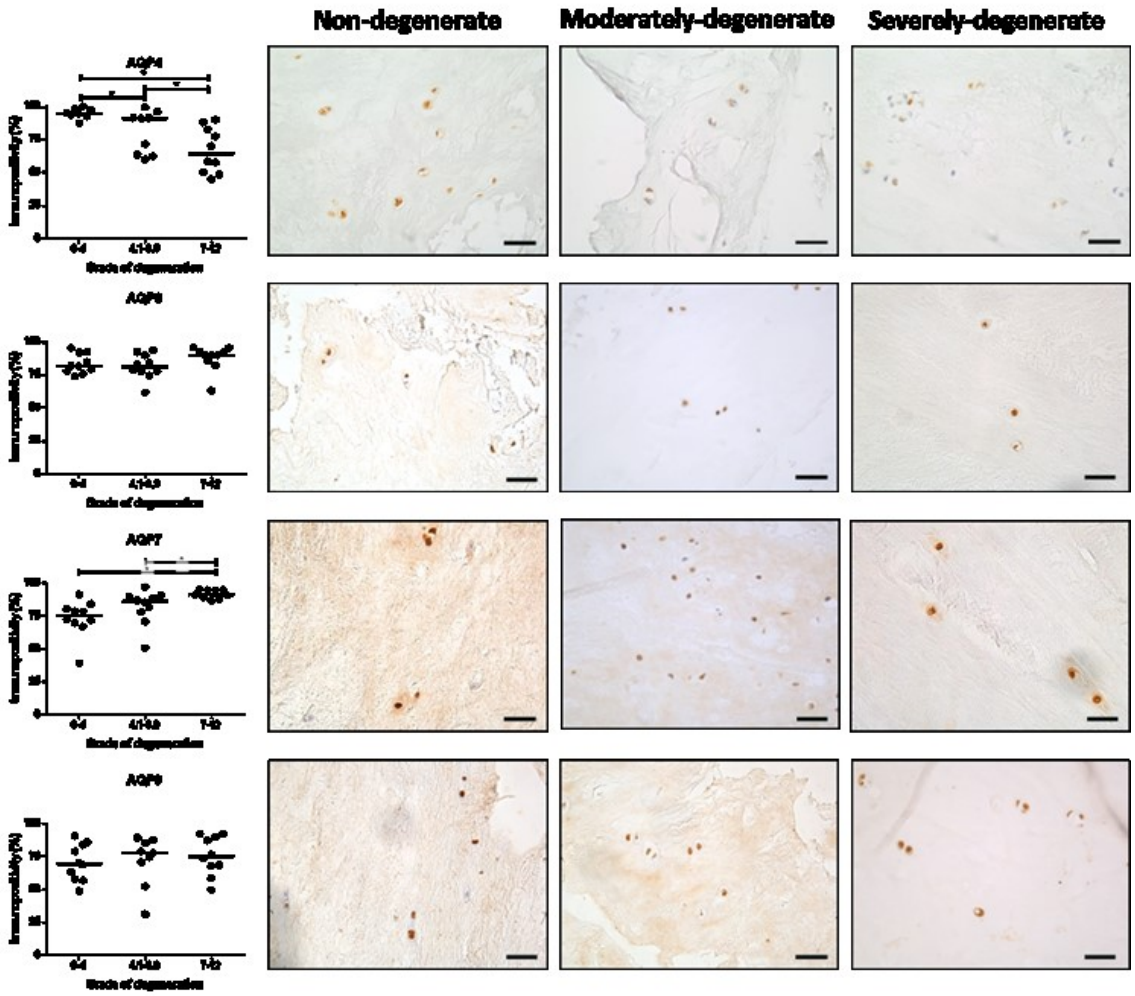

Figure 2.4. Immunopositivity of AQP4, 6, 7 and 9 within human NP tissue. Three cohorts were investigated for the expression of AQP family members in human IVD; non-degenerate (grade 0-4, n=10), moderately degenerate (grade 4.1-6.9, n=10), severely degenerate (grade 7-12, n=10). Immunopositive cells were expressed as a percentage of total count; the median value is represented by the bars. Statistical significances in % immunopositivity determined using Kruskal-Wallis test * = $p \leq 0.05$. Scale bar 50µm.

2.3.3 Aquaporin expression and localisation in cultured human NP cells

All aquaporins, which were expressed in native human NP tissue (AQPs 0- 7 and 9) were also identified in monolayer cultured human NP cells. To identify potential localisation of AQPs, expression was compared to cytoskeletal components F-actin and β-tubulin. Differential localisation was seen for AQPs in human NP cells (Figure 2.5 A), interestingly the expression of AQP4 appeared to co-localise with β-tubulin (Figure 2.5 B), potentially indicating a means of transporting AQP4 throughout the cell in response to certain stimuli.

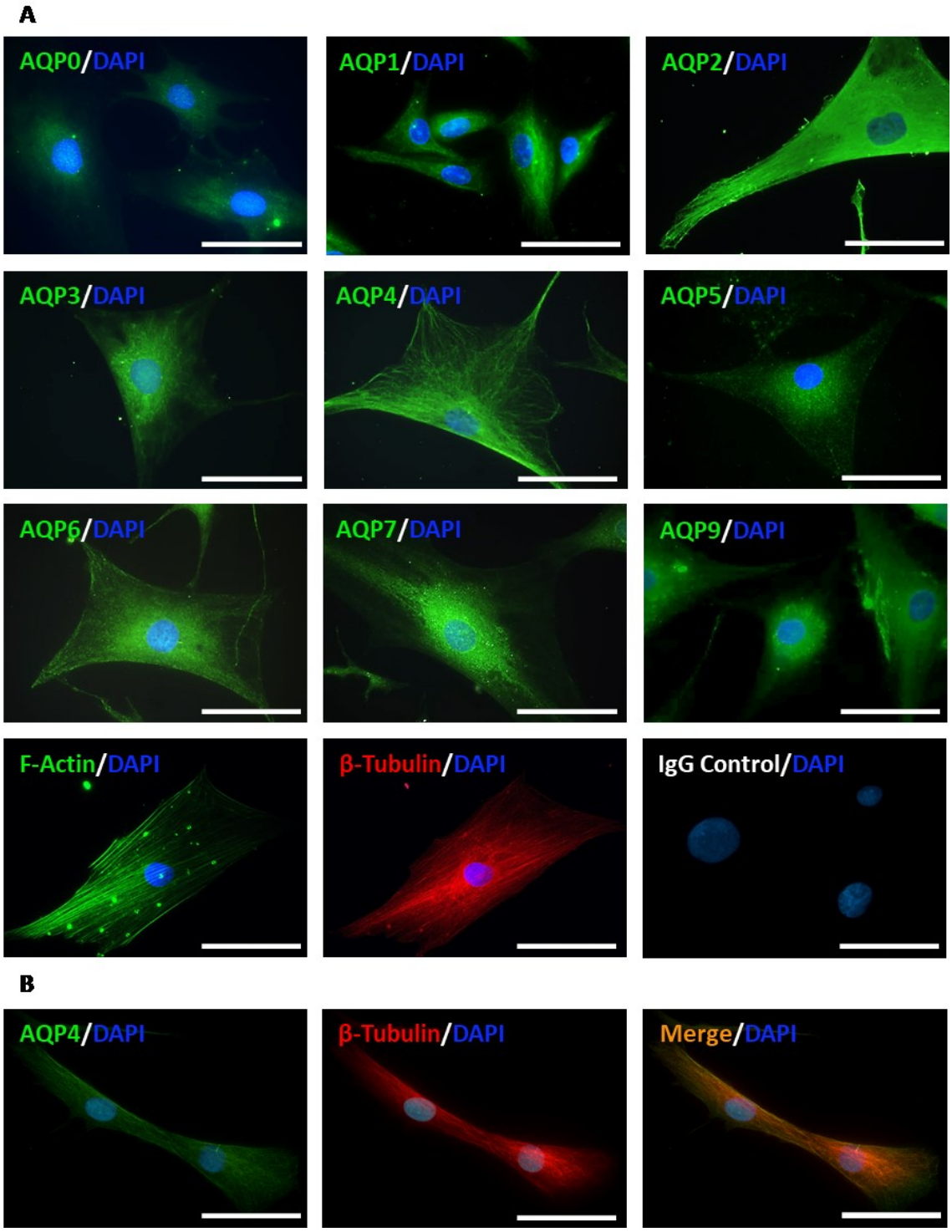

Figure 2.5. Localisation of AQPs within human NP cells. (A) All AQPs expressed in human NP tissue are also expressed in extracted human NP cells in monolayer culture at passage 2. The localisation of AQPs is compared to the expression of cytoskeletal components F-actin and β-tubulin within cells. (B) Within 2D cultured human NP cells, AQP4 co-localises with β-tubulin. Images taken on a BX60 fluorescent microscope (Olympus) at 100x objective magnification. Scale bar 20µm.

2.3.4 Aquaporin expression in canine IVD tissue

Expression of AQPs, identified in human NP tissue, was also investigated in native NC and NP cells within canine NP tissue. All AQPs investigated were expressed within both NC and NP cells in canine discs. Brachyury staining and the presence of distinct morphological features, such as clusters of large, vacuolated cells, enabled the distinction between NC and NP cells (Figure 2.6). AQP0-3 expression was maintained in NC cell clusters cultured in alginate beads for 28 days in αMEM at 400mOsm/L (Figure 2.6). Intense immunostaining was observed localised to the membranes of vacuoles within NC cell clusters, particularly for AQP2, (Figure 2.6).

IHC staining was performed on tissue to identify the immunopositivity of AQP0-3 across Thompson grades (Figure 2.6). NC cells were only observed in TG1-3 (Figure 2.6 and Figure 2.8). The number of NP cells expressing AQP2 decreased between TG1-3 when compared with TG4 ($p \leq 0.05$) (Figure 2.7), but the number of NC cells expressing AQP2 was not altered by TG (Figure 2.7). Immunopositivity of AQP0, 1 and 3 was not significantly altered by TG in both NC and NP cells (Figure 2.7). The percentage of NC cells expressing brachyury, AQP2 and 3 was significantly higher than the percentage of NP cells expressing these proteins in pair matched canine IVD samples ($p \leq 0.05$). The percentage of NC cells expressing AQP1 was significantly reduced compared to the percentage of NP cells expressing AQP1 in pair matched canine IVD samples ($p \leq 0.05$) (IgG controls, Appendix V).

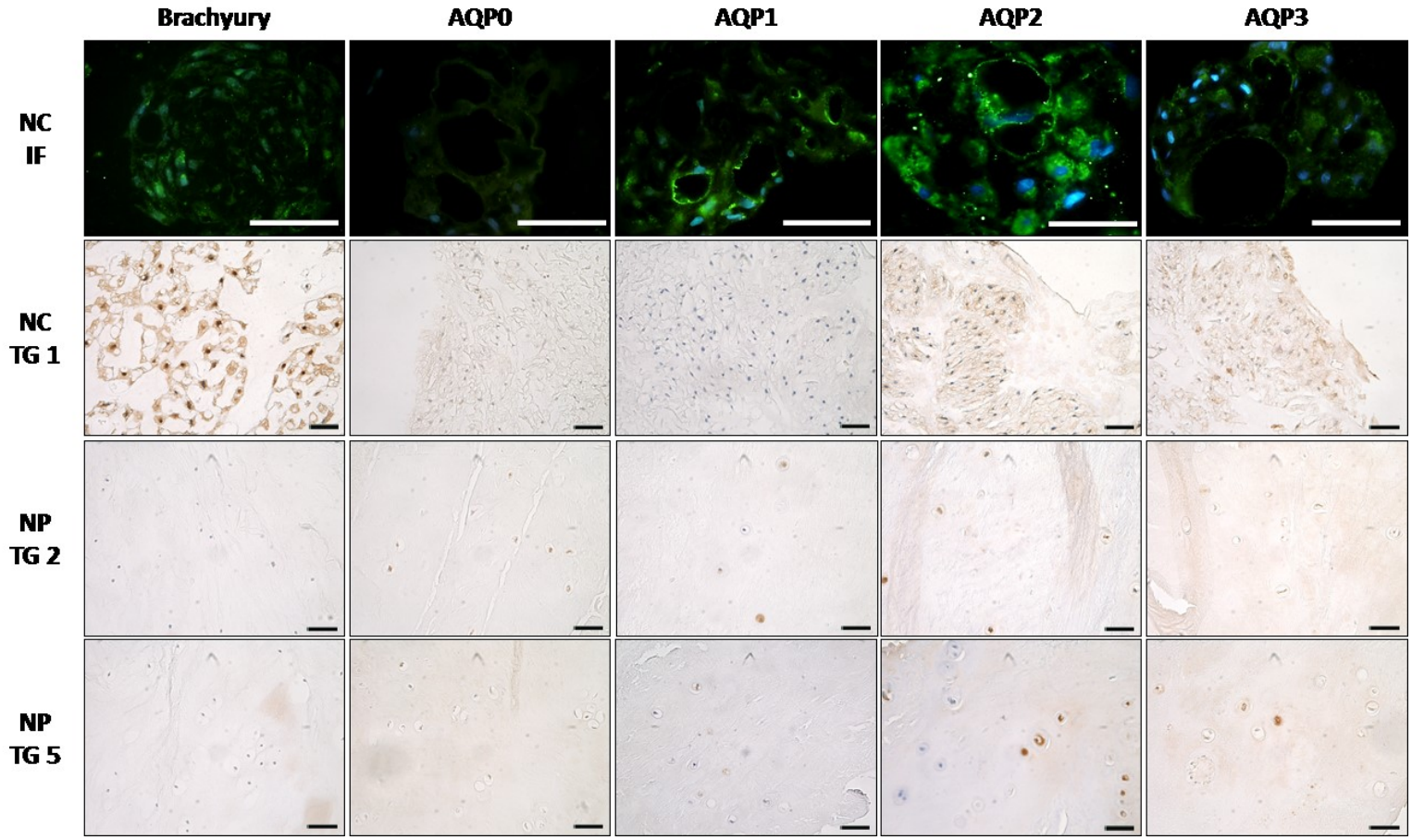

Figure 2.6. Expression and localisation of AQP0-3 in native canine IVD tissue. Immunofluorescence (IF) images show expression of AQPs in NC cell clusters after 3D culture and localisation at vacuolar-like membranes. Scale bar 20µm. IHC staining represents AQP expression in canine NC cells, at Thompson grade (TG) 1, and NP cells across TG2 and TG5. Scale bar 50µm. Brachyury staining was used as a positive marker of NC cells.

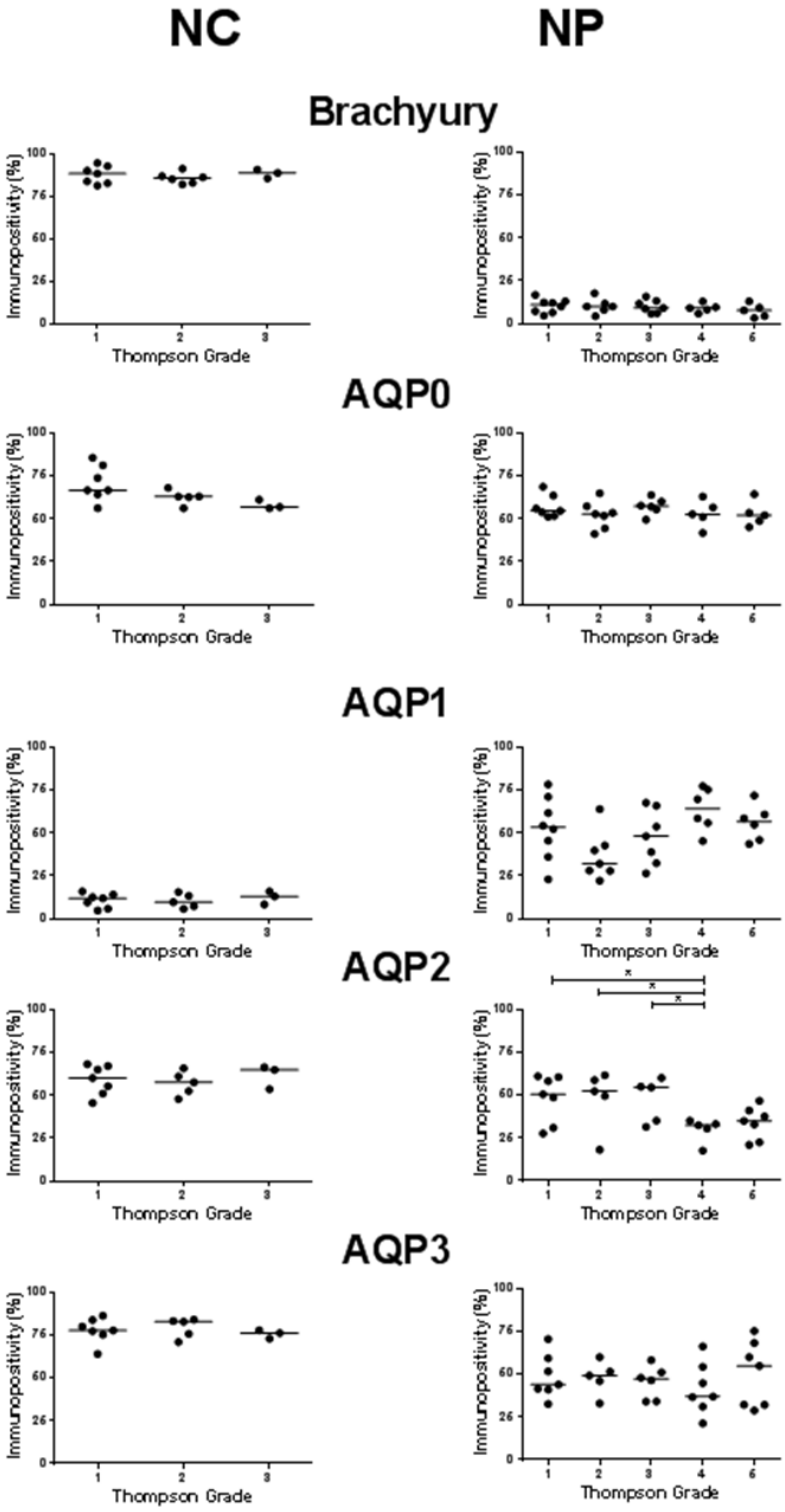

Figure 2.7. Immunopositivity of AQP1, 2, and 3 in canine NC and NP cells. Three cohorts were investigated for the expression of AQP family members in NC cells; Thompson grade (TG) 1-3, and NP cells; TG1-5. Brachyury staining was used as a positive marker of NC cells. Immunopositive cells were expressed as a percentage of total count; the median value is represented by the bars. Statistical significances in % immunopositivity determined using Kruskal-Wallis test * = $p \leq 0.05$

.

AQP4-9 expression was also maintained in NC cell clusters cultured in alginate beads for 28 days in αMEM at 400mOsm/L (Figure 2.8). Intense immunostaining was observed localised to the membranes of vacuoles within NC cell clusters, particularly for AQP5, 6 and 9 (Figure 2.8). IHC also indicated that AQP4-9 isoforms were expressed in NC and NP cells across Thompson grades (Figure 2.8). AQP4 immunopositivity in both NC and NP cells was unaffected by changes in TG in canine IVD tissue (Figure 2.9). Immunopositivity of AQP5 in canine NP cells significantly decreased from TG1 to TG4 ($p \leq 0.05$) (Figure 2.9) whilst AQP5 expression in canine NC cells remained unaffected by degeneration (Figure 2.9). As degeneration increased from TG1-2 up to TG4-5, AQP6 expression in NP cells significantly increased ($p \leq 0.05$) (Figure 2.9), however AQP6 expression in NC cell populations decreased with increasing TG from 1 to 3 ($p \leq 0.05$) (Figure 2.9). NP cell expression of AQP7 also increased from TG1-2 to TG5 ($p \leq 0.05$) (Figure 2.9), whereas AQP7 immunopostivity in NC cells remained constant across all grades of degeneration (Figure 2.9). AQP9 immunopositivity significantly decreased in NP cells between TG1-2 to TG5 ($p \leq 0.05$) (Figure 2.9) and in NC cells between grade TG1 and TG3 ($p \leq 0.05$) (Figure 2.9). The percentage of NC cells expressing AQP6 and 9 was significantly higher when compared to the percentage of NP cells expressing AQP6 and 9 in pair matched canine IVD samples ($p \leq 0.05$) (Appendix V).

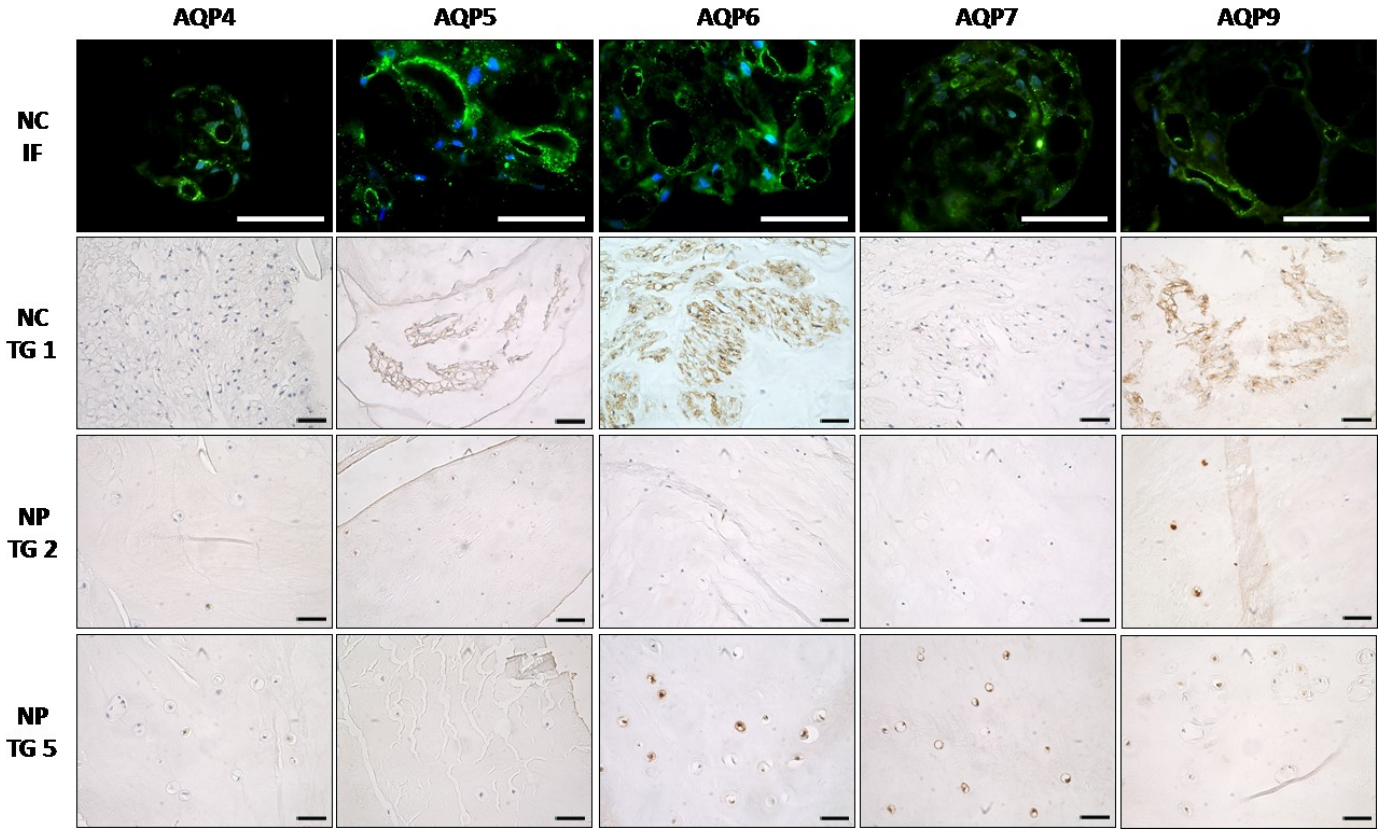

Figure 2.8. Expression and localisation of AQP4-9 in native canine IVD tissue cells. Immunofluorescence (IF) images show expression of AQPs in NC cell clusters after 3D culture and localisation at vacuolar-like membranes. Scale bar 20µm. IHC staining represents AQP expression in canine NC cells, at Thompson grade (TG) 1, and NP cells across TG2 and TG5. Scale bar 50µm.

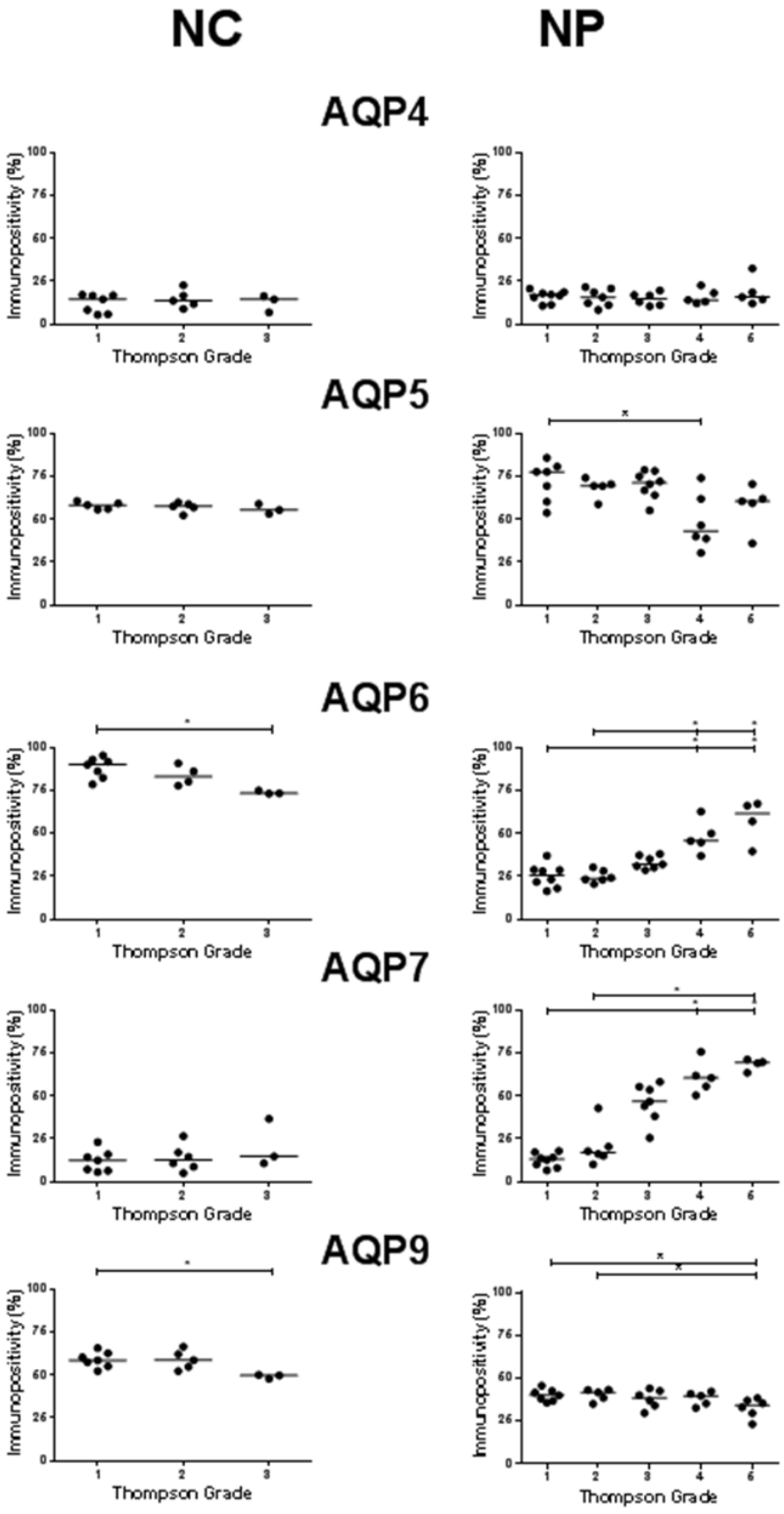

Figure 2.9. Immunopositivity of AQP4, 5 ,6 and 9 in NC and NP cells within canine IVDs. Three cohorts were investigated for the expression of AQP family members in NC cells; Thompson grade (TG) 1-3, and NP cells; TG 1-5. Immunopositive cells were expressed as a percentage of total count; the median value is represented by the bars. Statistical significances in % immunopositivity determined using Kruskal-Wallis test * = $p \leq 0.05$.

2.4 Discussion

NP cells reside within an osmotically challenging environment (Kraemer, Kolditz and Gowin, 1985; Urban, 2002; van Dijk, Potier and Ito, 2011; Johnson, Shapiro and Risbud, 2014a), where cells must be able to adapt to their environment to allow correct function. Previously AQPs 1, 2, 3 and 5 have been shown to be expressed by NP cells (Richardson *et al.*, 2008; Gajghate *et al.*, 2009; Wang and Zhu, 2011; Taş *et al.*, 2012; Johnson *et al.*, 2015), expression of AQP1, 2, and 5 are regulated by physiological conditions found in the disc such as hyperosmolality (Gajghate *et al.*, 2009) and AQP1 and 5 expression levels decreased with IVD degeneration (Johnson *et al.*, 2015). This highlights that water transport via AQPs in the disc must be tightly controlled to allow the survival and function of NP cells, and such regulation is diminished in degeneration, possibly aggravating the catabolic cascade. However, to date, no studies have investigated the expression of all AQP family members in the IVD or determined how their expression is altered with degeneration, thus it is difficult to gain a complete understanding of the roles for AQPs in the IVD. For the first time the expression of ten AQP isoforms, AQPs 0-9, in human and canine NP tissue were shown. We determined that the expression of certain AQPs is altered during IVD degeneration of humans and canines. Utilising canine discs, we were also able to investigate expression and localisation during cellular maturation and demonstrated nine AQPs were expressed in canine NC cells, which were particularly associated with vacuolar membranes, suggesting a role in water transport into vacuoles.

2.4.1 AQP expression in IVD tissues

Our results agree with studies that have shown AQP1, 2, 3 and 5 expression in NP cells (Richardson, Knowles, Marples, *et al.*, 2008; Gajghate *et al.*, 2009; Wang and Zhu, 2011; Taş *et al.*, 2012; Johnson *et al.*, 2015). However, whilst Richardson *et al*. 2008 identified that AQP1 and AQP3 were expressed within human IVD in agreement with our study, they failed to demonstrate expression of AQP2. However, in the current study both gene and protein expression of AQP2 was identified in human discs and protein in canine discs. In the earlier study (Richardson, Knowles, Marples, *et al.*, 2008) only ten PM samples from human discs were used for the identification of AQP protein expression, in contrast, here we have used a larger sample size with a total of 102 human samples to assess gene expression, and 30 surgical and PM human and 35 PM canine samples for IHC analysis. Our data is in agreement with a study by Gajghate *et al.* which demonstrated AQP2 gene and protein expression in rat and human IVD tissues (Gajghate *et al.*, 2009).

Limited AQP family members have been identified in other musculoskeletal tissues, including AQP1, 3, 4 and 9 in articular cartilage (Mobasheri *et al.*, 2004; Trujillo *et al.*, 2004; Cai *et al.*, 2017; Steinberg *et al.*, 2017; Takeuchi *et al.*, 2018), AQP1 and AQP9 in synovial tissues (Trujillo *et al.*, 2004; Nagahara *et al.*, 2010), AQP1 and 3 in osteoblasts (Mobasheri, Wray and Marples, 2005; Barron *et al.*, 2017) and AQP9 expression in osteoclasts (Aharon and Bar-Shavit, 2006; Liu *et al.*, 2009). Here, for the first-time gene expression of AQPs0, 4, 6-9 was shown in human NP tissue, although AQP8 was only expressed in a small number of samples at gene level (n=4). Furthermore we demonstrate for the first time protein expression of AQPs 0, 4, 6, 7 and 9. Together this data demonstrates NP cells express many AQPs which may play important roles in

the disc such as contributing towards water homeostasis, solute transport, cell volume regulation, cell adhesion and protein localisation (Day *et al.*, 2014; Kitchen *et al.*, 2015).

All AQPs expressed within human discs were also identified in canine discs from NCD and CD dog breeds, which were used to study AQP expression in the transition from NCs to NPs. Both NC and NP cells from canine discs expressed all AQPs investigated suggesting AQP family members are important during the development and maturation of the IVD. In canines and humans, the proportion of cells expressing AQPs and changes in their expression during degeneration differed, suggesting functions of AQPs during different stages of disc biology and within different species may vary. On the other hand, differences in sample preparation methods between human and canine samples may have resulted in the differences in immunopositivity results between species, as decalcification which was utilised for canine but not human samples, has been shown to effect IHC staining on IVD tissue previously (Binch *et al.*, 2015).

2.4.2 AQP expression during maturation of the IVD

Whilst NC and NP cells were seen to express all AQPs investigated, AQP expression was observed on higher numbers of NC cells v/s NP cells for AQPs 2, 3, 6, and 9, whilst AQP1 was seen on higher numbers of NP cells than NCs in pair matched canine discs. This may be due to differences in the disc environment, such as osmolality, nutrition, pH and mechanical loading that both NC and NP cells withstand during development, suggesting a role for AQPs in NC physiology. Of particular note IHC on native canine tissue and immunocytochemistry on cultured canine NC cells revealed AQP expression along vacuolar membranes, particularly for AQP2, 5, 6 and 9. The expression of these AQPs may be indicative of the roles vacuoles may play within NC cells. AQP5, along with AQP1 and 4, contributes to regulatory volume decrease and the

control of cell volume in response to osmotic flux, there is also evidence to suggest AQP2 is also involved (Galizia *et al.*, 2012). Therefore, AQP2 and 5 expression may indicate that vacuoles regulate NC cell responses to their hyperosmolar environment, and their decreased expression during NC to NP transition could regulate the decreased cell size seen during maturation. AQP6 expression potentially indicates that vacuoles play a role in regulating acid-base balance in NC cells. In the kidney, where AQP6 is expressed intracellularly, low pH activates the anion permeability of AQP6 (Yasui *et al.*, 1999) and increases AQP6 expression (Promeneur *et al.*, 2000). An increase in AQP6 expression in response to low pH also potentially explains the increase in AQP6 observed in canine NP cells during degeneration, where extracellular pH decreases.

2.4.3 AQP expression during degeneration of the IVD

Expression of AQP1 and 5 in the disc has been shown to be sensitive to degeneration within human IVD tissue previously (Johnson *et al.*, 2015), with levels decreasing with degeneration. Here, AQP4 protein expression was also shown to decrease during human IVD degeneration. This potentially indicates shared functions of these AQPs which, during degeneration when expression is decreased, results in a diminished ability of NP cells to control water transport and cell volume regulation as the surrounding environment becomes increasingly osmotically challenging. This decrease in AQP4 expression is of particular importance as within the AQP family, AQP4 has the fastest rate of water permeability followed by AQP1 and 5 (Yang and Verkman, 1997; Kitchen *et al.*, 2015), and these AQPs have all been implicated in the control of regulatory volume decrease when cells are exposed to hypo-osmotic stimuli (Benfenati *et al.*, 2011a; Mola *et al.*, 2016). Thus the decreased expression of AQPs 1, 4 and 5 seen

during human IVD degeneration could be a result of hypo-osmotic stimuli observed during IVD degeneration (Ishihara *et al.*, 1997).

An important response to osmotic stress is translocation of AQPs to the plasma membrane, in primary rat cortical astrocytes, HEK293 and MDCK cells AQP4 is rapidly translocated to the plasma membrane in response to osmotic changes (Mazzaferri, Costantino and Lefrancois, 2013; Kitchen *et al.*, 2015). This translocation is governed by many mechanisms including vesicle transport along microtubules (Mazzaferri, Costantino and Lefrancois, 2013; Kitchen *et al.*, 2015). In human NP cells we observed that AQP4 co-localised with β-tubulin, a major component of microtubules, indicating AQP4 is possibly translocated between the cytosol and plasma membrane in order to respond and adapt to changes in the extracellular osmolality.

In contrast to the decrease seen in AQP1, 4 and 5 with degeneration, the number of NP cells expressing AQP2 and AQP7 increased in moderate or severely degenerate human IVD tissues respectively. This may indicate that AQP2 and 7 are regulated by different underlying mechanisms and have different functions compared to AQP1, 4 and 5. The increase in the number of cells expressing these proteins may be a consequence of degeneration or a potential repair mechanism employed by NP cells to re-establish homeostasis dysregulated during degeneration. As the disc degenerates, the micro-environment in which cells reside, irreversibly changes, such as a decrease in disc pH (Urban, 2002). This potentially explains the increase in AQP2 protein expression, as AQP2 expression is increased in the rat kidney when exposed to lowered pH (Amlal, Sheriff and Soleimani, 2004). Immunopositivity of AQP3, 6 and 9 in human IVD tissue was not altered during degeneration, yet the majority of NP cells in native IVD tissue expressed all three AQPs, potentially indicating roles which may not be sensitive to IVD

degeneration. Within canine discs some effects mirrored the effects seen in human discs; however, some AQPs showed differential responses between species that remain to be explored. AQP5 immunopositivity decreased (Johnson *et al.*, 2015) and AQP7 immunopositivity increased in human and canine NP cells with IVD degeneration.

2.4.4 *Conclusion*

As the disc is an osmotically challenged tissue which is further altered during degeneration, NP cells must employ several tightly regulated mechanisms to survive and function within their unique environment. We postulate that the expression of numerous AQP family members in the disc highlights the importance of maintaining intricate control over regulation of water transport and cell volume in NP cells (Figure 2.10). The increased proportion of NP cells expressing AQP2 and AQP7 during degeneration may reflect consequences or potential repair mechanisms employed by the disc as NP cells lose their ability to adapt to the degenerate hypo-osmolar environment, which is identified by the loss of AQP1, AQP4 and AQP5 expression during degeneration. The expression of numerous AQPs within the disc may highlight the importance of controlling water and solute transport in relation to maintaining NC and NP cell function. As yet the actual roles of AQPs within disc maturation and degeneration are unknown; further investigation is warranted to identify mechanisms of regulation and functions of AQPs to elucidate the true action of these transmembrane channel proteins on the overall behaviour and health of the disc.

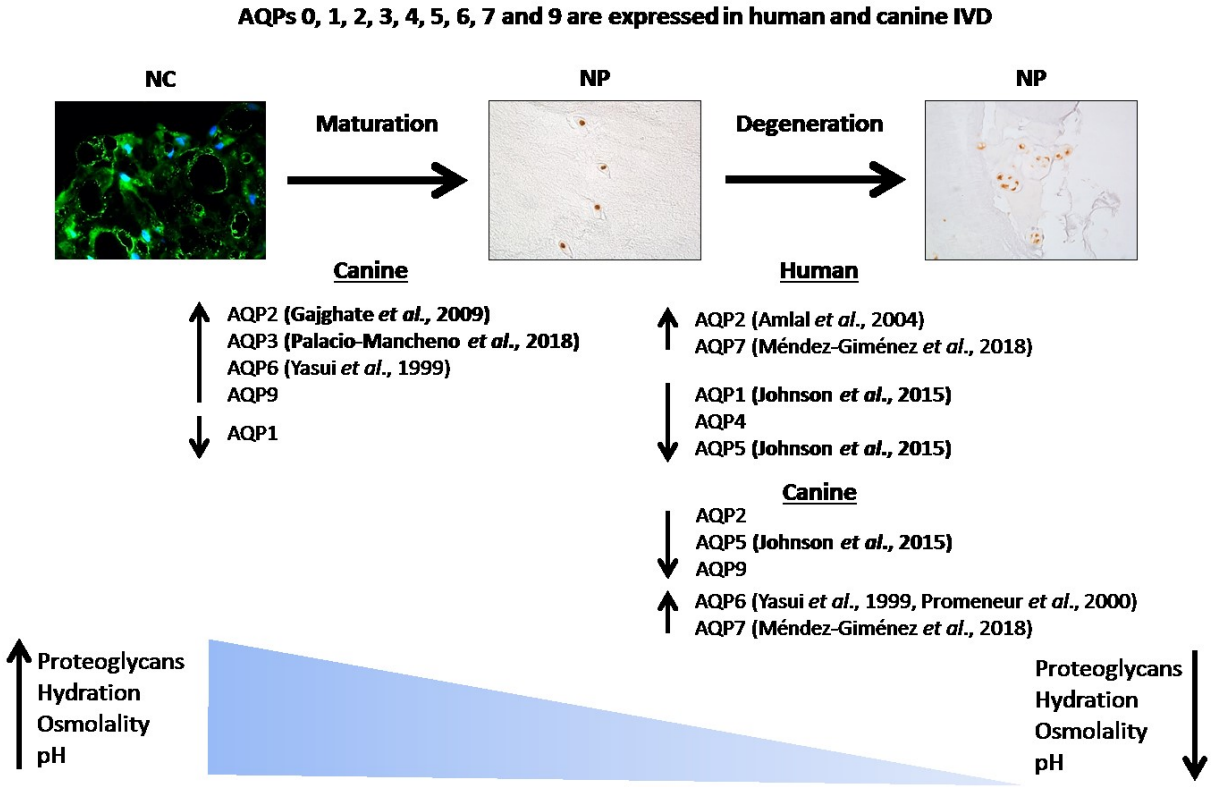

Figure 2.10. How AQP expression is altered during canine IVD maturation and degeneration and human IVD degeneration. AQPs are present in both NC cells during maturation and NP cells during degeneration. Alterations in AQP expression and the disc environment are shown as ↓=decrease and ↑=increase. References indicate where similar changes in expression, due to changes in the extracellular environment, have been observed. References in bold indicate where AQP expression in the disc has been investigated.

Chapter 3: Hyperosmotic regulation of AQP1 and 5 in nucleus pulposus cells.

3.1 Introduction

Many factors contribute to the correct function of the NP. The environment in which NP cells reside plays a big role in the physiology of the tissue; the correct biomechanical loading, pH, nutrition, O_2 tension and adaptation to a diurnal cycle all allow NP tissues to function correctly (McMillan, Garbutt and Adams, 1996; Ishihara *et al.*, 1997; Urban, 2002; Bibby *et al.*, 2005; Hartman *et al.*, 2018). As the NP has a high content of negatively charged, hydrophilic GAGs within its matrix, allowing water and cation retention, this provides a high osmotic pressure environment within the disc (Ishihara *et al.*, 1997; van Dijk, Potier and Ito, 2011; Johnson, Shapiro and Risbud, 2014a). This physiologically hyperosmotic environment has been shown to stimulate matrix synthesis (van Dijk, Potier and Ito, 2011; Neidlinger-Wilke *et al.*, 2012; O'Connell, Newman and Carapezza, 2014), providing evidence that NP cells have adapted to the higher osmolality and hydrostatic pressure imposed on them by the NP tissue environment. However, osmotic stress (both hyper- and hypo-) is known to cause many disruptions to cellular activity such as elevation of ROS, cytoskeletal rearrangement, inhibition of transcription and translation, damage to DNA and proteins and eventually cell death (Burg, Ferraris and Dmitrieva, 2007). So how have NP cells been able to adapt to this constantly changing hyperosmotic environment?

3.1.1 TonEBP

There are many cell signalling pathways that are activated during osmotic stress including p38 MAPK (Han *et al.*, 1994), Jnk (Galcheva-Gargova *et al.*, 1994) and ERK1/2 (Burg, Kwon and Kültz, 1996), but one of the most well-known, classical pathways, which many tissues and cell types employ to counter osmotic stress involves the function of

tonicity enhancer binding protein (TonEBP). TonEBP, is also known as nuclear factor of activated T cells 5 (NFAT5), is part of a family of transcription factors (NFAT1-5) that contains rel homology domains (DNA binding domains), but unlike NFAT1-4, TonEBP function is independent of calcineurin (a calcium-dependent serine/threonine phosphatase that activates T cells) and activator protein 1 (AP-1 ,a transcription factor controlling cellular processes such as growth and differentiation) (Macián, López-Rodríguez and Rao, 2001). Within many tissues TonEBP has the role of hyperosmotic adaptation; the exact mechanisms by which cells sense osmotic shifts is unknown, but studies suggest that integrins $\alpha_6\beta_4$ (Jauliac *et al.*, 2002) and $\alpha_1\beta_1$ (Moeckel *et al.*, 2006), a guanine nucleotide exchange factor, Brx (also known as A-kinase anchoring protein 13 (AKAP13)) (Kino *et al.*, 2009), and biomechanical stretching (Scherer *et al.*, 2014) may all activate TonEBP signalling. When cells are exposed to hyperosmotic stimuli, TonEBP is translocated into the nucleus. In the nucleus it forms homodimers and binds to tonicity response elements (TonE) on target genes, via rel homology domains, causing their upregulation (Miyakawa *et al.*, 1999). These well-described target genes include Sodium myo-inositol transporter (SMIT), aldose reductase (AR), Betaine-γ-amino butyric acid transporter (BGT1) and taurine transporter (TauT), that all facilitate the exchange of charged ions within cells for small non-ionic osmolytes (Miyakawa *et al.*, 1999; Burg, Ferraris and Dmitrieva, 2007; Halterman, Kwon and Wamhoff, 2012; Johnson, Shapiro and Risbud, 2014a) (Figure 3.1). Thus, restoring the osmotic pressure across the cell membrane and enabling cellular adaptation to the hyperosmotic extracellular environment.

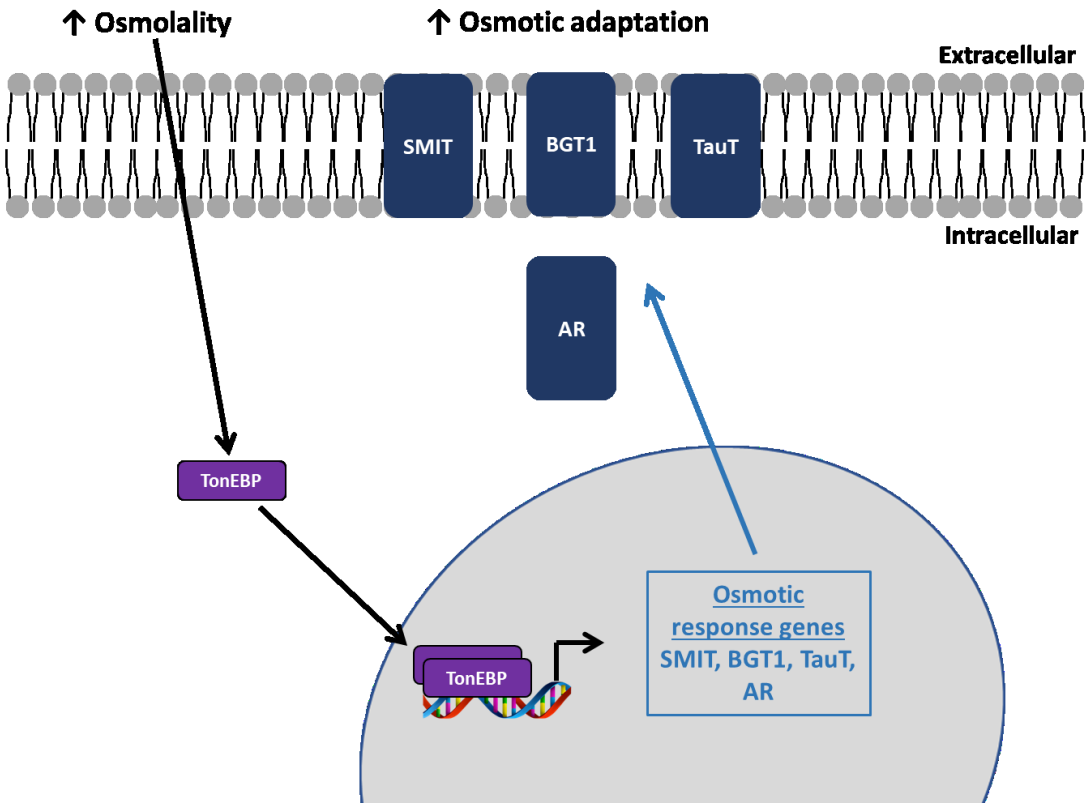

Figure 3.1. The function of TonEBP. Increased extracellular osmolality are sensed by the cell. These mechanisms activate TonEBP in the cytosol by phosphorylation. Activated TonEBP is translocated to the nucleus where it dimerises and binds to tonicity response elements (TonE) upstream of osmotic response genes. The expression of osmotic response genes (SMIT, BGT1, TauT and AR) is upregulated, enabling the cell to produce and transport non-ionic osmolytes across the cell membrane, restoring the osmotic balance in and out of the cell. Thereby controlling the cellular adaptation to hyperosmolality.

TonEBP has an emerging role in the function of the IVD and similar tissues. It has been shown that TonEBP is a key regulator of aggrecan (Tsai *et al.*, 2006) and the synthesis of chondroitin sulphate sidechains (Hiyama *et al.*, 2009) in NP cells. Whilst in the chondrogenic ATDC5 cell line, TonEBP was involved in the hyperosmotic induction of sox9, collagen type II and X, Runx2 and aggrecan (Caron *et al.*, 2013). As TonEBP allows NP cells to adapt to their hyperosmotic surroundings, regulate the matrix composition and osmotic status of the NP, it is important to determine what other pathways are potentially regulated by TonEBP to provide the correct function to the IVD.

3.1.2 Osmotic regulation of AQP expression

Many AQPs are present within NP tissue (Chapter 2). Their presence suggests that water transport is tightly controlled and very important for NP cell function. AQP1 and 5 expression in human NP tissue has previously been shown to decrease during IVD degeneration (Johnson *et al.*, 2015). The basal expression levels of AQP1 and 5 in NP cells is regulated by HIF-1α (Johnson *et al.*, 2015) which does not explain their decreased expression, therefore other degenerative changes may be implicated in the dysregulation of AQP1 and 5. AQP expression across many tissues and cell types has been shown to be regulated by alterations in extracellular osmolality, with many pathways implicated (Table 3.1), however only one study to date has investigated this within the IVD, which showed increased AQP2 expression (Gajghate *et al.*, 2009).

	Tissue/cell type	AQP	Treatment	Regulation	Pathways	References
Bladder	Rat bladder	AQP1	Hyperosmotic	–		(Spector *et al.*, 2002)
	Rat bladder	AQP2, 3	Hyperosmotic	↑		(Spector *et al.*, 2002)
	Human urothelium	AQP3, 9	Hyperosmotic	↑		(Rubenwolf *et al.*, 2012)
	Human urothelium	AQP4, 7	Hyperosmotic	–		(Rubenwolf *et al.*, 2012)
Brain	Primary rat astrocytes	AQP4, 9	Hyperosmotic	↑	p38	(Arima *et al.*, 2003)
	Rat brain	AQP4	Hyperosmotic	↑		(Mesbah-Benmessaoud *et al.*, 2011)
	Mouse brain	AQP4	Hyperosmotic	↓		(Cao *et al.*, 2012)
	Rat choroid plexus	AQP1	Hypo-osmotic	↑		(Moon *et al.*, 2006)
Eye	Human retinal epithelial cells	AQP5, 8	Hyperosmotic	↑	p38, ERK1/2, NF-κB, TonEBP	(Hollborn *et al.*, 2015)
	Human retinal epithelial cells	AQP5	Hypo-osmotic	↓		(Hollborn *et al.*, 2015)
	ARPE-19 cell line	AQP4	Hyperosmotic	↓	Proteasomal degradation	(Willermain *et al.*, 2014)
	Rat retina	AQP1	Hyperosmotic	↓		(Qin *et al.*, 2009)
	Rat retina	AQP4	Hyperosmotic	–		(Qin *et al.*, 2009)
Heart	Mouse cardiac endothelial cells	AQP1	Hyperosmotic	↑		(Rutkovskiy, Mariero, *et al.*, 2012a)
	Mouse cardiomyocytes	AQP4	Hyperosmotic	↓		(Rutkovskiy, Mariero, *et al.*, 2012a)
IVD	Rat NP cells	AQP2	Hyperosmotic	↑	TonEBP	(Gajghate *et al.*, 2009)
	Mouse NC cells	AQP3	Hyperosmotic	↑		(Palacio-Mancheno *et al.*, 2018)
Lung	Rat alveolar epithelial cells	AQP5	Hyperosmotic	↑	HIF-1α	(Zhou *et al.*, 2007)

	Tissue/cell type	AQP	Treatment	Regulation	Pathways	References
Kidney	mIMCD-3 cell line	AQP1	Hyperosmotic	↑		(Jenq *et al.*, 1998)
	mIMCD-3 cell line	AQP1	Hyperosmotic	↑	p38, ERK1/2, JNK, TonE	(Umenishi *et al.*, 2003)
	mIMCD-3 cell line	AQP1	Hyperosmotic	↑	TonEBP	(Lanaspa, Miguel A *et al.*, 2010)
	Rat kidney collecting duct cells	AQP2	Hyperosmotic	↑	p38, ERK1/2, JNK	(Hasler *et al.*, 2008)
	MDCK cell line	AQP3	Hyperosmotic	↑		(Matsuzaki *et al.*, 2001)
Ovary	3AO ovarian cancer cell line	AQP1, 5	Hyperosmotic	−		(Chen *et al.*, 2015)
	3AO ovarian cancer cell line	AQP3, 9	Hyperosmotic	−		(Chen *et al.*, 2015)
Skin	Human keratinocytes	AQP3	Hyperosmotic	↑		(Sugiyama *et al.*, 2001)
	Human keratinocytes	AQP9	Hyperosmotic	−		(Sugiyama *et al.*, 2001)

Table 3.1. Regulation of AQP expression by alterations in extracellular osmolality. The expression of many AQP isoforms, across many tissue and cell types is upregulated (↑) or downregulated (↓) by osmolality. AQP expression may also be unaltered by changes in osmolality (−).

Specifically, AQP1 expression is upregulated by hyperosmolality in mIMCD-3 kidney cells (Jenq *et al.*, 1998; Umenishi and Schrier, 2003; Lanaspa, Miguel A *et al.*, 2010) and mouse cardiac endothelial cells (Rutkovskiy, Mariero, *et al.*, 2012a). AQP5 expression has also been shown to be upregulated by hyperosmolality in 3AO ovarian cancer cells (Chen *et al.*, 2015), rat alveolar epithelial cells (Zhou *et al.*, 2007) and human retinal epithelial cells (Hollborn *et al.*, 2015), in which AQP5 expression was reduced after hypo-osmotic treatment (Hollborn *et al.*, 2015). TonEBP has also been implicated with the hyperosmotic upregulation of both AQP1 (Umenishi and Schrier, 2003; Lanaspa, Miguel A *et al.*, 2010) and AQP5 (Hollborn *et al.*, 2015). This potentially

indicates that both AQPs are also regulated in the same manner in NP cells, as the osmolality of NP tissue decreases during degeneration. There is also a precedence of AQP regulation in the IVD; AQP3 expression was upregulated by hyperosmolality in 3D cultured murine NC cells (Palacio-Mancheno *et al.*, 2018) and the hyperosmotic upregulation of AQP2 in 2D cultured murine NP cells was dependent on TonEBP (Gajghate *et al.*, 2009). If AQP1 and 5 are regulated in this manner, it may implicate them in enabling the adaptation of NP cells to their hyperosmotic environment along with other TonEBP target genes. This adaptation may be diminished during degeneration when their expression is reduced, possibly by the lowered extracellular osmolality.

AQP expression and function has also been implicated in enabling cells to sense osmotic stress via membrane tension changes (Ozu *et al.*, 2018), interactions with other osmotically activated membrane channels (Benfenati *et al.*, 2011a; Mola *et al.*, 2016) and the control of cell volume regulation (Kitchen *et al.*, 2015), indicating that AQPs may also function upstream of TonEBP to enable cellular adaptation to osmolality changes. As TonEBP also regulates the expression of NP matrix genes, if AQP1 and 5 expression in NP cells is linked to TonEBP, they may also be linked to matrix production and therefore the fundamental function of NP cells to maintain the integrity of the IVD.

This study aimed to investigate if AQP1 and 5 expression was regulated by hyperosmolality in 2D and 3D cultured human NP cells to determine why their expression is decreased during degeneration. Also, to identify if AQP1 and 5 are similarly regulated in rat NP cells, which may determine if this response is common across different species, highlighting that it is a fundamental process for IVD function, and how TonEBP is involved in the osmotic regulation of both AQPs. To assess the *in vivo* role of

TonEBP in the expression of AQP1 and 5, expression in wildtype (WT) and TonEBP -/- mice embryos were also investigated.

3.2 Materials and methods

3.2.1 Experimental design

As the reasons for the decrease in AQP1 and 5 expression during in NP tissue during IVD degeneration are unknown, 2D cultured human NP cells were treated with hyperosmotic media (representative of physiological to healthy IVD). qRT-PCR and western blotting were utilised to determine if AQP1 and 5 gene and protein expression were sensitive to alterations in extracellular osmolality, which has been shown in a number of other tissue types. Furthermore, gene expression was also investigated in 3D cultured human NP cells exposed to hyperosmotic treatment to determine if AQP1 and 5 were regulated in a similar manner in more *in vivo*-like NP cells. Similarly, gene and protein regulation of AQP1 and 5 was investigated in 2D cultured rat NP cells, to determine if responses to hyperosmolality were similar across species. Subsequently, TonEBP was knocked down in rat NP cells prior to the application of hyperosmotic stimuli to determine if TonEBP controlled the hyperosmotic regulation of AQP1 and 5 expression. To investigate if TonEBP regulated *in vivo* expression of AQP1 and 5, IHC was performed on the spines and tails of WT and TonEBP -/- mouse embryos and fluorescence intensities compared. The experimental design is summarised in Figure 3.2.

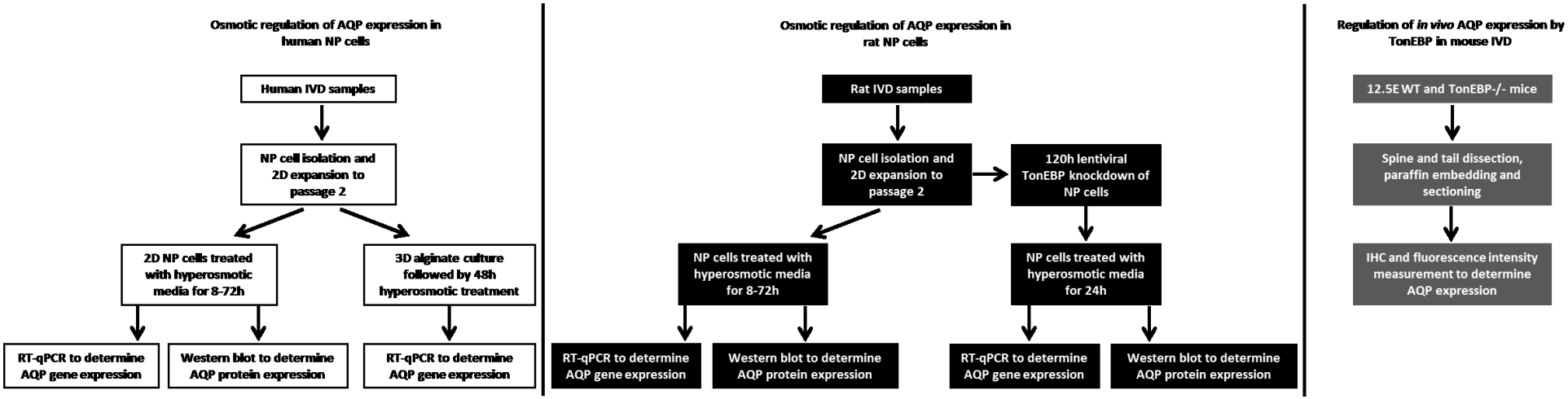

Figure 3.2 Experimental design to investigate the *in vitro* osmotic regulation of AQP1 and 5 in NP cells and *in vivo* regulation of AQP1 and 5 by TonEBP in IVD tissue.

3.2.2 Human Tissue

Human IVD tissue was obtained from patients undergoing microdiscectomy surgery for the treatment of nerve root compression as a result of IVD herniation or post-mortem (PM) examination with informed consent of the patients or relatives. Ethical approval was granted from Sheffield Research Ethics Committee (09/H1308/70) (Section 2.2.2).

3.2.3 Tissue Processing

Human tissue was fixed in 10% (v/v) neutral buffered formalin (Leica Microsystems) and embedded into paraffin wax. Following embedding, 4µm sections were cut and human IVDs histologically graded using methods described previously (section 2.2.4) to determine severity of IVD degeneration.

3.2.4 Human NP cell extraction and culture

Human NP cells were isolated from surgical and PM tissue and expanded in 2D culture as described previously (Section 2.2.5). Human NP cells at passage 2 were utilised for all experiments.

3.2.5 Hyperosmotic gene regulation of AQPs in human NP cells

Once expanded, human NP cells were seeded into 6-well plates in standard culture media (Section 2.2.8) with an osmolality of 325mOsm/kg. Cells were treated with 425mOsm/kg media for 8, 12, 24, 48 and 72h to mimic the osmolality of the native, non-degenerate disc in monolayer (2D) culture. To alter the osmolality from 325 to 425mOsm/kg, 50mM NaCl was added to media and the osmolality of all

solutions was determined using a freezing point osmometer (Model 3320, Advanced Instruments, Horsham, UK). NP cells in 325mOsm/kg media at 0h time point were used as untreated controls. Following treatment, media was aspirated and 1mL Trizol (Life Technologies) was added to lyse cells. Lysate was collected and 200µL Chloroform (Sigma-Aldrich) added per mL Trizol (Life Technologies). Samples were vortexed for 15 seconds and left to stand at room temperature for 10min, prior to 4°C centrifugation at 12000g for 15min to separate protein, DNA and RNA-containing layers. The clear, upper phase containing RNA was taken forward and 500µL of molecular grade 2-propanol was added and samples were stored at -80°C for at least 1h to precipitate RNA. Samples were then centrifuged at 12,000g for 30min at 4°C and supernatant was discarded. Pellets were resuspended and washed in 200-proof ethanol (Sigma-Aldrich) and centrifuged at 7500g for 15min at 4°C. Supernatant was removed and samples were allowed to air-dry for 10min. RNA was finally resuspended in 14µL RNase-free water (Qiagen, Manchester, UK) before proceeding to cDNA synthesis.

To explore how AQP gene expression was potentially altered by hyperosmotic stimulus in an environment mimicking the *in vivo* IVD conditions, as compared to 2D culture where NP cells are known to de-differentiate. Human NP cells were resuspended, cultured and treated following encapsulation into alginate beads. After expansion up to passage 2, human NP cells were resuspended at a density of $4x10^6$ cells/mL in sterile filtered 1.2% (w/v) alginic acid (Sigma-Aldrich) in 0.15M NaCl. Human NP cell-containing alginate was polymerised by passing through a 20G needle into 0.2M $CaCl_2$ drop-by-drop to produce alginate beads and left for 10 mins to fully

gel. Newly formed beads were washed with 0.15M NaCl to remove excess $CaCl_2$ and washed twice with DMEM before standard culture media was added. Alginate beads were polymerised and cultured in 24-well plates with 6 beads per well. Alginate beads were cultured in standard conditions for 2 weeks prior to treatment to allow human NP cells to differentiate into an *in vivo*-like phenotype (Le Maitre, Freemont and Hoyland, 2004). Once differentiated, alginate beads were treated (2 beads per well of a 96-well plate) with 325mOsm/kg (standard culture media), 425mOsm/kg or 525mOsm/kg, produced by adding 50mM or 100mM NaCl added to standard culture media respectively, for 48h. Following treatment, beads were added to alginate dissolving buffer (55mM sodium citrate, 30mM EDTA, 0.15 M NaCl in H_2O) for 10min at 37°C on an orbital shaker before centrifugation at 300g for 10min. Supernatant was discarded and pellets resuspended in DMEM containing 0.4mg/mL collagenase (Sigma-Aldrich) for 10min at 37°C on an orbital shaker to degrade ECM which had been deposited by NP cells during 3D culture. Samples were centrifuged for a further 10min at 300g, supernatant removed and 1mL Trizol (Life Technologies) added to each sample. RNA was extracted using RNeasy mini kit (Qiagen) (Section 2.2.5). RNA was finally eluted from RNeasy mini kit columns with 14µL RNase free water (Qiagen). RNA from both 2D and 3D alginate samples was synthesised into cDNA following protocols outlined in section 2.2.5. qRT-PCR was utilised to identify regulation of gene expression of AQP1 and 5, employing pre-designed primer/probe mixes (Life Technologies) (section 2.5.5).

3.2.6 Hyperosmotic protein regulation of AQPs in human NP cells

Human NP cells were seeded into T25 culture flasks (Nunc, Paisley, UK) and treated with 425mOsm/kg media for 8, 24 or 48h. Cells in standard culture media (325mOsm/kg) at 0h were used as controls. Following treatment, cells were washed twice with ice-cold PBS before 500µL Radioimmunoprecipitation assay (RIPA) buffer was added to lyse cells. RIPA buffer was used to lyse cells as it contains both ionic and non-ionic surfactants that enable the effective lysis of whole cell extracts and membrane-bound proteins. Components of RIPA buffer are outlined in Table 3.2.

RIPA buffer component	Concentration
Sodium chloride	150mM
Triton X-100	1% (v/v)
Sodium deoxycholate	0.5% (w/v)
Sodium dodecyl sulphate	0.1% (w/v)
Tris	50mM
cOmplete™ protease inhibitor cocktail tablets	1 tablet/50mL
PhosSTOP phosphatase inhibitor tablets	1 tablet/10mL
pH 8	-

Table 3.2. RIPA buffer components and final concentration when added to H_2O. All reagents purchased from Sigma-Aldrich.

Lysates were vortexed at 4°C for 20min to complete cell lysis. The protein concentration of lysates was determined using the BCA assay. BCA reagent was produced by adding 4% (w/v) copper (II) sulphate (Sigma-Aldrich) to bicinchoninic acid solution (Sigma-Aldrich) at a ratio of 1:50 (e.g. 100µL copper (II) sulphate was

added to 4900µL bicinchoninic acid solution). A standard curve of protein standards (0, 0.05, 0.5, 0.1, 1 and 2mg/mL BSA in RIPA buffer) was performed in triplicate. To samples and protein standards BCA reagent was added at a ratio of 1:8 (e.g. 160µL of BCA reagent added to 20µL of standard/sample). Plates were incubated at 37°C protected from light for 30min. BCA assay works by the formation of Cu^{2+}-protein complexes followed by reduction of Cu^{2+} to Cu^{1+} in alkaline solutions. Cysteine, cystine, tryptophan, tyrosine and the peptide bond are able to reduce Cu^{2+} to Cu^{1+} and the amount of reduction is proportional to the amount of protein present. As reduction occurs BCA forms a complex with Cu^{1+}, changing colour to purple-blue, allowing the measurement of proteins at absorbance 562nm. Once incubation was completed the absorbance of standards and samples was recorded at 562nm on a CLARIOstar plate reader (BMG Labtech). Protein concentration of samples was determined by producing a standard curve from the absorbance of BSA protein standards from which to extrapolate the concentration of total protein.

SDS-polyacrylamide gel electrophoresis (SDS-PAGE) was used to separate whole cell lysates according to molecular mass. Gels consisted of a lower separating gel and stacking gel layered above (Table 3.3).

Gel component	Separating gel (mL)	Stacking gel (mL)
H_2O	3.4	2.9
40% (w/v) acrylamide	2.4	0.75
1.5M Tris-HCl pH 8.8	2	-
0.5M Tris-HCl pH 6.8	-	1.25
10% (w/v) SDS	0.08	0.05
10% (w/v) Ammonium persulphate	0.08	0.05
N, N, N′, N′-Tetramethylethylenediamine	0.008	0.005

Table 3.3. The composition of 12% SDS-PAGE gel. Tris acquired from Fisher Scientific. All other reagents acquired from Sigma-Aldrich.

Before SDS-PAGE, samples were diluted with 4x Laemmli protein sample buffer (Bio-Rad) and incubated at 70°C in a water bath to denature proteins. Samples were not boiled as this may cause membrane-bound proteins to aggregate, stopping movement through gels. Samples were loaded into gels at 30µg total protein per well. To determine molecular weight of proteins 5µL Chameleon™ duo pre-stained protein ladder (LI-COR) was loaded into one well. Samples where electrophoresed at 100V for 90min in 1x running buffer, after dilution with H_2O from 10x running buffer (Table 3.4).

10x running buffer component	Concentration
Tris-HCl	250mM
Glycine	1920mM
SDS	1%(w/v)
pH 8.3	-

Table 3.4. 10x running buffer composition. Tris and glycine acquired from Fisher Scientific. SDS acquired from Sigma-Aldrich.

Following completion of SDS-PAGE, proteins were transferred from gels onto polyvinylidene (PVDF) membranes (Amersham). PVDF membranes were activated in methanol for 5min before the assembly of transfer cassettes containing sponges, filter paper, gel and PVDF membrane. Cassettes were orientated with the PVDF membrane towards the anode within western blot apparatus. Proteins were transferred at 90V for 3h on ice at 4°C in 1x transfer buffer containing 20% (v/v) methanol, diluted from 10x transfer buffer (Table 3.5).

10x Transfer buffer component	Concentration
Tris	250mM
Glycine	1920mM
pH 8.3	-

Table 3.5. 10x transfer buffer composition. All reagents purchased from Fisher Scientific.

Membranes were then blocked in TBS 0.1% (v/v) tween 20 (TBS-T) containing 5% (w/v) non-fat dried milk (NFDM) (Marvel) for 1h at RT, followed by overnight incubation with rabbit polyclonal antibody against AQP1 (1:5000, AB3272, Millipore) and mouse monoclonal antibody against β-actin (1:5000, Abcam) in TBS-T containing 1% (w/v) NFDM. Membranes were washed in TBS-T 3 x 5min before incubation with

IRDye® 800CW goat anti-rabbit IgG (H + L) antibody (1:10000, 926-32211, LI-COR) and IRDye® 680RD goat anti-mouse IgG (H + L) antibody (1:10000, 926-68070, LI-COR) in TBS-T containing 1% (w/v) NFDM for 1h at RT. Membranes were washed in TBS-T 3 x 5min before visualisation of protein bands using LI-COR Odyssey and Odyssey infrared imaging software (LI-COR).

3.2.7 Rat NP cell extraction and culture

Wistar rats (200-250g) were euthanised with CO_2 and spinal columns dissected under aseptic conditions. Lumbar IVDs were separated from the spinal column and the NP separated from the AF using a dissecting microscope. NP tissue was partially digested with 0.1% (w/v) collagenase (Sigma-Aldrich) and 10U/mL hyaluronidase (Sigma-Aldrich) for 4-6h and then maintained in DMEM supplemented with 10% (v/v) FBS and P/S. Rat NP cells migrated out of explant tissue after 1w; when confluent, cells were passaged using trypsin (0.25%) EDTA (1mM) and subsequently cultured.

3.2.8 Hyperosmotic gene regulation of AQPs in rat NP cells

Rat NP cells were seeded at $3x10^4$ cells/well in 6-well plates and treated with altered osmolality media (425mOsm/kg or 525mOsm/kg) for 8 and 24h. NP cells cultured in standard media (325mOsm/kg) at time point 0h were used as controls. After treatment cells were washed in ice-cold PBS before cell lysis and RNA extraction as described in section 2.2.5. RNA was finally eluted in 20µL RNase-free water. Extracted RNA was then converted to cDNA by adding 20µL RNA to EcoDry™ premix (Takara) and incubated at 42°C for 1h, followed by 10min at 70°C. cDNA was stored

at -20°C. To determine regulation of AQP1 and 5 gene expression under hyperosmotic treatment qRT-PCR was performed using Taqman methods outlined in section 2.2.5. Pre-designed primer/ probe mixes (Life Technologies) were used to determine gene expression of AQP1, 5 and GAPDH, which was used as a housekeeping control.

3.2.9 Hyperosmotic protein regulation of AQPs in rat NP cells

Rat NP cells were seeded at $4x10^4$ cells/well in 6-well plates and treated with altered osmolality media (425mOsm/kg or 525mOsm/kg) for 8 and 24h. NP cells cultured in standard media (325mOsm/kg) at time point 0h were used as controls. After treatment cells were washed in ice-cold PBS before adding 200µL homemade lysis buffer, (made up in mammalian protein extraction reagent MPER, Sigma-Aldrich) (Table 3.6) per well, cell lysates were collected and vortexed for 20min at 4°C.

Cell lysis buffer component	Concentration
cOmplete™ protease inhibitor cocktail tablets	1 tablet/50mL
NaCl	150mM
NaF	4mM
Na_3VO_4	20mM
β-glycerophosphate	25mM
Dithiothreitol (DTT)	0.2mM

Table 3.6. Cell lysis buffer composition. used to lyse rat NP cells for western blot analysis of proteins. All reagents made up to final concentration in mammalian protein extraction reagent (MPER). All reagents purchased from Sigma-Aldrich.

Determination of cell lysate protein concentration, separation of proteins using SDS-PAGE and transfer onto PVDF membranes is described in section 3.2.6. The only difference in the SDS-PAGE procedure was the use 5µL of pPrecision plus protein™ dual colour standards ladder (Bio-rad) to determine the molecular mass of proteins. After transfer PVDF membranes were cut horizontally at ~45kDa to separate higher molecular mass proteins (β-tubulin, 55kDa, used as housekeeping control) and lower molecular mass proteins (AQP1 and 5, 28kDa, proteins of interest). Membranes were blocked in TBS-T containing 5% (w/v) NFDM for 1h at RT, before overnight incubation with either rabbit polyclonal antibody against AQP1 (1:500, AB3272, Millipore), rabbit polyclonal antibody against AQP5 (1:500, A4979, Sigma-Aldrich) or mouse monoclonal antibody against β-tubulin (1:1000, MA5-16308, Invitrogen). Membranes were washed in TBS-T 3 x 5min before incubation with goat anti-rabbit IgG (H+L) secondary antibody, HRP conjugated (1:1000, 31460, Invitrogen, for AQP1 and 5 probed membranes) or goat anti-mouse IgG (H +L)

secondary antibody, HRP conjugated (1:2000, 31430, Invitrogen, for β-tubulin probed membranes) for 1h at RT. All antibodies were diluted in TBS-T containing 1% (w/v) NFDM. Immunolabelling of protein bands was detected by adding ECL reagent (Amersham) to membranes for 2min before removing excess liquid and visualised under chemiluminescence using ImageQuant™ LAS 4000 (GE Healthcare).

3.2.10 TonEBP knockdown in rat NP cells

To investigate the potential role of TonEBP in the hyperosmotic regulation of AQP1 and 5 in rat NP cells, the expression of this transcription factor was knocked down. HEK293T cells were seeded in $10cm^2$ culture plates at $5x10^6$ cells/plate in DMEM with 10% (v/v) heat-inactivated FBS 24h prior to transfection. Cells were transfected with 9µg shCTR (no knockdown control) or shTonEBP (TonEBP knockdown) plasmids along with 6µg psPAX2 packaging plasmid and 3µg pMD2.G VSV-G envelope expressing plasmid using Lipofectamine 2000 (Invitrogen). After 6h transfection media was replaced with fresh DMEM with 10% (v/v) FBS. Lentiviral media was harvested at 48h and 60h post transfection and virus was precipitated by adding 7% PEG 6000 solution and storing at 4°C for at least 12h. Supernatant/PEG mixture was centrifuged at 1500g for 30min at 4°C to pellet lentiviral particles. Rat NP cells were transduced with fresh media containing viral particles and 8µg/mL polybrene (Sigma-Aldrich). Knockdown of TonEBP occurred for 5 days. On day 4, hyperosmotic media (425mOsm/kg) was added to rat NP cells for 24h of hyperosmotic treatment. Cells were harvested on day 5 of TonEBP knockdown and downstream experiments were performed to assess gene and protein regulation of AQP1 and 5, as described previously (Section 3.2.8 and 3.2.9).

3.2.11 TonEBP -/- mice immunohistochemistry

The generation of TonEBP -/- mice was performed as described by Mak *et al.*, 2011. The generation of TonEBP -/- mice used in these experiments were generated by Makarand Risbud's laboratory (Thomas Jefferson University, Philadelphia, PA, USA). The gene-targeting vector contained the tyrosine kinase gene and a 2.5kb TonEBP genomic DNA with part of exon 5 and 6 replaced by neomycin resistance gene. The TonEBP targeting vector was transfected into AB2.2 embryonic stem cells by electroporation. Cells with the vector incorporated into their genome by homologous recombination were selected by the addition of G418 and FIAU into culture media after transfection. Vector-integrated cells were then injected into blastocytes from C57BL/6J mice. Blastocytes were then implanted into the uterus of ICR mice to carry the embryos to term. Mice with deletion of part of exon 5 and 6 were detected with PCR. TonEBP+/- mice were then backcrossed to C57BL/6J mice once and germline transmission confirmed with PCR and southern blotting. TonEBP -/- embryos were generated by timed mating of TonEBP +/- mice. The morning of vaginal plug detection was considered to be embryonic day 0.5 (E0.5) (Mak *et al.*, 2011). TonEBP-/- embryos did not develop normally and died after 14.5 days of embryonic development due to impaired cardiac development and function (Mak *et al.*, 2011). Spines and tails from wildtype TonEBP+/+ (WT) and TonEBP-/- mouse embryos were dissected and paraffin embedded. Paraffin embedded 4µm sections of spines and tails from WT and TonEBP-/- complete knockout mice at 12.5 days of embryonic development (E12.5) were used to investigate the effect of TonEBP

knockdown on the *in vivo* protein expression of AQP1 and 5 within the IVD using immunohistochemistry.

Sections were dewaxed in histoclear (Leica Microsystems) (3 x 5min), rehydrated through 100% ethanol (3 x 5min), 95% ethanol (3 x 1min) and water (5min) before washing in PBS (5min). Antigens were retrieved by placing slides in citric acid-based antigen unmasking solution (1:100, Vector Laboratories), the solution was boiled for 2min and allowed to incubate in solution for 10min at RT. Heat antigen retrieval methods were repeated with fresh antigen unmasking solution and then slides were cooled at RT for 30min before washing in PBS (2 x 2min). Tissues were blocked in 5% (v/v) donkey serum (Abcam), 0.4% (v/v) triton X-100 (Sigma-Aldrich) in PBS for 1h at RT. All antibodies and wash steps were performed using blocking solution. Slides were incubated overnight at 4°C with either rabbit polyclonal antibody against AQP1 (1:100, AB3272, Millipore) or rabbit polyclonal antibody against AQP5 (1:100, A4979, Sigma-Aldrich). Slides were washed (3 x 5min) and incubated with donkey anti-rabbit IgG (H+ L) highly cross-adsorbed secondary antibody conjugated to Alexa Fluor® 594 (1:700, A-21207, Invitrogen) for 1h at RT. Slides were washed (3 x 5min), mounted with ProLong™ diamond antifade mountant with DAPI (Life Technologies) and allowed to cure at RT overnight, protected from light. Slides were stored at 4°C. Mounted slides were visualised using an Axio Imager A2 (Zeiss). All images were taken at identical exposures to enable the quantification of fluorescent intensities.

3.2.12 Statistical analysis

The regulation of AQP1 and 5 gene and protein expression, in both human and rat NP cells, was performed in triplicate on 3 patients or pooled rat cells on different days. Data was found to be non-parametric, therefore Kruskall-Wallis with Dwass-Steel-Critchlow-Fligner post hoc analysis test was used to identify significant differences between AQP1 and 5 gene expression (investigated by qRT-PCR), and protein expression (investigated by western blotting). IHC was performed on 3 WT and TonEBP-/- rats each, in at least duplicate. Fluorescent images were taken, all at the identical exposure, gain and magnification. Fluorescent intensity of NP regions was determined using ImageJ software and normalised to the number of NP cells within the same IVD. Data was found to be non-parametric, therefore Kruskall-Wallis with Dwass-Steel-Critchlow-Fligner post hoc analysis test was used to identify significant differences between fluorescent intensities of WT and TonEBP-/- mice, after AQP1 and 5 IHC experiments, to determine putative changes in expression.

3.3 Results

3.3.1 Hyperosmotic regulation of AQP1 and 5 expression in human NP cells

AQP1 gene expression was significantly upregulated in 2D monolayer cultured human NP cells after 24h and 72h hyperosmotic treatment (425mOsm/kg) ($p \leq 0.05$) when compared to untreated controls (325mOsm/kg) at time 0 (Figure 3.3A). The gene expression of AQP5 in 2D monolayer cultured human NP cells was upregulated by the same hyperosmotic treatment at 12, 24, 48 and 72h, when compared with untreated controls ($p \leq 0.05$) (Figure 3.3B). During 3D alginate culture of human NP cells, to restore their *in vivo* phenotype, AQP1 gene expression was upregulated by 48h of both hyperosmotic treatments (425 and 525mOsm/kg) ($p \leq 0.05$) (Figure 3.3C), whereas AQP5 expression was only upregulated by 425mOsm/kg treatment for 48h, compared to untreated controls ($p \leq 0.05$) (Figure 3.3D). No osmotic treatments effected NP cell viability (Appendix VI).

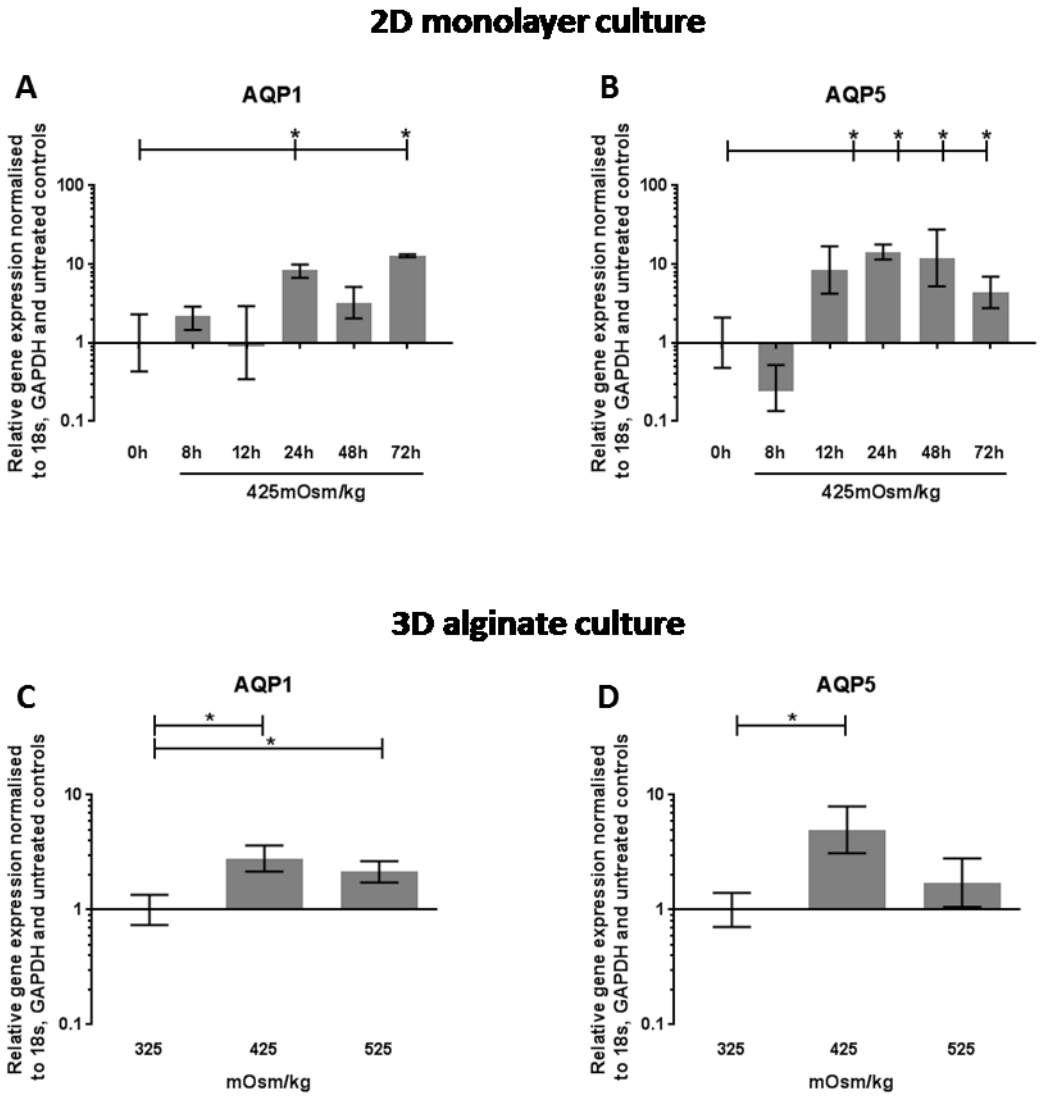

Figure 3.3. Hyperosmotic regulation of AQP1 and 5 gene expression in human NP cells. (A, B) Regulation of AQP1 and AQP5 gene expression, after 8 - 72h treatment with 425mOsm/kg media, in human NP cells cultured in monolayer up to passage 2 prior to treatment. (C, D) Regulation of AQP1 and AQP5 gene expression, after 48h treatment with 425 or 525mOsm/kg media, in human NP cells cultured for 2w encapsulated in alginate beads prior to treatment. The osmolality of untreated controls in standard culture media was 325mOsm/kg. The osmolality of treatment media was altered using NaCl and was measured using a freezing point depression osmometer (Model 3320 osmometer, Advanced Instruments). Statistical significance determined using Kruskal-Wallis test * = $p \leq 0.05$.

AQP1 protein expression in human NP cells, in 2D monolayer culture, was significantly upregulated after 8, 24 and 48h of hyperosmotic treatment (425mOsm/kg) when compared to untreated controls (325mOsm/kg) at 0h ($p \leq 0.05$) (Figure 3.4).

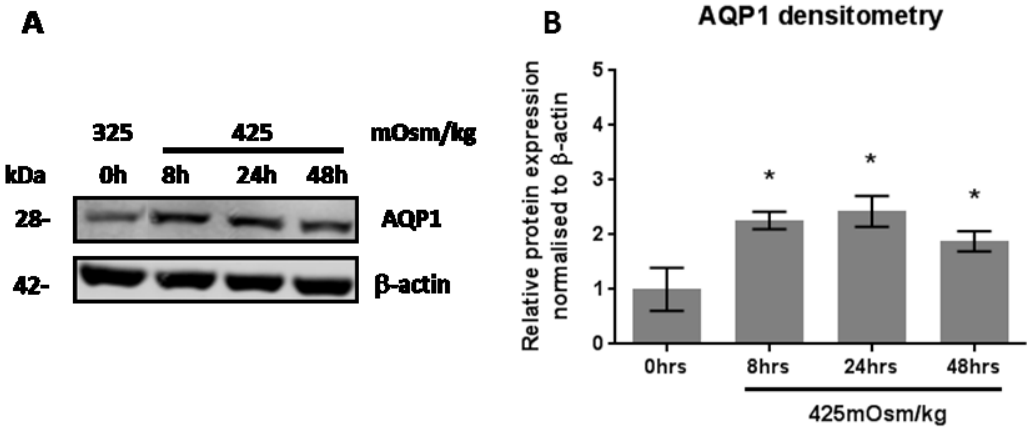

Figure 3.4. Hyperosmotic regulation of AQP1 protein expression in human NP cells. (A) Western blot analysis of AQP1 expression in human NP cells when exposed to 8, 24 and 48h of 425mOsm/kg media treatment, when compared to 325mOsm/kg (untreated) media controls at 0h. β-actin was used as a loading control. Chameleon® duo pre-stained protein ladder (LI-COR) was used to determine the size (kDa) of protein bands on blots. (B) Densitometry measurements of AQP1 protein expression, in human NP cells, when exposed to 8, 24, and 48h 425mOsm/kg media treatment compared to 325mOsm/kg control at 0h. The relative AQP1 expression is normalised to β-actin expression. Statistical significance determined using Kruskal-Wallis test * = $p \leq 0.05$.

3.3.2 TonEBP expression in native human NP tissue

TonEBP is expressed in non-degenerate (Figure 3.5A), moderately degenerate (Figure 3.5B) and severely-degenerate (Figure 3.5C) native human NP tissue. The percentage of cells expressing TonEBP within the human NP is high and there is no significant difference across any grade of degeneration (Figure 3.5D).

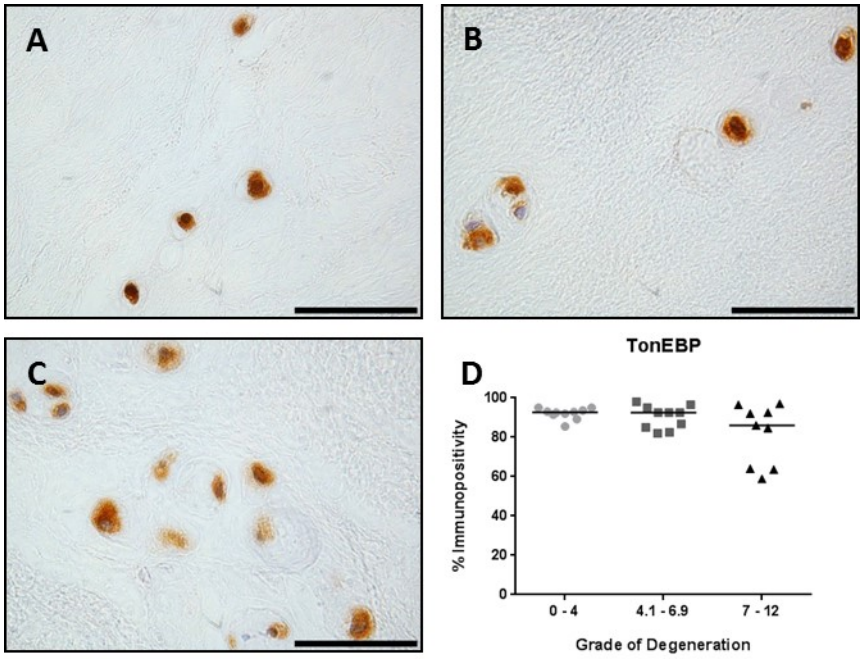

Figure 3.5. Protein expression of TonEBP within native human NP tissue, determined using IHC on 4µm sections. Representative images if IHC from non-degenerate (A), moderately-degenerate (B) and severely-degenerate (C) human NP tissue. (D) Immunopositivity results determining the percentage of cells within NP tissue expressing TonEBP. Two-hundred cells per patient sample were counted as positive or negative. Each point represents an individual patient NP sample. The grades of degeneration are described as followed: non-degenerate (0-4), moderately-degenerate (4.1-6.9) and severely-degenerate (7-12). Positive staining for TonEBP is indicated by brown staining and cell nuclei are counterstained blue with Mayer's haematoxylin.

3.3.3 Hyperosmotic regulation of AQP1 and 5 expression in rat NP cells

AQP1 gene expression was significantly upregulated in rat NP cells after 8h treatment with 425mOsm/kg media ($p \leq 0.05$) (Figure 3.6A) and after 8h and 24h treatment with 525mOsm/kg media ($p \leq 0.05$) (Figure 3.6A). After 8h of 525mOsm/kg media treatment AQP1 gene expression was significantly higher compared to when rat NP cells were exposed to the same treatment for 24h ($p \leq 0.05$) (Figure 3.6A). Although both time points with 525mOsm/kg treatment significantly upregulated AQP1 expression when compared to untreated controls (Figure 3.6A). Treatment

with 425mOsm/kg media failed to significantly regulate AQP1 gene expression (Figure 3.6A). AQP1 protein expression was upregulated following 8h and 24h of 425mOsm/kg media treatment and 8h 535mOsm/kg media treatment, when compared to untreated controls at 0h ($p \leq 0.05$) (Figure 3.6B). The localisation of AQP1 protein within monolayer cultured rat NP cells is observed after immunofluorescence staining (Figure 3.6C) (secondary antibody controls, Appendix VII).

Treatment with 525mOsm/kg media, at both 8h and 24h, significantly upregulated AQP5 gene expression in rat NP cells compared to untreated controls ($p \leq 0.05$) (Figure 3.6D). Similar to AQP1 gene regulation, AQP5 gene expression was significantly increased after 8h of 525mOsm/kg treatment when compared to 24h of the same treatment in rat NP cells (Figure 3.6D). All hyperosmotic treatments (425 and 525mOsm/kg) at 8h and 24h upregulated the protein expression of AQP5 in rat NP cells, when compared to 325mOsm/kg (untreated) controls at 0h ($p \leq 0.05$) (Figure 3.6E). The localisation of AQP5 protein within monolayer cultured rat NP cells is observed after immunofluorescence staining (Figure 3.6F) (secondary antibody controls, Appendix VII).

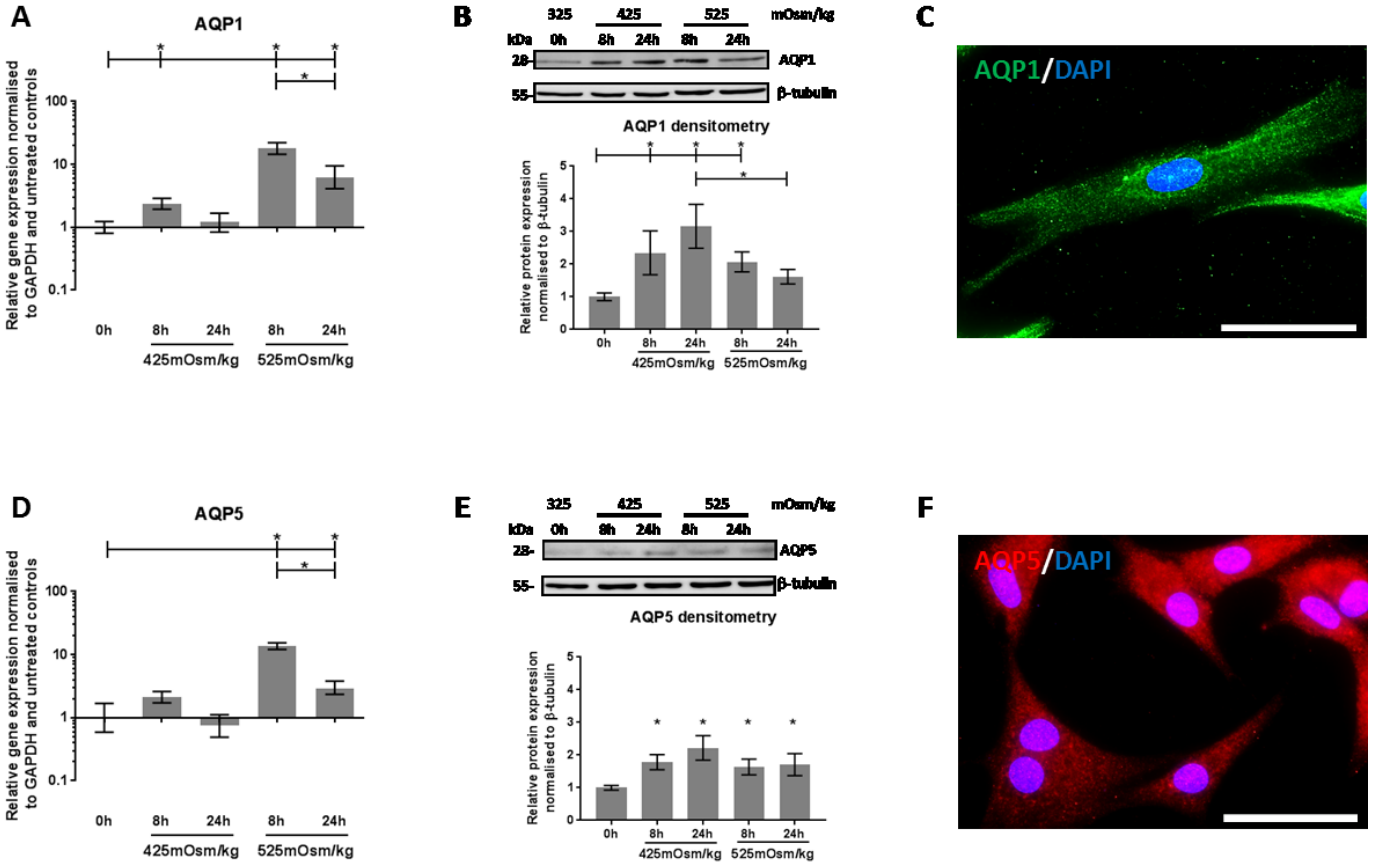

Figure 3.6. Hyperosmotic regulation and localisation of AQP1 and 5 in monolayer cultured rat NP cells. Gene regulation of AQP1 (A) and AQP5 (D) under hyperosmotic conditions. Western blotting results identifying the regulation of AQP1 (B) and AQP5 (F) protein expression under hyperosmotic conditions. The localisation of AQP1 (C) and AQP5 (F) within monolayer cultured rat NP cells. Statistical significance determined using Kruskal-Wallis test * = $p \leq 0.05$.

3.3.4 The effect of TonEBP knockdown on the hyperosmotic regulation of AQP1 and 5 in rat NP cells

In rat NP cells, transduced with shTonEBP lentiviral vector (325 and 525mOsm/kg treatments), the gene and protein expression of TonEBP was significantly reduced compared to TonEBP expression in rat NP cells transduced with shCTR (325 and 525mOsm/kg treatments) ($p \leq 0.05$) (Figure 3.7A and B). In shCTR cells, TonEBP gene and protein expression was significantly upregulated in cells treated with 525mOsm/kg media when compared with untreated controls (325mOsm/kg) ($p \leq 0.05$) (Figure 3.7A and B). These results highlight that TonEBP is functional within shCTR cells and expression is successfully knocked down in shTonEBP cells. AQP1 gene and protein (expression was upregulated when rat NP cells were treated for 24h with hyperosmotic media (525mOsm/kg) in shCTR NP cells ($p \leq 0.05$) (Figure 3.7C and D). When TonEBP expression was knocked down, AQP1 gene expression in both untreated and hyperosmotic treatment groups was significantly reduced ($p \leq 0.05$) (Figure 3.7C). However, AQP1 protein was still upregulated after 24h hyperosmotic treatment in shTonEBP transduced cells ($p \leq 0.05$), comparable to the relative expression of AQP1 observed in 24h hyperosmotic treatment of shCTR cells (Figure 3.7D). AQP5 gene and protein expression was still upregulated when rat NP cells were treated for 24h with hyperosmotic media (525mOsm/kg) in shCTR NP cells (Figure 3.7E and F). When TonEBP expression was knocked down, AQP5 gene and protein expression in both untreated and hyperosmotic treatment groups was significantly reduced ($p \leq 0.05$) when compared to the same treatment in shCTR cells (Figure 3.7E and F).

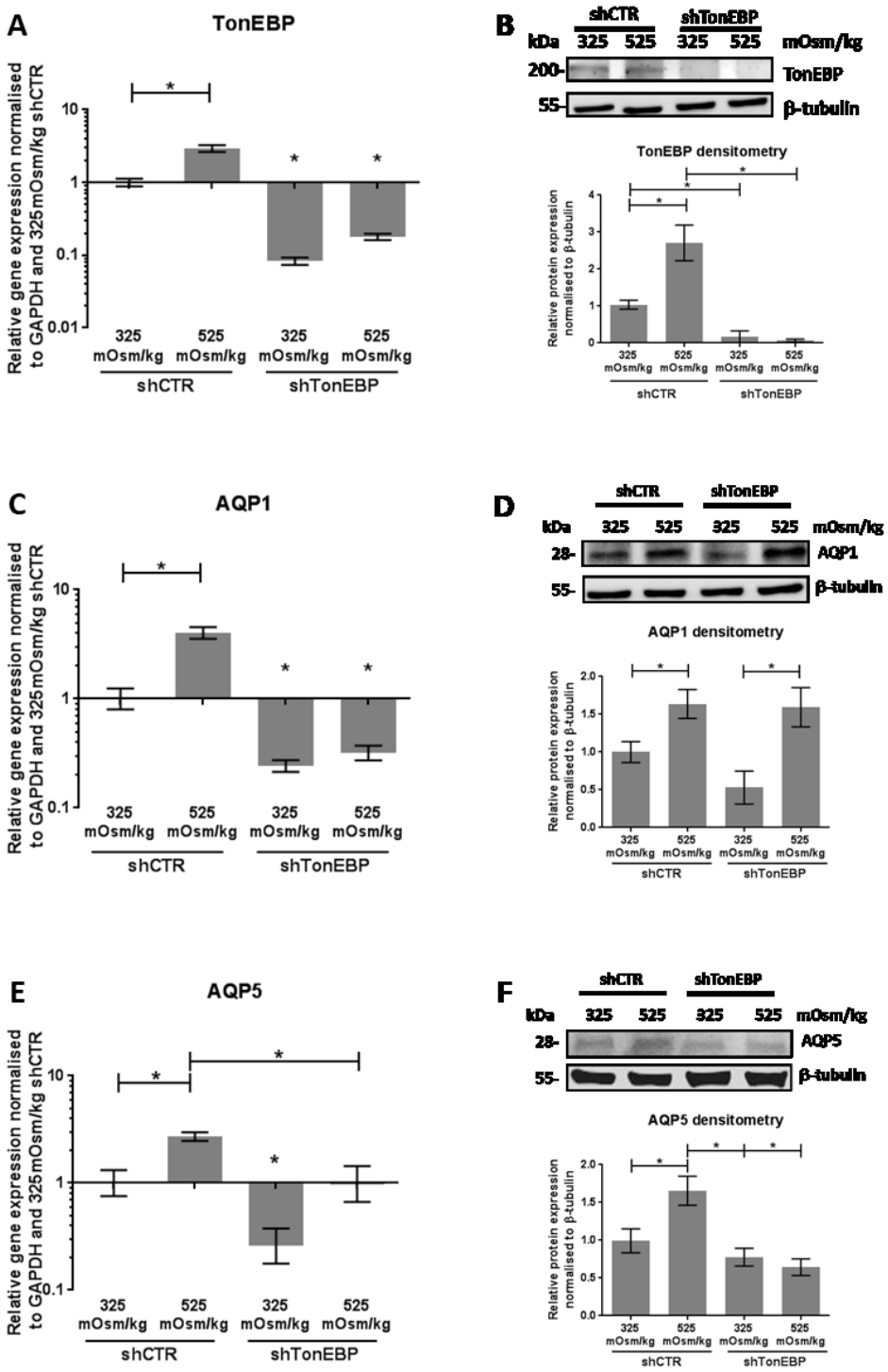

Figure 3.7. The effects of TonEBP knockdown on the hyperosmotic regulation of AQP1 and 5 in rat NP cells. Rat NP cells were exposed to control (325mOsm/kg) or hyperosmotic (525mOsm/kg) treatment for 24hr, after 4d of TonEBP knockdown (shTonEBP) or no knockdown control (shCTR). After knockdown and treatment, the gene and protein expression of TonEBP (A, B), AQP1 (C, D) and AQP5 (E, F) was determined respectively. Results were normalised to 325mOsm/kg shCTR controls. Statistical significance determined using Kruskal-Wallis test * = $p \leq 0.05$.

3.3.5 Effect of TonEBP expression on in vivo expression of AQP1 and 5

AQP1 was expressed in the spine and tail discs of wild type TonEBP +/+ (Figure 3.8A and B), and complete knockout TonEBP -/- (Figure 3.8C and D) embryonic mice. The relative fluorescence of AQP1 immunostaining in TonEBP +/+ spine discs was significantly higher when compared with TonEBP +/+ tail discs, spine and tail discs from TonEBP -/- mice ($p \leq 0.05$) (Figure 3.8E) (secondary antibody controls, Appendix VII).

AQP5 was expressed in the spine and tail discs of wild type TonEBP +/+ (Figure 3.9A and B), and complete knockout TonEBP -/- (Figure 3.9C and D) embryonic mice. The relative fluorescence of AQP1 immunostaining in TonEBP +/+ spine discs was significantly higher when compared with TonEBP +/+ tail discs, spine and tail discs from TonEBP -/- mice ($p \leq 0.05$) (Figure 9.8E) (secondary antibody controls, Appendix VII).

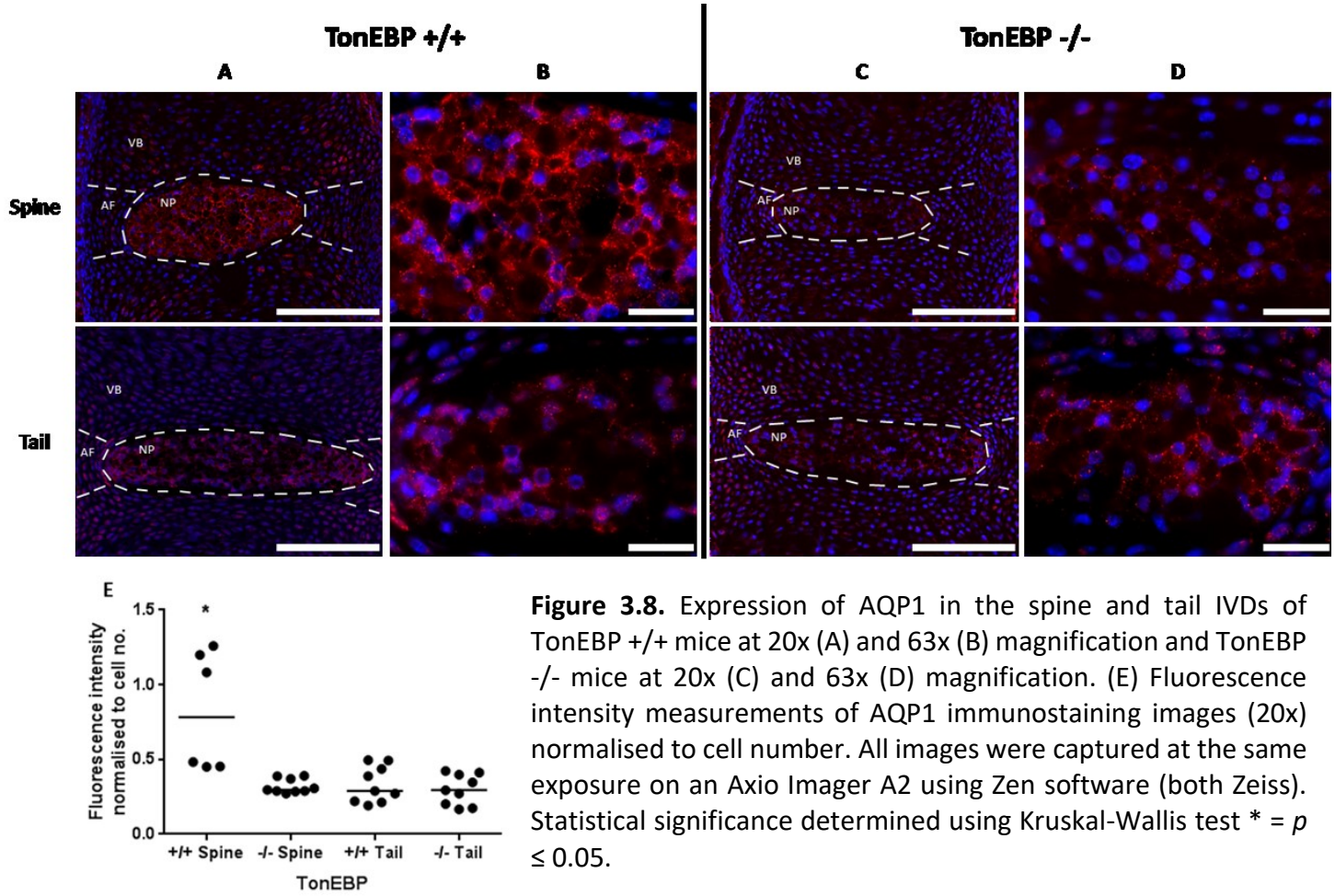

Figure 3.8. Expression of AQP1 in the spine and tail IVDs of TonEBP +/+ mice at 20x (A) and 63x (B) magnification and TonEBP -/- mice at 20x (C) and 63x (D) magnification. (E) Fluorescence intensity measurements of AQP1 immunostaining images (20x) normalised to cell number. All images were captured at the same exposure on an Axio Imager A2 using Zen software (both Zeiss). Statistical significance determined using Kruskal-Wallis test * = $p \leq 0.05$.

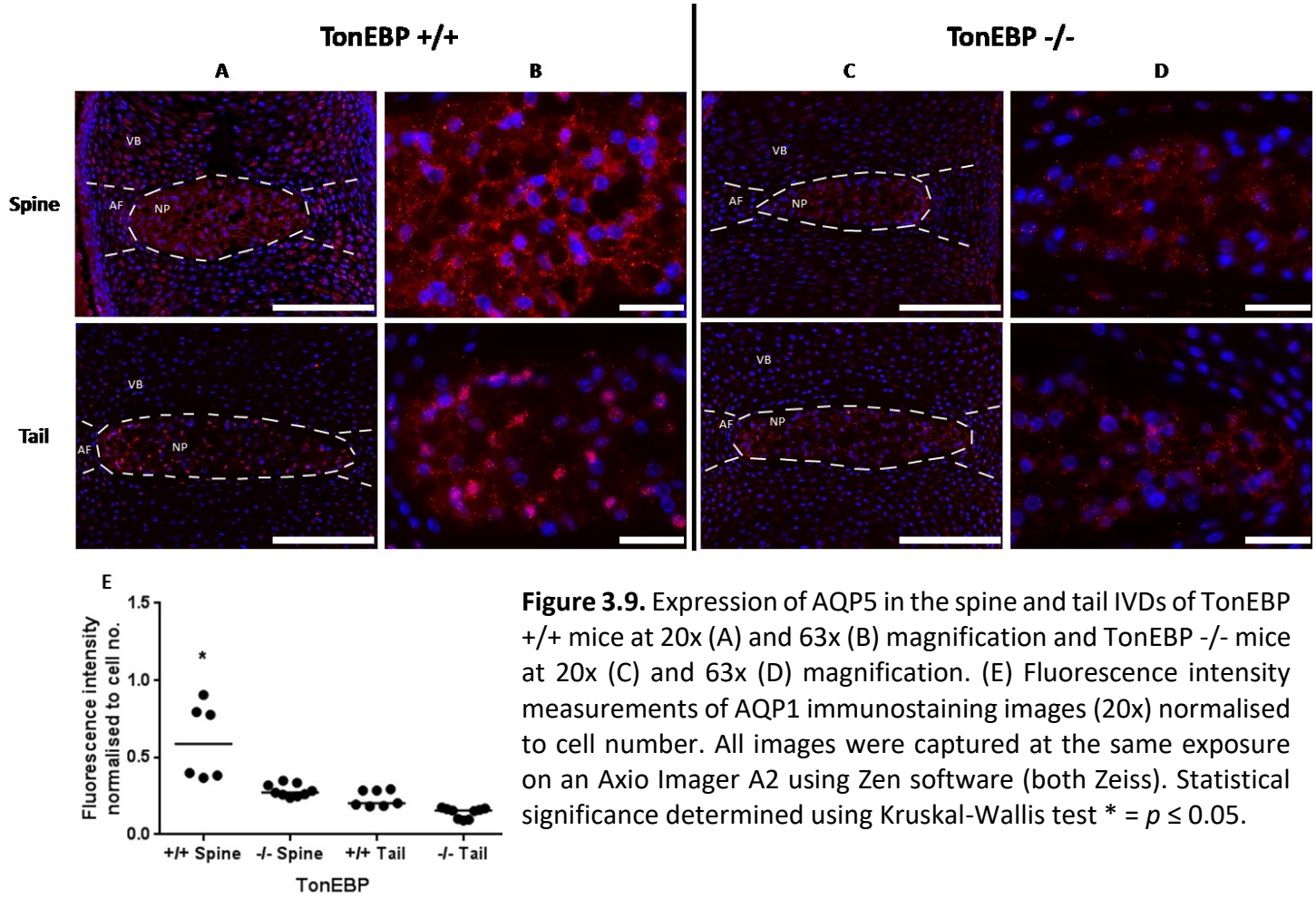

Figure 3.9. Expression of AQP5 in the spine and tail IVDs of TonEBP +/+ mice at 20x (A) and 63x (B) magnification and TonEBP -/- mice at 20x (C) and 63x (D) magnification. (E) Fluorescence intensity measurements of AQP1 immunostaining images (20x) normalised to cell number. All images were captured at the same exposure on an Axio Imager A2 using Zen software (both Zeiss). Statistical significance determined using Kruskal-Wallis test * = $p \leq 0.05$.

3.4. Discussion

NP cells have adapted to the environment in which they reside. The physiological O_2 tension (Fujita *et al.*, 2012), pH (Silagi *et al.*, 2018), nutrient diffusion (Urban, 2002), mechanical loading (Neidlinger-Wilke *et al.*, 2012) and osmolality (O'Connell, Newman and Carapezza, 2014) of the healthy disc allows NP cells to function correctly. When the IVD undergoes degeneration, this environment is altered, exacerbating cellular dysfunction. Previous studies, along with results presented in this thesis (Chapter 2), have identified that many AQPs are expressed by NP tissue (Richardson *et al.*, 2008; Gajghate *et al.*, 2009; Wang and Zhu, 2011; Taş *et al.*, 2012; Johnson *et al.*, 2015). However, only a few studies identify how the expression of AQPs is regulated in the disc. Those that have investigated AQP regulation have found that AQP2 and 3 are upregulated by hyperosmolality, physiological to healthy IVD, in murine NP (Gajghate *et al.*, 2009) and NC cells (Palacio-Mancheno *et al.*, 2018) respectively. AQP1 and 5 expression is decreased during human IVD degeneration (Johnson *et al.*, 2015), yet the cause of this, and how both AQPs are regulated, is unknown. Therefore, for the first time this study has identified that AQP1 and 5 gene and protein expression in NP cells is upregulated by hyperosmolality, which potentially explains why their expression decreases during IVD degeneration, as the osmolality of the NP decreases. This study also determined that the *in vitro* and *in vivo* expression of AQP1 and 5 expression in NP cells is reliant on TonEBP. As TonEBP is an important transcription factor involved in the overall function of the IVD, the regulation of AQPs by TonEBP may also implicate that their function is also important for the health of the IVD.

3.4.1 Hyperosmotic regulation of AQP1 and 5 in NP cells

AQP1 and 5 in human and rat NP cells were upregulated in hyperosmotic conditions that mimic the physiological conditions of the healthy IVD. AQP1 and 5 are also regulated in a similar manner, under similar hyperosmotic conditions, in a range of other tissues and cell types (Jenq *et al.*, 1998; Umenishi and Schrier, 2003; Zhou *et al.*, 2007; Lanaspa *et al.*, 2010; Rutkovskiy *et al.*, 2012; Chen *et al.*, 2015; Hollborn *et al.*, 2015), possibly indicating shared mechanisms of regulation. However, hyperosmotic treatment has also led to the reduction of AQP1 and 5 expression (Muller, Sendler and Hildebrandt, 2006) and hypo-osmotic treatment has led to increased expression of AQP1 (Moon *et al.*, 2006) in other tissues, highlighting that the osmotic regulation of AQP expression is also tissue and cell type-specific. 3D hyperosmotic treatment of human NP cells also showed upregulation of AQP1 and 5, along with 2D treatment, indicating that this response may be relevant *in vivo*, as NP cells are known to re-differentiate into an *in vivo*-like state when cultured in 3D.

AQP1 and 5 gene expression in human NP cells was upregulated by hyperosmotic conditions with an osmolality of 425mOsm/kg, yet the highest upregulation of AQP1 and 5 gene expression in rat NP cells was observed with 525mOsm/kg treatment. This potentially indicates that there are differences in regulation across species, possibly due to the differences in NP environments between adult human and young rat discs. NC cells are preserved within rat IVDs compared to adult human IVDs where NC cells are replaced by NP cells; NC cells produce more hydrophilic matrix when compared to NP cells and therefore may raise the osmolality of the young rat NP to higher levels when compared to a mature

human IVD. Consequently, rat NP cells may respond to a higher osmolality treatment (with regards to AQP1 and 5 upregulation), compared to human NP cells, as this mimics the *in vivo* environment more closely, the same going for the response in human NP cells, where 425mOsm/kg may represent NP tissue osmolality more closely. The differences in gene expression may also be a result of the treatment timeframe. AQP1 expression in rat NP cells is significantly upregulated after 8h treatment, yet after 24h there is no significant difference compared to baseline levels, and AQP5 is not upregulated at either time point. This may simply be due to AQP regulation by 425mOs/kg occurring before 8h or after 24h.

However, the protein expression of AQP1 and 5 in both human and rat NP cells was significantly upregulated by 425mOsm/kg treatment, highlighting that protein expression is regulated similarly across species. Yet the results for AQP1 and 5 protein expression in rat NP cells may not be entirely trustworthy as membranes were cut horizontally to separate differently sized protein bands; so AQP1/5 and β-tubulin could be probed at the same time without needing to strip PVDF membranes. This is not best practice as there is the potential to miss out staining of differently sized bands which may relate to protein dimers/trimers and post-translationally modified proteins, and therefore results may not reflect changes in the total protein concentration, only selected species. In human NP cell western blotting the whole intact membrane was scanned which may have provided more accurate results. Only 1 band, at ~28kDa, for AQP1 was observed in human experiments; this increases confidence in the observed band, also at ~28kDa, in rat experiments. Also, housekeeping proteins were used to normalise against for western blotting analyses.

This poses questions as to whether these proteins are really stably expressed under treatment and whether there is biological variation between different samples, however, published research articles have used the same housekeeping proteins, suggesting they are suitable controls under similar treatments in identical cell types (Gajghate *et al.*, 2009; Johnson *et al.*, 2017; Choi *et al.*, 2018).

As AQP1 and 5 are regulated by osmolality in a similar manner in human and rat NP cells, this indicates there are shared mechanisms of regulation and that AQP regulation is important for IVD function across species. AQP1 and -5 may enable NP cells to adapt to their hyperosmolar environment, and when expression decreases in degeneration (Johnson *et al.*, 2015) this may be due to the decrease in the extracellular osmolality, causing further dysfunction of NP cells. This may mean that AQP1 and 5 expression is decreased as a consequence of initial degeneration, but also leads to a continuation of the degenerative cascade where cells can no longer adapt to their environment.

3.4.2 The role of TonEBP on the expression of AQP1 and 5

TonEBP is important in enabling cells to adapt to a hyperosmotic environment, which is essential for NP cells, which reside within a hyperosmotic environment during healthy IVD physiology. Hyperosmolality increases TonEBP mRNA and protein expression and causes nuclear import and upregulation of target genes (TauT, SMIT, BGT1, AR) (Burg, Ferraris and Dmitrieva, 2007) to enable cellular adaptation to the IVD environment. TonEBP also controls aggrecan and GAG synthesis under hyperosmotic conditions in NP cells (Tsai *et al.*, 2006; Hiyama *et al.*,

2009), therefore TonEBP function has important implications for IVD function and the maintenance of NP osmolality.

This study identified that AQP1 and 5 gene expression, along with their hyperosmotic upregulation, in rat NP cells was significantly reduced when TonEBP expression was knocked down. These results highlight that AQP1 and 5 expression in NP cells is potentially governed by the expression and function of TonEBP. TonEBP has also been shown to regulate the expression of AQP1 and 5 in other tissues (Umenishi and Schrier, 2003; Lanaspa, Miguel A. *et al.*, 2010; Hollborn *et al.*, 2015), providing a precedent for results observed in this study. TonEBP expression is also required for the hyperosmotic upregulation of AQP2 in NP cells (Gajghate *et al.*, 2009), therefore AQP1, 2 and 5 may enable the adaptation of NP cells to their hyperosmolar environment along with the classical TonEBP-targeted osmotic response genes.

Expression and hyperosmotic upregulation of AQP5 protein is significantly down-regulated by TonEBP knockdown suggesting that TonEBP is essential for the correct expression of AQP5 in NP cells. However, basal levels of AQP1 protein expression were slightly reduced (not significantly) by TonEBP knock down, yet the hyperosmotic up-regulation of AQP1 remained unaffected under the same conditions. Even though AQP1 gene expression was clearly regulated by TonEBP, other mechanisms may control protein expression. A possible explanation is that under hyperosmotic conditions, AQP1 protein expression is somehow stabilised for longer periods. Evidence for such an explanation is provided by Leitch, Agre and King, 2001, who identified that in fibroblasts isolated from BALB/c mice AQP1 expression

was upregulated by hyperosmotic treatment, which reduced ubiquitination and proteasomal degradation of AQP1, ultimately leading to increased protein stability under these conditions (Leitch, Agre and King, 2001). This is potentially how AQP1 protein expression is still upregulated in response to hyperosmolality, when TonEBP is knocked down in NP cells, even though gene expression is significantly reduced.

Along with the classical function in regulating the cell's response to hyperosmotic stress, TonEBP has also been shown to increase the expression of TNF-α (Esensten *et al.*, 2005), IL-6 (Ueno *et al.*, 2013) and MCP-1 (Küper, Beck and Neuhofer, 2012; Ueno *et al.*, 2013) under hyperosmotic conditions, all of which are upregulated in IVD degeneration (Le Maitre, Hoyland and Freemont, 2007a; Andrade *et al.*, 2013; Phillips *et al.*, 2015). Parallel to the role under hyperosmotic stress, TonEBP is also activated by TNF-α signalling in NP cells, which leads to the upregulation of genes involved in IVD degeneration, rather than the classical osmotic response genes (Johnson *et al.*, 2017). This highlights that TonEBP may also play a role during IVD degeneration; as the osmolality decreases TonEBP no longer upregulates osmotic response genes, possibly including AQP1, 2 and 5, but rather is activated by TNF-α signalling, intensifying the degenerative cascade (Johnson *et al.*, 2017). This could also explain why altered TonEBP signalling has been seen during degeneration, yet this study demonstrated no change in numbers of cells expressing TonEBP.

It is currently unknown if AQP1 and 5 could also function upstream of TonEBP, this may be possible if AQP1 and 5 at the membrane are able sense changes in membrane tension, via modulating the flow of water in response to changes in

osmolality (Ozu *et al.*, 2018). They may also contribute to the activation of TonEBP along with other proposed mechanisms (Moeckel *et al.*, 2006; Kino *et al.*, 2009). Activated TonEBP consequently upregulates AQP1 and 5, forming a positive feedback loop, to ensure adaptation to the environment.

NP expression of AQP1 and 5 was shown to be higher in the spines of WT mice compared to TonEBP-/- mice. This suggests that *in vivo* expression of AQP1 and 5 in the IVD is reliant upon TonEBP expression, strengthening the *in vitro* regulation also discovered in this chapter. WT spine expression was also higher than WT tail expression. This highlights that AQP1 and 5 expression may be different in mouse spine IVDs compared to mouse tail IVDs, but as humans do not have tails, this may not be completely relevant to human physiology. It does, however, potentially indicate that other factors may contribute to AQP expression in the IVD, along with TonEBP, such as mechanical stimuli. Due to the anatomical position of spinal and caudal IVDs in mice, there may be differences to the NP microenvironment, such as the levels of mechanical stimuli that also provide vital cues to finely tune AQP expression. The *in vivo* expression of AQP1 and 5 was only able to be investigated during embryonic development due to the lethality of TonEBP knockdown (Mak *et al.*, 2011). Results highlight that during development TonEBP is essential for the maintenance of AQP1 and 5, at least in IVDs in the spine. However, it is still unknown if TonEBP contributes to *in vivo* expression in the adult NP, where many other factors (which are altered compared to the embryonic environment). Which would implicate a role for TonEBP regulation of AQPs in physiology of mature NP cells, as compared

to the physiology of notochordal cells, which are the abundant cell type of the NP during development.

3.4.3 Conclusion

AQP1 and 5 expression is decreased during human IVD degeneration (Johnson *et al.*, 2015). This study has identified that AQP1 and 5 are upregulated by hyperosmolality, mimicking the healthy NP, and may explain why expression is decreased during degeneration, when the osmolality is decreased. This suggests AQP1 and 5 may be part of the mechanisms that allow NP cells to adapt to their hyperosmotic environment. TonEBP has already been established as an integral part of those mechanisms; as the hyperosmotic upregulation of AQP1 and 5 is dependent on TonEBP, this implies they both participate in the osmoadaptation process and matrix synthesis (Figure 3.10). During IVD degeneration TonEBP function is uncoupled from the altered osmolality and catabolic genes are upregulated instead of the classical osmotic response genes, which may also include AQP1 and 5. As expression of these genes (and AQP1 and 5) is reduced, NP cells can no longer adapt to the degenerate environment and degeneration is exacerbated (Figure 3.10). Therefore, AQPs may play a role in adapting NP cells to their environment and maintaining the function of NP tissue.

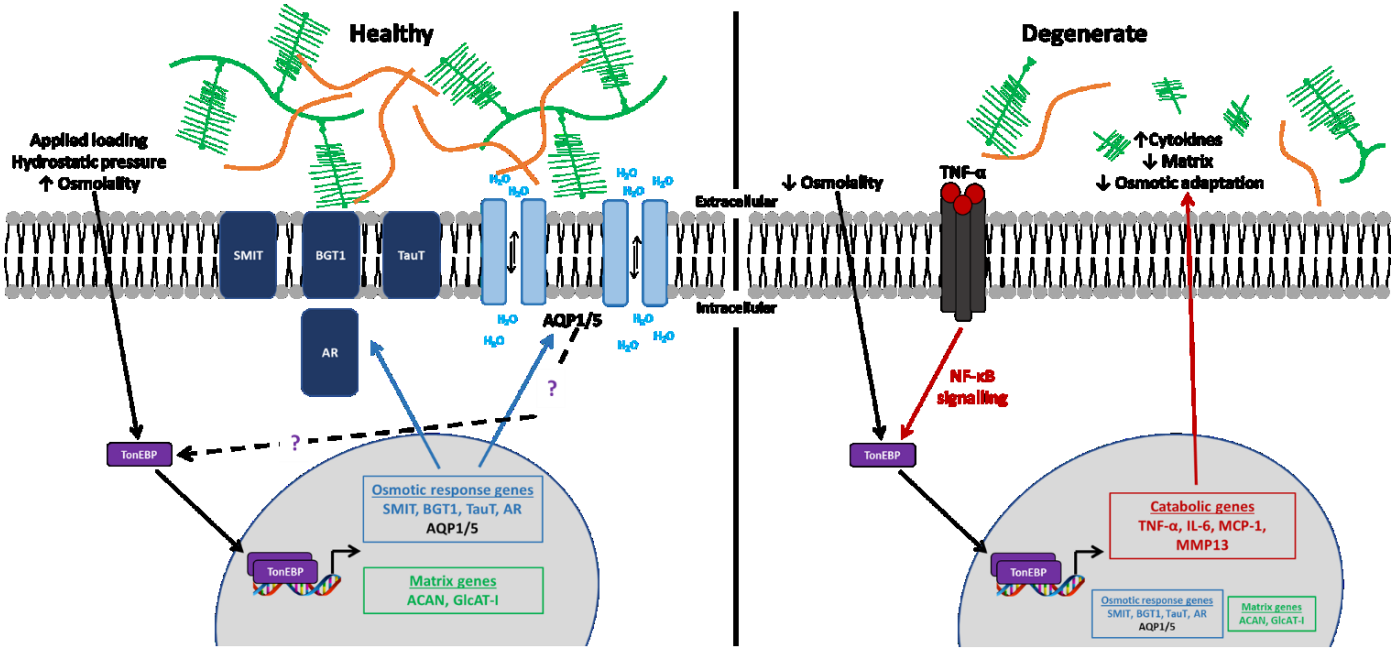

Figure 3.10. Hyperosmotic regulation and potential roles of AQP1 and 5 in NP cells. Under hyperosmotic conditions AQP1 and 5 expression is upregulated in NP cells. Hyperosmotic upregulation of AQP1 and 5 is controlled by TonEBP, along with the classical osmotic response genes. Therefore, possibly indicating that AQP1 and 5 also enable the adaptation of NP cells to their environment and contribute to the maintenance of matrix expression during healthy physiology. There is evidence that AQPs may also function as osmosensors when membrane tension is altered, potentially implicating AQP1 and 5 in the activation of TonEBP, however this is speculative at present (dashed arrow). During IVD degeneration osmolality is decreased and cytokines, such as TNF-α, are present. This may lead to the activation of TonEBP by non-canonical pathways which changes the genes TonEBP targets. TonEBP now favours catabolic gene expression over osmotic and matrix genes, contributing to degeneration. This may explain why AQP1 and 5 expression is decreased during IVD degeneration; decreased osmolality means TonEBP no longer increases expression of osmotic response genes (including AQP1 and 5), NP cells fail to adapt to their altered environment and start to produce catabolic factors that intensify the degenerative cascade.

Chapter 4: Effect of AQP4 and TRPV4 function on the water permeability of human nucleus pulposus cells

4.1 Introduction

The local environment of the NP is hyperosmotic, when compared to many other tissues (Ishihara *et al.*, 1997). Yet, the osmolality never remains constant as loading applied onto the disc forces water and ions out of the tissue as proteoglycans are compressed (McMillan, Garbutt and Adams, 1996). Therefore, the IVD and its environment undergo a diurnal cycle where NP cells must adapt to daily fluctuations in tissue osmolality and mechanical loading. The diurnal cycle of loading and consequential changes to the NP environment are important for regulating the correct function of NP cells (Ishihara *et al.*, 1997; Wuertz *et al.*, 2007; Neidlinger-Wilke *et al.*, 2012; O'Connell, Newman and Carapezza, 2014). During degeneration, when proteoglycan content of the IVD is reduced, the osmolality and mechanical loading of the tissue is permanently altered, interfering with the usual diurnal cycle. The altered environment contributes to degenerative processes, during which cells lose their ability to adapt to osmotic and mechanical cues and start producing catabolic factors (Le Maitre *et al.*, 2009; Gilbert, Hoyland and Millward-Sadler, 2010; Gilbert *et al.*, 2011; Sowa *et al.*, 2012). The ability of cells to perceive and respond to their environment is essential for their correct function, yet the exact mechanisms NP cells employ to adapt to the osmotic and mechanical environment, and how these are altered during degeneration, aren't completely understood.

This thesis has identified that AQPs are upregulated by the hyperosmotic environment of the healthy IVD and their expression is regulated at least in part by TonEBP, indicating roles relating to the adaptation of NP cells to their environment (Chapter 3). An adaptation that is lost during degeneration, when AQP expression is decreased (Johnson *et al.*, 2015). However, the regulation of AQPs by osmolality in the

IVD does not determine how they function or may contribute to physiological adaptations and cellular dysregulation during degeneration.

4.1.1 AQP function and cellular water permeability

Changes in extracellular osmolality causes flux of water, which results in cell swelling or shrinkage, depending on the osmotic gradient. The ability of cells to regulate their volume is essential for the maintenance of cellular homeostasis. AQPs allow the bi-directional movement of water and other small solutes through the cell membrane and control the water permeability of cells in response to even very small osmotic gradients (Agre *et al.*, 2002). Thus, AQPs provide cells a means by which to alter their volume in response to changes to the osmotic environment. AQP expression and function allows the control of water permeability, enabling fundamental functions of cells (Krane *et al.*, 2001b; Tanaka and Koyama, 2011; Day *et al.*, 2014; Kitchen and Conner, 2015; Galan-Cobo, Ramirez-Lorca and Echevarr, 2016; Ozu *et al.*, 2018). However, changes in cell size do not go unchecked; cells initiate complex mechanisms to regulate volume changes which prevent excessive swelling or shrinkage which could lead to cell damage.

4.1.2 TRPV4

Cells have adapted complex mechanisms to sense and respond to environmental stimuli. A group of transmembrane proteins that play a key role in adaptation to the environment are TRP channels. The TRP channel family (of which there are 28 members) is classified into six subfamilies that enable the cell to respond to a variety of environmental stimuli by altering the intracellular Ca^{2+} concentration. These changes in Ca^{2+} concentration induce transduction of signalling pathways, enabling cells to respond to their environment (Samanta *et al.*, 2018). The TRPV subfamily (TRPV1-6) were

thought to be activated by alterations in temperature as the first member to be identified, TRPV1, is a nociceptor activated by temperature (>42°C) and capsaicin (Caterina *et al.*, 1997). However the remaining TRPV family members have diverse functions, TRPV4 has been shown to play an important role in the cellular response to osmotic and mechanical stress (Liedtke *et al.*, 2000; Strotmann *et al.*, 2000; Nilius *et al.*, 2001; Köhler *et al.*, 2006; Toft-Bertelsen, Larsen and Macaulay, 2018)

TRPV4 is expressed in a wide variety of tissues (Everaerts, Nilius and Owsianik, 2010a) and is activated by hypo-osmotic stimuli, when cell volume increases, enabling the influx of Ca^{2+}. This leads to the activation of Ca^{2+}-dependent K^+ channels (Arniges *et al.*, 2004) and RVD mechanisms (Liedtke and Friedman, 2003; Wu *et al.*, 2007) as cells balance external and intracellular osmotic pressure, to regulate cell volume changes (Figure 4.1).

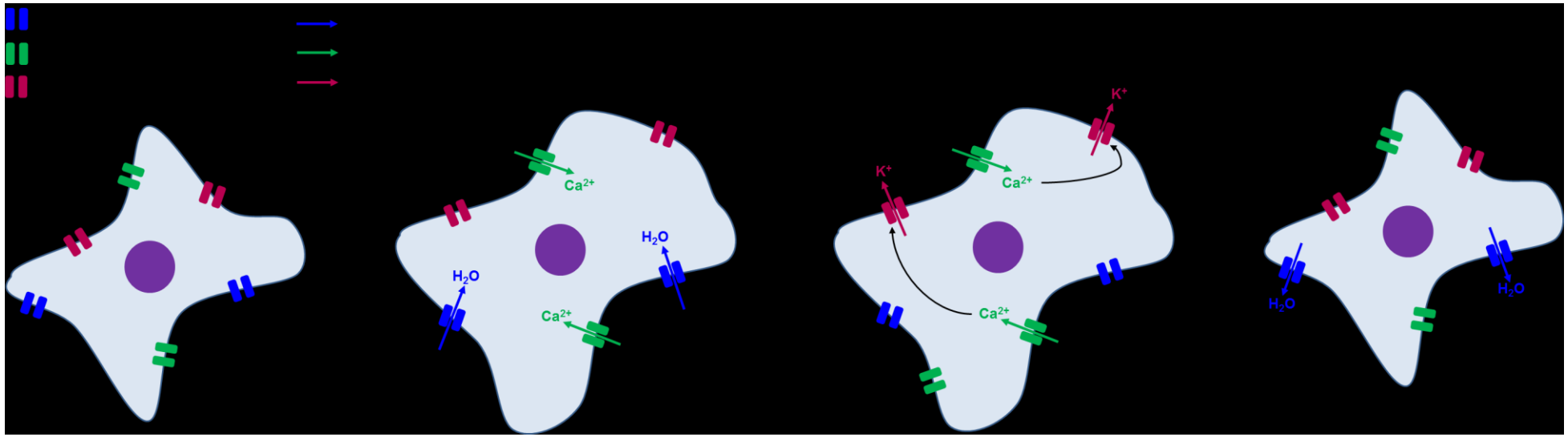

Figure 4.1. Function of TRPV4 during hypo-osmotic stress and activation of regulatory volume decrease mechanisms. Cell swelling during a decrease in extracellular osmolality activates TRPV4 and causes rapid Ca^{2+} influx. Intracellular Ca^{2+} activates dependent K^+ channels and K^+ is transported out of the cell. AQPs transport water out of the cell along the osmotic gradient produced by K^+ efflux, decreasing cell volume and restoring the osmotic balance inside and outside of the cell.

However, there have been limited studies on TRPV4 expression and function in the IVD. It has been shown that exposing mouse MSCs to low magnitude compression enables their differentiation to an NP cell-like phenotype via a TRPV4-dependent pathway (Gan *et al.*, 2018) and in bovine NP cells TRPV4 expression was upregulated by hypo-osmolality (Walter *et al.*, 2016). The same study also showed preliminary data that suggested TRPV4 expression in human IVDs was decreased during degeneration, however results were only reported for 2 human discs (Walter *et al.*, 2016). However, no studies to date have identified how TRPV4 function potentially affects NP cell physiology in response to osmotic stimuli.

However, TRPV4 has a more established role in cartilage physiology. Mechanotransduction of human articular chondrocytes under dynamic loading has been shown to be TRPV4-mediated, which regulates expression of matrix genes (O'conor *et al.*, 2013). Furthermore, TRPV4 plays an important role in regulating RVD mechanisms in chondrocytes after hypo-osmotic stimuli (Lewis, Feetham and Barrett-Jolley, 2011), indicating that TRPV4 contributes to healthy cartilage physiology. Indeed, mutations to TRPV4 have been shown to reduce channel activity and induce osteoarthritis (Lamandé *et al.*, 2011) and deletion of TRPV4 in a mouse model leads to a lack of osmotically-driven Ca^{2+} influx and the onset of osteoarthritis (Clark *et al.*, 2010). As TRPV4 is clearly important for the correct function of chondrocytes and a lack of expression/function leads to osteoarthritis, which has similar pathology to IVD degeneration; TRPV4 may also be implicated in the adaptation of NP cells to their hyperosmotic environment and the overall health of the disc.

Interestingly, there is also evidence that the functions of AQPs and TRPV4 may be linked. The ability of many cell types to sense changes in extracellular osmolality and

trigger RVD mechanisms may rely on AQPs and TRPV4 functioning in synergy. In rabbit cortical collecting duct cells hypo-osmotic activation of TRPV4 and RVD mechanisms were reliant on AQP2 expression (Galizia *et al.*, 2012). Similar activation of TRPV4 and RVD was reliant on AQP5 in mouse salivary gland cells (Liu *et al.*, 2006) and AQP4 and TRPV4 have been shown to interact to control RVD in mouse retinal Müller cells (Jo *et al.*, 2015). AQP4 has also been shown to co-localise with TRPV4 in mouse astrocytes and form a complex that controls the regulation of cell volume (Benfenati *et al.*, 2011a) and Mola *et al.*, 2016 identified that AQP1 and 4-influenced swelling was the main trigger for RVD and TRPV4 mediated calcium signalling in mouse astrocytes. This regulatory role suggests AQPs have many fundamental roles in cell biology other than their function as a passive water channel. Which have been suggested as one of many mechanisms that potentially enable NP cells to sense changes in their extracellular environment (Sadowska *et al.*, 2018). As AQP4 is the isoform that is most permeable to water (Yang and Verkman, 1997; Kitchen *et al.*, 2015), understanding its role in NP cells and whether it works in unison with TRPV4, to enable adaptation to the fluctuating osmotic environment is important to determine. Especially as a decrease in AQP4 is seen in IVD degeneration (Chapter 2), which could result in a loss of adaptation, when the environment becomes hypo-osmotic.

To determine the physiological roles of AQP4 and TRPV4 in the IVD, this study investigated the expression of TRPV4 in native human NP tissue to determine if levels were altered during degeneration. Furthermore, how human NP cells adapt to changes in extracellular osmolality was determined by measuring changes in cell volume and the rate at which cell size changed within altered osmolality. In addition, the potential involvement of AQP4 and TRPV4 was investigated using specific inhibitors and the water

permeability of NP cells following osmotic challenge was determined in the presence and absence of channel inhibitors. Finally, calcium influx in human NP cells, when exposed to altered osmolality, was investigated as changes in extracellular osmolality often cause calcium flux in cells which leads to cell volume regulation. To determine whether AQP4 and TRPV4 facilitated this, calcium influx was investigated in the presence and absence of channel inhibitors.

4.2 Materials and methods

4.2.1 Experimental Design

To investigate TRPV4 expression, IHC was performed on non-degenerate and degenerate human NP tissue and co-localisation of AQP4 and TRPV4 in human NP cells was determined using confocal microscopy. To investigate how human NP cells responded to shifts in extracellular osmolality, human NP cells were exposed to rapid physiological alteration to osmolality to mimic healthy and degenerate conditions. A plate-reader based assay, utilising the self-quenching effects of Calcein-AM in response to relative intracellular concentration, was used to determine the rate at which NP cells respond to extracellular osmolality changes by modulating their size (Fenton *et al.*, 2010). To determine the actual change in cell volume to rapid changes in osmolality, flow cytometry and fluorescent microscopy methods were utilised. Measurements taken from both the rate of cell volume change and the actual cell volume change were used to determine the relative water permeability from equations outlined by Fenton *et al.*, 2010. Calcium influx in response to altered osmolality, an important cellular adaptation response, was measured using Fluo-4 direct calcium assay in a plate reader setup. To investigate the effects of AQP4 and TRPV4 function on these processes, NP

cells were either treated with specific inhibitors to block channel function or left as controls during all experiments. The experimental design is outlined in Figure 4.2.

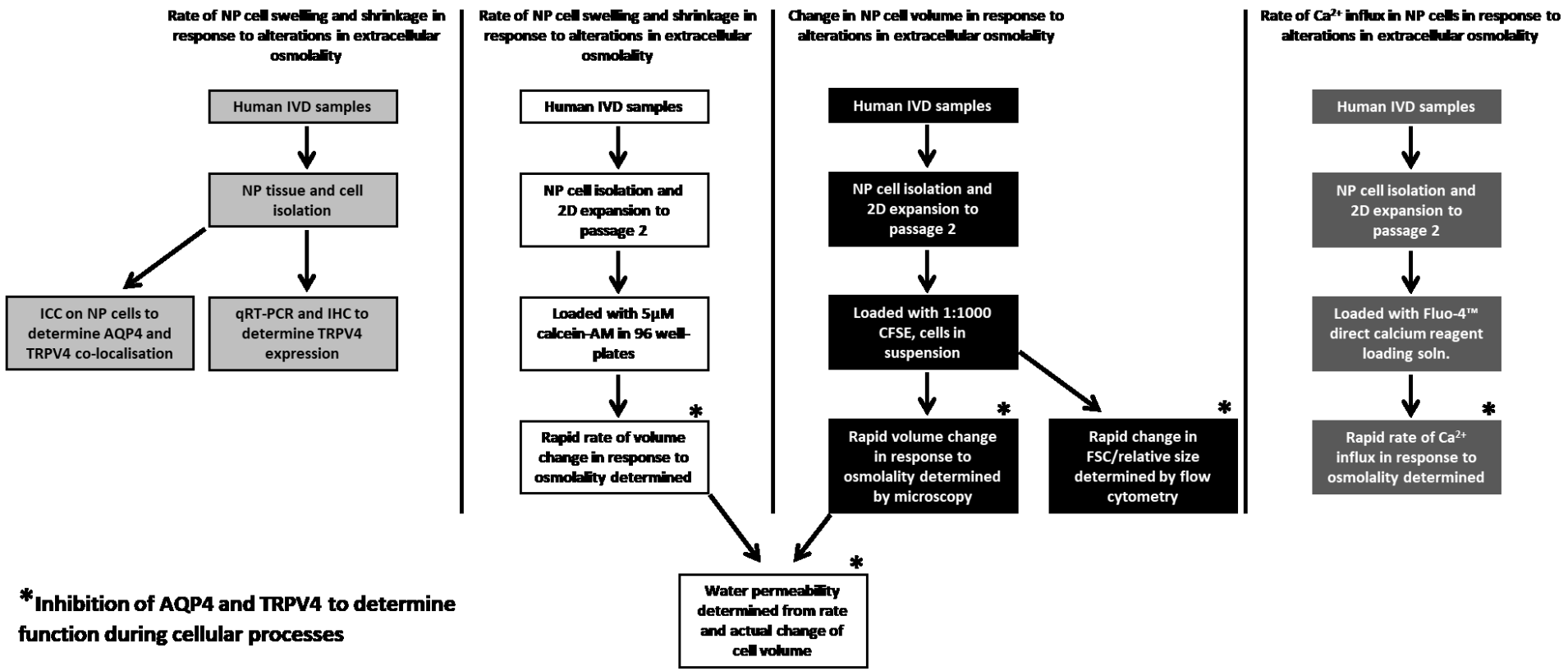

Figure 4.2. Experimental design of methods used in this chapter.

4.2.2 Human Tissue, NP cell extraction and culture

Human IVD tissue was obtained with ethical consent, NP cells extracted and monolayer cultured according to methods outlined in section 2.2**.**

4.2.3 TRPV4 gene expression in native human NP tissue

The gene expression of *TRPV4* was identified from directly extracted RNA, subsequent cDNA synthesis and qRT-PCR of non-degenerate and degenerately graded human NP tissue, using methods outlined in section 2.2. Pre-designed primer/probe mix for human *TRPV4* gene (Hs01099348_m1, Life Technologies) was used and normalised to GAPDH and 18s.

4.2.4 TRPV4 protein expression in native human NP tissue

The expression of TRPV4 protein in non-degenerate and degenerately graded human NP tissue was assessed using IHC as outlined in section 2.2.7. Slides were blocked in 1% (w/v) BSA in 25% (v/v) goat serum (Abcam) and 75% (v/v) TBS. Using rabbit polyclonal primary antibody against TRPV4 (1:200, ab94868, Abcam) and goat anti-rabbit IgG (H&L) (Biotin) secondary antibody (1:500, ab6720, Abcam).

4.2.5 Immunofluorescence

Human NP cells were seeded into chamber slides and immunofluorescence protocols were performed as described in section 2.2.8. To determine potential co-localisation of TRPV4 and AQP4, dual immunostaining was performed by incubating fixed NP cells with rabbit polyclonal antibody against TRPV4 (1:200, ab94868, Abcam) and mouse monoclonal antibody against AQP4 (1:200, ab9512, Abcam). During secondary antibody staining, fixed cells were incubated with goat anti-rabbit IgG (H +L)

cross-adsorbed, Alexa Fluor® 488 (1:500, A-11008, Invitrogen) and goat anti-mouse IgG (H+L) cross-adsorbed, Alexa Fluor® 633 (1:500, A-21050, Invitrogen). Staining and co-localisation images were captured with a LSM 800 confocal microscope (Zeiss) using Zen software (Zeiss).

4.2.6 Rate of human NP cell swelling and shrinkage

Human NP cells were seeded into black-walled 96-well plates (Corning) at a density of $1x10^4$ cells/well for 48h prior to experiments. Calcein, AM (C1430, Invitrogen) stock at 5mM in DMSO was produced. Cells were loaded with 5µM calcein, AM (1:1000 from stock) in standard culture media for 90min at 37°C. After calcein incubation, cells were washed twice with standard culture media, a final volume of 75µL standard culture media was added per well and cells were allowed to equilibrate to new media for at least 5min at 37°C. Prior to experiments, protocols to measure the rapid rate of change in calcein fluorescence (Figure 4.3) within cells treated with altered osmolality media were set up on a CLARIOstar plate reader (BMG Labtech). Utilising the well mode to detect fluorescent intensity, protocols was set up with a preset of calcein optical settings (ex. 483-14, em. 530-30). Two kinetic windows were setup: a baseline reading of 5s (time -5s to 0s) at 50ms intervals, followed by injection (at time 0s) of 75µL osmotically altered media and a final kinetic window reading for 50s (0s - 45s) at 50ms intervals (total of 1000 intervals). Protocol setup and timing is shown in Figure 4.4.

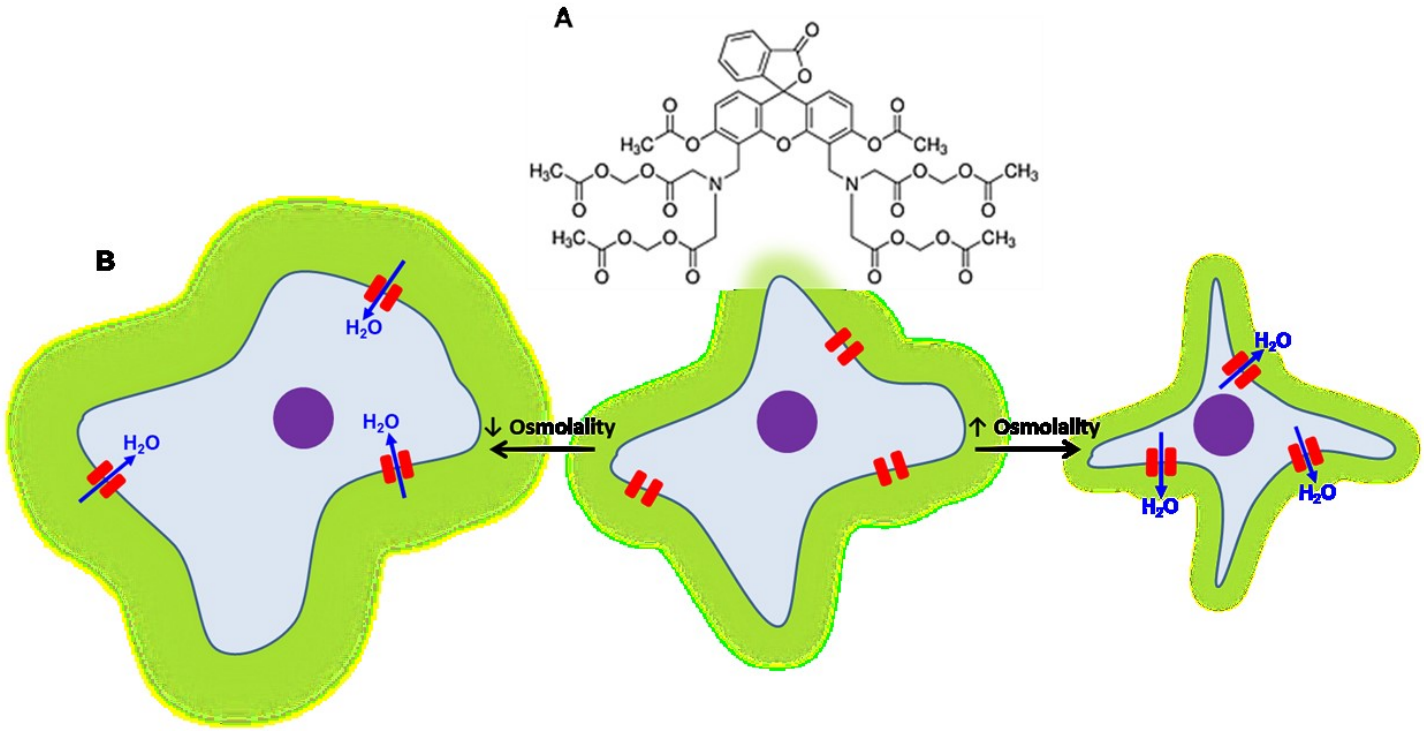

Figure 4.3. Mechanism of calcein-AM fluorescence in response to cell size. (A) Calcein-AM structure. (B) The fluorescence of intracellular calcein is dependent on its relative concentration within the cell. At higher intracellular concentrations, when the cell shrinks in response to hyperosmolality, calcein undergoes self-quenching; at lower intracellular concentrations, when the cell swells in response to hypo-osmolality, calcein fluorescence increases. These rapid changes in calcein fluorescence can be recorded on a plate reader and the rate of cell volume change determined (Fenton *et al.*, 2010). The process of calcein self-quenching is not completely understood, but it may depend on dye dimerisation, energy transfer to non-fluorescent dimers and collisional quenching interactions between dye monomers (Chen and Knutson, 1988).

A

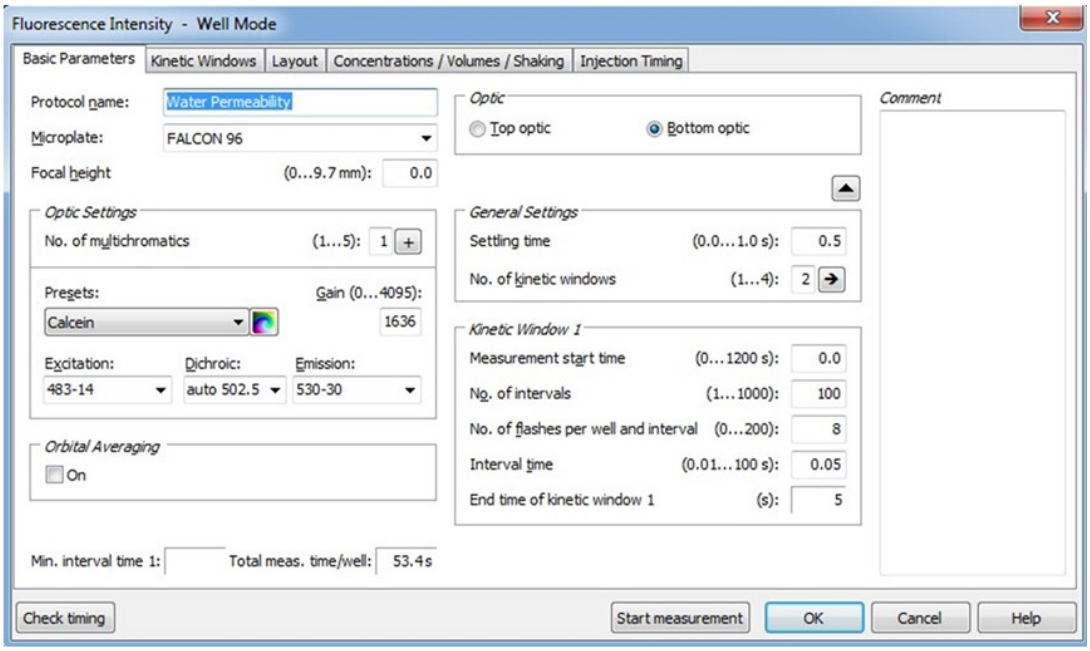

B

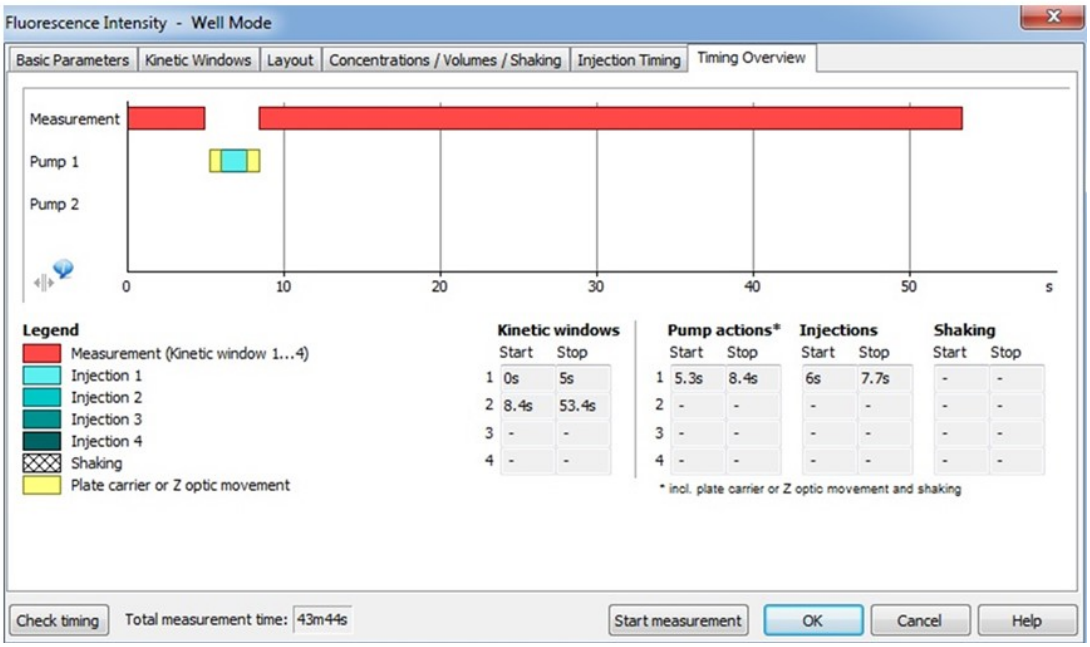

Figure 4.4. Plate reader parameters. (A) Basic parameters of protocol to determine rapid rate of change in calcein fluorescence using a CLARIOstar plate reader (BMG Labtech). (B) Timing overview of kinetic windows and injection within protocol to determine rapid rate of change in calcein fluorescence using a CLARIOstar plate reader (BMG Labtech).

The protocol temperature was set to 37°C and the plate reader injector and tubing was primed with an appropriate amount of treatment media prior to experiments. The production of treatment media from standard culture media is outlined in Table 4.1.

Treatment media (mOsm/kg)	Production of treatment	Final mOsm/kg once injected onto cells
125	38.5%(v/v) dH_2O	225
325	Nothing added - control	325
525	200mM Sucrose	425
725	400mM Sucrose	525

Table 4.1 Production of the final osmotically altered treatment media, within a physiological range, to induce NP cell swelling and shrinkage when 75µL is injected into wells containing 75µL of standard culture media. All media used in experiments was phenol red-free.

Plates were loaded into the plate reader and protocols were performed on NP cells from 3 patients in triplicate to determine the rate of human NP cell swelling and shrinkage in response to physiological alterations in extracellular osmolality. Experiments were repeated after 1h incubation of NP cells (already seeded into 96-well plates at $1x10^4$ cells/well) with 300µM AQP4 inhibitor (AQP4i) (TGN 020, Tocris) or 4.8µM TRPV4 inhibitor (TRPV4i) (HC-067047, Sigma-Aldrich) to determine the function of these channels on the rate of NP cell swelling and shrinkage. During inhibition experiments, all washes and treatment injections were performed with media containing 300µM AQP4i or 4.8µM TRPV4i when appropriate. Relative fluorescence of calcein (F_1/F_0) over time (s) curves were plotted and the rate of the change in F_1/F_0 was determined by fitting plateau followed by one phase association/decay nonlinear regression analysis to curves using GraphPad Prism v7.03 software.

4.2.7 Cell size determination

Human NP cells (from 3 individual patients in triplicate) were trypsinised and resuspended in standard culture media at a density of $2x10^5$ cells/mL. Live cells were labelled with CFSE - Cell Labelling Kit (1:1000, ab113853, Abcam) for 10min at RT protected from light and washed before being resuspended in 1mL standard culture media (without phenol red). An equivalent amount (1mL) of altered osmolality treatment media (Table 4.1) was added to cells for approx. 30s (time taken for calcein F_1/F_0 curves to plateau) before forward scatter (FSC) (proportional to cell size) was determined on 10,000 events using a FACSCalibur flow cytometer (BD Biosciences) and CellQuest Pro v5.2.1 software (BD Biosciences). Furthermore, to determine actual cell size after 30s treatment, cells at a density of $2x10^5$ cells/mL were added to Countess™ cell counting chamber slides (Invitrogen) and images of live (CFSE stained), suspended NP cells were captured using a BX60 fluorescent microscope (Olympus) using cellSens software (Olympus). The area of at least 200 cells/repeat from 2D images was determined using ImageJ; cells that had an aspect ratio of ≥1.5 and an area of ≤100 pixels were excluded to remove doublets/clumps of cells and cell debris. Size calculations of cells in suspension relied on the presumption that all suspended cells used for the analysis of 2D and 3D cell size had spherical morphology. Cell size was calculated from a series of equations, firstly to determine the radius of cells from 2D area measurements (Equation 4.1).

$$r = \sqrt{\frac{A}{\pi}}$$

Equation 4.1. Radius of a circle. Where *r* = radius, *A* = area, *π* = pi.

Once the average radius of cells was determined this was used to determine the average cell surface area (Equation 4.2) and average cell volume (Equation 4.3) for each repeat experiment.

$$A = 4\pi r^2$$

Equation 4.2. Surface area of a sphere. Where *A* = surface area, *π* = pi, *r* = radius.

$$V = \frac{4}{3}\pi r^3$$

Equation 4.3. Volume of a sphere. Where *V* = volume, *π* = pi, *r* = radius.

Both cell surface area and cell volume measurements, along with the rate of change in F_1/F_0 over time, were used to determine the water permeability of human NP cells in response to altered extracellular osmolality (Section 4.2.8). All cell size determination experiments were also performed after 1h incubation of NP cells with either AQP4i (300µM TGN 020, Tocris) or TRPV4i (4.8µM HC-067047, Sigma-Aldrich), which were also added to each wash, resuspension and CFSE incubation steps throughout the experimental procedure.

4.2.8 Water permeability determination

Using values calculated from the rate of NP cell swelling and shrinkage (section 4.2.6) and NP cell size determination (section 4.2.7), the water permeability of human

NP cells in response to alterations in extracellular osmolality, and the potential involvement of AQP4 and TRPV4, was determined using Equation 4.4.

$$Pf = \frac{K \times [V0 - Vmin^2]}{A \times \Delta\pi \times Vw}$$

Equation 4.4. Water permeability. Where *Pf* = water permeability, *K* = rate constant for one phase decay/association, *V*0 = starting cell volume, $Vmin^2$ = cell volume after treatment, *A* = cell surface area, *Δπ* = applied osmotic gradient, *Vw* = partial molar volume of water ($1.8x10^{-5}m^3$/mol). As [*V*0 - $Vmin^2$] reflects the total cell volume change in response to the change in extracellular osmolality, *K* x [*V*0 - $Vmin^2$] describes the theoretical fraction of total volume change per one x-axis unit change (50ms) at the initial rate of volume change. Adapted from (Fenton *et al.*, 2010).

Average *Pf* of human NP cells, for each patient, was calculated in response to physiological changes in osmolality (325mOsm/kg → 225, 425 or 525mOsm/kg) with or without AQP4i and TRPV4i. All *Pf* values were normalised to the average *Pf* of controls in the absence of inhibitors, to determine the effect of AQP4i and TRPV4i on the *Pf* of human NP cells at each extracellular osmolality change.

4.2.9 Fluo-4 Direct™ Calcium influx assay

Calcium influx into human NP cells in response to extracellular osmolality alterations was measured using Fluo-4 Direct™ calcium assay kit (F10471, Invitrogen). Human NP cells were seeded into black-walled 96-well plates (Corning) at a density of $1x10^4$ cells/well for 48h prior to experiments. Fluo-4 Direct™ (2x) calcium reagent loading solution (Invitrogen) was prepared following the manufacturer's guidelines: 10mL Fluo-4 Direct™ calcium assay buffer was added to one bottle of Fluo-4 Direct™ calcium reagent (component A). Media was aspirated from cells and an equal volume of Fluo-4 Direct™ (2x) calcium reagent loading solution (37.5µL) and standard culture

media (37.5µL) was added to cells, for a total volume of 75µL per well. Plates were incubated for 1h at 37°C protected from light. Following incubation, plates were ready for experimental use without removing Fluo-4 Direct™ (2x) calcium reagent loading solution and standard culture media from wells. Calcium influx into human NP cells in response to physiological alterations of extracellular osmolality (325mOsm/kg →225, 325, 425 or 525mOsm/kg) was performed on a CLARIOstar plate reader (BMG Labtech) following the same protocol outlined in section 4.2.6, with optic settings changed to excitation at 494nm and emission at 516nm. Treatment media (Table 4.1) injected into wells after the first kinetic window (-5s to 0s). Experiments were also performed after 1h incubation of cells with either AQP4i (300µM TGN 020, Tocris) or TRPV4i (4.8µM HC-067047, Sigma-Aldrich), simultaneously added to cells with Fluo-4 Direct™ (2x) calcium reagent loading solution and media. During AQP4i and TRPV4i experiments, inhibitors were also added to treatment media prior to injection.

4.2.10 Statistical Analysis

TRPV4 protein expression in human NP tissue (assessed by IHC) was found to be non-parametric, therefore Kruskall-Wallis with Dwass-Steel-Critchlow-Fligner post hoc analysis test was used to identify significant differences between expression across grades of degeneration. The rate of cell swelling/shrinkage (determined by calcein fluorescence) was investigated in triplicate in human NP cells from 3 patients. Data was non-parametric and to determine significance between paired samples from the same patient across 3 treatment groups (CTR, AQP4i and TRPV4i), the Friedman test was used with Conover post hoc analysis. Cell volume data was non-parametric, therefore Kruskall-Wallis with Dwass-Steel-Critchlow-Fligner post hoc analysis test was used to identify significant differences in cell volume, at a fixed osmolality, when comparing

treatment groups (CTR, AQP4i and TRPV4i). The Friedman test was used to determine significance between the geometric mean of the FSC, and the *Pf*, from paired patient samples when comparing 3 treatment groups (CTR, AQP4i and TRPV4i), at a fixed osmolality. Ca^{2+} influx data was non-parametric, therefore Kruskall-Wallis with Dwass-Steel-Critchlow-Fligner post hoc analysis test was used to identify significant differences in the max-min F_1/F_0 and time taken to reach maximum F_1/F_0 in NP cells treated with different osmolalities, or inhibitors (CTR, AQP4i and TRPV4i) at 225mOsm/kg.

4.3 Results

4.3.1 Expression of TRPV4 within native human NP tissue

TRPV4 was expressed at both gene and protein level within native human NP tissue (Figure 4.5). The relative gene expression of TRPV4 did not change significantly during IVD degeneration ($p \leq 0.05$) (Figure 4.5A). The majority of NP cells expressed TRPV4 protein in native tissue, however, immunopositivity was unaffected by IVD degeneration (Figure 4.5B) (IgG controls, Appendix VIII). TRPV4 was also still expressed by NP cells extracted from human IVD tissue at passage 2. (Figure 4.5C) Within 2D cultured human NP cells TRPV4 was found to co-localise with AQP4 (Figure 4.5C), potentially suggesting related functions shared between these transmembrane channel proteins (IgG controls, Appendix VIII).

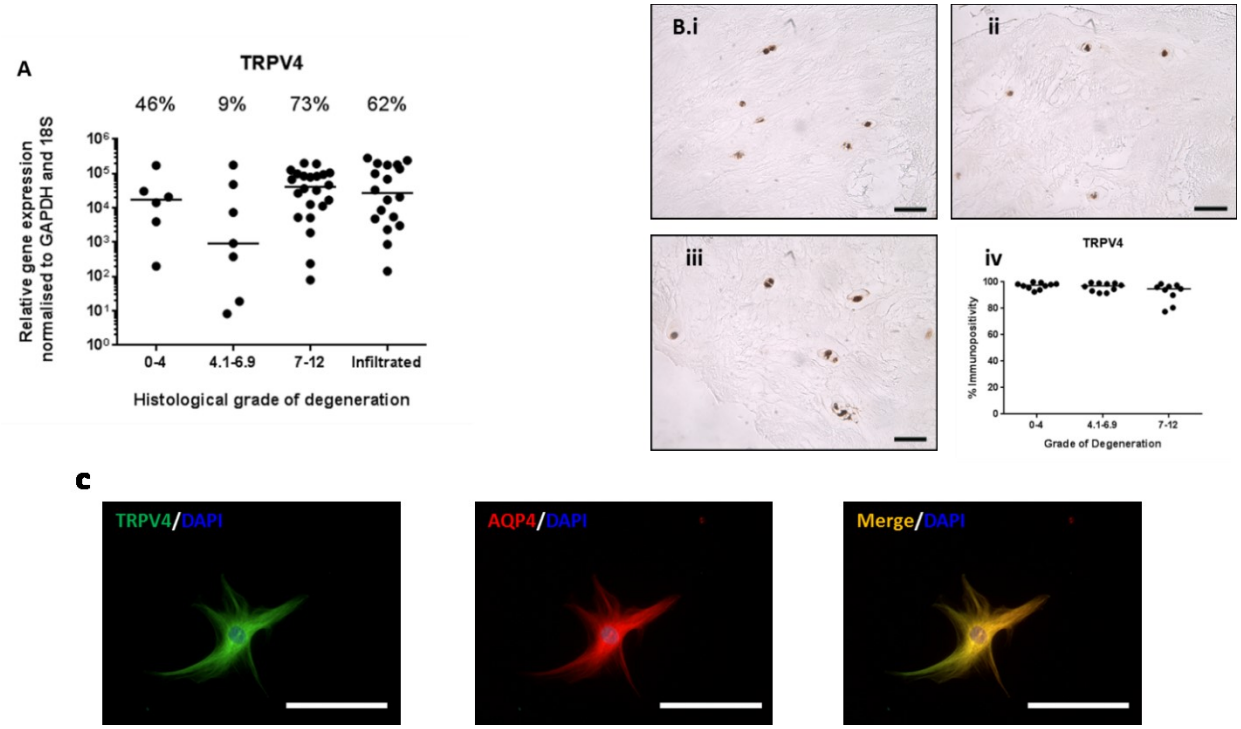

Figure 4.5. TRPV4 expression within native human NP tissue and cultured NP cells. (A) Gene expression of TRPV4. Each point indicates an individual patient. (B) Immunopositivity results determining the percentage of cells within NP tissue expressing TRPV4. Two-hundred cells per patient sample were counted as positive or negative (B.iv). Each point represents an individual patient. NP tissue was graded: non-degenerate (0-4, B.i), moderately-degenerate (4.1-6.9, B.ii) and severely-degenerate (7-12, B.iii). Positive staining for TRPV4 is indicated by brown staining and cell nuclei are counterstained blue with Mayer's haematoxylin. (C) Immunofluorescence highlighting the expression of TRPV4 (green) in 2D cultured human NP cells co-localises with AQP4 (red). Cell nuclei counterstained with DAPI (blue). Images taken at 63x objective magnification, using a LSM 800 confocal microscope (Zeiss). Scale bar 20µm. Statistical significance determined using Kruskal-Wallis test * = $p \leq 0.05$.

4.3.2 Rate of NP cell swelling and shrinkage in response to extracellular osmolality

The relative fluorescence (F_1/F_0: F_1 = fluorescence at time n / F_0 = fluorescence at baseline) of intracellular calcein was altered, in real-time, when no-inhibition control NP cells were exposed to altered extracellular osmolality (225, 425 and 525mOsm/kg), after 5s baseline readings in standard culture media (325mOsm/kg) (Figure 4.6A). When control media (325mOsm/kg) was added after baseline, the F_1/F_0 was unchanged (Figure 4.6A). Incubation with AQP4i (300µM, TGN 020) or TRPV4i (4.8µM, HC-067047) altered the real-time change in intracellular calcein F_1/F_0 when NP cell were exposed to 225mOsm/kg (Figure 4.5B.i), 325mOsm/kg (Figure 4.6B.ii), 425mOsm/kg (Figure 4.6B.iii) and 525mOsm/kg (Figure 4.6B.iv) treatments (Determination of rate of cell volume change, Appendix IX and X).

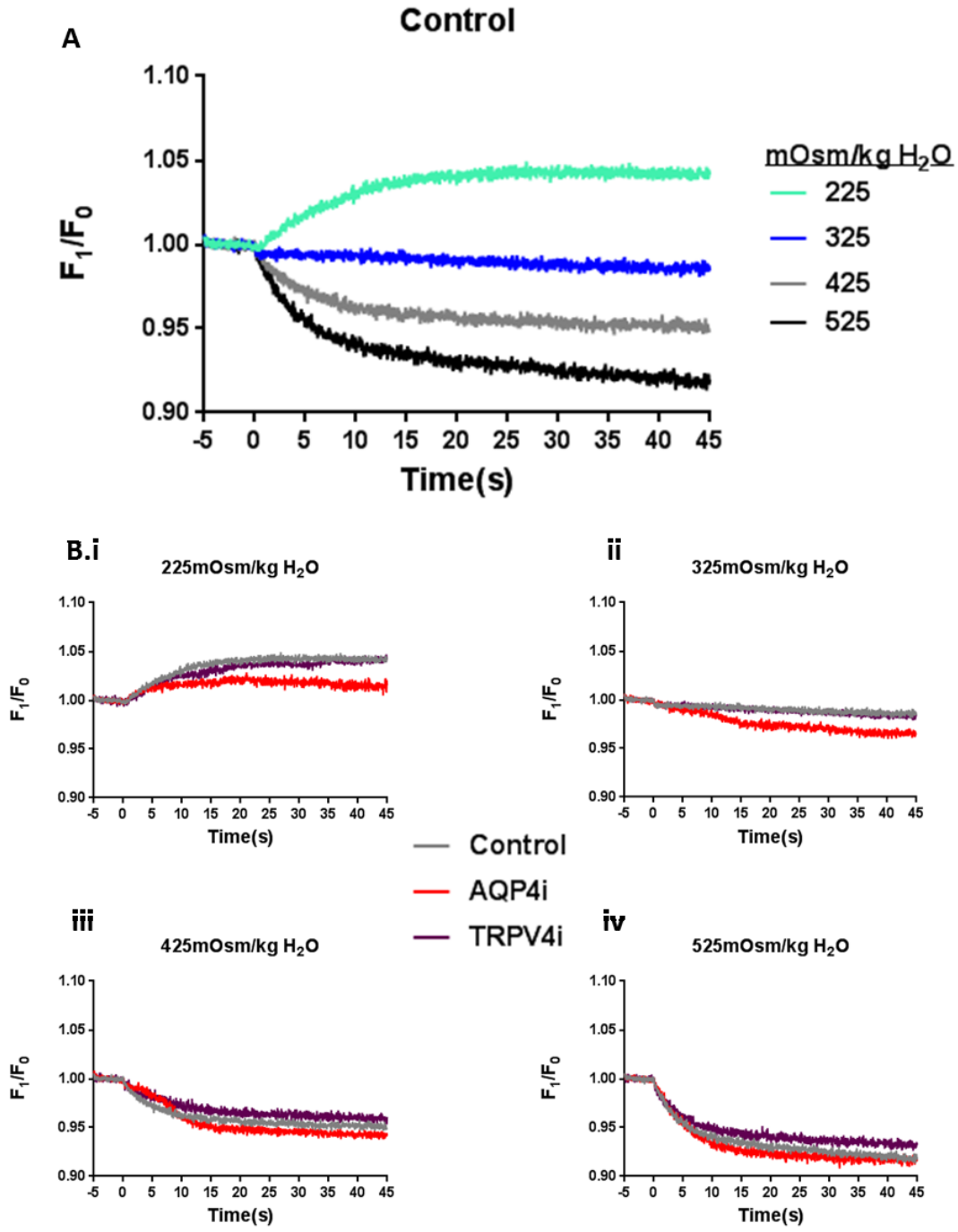

Figure 4.6. The real-time rate of change in the relative fluorescence (F_1/F_0) of calcein, when NP cells are exposed to physiological alterations in extracellular osmolality (A). Baseline fluorescence of calcein-loaded NP cells was recorded for 5s (-5s - 0s), before injection of altered osmolality media and change in calcein fluorescence recorded for a further 45s (0s - 45). Change in F_1/F_0 was recorded in control cells and NP cells treated with AQP4i (300µM, TGN 020) or TRPV4i (4.8µM, HC-067047) for 1hr prior to injection with (B.i) 225, (B.ii) 325, (B.iii) 425 and (B.iv) 525mOsm/kg.

The rate of change in fluorescence (K Δ F_1F_0) at 225mOsm/kg treatment was significantly reduced in AQP4i and TRPV4i treated NP cells when compared to no-inhibition control NP cells (CTR) ($p \leq 0.05$) (Figure 4.7A). At 425mOsm/kg treatment K Δ F_1F_0 was significantly decreased in AQP4i and TRPV4i compared to CTR ($p \leq 0.05$) (Figure 4.7B). At 525mOsm/kg treatment K Δ F_1F_0 was significantly decreased in TRPV4i compared to CTR ($p \leq 0.05$) (Figure 4.7C).

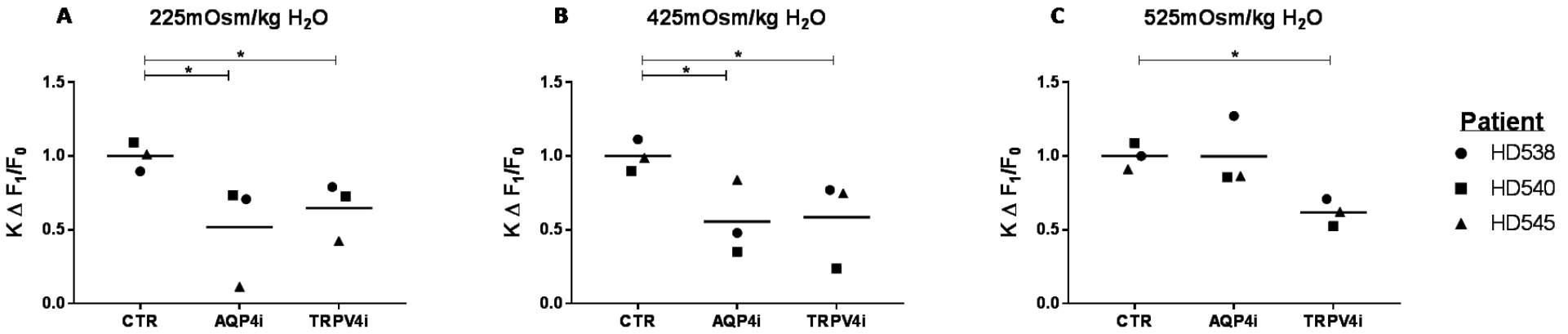

Figure 4.7. The rate of change in intracellular calcein fluorescence during alterations to extracellular osmolality. The rate of change in relative fluorescence ($K \Delta F_1/F_0$) was determined from curves showing the real-time change in fluorescence of calcein, which is proportional to cell swelling and shrinkage in response to alterations in extracellular osmolality. Rate values were extrapolated by fitting plateau followed by one-phase association (225mOsm/kg)/ decay (425, 525mOsm/kg) non-linear regression analysis to curves. $K \Delta F_1F_0$ was determined for 3 patient sample NP cells in triplicate, average values are plotted and normalised against no inhibition controls (CTR) for each treatment: (A) 225, (B) 425 and (C) 525mOsm/kg. Extracellular osmolality was altered for each treatment from a starting osmolality of 325mOsm/kg. Statistical significance determined using Freidman test * = $p \leq 0.05$.

4.3.3 Change in NP cell volume in response to extracellular osmolality alterations

The volume of AQP4i and TRPV4i treated human NP cells exposed to 225mOsm/kg was significantly reduced, when compared to no-inhibition control (CTR) NP cells ($p \leq 0.05$) (Figure 4.8A). The volume of TRPV4i treated NP cells was significantly reduced compared to CTR cells at 325mOsm/kg ($p \leq 0.05$) (Figure 4.8B). AQP4i and TRPV4i failed to significantly alter cell volume of NP cells, compared to CTR, when exposed to 425 (Figure 4.8C) and 525mOsm/kg (Figure 4.8D) (CFSE-loaded NP cells, Appendix XI).

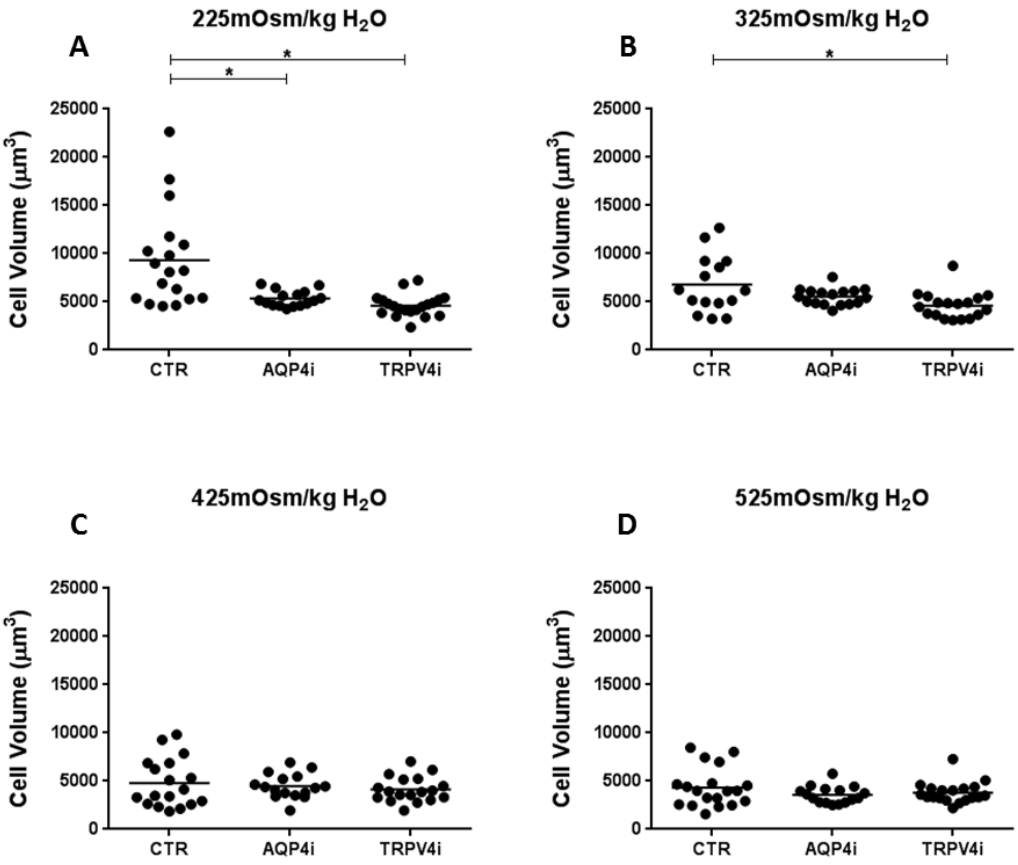

Figure 4.8. NP cell volume changes in response to altered extracellular osmolality. Effect of AQP4i (1h, 300µM, TGN 020) and TRPV4i (1h, 4.8µM, HC-067047) on NP cell volume, when compared to no inhibition controls (CTR), after standard culture media (325mOsm/kg) was altered to a final osmolality of 225 (A), 325 (B), 425 (C) and 525mOsm/kg (D). Cell volume was calculated from the area of 2D images of at least 200 CFSE-stained live NP cells in suspension from 3 patients in triplicate. Each point represents an individual image used for the analysis of cell volume. Statistical significance determined using Kruskal-Wallis test * = $p \leq 0.05$.

The forward scatter of the geometric mean (FSC-Geo. Mean) of human NP cells was altered when extracellular osmolality was decreased or increased from control osmolality (325mOsm/kg) (Figure 4.9 and 4.10). Pre-treatment with AQP4i (Figure 4.9) and TRPV4i (Figure 4.10) also altered FSC-Geo. Mean at 225 (Figure 4.9A and 4.10A), 325 (Figure 4.9B and 4.10B), 425(Figure 4.9C and 4.10C) and 525mOsm/kg (Figure 4.9D and 4.10D) (Flow cytometry gating, Appendix XI).

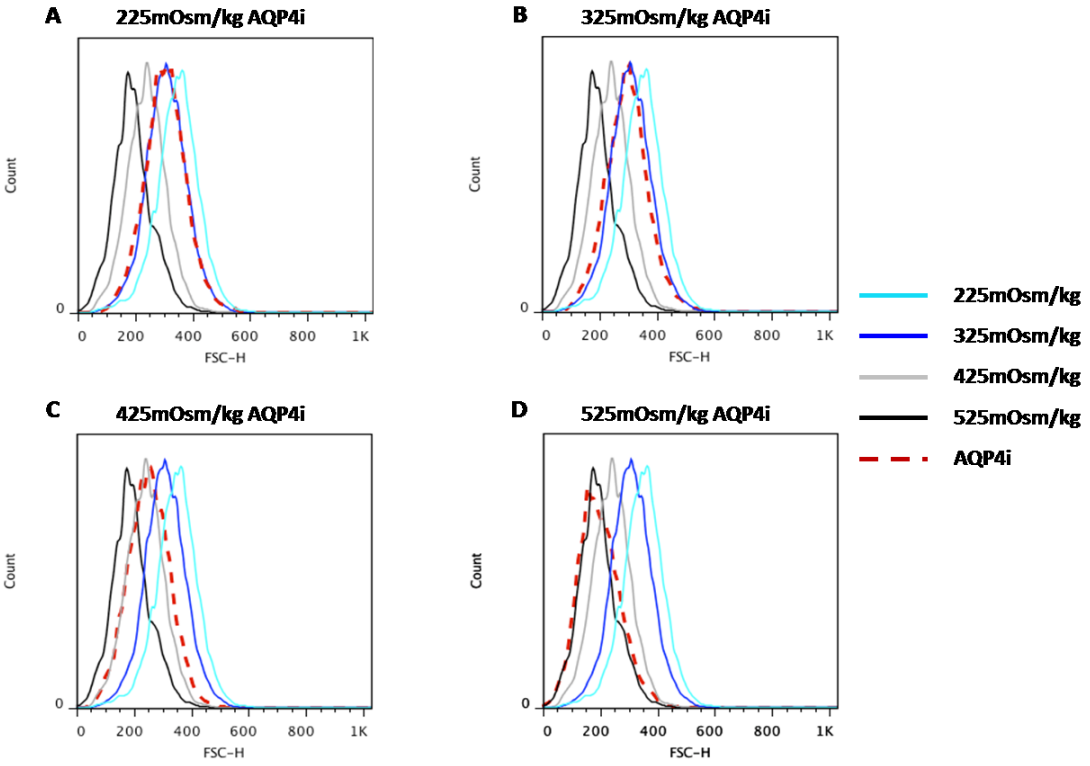

Figure 4.9. Flow cytometry analysis of NP cell geometric mean of forward scatter (FSC-H) changes in response to extracellular osmolality changes and the effect of AQP4i (1h, 300µM, TGN 020) at 225 (A), 325 (B), 425 (C) and 525mOsm/kg (D). Histograms show representative experiments from an individual patient (HD540).

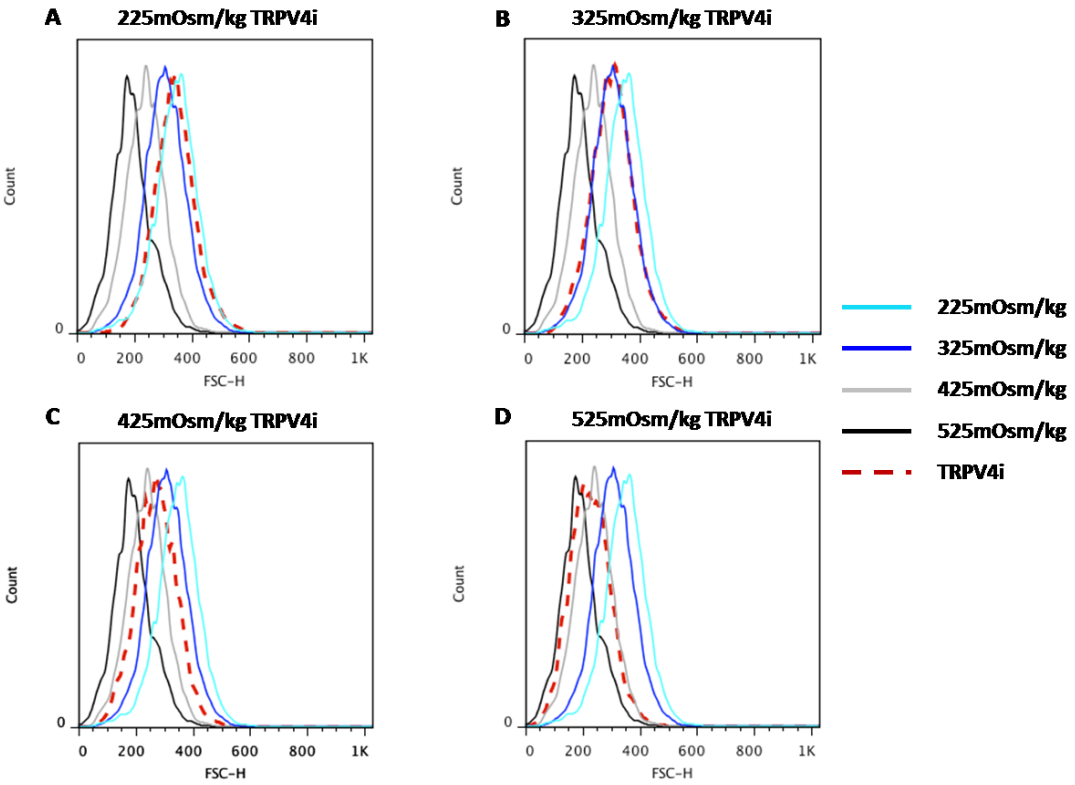

Figure 4.10. Flow cytometry histogram analysis of NP cell geometric mean of forward scatter (FSC-H) changes in response to extracellular osmolality changes and the effect of TRPV4i (1h, 4.8µM, HC-067047) at 225 (A), 325 (B), 425 (C) and 525mOsm/kg (D). Histograms show representative experiments from an individual patient (HD540).

FSC-Geo. Mean of AQP4i and TRPV4i treated NP cells was significantly reduced when compared to FSC-Geo. Mean of CTR NP cells at 225mOsm/kg treatment ($p \leq 0.05$) (Figure 4.11A). FSC-Geo. Mean was also significantly reduced in TRPV4i treated cells at 325mOsm/kg treatment, when compared with CTR NP cells ($p \leq 0.05$) (Figure 4.11B). Treatment with 425 (Figure 4.11C) or 525mOsm/kg (Figure 4.11D) media failed to significantly alter the FSC-Geo. Mean of AQP4i or TRPV4i treated NP cells when compared to CTR.

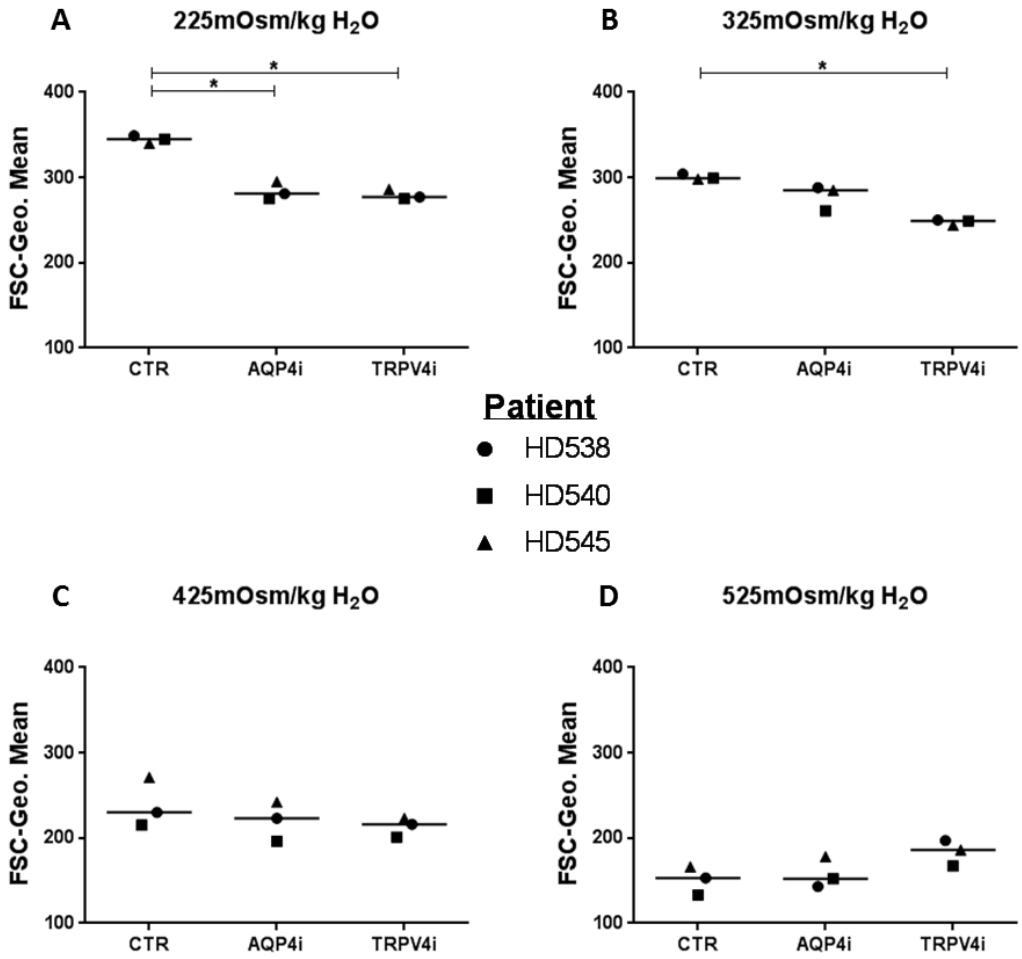

Figure 4.11. Forward scatter of geometric mean (FSC-Geo. Mean) measurements of NP cells exposed to extracellular osmolality changes. Average FSC-Geo. Mean is determined for each patient after NP cells are exposed to (A) 225, (B) 325, (C) 425 and (D) 525mOsm/kg. Prior to treatment, media osmolality was 325mOsm/kg. At each treatment osmolality, the FSC-Geo. Mean of AQP4i (1h, 300µM, TGN 020) and TRPV4i (1h, 4.8µM, HC-067047) treated cells was compared to no inhibition control cells (CTR). Statistical significance determined using Freidman test * = $p \leq 0.05$.

4.3.4 Effect of AQP4 and TRPV4 inhibition on the water permeability of human NP cells

The normalised water permeability of human NP cells was significantly reduced with AQP4i and TRPV4i, when compared with no-inhibition control cells, at both 225mOsm/kg ($p \leq 0.05$) (Figure 4.12A) and 425mOsm/kg ($p \leq 0.05$) (Figure 4.12B). At 525mOsm/kg treatment, the normalised water permeability of TRPV4i treated NP cells was also significantly reduced when compared to no-inhibition control cells ($p \leq 0.05$) (Figure 4.12C). AQP4i did not significantly change the water permeability of human NP cells, when compared to no-inhibition controls, at 525mOsm/kg treatment (Figure 4.12C).

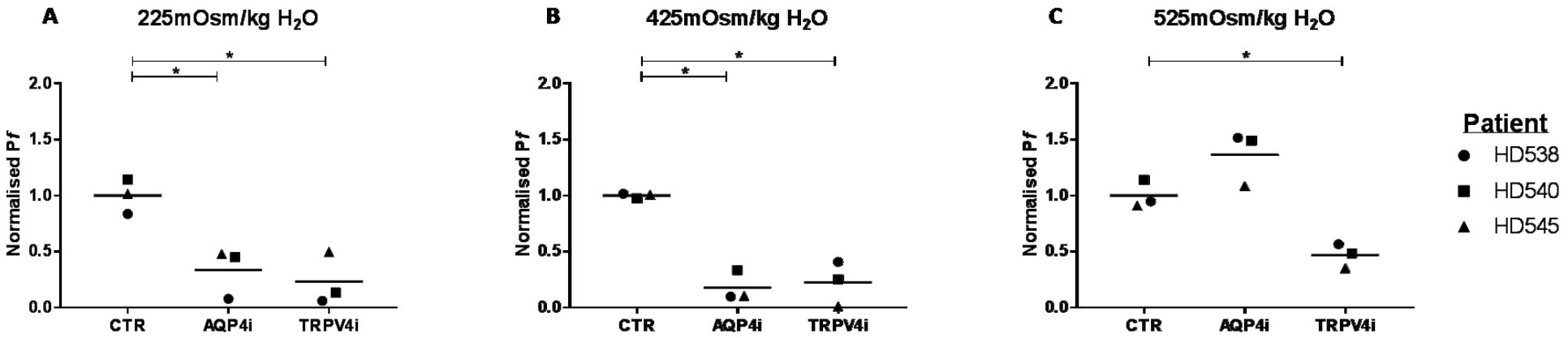

Figure 4.12. Water permeability of human NP cells in response to extracellular osmolality alterations and the effect of AQP4 and TRPV4 inhibition. Water permeability (P*f*) is calculated using the rate of change in calcein fluorescence ($K \Delta F_1F_0$), the actual change in cell volume and cell surface area, after alterations to extracellular osmolality, and applied to Equation 4.4. All P*f* values were normalised to the average of no inhibition controls (CTR) and averaged per patient. The normalised P*f* of AQP4i (1h, 300µM, TGN 020) and TRPV4i (1h, 4.8µM, HC-067047) was compared to CTR at (A) 225, (B) 425 and (C) 525mOsm/kg treatments. Prior to treatment, media osmolality was 325mOsm/kg. Statistical significance determined using Freidman test * = $p \leq 0.05$.

4.3.5 Human NP cell Ca^{2+} influx in response to altered extracellular osmolality

The F_1/F_0 of intracellular Fluo-4 direct, relative to Ca^{2+}, was altered in real-time, when NP cells were exposed to altered extracellular osmolality (225, 325, 425 and 525mOsm/kg), after 5s baseline readings in standard culture media (325mOsm/kg) (Figure 4.13A). The max-min F_1/F_0 of intracellular Fluo-4 direct was significantly increased in 225mOsm/kg treated NP cells, compared to all other osmotic treatments ($p \leq 0.05$) (Figure 4.13B). The max-min F_1/F_0 of intracellular Fluo-4 direct was significantly increased in 325 and 425mOsm/kg treated NP cells, compared to 525mOsm/kg treated NP cells ($p \leq 0.05$) (Figure 4.13B). The time taken to reach maximum F_1/F_0 of intracellular Fluo-4 direct in 225mOsm/kg treated NP cells was significantly decreased when compared to all other osmotic treatment groups ($p \leq 0.05$) (Figure 4.13C).

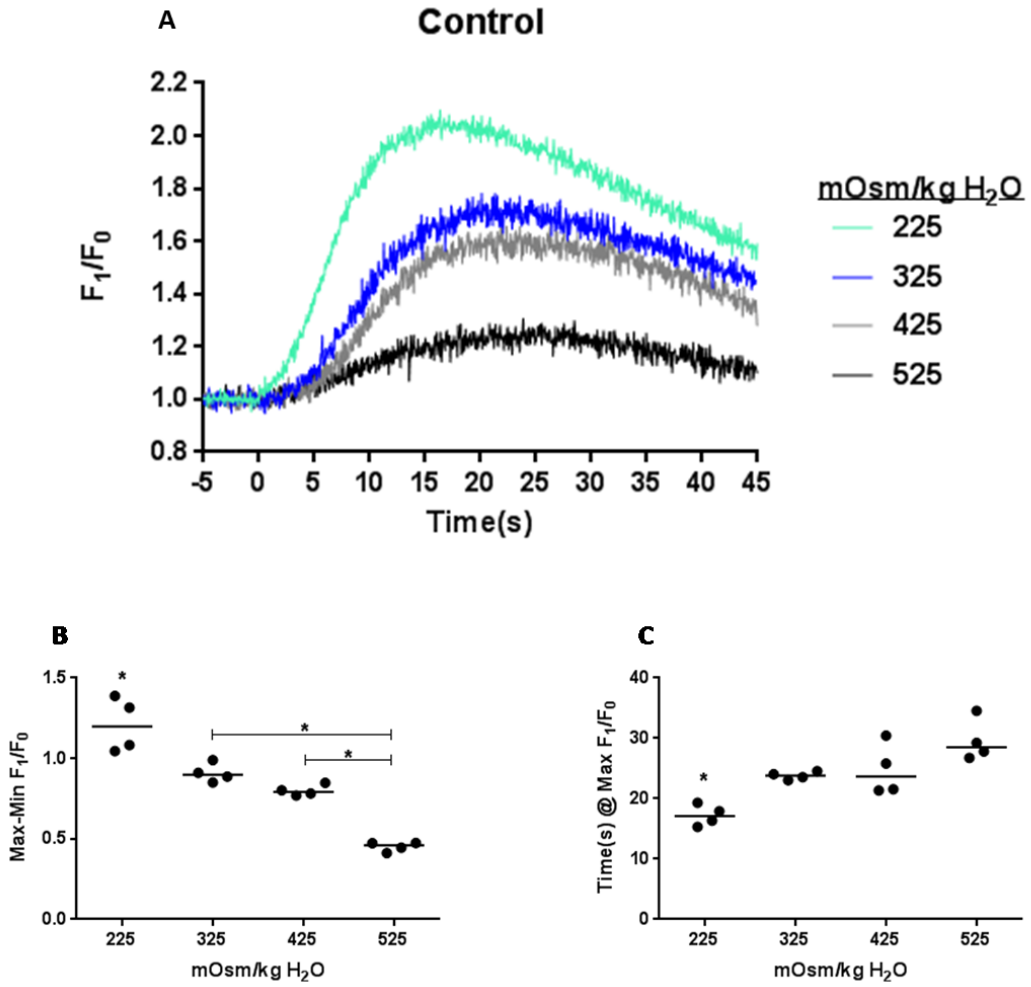

Figure 4.13. Ca^{2+} influx in human NP cells when exposed to altered extracellular osmolality. (A) Fluo-4 direct assay (Invitrogen) was used to measure the rate of Ca^{2+} influx into human NP cells. Baseline fluorescence of calcein-loaded NP cells was recorded for 5s (-5s - 0s), before injection of altered osmolality media and change in relative Fluo-4 fluorescence (F_1/F_0), dependent on the intracellular Ca^{2+} concentration, was recorded for a further 45s (0s - 45). (B) Max-min F_1/F_0 values for Ca^{2+} influx at each treatment osmolality, indicating total Ca^{2+} influx over time. (C) Time (s) taken for max F_1/F_0 (Ca^{2+} influx) to be reached in human NP cells at each treatment osmolality. Statistical significance determined using Kruskal-Wallis test * = $p \leq 0.05$.

4.3.6 Effect of AQP4 and TRPV4 inhibition on hypo-osmotic Ca^{2+} influx in human NP cells

The F_1/F_0 of intracellular Fluo-4 direct, relative to Ca^{2+}, was altered in real-time, when NP cells were exposed to 225mOsm/kg extracellular osmolality after AQP4i, TRPV4i or CTR treatment, and 5s baseline readings in standard culture media (325mOsm/kg) (Figure 4.14A). The max-min F_1/F_0 of intracellular Fluo-4 direct was significantly increased in CTR treated NP cells, compared to AQP4i and TRPV4i treated NP cells ($p \leq 0.05$) (Figure 4.14B). The time taken to reach maximum F_1/F_0 of intracellular Fluo-4 direct in AQP4i treated NP cells was significantly increased when compared to CTR and TRPV4i treated NP cells ($p \leq 0.05$) (Figure 4.14C).

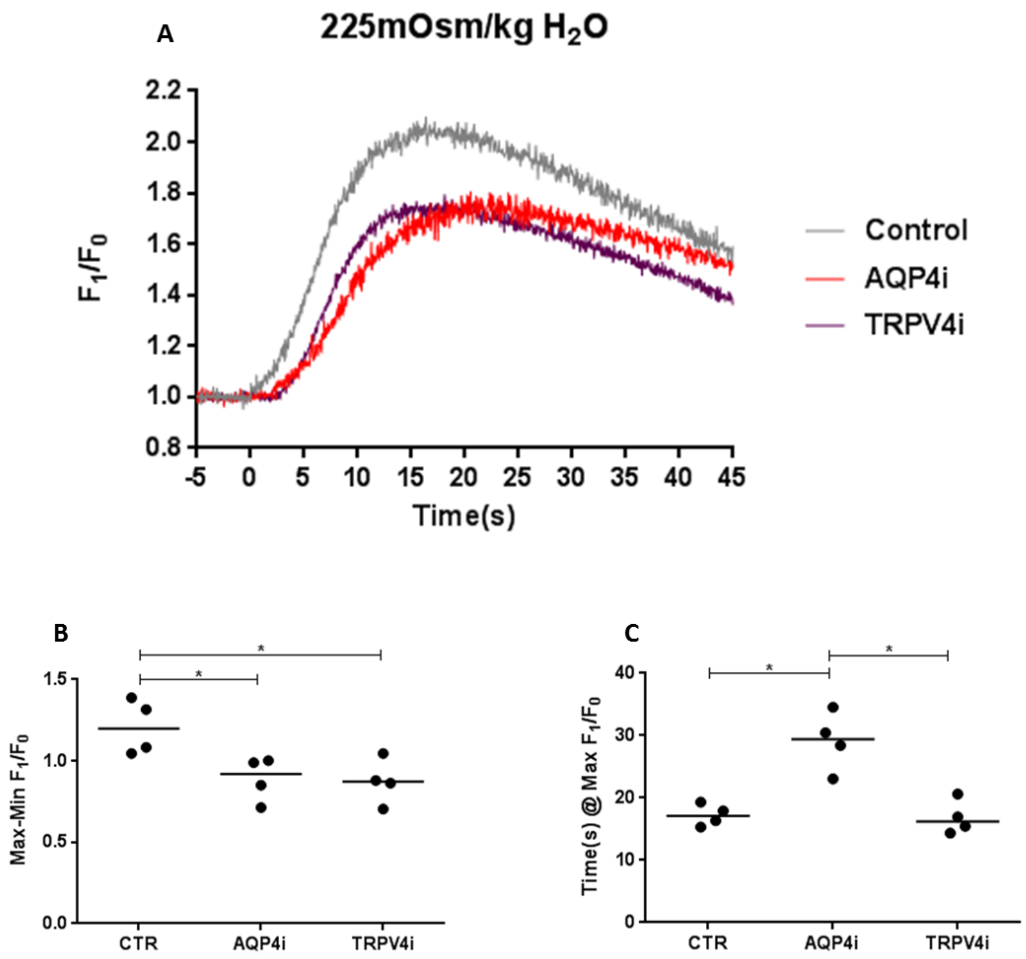

Figure 4.14. Effect of AQP4 and TRPV4 inhibition on the hypo-osmotic induction of Ca^{2+} influx. (A) Fluo-4 direct assay (Invitrogen) was used to measure the rate of Ca^{2+} influx into human NP cells when exposed to hypo-osmotic treatment (225mOsm/kg). Baseline fluorescence of calcein-loaded NP cells was recorded for 5s (-5s - 0s), before injection of 225mOsm/kg media and change in relative Fluo-4 fluorescence (F_1/F_0), dependent on the intracellular Ca^{2+} concentration, was recorded for a further 45s (0s - 45). (B) Max-min F_1/F_0 values for Ca^{2+} influx at 225mOsm/kg.(C) Time (s) taken for max F_1/F_0 (Ca^{2+} influx) to be reached in human NP cells. Change in F_1/F_0 was recorded in control cells (CTR) and NP cells treated with AQP4i (300µM, TGN 020) or TRPV4i (4.8µM, HC-067047) for 1hr prior to injection. Statistical significance determined using Kruskal-Wallis test * = $p \leq 0.05$.

4.4 Discussion

The hyperosmotic environment of the IVD is constantly changing due to diurnal loading, where water is imbibed and then dissipated as the mechanical loading of the spine changes. In physiologically-matched osmolality, matrix expression is increased in NP cells (Wuertz *et al.*, 2007; Neidlinger-Wilke *et al.*, 2012; O'Connell, Newman and Carapezza, 2014), indicating NP cells have adapted their function to the hyperosmotically fluxing environment within the IVD. Therefore, mechanisms must be in place to protect NP cells, and enable their adaptation to hypo- and hypertonic shifts in extracellular osmolality. It is well documented that TonEBP contributes to NP cells' long-term adaptation to hyperosmolality (Chapter 3) and the expression of matrix molecules (Tsai *et al.*, 2006; Hiyama *et al.*, 2009; Johnson, Shapiro and Risbud, 2014b). However, the mechanisms that control the initial response to altered extracellular osmolality, such as the rapid flux of water and ions and changes in cell volume, in NP cells are not completely understood. Especially how hypo-osmotic conditions, observed during IVD degeneration, may impacts these fundamental cellular processes and the overall function of the IVD.

This study identified that NP cells rapidly modulate their cell volume and the rate which volume is changed in response to extracellular osmolality alterations that mimicked the environment of the healthy and degenerate IVD. The magnitude of the rate of cell volume change, actual cell volume change and water permeability responses to extracellular osmolality alterations in NP cells was reliant upon the function of AQP4 and TRPV4. Under hypo-osmotic treatment, AQP4i decreased NP cell water permeability, maximum Ca^{2+} influx and time taken to reach maximum Ca^{2+}

influx; this indicates that during degeneration, when osmolality and AQP4 expression is decreased (Chapter 2), NP cells are no longer adapting to their environment. The expression of TRPV4 in human NP tissue was not sensitive to IVD degeneration and its function was required to maintain water permeability across all osmotic treatments, indicating TRPV4 enables fundamental cellular processes, such as volume regulation, regardless of IVD degeneration. As TRPV4i decreased the water permeability, and AQP4i decreased hypo-osmotic Ca^{2+} influx, in NP cells; this suggests that the function of both channels is linked and may play joint roles during NP cell adaptation to its microenvironment.

4.4.1 NP cell volume change in response to extracellular osmolality

Upon exposure to alterations in extracellular osmolality, cells adapt by altering their volume accordingly via osmotically driven water transport and the activation of regulatory volume changes (Corasanti, Gleeson and Boyer, 1990; Lang *et al.*, 1998). This study has shown that human NP cells are no different; under hypo-osmotic treatment cell volume was increased, and under hyperosmotic treatment, cell volume was reduced. These results may indicate that during IVD degeneration, when osmolality is decreased compared to healthy conditions, human NP cell size increases. Bovine NP cells show a similar trend when exposed to low osmolality (Maidhof *et al*,. 2014) and rabbit NP cell size was also increased after an AF puncture model of degeneration (He *et al.*, 2013), indicating that NP cell size could possibly be used to determine the degenerative state of the IVD.

Fluorescent microscopy was used to quantify the volume of CFSE-labelled NP cells when exposed to altered osmolality. Flow cytometry, specifically shifts in FSC,

was used alongside microscopy to determine how NP cell size was altered. Shifts in FSC have been previously used to determine changes in cell size after osmotic alteration (MacDonald and Zaech, 1982; Sloot, Hoekstra and Figdor, 1988; Adan *et al.*, 2017) and NP cell size has been characterised using the same method (Chen, Yan and Setton, 2006). As results from independently analysed microscopy and flow cytometry experiments on NP cell size both indicate a similar response to osmotic stimuli, this strengthens the observations presented in this study.

However, FSC measurements may not be directly related to the changes in cell size, as it may alter depending on the light scattering properties of different cells (McGann, Walterson and Hogg, 1988; Adan *et al.*, 2017; Yurinskaya *et al.*, 2017), therefore flow cytometry results presented here may only reflect the relative change in NP cell size, rather than the actual change in size. Furthermore, the actual size of human NP cells could not be determined from flow cytometry measurements because the FSC of NP cells could not be integrated with the FSC of size calibration beads, indicating again that FSC is not always directly proportional to cell size. Many properties may effect FSC, such as cell hydration state (Yurinskaya *et al.*, 2017). This may explain why the FSC of NP cells and calibration beads did not align; as the pericellular matrix surrounding NP cells in culture (Sato *et al.*, 2001, Sato *et al.*, 2004; Horner *et al.*, 2002) changes the hydration and light scattering properties of NP cells compared to non-fluorescent polystyrene size calibration beads. Both microscopy and flow cytometry results relied on the presumption that analysed cells were spherical in morphology, in order to calculate the 3D cell volume from 2D measurements. A coulter counter enables the experimental determination of actual

cell size; cells are pulled through microchannels (separating two chambers of electrolyte solution) at the same time as an electrical current, causing impedance which is proportionate to the volume of the cells traversing the channels (Behind the Coulter Principle - Beckman Coulter, 2018). This would be a more accurate measure of cell volume in response to altered osmolality (Fenton *et al.*, 2010), enabling measurements of precise volume change in NP cells.

4.4.2 Role of AQP4 and TRPV4 on NP cell size

When exposed to decreased extracellular osmolality (225mOsm/kg), NP cell volume was increased compared to osmotic controls (325mOsm/kg). In the presence of either AQP4i or TRPV4i, the hypo-osmotic increase in NP cell size was significantly reduced. These results indicate that the function of both AQP4 and TRPV4 is required for NP cells to respond in the correct manner to decreased osmolality, by increasing volume. Potentially indicating that both channels work synergistically, enabling NP cells to correctly regulate their volume and trigger downstream mechanisms (such as RVD), in order to adapt to their environment. This synergistic function of AQP4 and TRPV4 has been observed in astrocytes and the regulation of the blood-brain-barrier previously (Solenov *et al.*, 2004; Jo *et al.*, 2015; Kitchen *et al.*, 2015; Mola *et al.*, 2016). Cell volume responses to increased osmolality (425 and 525mOsm/kg) showed no significant change, possibly meaning there is no effect of channel inhibition or the methods used to measure cell volume were not sensitive enough to detect the decrease in cell size that normally follows a decrease in extracellular osmolality.

4.4.3 The rate of NP cell volume change in response to altered osmolality

This is the first time the rate of NP cell volume change in response to altered osmolality, and the effects of AQP4 and TRPV4 inhibition, has been investigated. The rate of NP cell swelling and shrinkage was determined using calcein-AM loaded cells in a plate reader-based method, used previously to investigate volume change rates and AQP function within vesicles, proteoliposomes, MDCK and CHO cell lines, astrocytes, erythrocytes and fibroblasts (Mola *et al.*, 2009; Fenton *et al.*, 2010; Kitchen *et al.*, 2016).

Calcein-AM has been used in experimental systems such as vesicles (Chen and Knutson, 1988), proteoliposomes (Zeidel *et al.*, 1992), and mammalian cells (Solenov *et al.*, 2004) to determine rapid changes in volume and AQP function. These measurements are achieved by the self-quenching properties of calcein at higher concentrations (Chen and Knutson, 1988) and insensitivity to pH, Ca^{2+} or NaCl concentration (Wehner *et al.*, 1995; Solenov *et al.*, 2004). Hamann *et al.*, 2002 were the first to discover that the fluorescent intensity of calcein-loaded mammalian cells was rapidly altered according to the osmotic challenge applied (increase during hypo-osmotic, decrease during hyperosmotic), demonstrating the usefulness of calcein to measure the rapid changes and rate of cell volume. The first methods utilising this technique relied on fluorescent microscopy (Wehner *et al.*, 1995; Hamann *et al.*, 2002; Solenov *et al.*, 2004), more recently plate reader methods have been developed which enable rapid and reproducible investigations into the rapid real-time rate of cell volume changes and screening of membrane protein modulators (Mola *et al.*, 2009; Fenton *et al.*, 2010).

This study followed protocols of Fenton *et al.*, 2010, who determined how calcein fluorescence intensity was related to cell volume, and speculated that a variety of cell types could be tested with their protocols (Fenton *et al.*, 2010). This is also the first time that this method has been used to determine the rate of cell volume change in response to extracellular osmolality in human NP cells. Calcein fluorescence depends linearly on extracellular osmolality in MDKC cells (Fenton *et al.*, 2010), which has also been shown to be the case for human NP cells (Appendix X). Demonstrating these methods can be used to accurately investigate the fundamental functions of NP cells, regarding how they respond to their osmotically fluxing environment, and what molecules/proteins/pathways contribute to their adaptation. One caveat to this technique is that it is performed on 2D cultured cells, therefore cell volume and the rate at which it changes may not represent how NP cells respond in their *in vivo* environment.

4.4.4 Role of AQP4 and TRPV4 on the rate of NP cell volume change

AQP4 function was required for NP cells to swell at the normal rate under 225mOsm/kg treatments and shrink at the normal rate under 425mOsm/kg treatment. TRPV4 function was required for NP cells to alter their volume at the correct rate across all osmotic treatments (225, 425 and 525mOsm/kg). Highlighting that AQP4 and TRPV4 not only contribute to overall NP cell volume, but also dictate the rate at which the desired volume is reached, further implicating both channels in the control of NP cell responses to their osmotically fluxing environment.

4.4.5 Control of NP cell water permeability

The water permeability of NP cells was determined by combining cell volume changes and the rates of change in volume (Fenton *et al.*, 2010). AQP4i decreased the water permeability of NP cells when exposed to healthy (425mOsm/kg) and degenerate (225mOsm/kg) osmolalities, but not when NP cells were exposed to higher osmolality (525mOsm/kg). This may indicate that AQP4 only controls NP cell responses under specific conditions within the microenvironment of the IVD. It has previously, been shown that AQP4 driven water permeability may depend on cell membrane compression and tension (Tong, Briggs and McIntosh, 2012; Ozu *et al.*, 2018), which changes as cells respond to altered osmolality. Thus, AQP4 may exert a greater effect on NP cells within a certain osmotic range, and multiple other AQPs expressed by NP cell may contribute outside this range.

TRPV4 function on the other hand, significantly impacted on the water permeability of NP cells across all osmolalities and was expressed by the vast majority of NP cells regardless of degenerative state. This indicates a potential overarching role during NP cell physiology and adaptation to the hyperosmotic environment of the IVD. TRPV4 is known to enable chondrocyte mechanotransduction and matrix synthesis (O'conor *et al.*, 2013) and lack of TRPV4 expression can induce osteoarthritis in animal models (Clark *et al.*, 2010; Lamandé *et al.*, 2011), thus may contribute to similar functions in the IVD. TRPV4 contributes to NP cell water permeability, yet it is not a water channel itself. Therefore, TRPV4 function must somehow be linked to the function of AQPs and cell volume regulation. TRPV4 has been shown to have physical and functional links with AQPs to enable cells to sense extracellular osmolality changes and initiate cell volume responses (Liu *et al.*, 2006;

Benfenati *et al.*, 2011a; Galizia *et al.*, 2012; Jo *et al.*, 2015; Mola *et al.*, 2016). TRPV4 was also found to co-localise with AQP4 in human NP cells suggesting related functions and interaction between both channels.

Increased osmolality treatments (425 and 525mOsm/kg) used in these experiments were produced using sucrose as the key osmolyte. This ensured that the actual water permeability of NP cells was able to be determined. NP cells contain transmembrane channel proteins that readily transport osmolytes such as Na^+ and Cl^+, urea and mannitol. Therefore, if any of these were used to alter osmotic treatments, cell volume may have reached equilibrium at a different rate as NP cells could utilise the movement of osmolytes used to regulate volume changes, rather than employing the actual mechanisms used to regulate cell volume. However, as IVD matrix is negatively charged, one of the main ions imbibed into the tissue will be Na^+ (Urban, 2002). So repeating experiments using NaCl will enable the comparison between methods of changing medium osmolality (determining if results are an osmotic or substrate effect) and may be more physiological to the *in vivo* environment of the IVD.

4.4.6 Ca^{2+} influx in response to extracellular osmotic shifts

Cellular response to osmotic shifts in their environment is to modulate calcium flux to trigger downstream pathways to enable adaptation to altering environment. TRPV4 in particular has a well-established role in regulating the cellular response to hypo-osmotic shifts in extracellular osmolality, where calcium influx is increased. This enables the triggering of RVD mechanisms and shrinkage to adapt (Caterina *et al.*, 1997; Liedtke and Friedman, 2003; Arniges *et al.*, 2004; Everaerts,

Nilius and Owsianik, 2010; Toft-Bertelsen, Larsen and Macaulay, 2018). NP cells showed they also increase Ca^{2+} influx under hypo-osmotic conditions, compared to hyper-osmotic conditions, suggesting they may employ similar pathways to adapt to their diurnal environment. Previous research has also shown that NP cells do not increase calcium influx under similar hyperosmotic conditions. (Pritchard, Erickson and Guilak, 2002). Pritchard, Erickson and Guilak, 2002 also identified that Ca^{2+} influx and cell volume may be controlled by an actin cytoskeletal-dependent mechanism. Which in turn could potentially be regulated by AQP4; as in astrocytes AQP4 knockdown lead to drastic rearrangement of the actin cytoskeleton network and reduced water permeability (Nicchia *et al.*, 2005). Cytoskeletal rearrangement under alterations in osmolality have also been observed in bovine NP cells (Maidhof, Jacobsen, Papatheodorou and Chahine, 2014). However, when NP cells were injected with control media (325mOsm/kg, same as pre-injection media) a Ca^{2+} influx response was still observed. This highlights that Ca^{2+} influx may also be due to mechanical pressure applied onto NP cells from the injection system of the plate reader, as TRPV4 and other Ca^{2+} channels are also known to be mechanotransducive (Samanta *et al.*, 2018). This may indicate Ca^{2+} influx observed was not solely attributable to the extracellular osmolality, however hypo-osmotic increased Ca^{2+} influx to a greater extent than control injection.

TRPV4i significantly reduced hypo-osmotic Ca^{2+} influx, suggesting important NP cell responses to hypo-osmotic stimuli and the potential activation of RVD. However, Ca^{2+} influx was not totally nullified, therefore other channels may also be involved in these processes. AQP4i significantly reduced the time taken for maximum

Ca^{2+} influx and the maximum Ca^{2+} influx, despite its sole function as a water channel. AQP4 and TRPV4 function is linked to osmosensing and the adaptation to extracellular osmolality of astrocytes (Benfenati *et al.*, 2011a; Jo *et al.*, 2015; Mola *et al.*, 2016; Chmelova *et al.*, 2019), and results described here also indicate there may be similar mechanisms employed by NP cells.

4.4.7 Conclusion

AQP4 and TRPV4 function may be linked in NP cells in order to control the rate of cell volume regulation, water permeability and Ca^{2+} influx, triggering downstream mechanisms enabling the adaptation of NP cells to their osmotically challenging environment (Figure 4.15). During IVD degeneration AQP4 expression is decreased (Chapter 2); as a result, NP cells will not be able to respond to the hypo-osmotic environment due to impaired cell volume regulation and Ca^{2+} influx (Figure 4.15). Due to the lack of osmotic response, downstream mechanisms may not be employed by NP cells to ensure their survival and function in the increasingly degenerate environment. Further study is warranted to determine what impact AQP4 and TRPV4 expression and function have on potential downstream mechanisms such as RVD, cell survival and matrix synthesis.

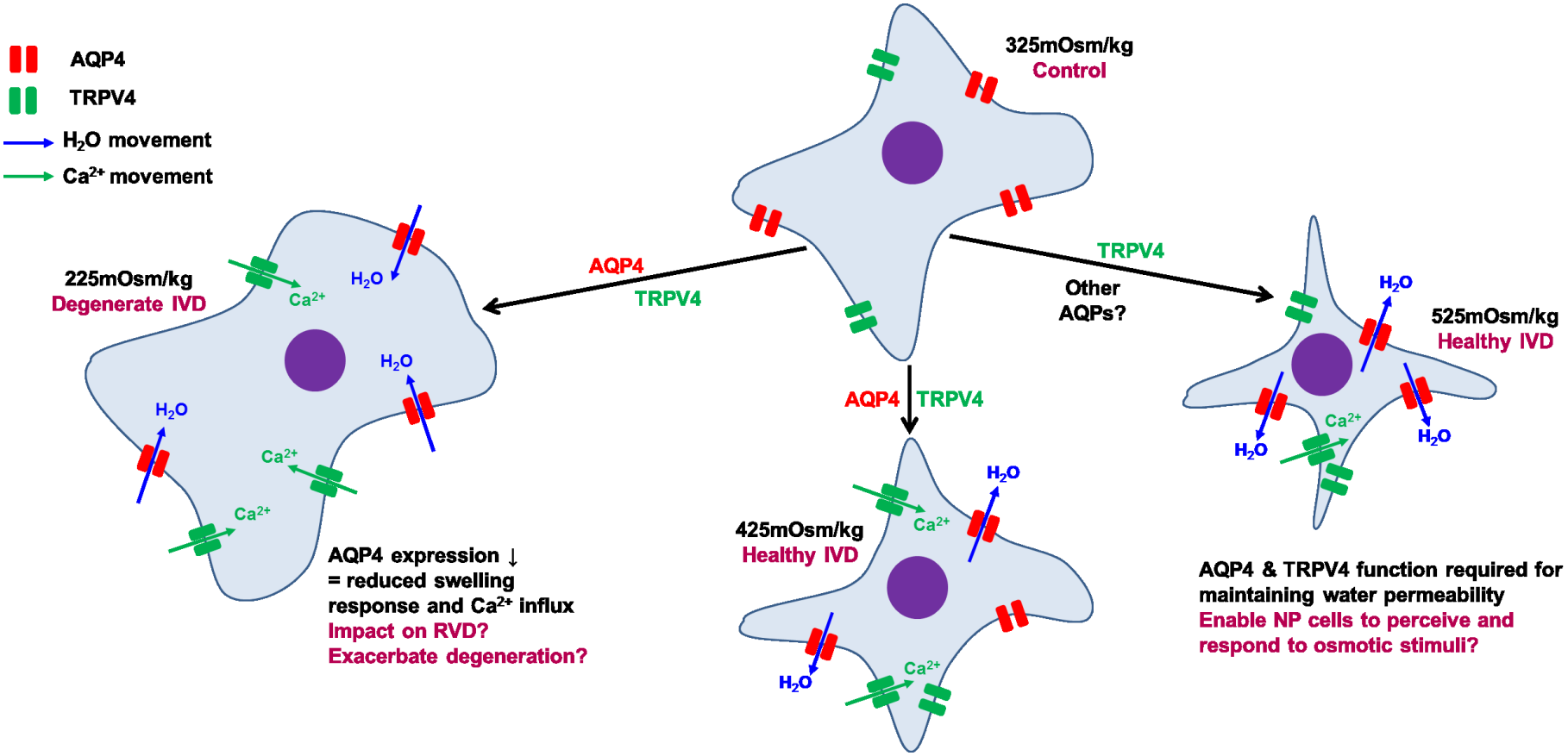

Figure 4.15. NP cell responses to extracellular osmolality alterations: potential roles of AQP4 and TRPV4.

Chapter 5: Regulation of AQP expression by physiological conditions within the intervertebral disc

5.1 Introduction

This thesis has identified that certain AQPs are regulated by the physiological osmolality of the IVD, which potentially indicates how they are regulated *in vivo* and alludes to the specific functions of these AQPs surrounding the osmotic adaptation of NP cells. However, the native environment in which NP cells reside is also hypoxic, acidic and has low nutrient supply, when compared to other tissues, and also has to withstand biomechanical loading (Urban, 2002). During degeneration these conditions can be severely altered and the degenerative cascade is exacerbated by the increased production of cytokines, which trigger degenerative processes (Takahashi *et al.*, 1996; Le Maitre, Freemont and Hoyland, 2005; Le Maitre, Hoyland and Freemont, 2007a; Risbud and Shapiro, 2014). Therefore, the functions of NP cells are, at least in part, regulated by their environment and dysregulated during degeneration when the environment is altered. This indicates that AQPs may also be regulated by many of the other environmental cues within the IVD.

AQP expression in many tissues has been shown to be regulated by physiological conditions which change in the IVD during degeneration, such as O_2 concentration, cytokines and pH (Tables 5.1-5.3 respectively). However, there have been few studies which have investigated the regulation of AQP expression by these conditions in NP cells. It was determined that AQP1 and 5 expression in rat NP cells was not regulated by changes in O_2 concentration, but basal expression levels were maintained under hypoxia by HIF-1α (Johnson *et al.*, 2015) (Table 5.1), indicating that within the native environment of the IVD, where O_2 concentration is always low and HIF-1α is stably expressed (Fujita *et al.*, 2012), the maintenance of AQP expression in

NP cells is controlled by the environment. In bovine NP cells it was determined that TNF-α decreased expression of AQP1 (Maidhof, Jacobsen, Papatheodorou and Chahine, 2014) (Table 5.2), signifying that during IVD degeneration, when TNF-α expression is increased (Le Maitre, Hoyland and Freemont, 2007a), AQP expression may be differentially regulated when compared to healthy IVD physiology. These studies show that potentially more than one environmental factor may contribute to the regulation of AQP expression and function within NP cells. No studies, to date have investigated pH regulation of AQP expression in NP cells, with only a few identifying such regulation in the kidney (Promeneur *et al.*, 2000; Amlal, Sheriff and Soleimani, 2004), where AQP2 and 6 are potentially involved in acid-base regulation (Table 5.3). It may be that AQPs are only regulated by pH within tissues that exhibit fluctuations which cells need to adapt to, such as the IVD.

	Tissue/cell type	AQP	Treatment	Regulation	Pathways	References
Brain	Mouse brain, 9L glioma cell line	AQP1	10% O_2, DMOG, $CoCl_2$	↑	HIF-1α	(Abreu-Rodríguez *et al.*, 2011)
	9L glioma cell line	AQP1	20 - 0 % O_2	↑		(Hayashi *et al.*, 2007)
	Mouse Schwann cells	AQP1	$CoCl_2$	↑	HIF-1α	(Zhang, J. *et al.*, 2013)
	Mouse cortical astrocytes	AQP5	0% O_2	↓		(Chai *et al.*, 2013)
	Rat spinal cord	AQP1, 4	Spinal cord injury	↑	HIF-1α	(Wang, Y. *et al.*, 2011)
	Rat brain	AQP4, 9	Middle cerebral artery occlusion	↑	HIF-1α	(Higashida *et al.*, 2011)
	Rat brain	AQP4, 9	traumatic brain injury	↑	HIF-1α	(Ding *et al.*, 2009)
Eye	Rat retina	AQP0, 9, 12	Ar laser-induced retinal vein occlusion	↑		(Hollborn *et al.*, 2012)

	Tissue/cell type	AQP	Treatment	Regulation	Pathways	References
	Rat retina	AQP1, 3, 4, 5, 6, 8, 11	Ar laser-induced retinal vein occlusion	↓		(Hollborn *et al.*, 2012)
	Human retinal vascular endothelia cells	AQP1	1% O_2	↑		(Kaneko *et al.*, 2008)
	Human retinal vascular endothelia cells	AQP1	1% O_2	↑	HIF-1α, HIF binding site	(Tanaka *et al.*, 2011)
Heart	Human heart tissue, mouse cardiomyocytes	AQP4	Coronary artery occlusion	↓		(Rutkovskiy, Stensløkken, *et al.*, 2012)
	Mouse cardiac endothelial cells	AQP1	Retrograde buffer-perfused global ischemia	↓		(Rutkovskiy *et al.*, 2013)
	Rabbit heart	AQP1	Coronary artery occlusion	↑		(Ran *et al.*, 2010)
	Mouse heart	AQP1, 4, 6	Coronary artery occlusion	↑		(Zhang, H. Z. *et al.*, 2013)
	Rat pulmonary arterial smooth muscle cells	AQP1	4 - 10% O_2, Ca^{2+} channel blockers	↑	Intracellular Ca^{2+}	(Leggett *et al.*, 2012)
Musculo-skeletal	Rat NP cells	AQP1, 5	1% O_2, DMOG	−	Basal expression regulated by HIF-1α	(Johnson *et al.*, 2015)
Reproductive	PC-3M prostate cancer cell line	AQP1	5% O_2, $CoCl_2$	↑	p38, PKC, Intracellular Ca^{2+}	(Tie *et al.*, 2012)
Respiratory	Mouse lung	AQP1	1% O_2, DMOG	↑	HIF-1α	(Kawedia *et al.*, 2013)
	Mouse lung	AQP5	1% O_2, DMOG	↓	HIF-1α, proteasome	(Kawedia *et al.*, 2013)

Table 5.1. Regulation of AQP expression by O_2 concentration. The expression of many AQP isoforms, across many tissue and cell types is upregulated (↑) or downregulated (↓) by O_2 concentration. AQP expression may also be unaltered by changes in O_2 concentration (−).

	Tissue/cell type	AQP	Treatment	Regulation	Pathways	References
Adipose	3T3-L1 adipocyte cell line	AQP7	TNF-α	↓		(Fasshauer *et al.*, 2003)
Brain	Rat primary astrocytes	AQP4	IL-1β	↑	NF-κB	(Ito *et al.*, 2006)
	Rat brain tissue/ astrocytes	AQP4	IL-1β, TNF-α	↑	NF-κB, p38	(Ding *et al.*, 2013)
	Rat cortical astrocytes	AQP4	IL-1β	↑		(Chastre *et al.*, 2010)
	Rat hippocampus/ entorhinal cortex	AQP4	TNF-α	↑	PKC	(Zou, Vetreno and Crews, 2012)
Digestive	Gingival epithelial tissue	AQP3	TNF-α	↑		(Tancharoen *et al.*, 2008)
	NS-SV-AC human salivary acinar cell line	AQP5	TNF-α	↓		(Yamamura *et al.*, 2012)
Kidney	Mouse kidney	AQP2	IL-1β	↓		(Boesen, 2013)
Musculo-skeletal	Human synoviocytes	AQP9	TNF-α	↑		(Nagahara *et al.*, 2010)
	Bovine NP cells	AQP1	TNF-α	↓		(Maidhof *et al.*, 2014)
Respiratory	Mouse lung epithelial cells	AQP5	TNF-α	↓		(Krane *et al.*, 2001a)
	Human bronchial epithelial cells	AQP1, 5	TNF-α	↓		(Mezzasoma *et al.*, 2013)
	Rat nasal mucosa	AQP5	IL-1β	↓	NF-κB	(Wang and Zheng, 2011)
Skin	DJM-1 keratinocyte cell line	AQP3	TNF-α	↓		(Horie *et al.*, 2009)

Table 5.2. Regulation of AQP expression by cytokines specific to IVD degeneration. The expression of many AQP isoforms, across many tissue and cell types is upregulated (↑) or downregulated (↓) by IL-1β or TNF-α.

	Tissue/cell type	AQP	Treatment	Response	Pathways	Reference
Kidney	Rat kidney	AQP6	$NaCO_3$-induced alkali loading	↑		(Promeneur *et al.*, 2000)
	Rat Kidney	AQP6	NH_4-induced acid loading	↑ only with free access to drinking water		(Promeneur *et al.*, 2000)
	Rat kidney	AQP2	NH_4-induced metabolic acidosis	↑	AVP	(Amlal, Sheriff and Soleimani, 2004)

Table 5.3. Regulation of AQP expression by pH alterations. The expression of AQPs is upregulated (↑) by altered tissue pH.

The regulation of AQP expression by these conditions occurs across many cell and tissue types and regulation of expression is potentially specific to each type. Many of the AQPs expressed in NP tissue (Chapter 2) are regulated by conditions in many tissues that are also present during healthy and degenerate IVD physiology, highlighting AQPs may also be regulated in a similar manner in NP cells. The potential regulation of AQP expression by physiological conditions may be an indication of the potential roles specific AQPs contribute towards with the disc.

This study aimed to investigate if AQPs expressed in human NP tissue were expressed in extracted NP cells and whether expression was regulated by culture conditions, including 2D and 3D culture and stimulation by cytokines, hypoxia and pH. Furthermore, these conditions were then combined to mimic the conditions representative of the IVD environment and effects on AQP expression determined.

5.2 Materials and methods

5.2.1 Experimental design

To determine that all AQPs expressed by native human NP tissue (AQP0-7 and 9, Chapter 2) were expressed by human NP cells during culture; IHC was performed on cytospins of human NP cells taken from passage 0 - 2 and after 2w alginate bead culture which is utilised to re-differentiate cells to an NP like phenotype. How AQP expression in NP cells is regulated has not been previously established. Therefore, human NP cells, encapsulated in alginate beads to re-differentiate into an *in vivo*-like phenotype, were treated with cytokines (IL-1β, IL-6 and TNF-α), altered pH (pH7.4 - 6.5) under 5% and 21% O_2. Furthermore, combined treatments mimicking healthy and degenerate IVD conditions were investigated to determine if AQP gene expression within NP cells is regulated by conditions observed during IVD physiology. The experimental design is outlined in Figure 5.1.

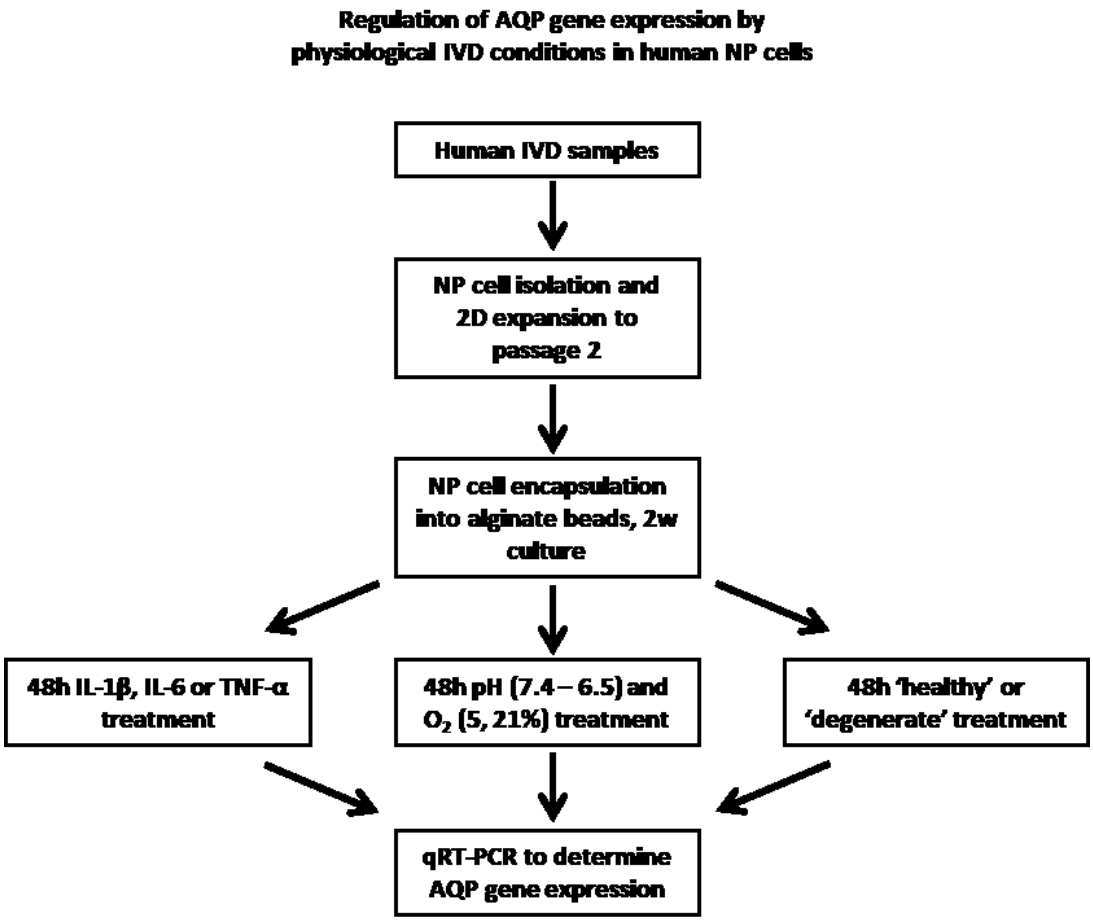

Figure 5.1. Experimental design of methods used in this study.

5.2.2 Human Tissue, NP cell extraction and culture

Human IVD tissue was obtained with ethical consent, NP cells extracted and monolayer cultured according to methods outlined in section 2.2.

5.2.3 Cytospins

Human NP cells were taken at passage 0 (straight after isolation from NP tissue), at passage 1, passage 2 during splitting and after 2 week culture and isolation from alginate beads (section 3.2.6), and centrifuged at 300g for 5min. Supernatant was discarded and cell pellets resuspended in 10% neutral buffered formalin for

5min. Fixed cells were centrifuged at 300g for 5min and pellets resuspended in PBS at $1x10^6$/mL. Cytospins, filter cards (Thermo Fisher, UK) and slides (Leica Microsystems) were assembled and 200µL of cell suspension was added to each cytospin and centrifuged at 300g for 5min to deposit a single layer of cells onto slides. Slides were stored at 4°C. IHC was performed (Section 2.2.7) to determine if the expression of AQPs in native human NP tissue (AQP0-7, 9) was retained in isolated human NP cells during culture duration and conditions used in experiments.

5.2.4 Regulation of AQP gene expression under physiological IVD conditions

At passage 2, human NP cells were encapsulated into alginate beads as previously described (section 3.2.6). To assess catabolic cytokine regulation of AQP gene expression in human NP cells, alginate beads were treated with 0 (control), 1, 10 and 100ng/mL recombinant human IL-1β (200-01B, Peprotech), recombinant human IL-6 (200-06, Peprotech) or recombinant human TNF-α (300-01A, Peprotech) for 48h. To determine the effect of physiological pH on the gene expression of AQPs, alginate beads were treated with standard culture media with altered pH: pH 7.4 (media control), pH 7.1 (healthy IVD), pH 6.8 (moderate IVD degeneration) or pH 6.5 (severe IVD degeneration) for 48h. The pH of standard culture media was adjusted using HCl and replaced every 12h to ensure treatment pH was constant and media remained unbuffered. All treatments were performed at 21% (v/v) O_2 (to represent standard culture conditions) and 5% (v/v) O_2 (to represent physioxia of the native IVD). All treatment conditions were combined to produce a set of treatments to represent the healthy and degenerate IVD niche (Table 5.4), which alginate beads were also treated with for 48h.

Treatment	Standard culture control	Healthy IVD niche	Degenerate IVD niche
Osmolality (mOsm/kg)	325	425	325
pH	7.4	7.1	6.8
Cytokines (1ng/mL)	-	-	IL-1β, IL-6, TNF-α
O_2 concentration (% v/v)	5, 21	5, 21	5, 21

Table 5.4 Healthy and degenerate IVD niche treatment components. Combined treatments represent the healthy and degenerate extracellular environments within the IVD; standard culture conditions were included as an untreated control. Human NP cells encapsulated in alginate beads were subjected to 48h treatment in either control, healthy or degenerate IVD conditions, to assess the effect on AQP gene expression.

Following 48h treatment, NP cells were released from alginate beads and RNA extracted (section 3.2.6), cDNA synthesised and the gene expression of AQPs investigated using previously described methods (section 2.2.5).

5.2.5 Statistical analysis

All experiments investigating AQP gene expression by physiological IVD conditions were performed on at least 3 patient-derived human NP cells in triplicate. Data was shown to be non-parametric, therefore, Kruskall-Wallis with Dwass-Steel-Critchlow-Fligner post hoc analysis test was used to identify significant differences in in AQP gene expression after 48h treatment ($p \leq 0.05$).

5.3 Results

5.3.1 AQP expression during 2D and 3D culture of human NP cells

Throughout all culture conditions (passage 0 - 2 and 2w 3D culture in alginate beads) prior to experimental procedures, immunopositivity was seen for all AQPs which were expressed in native human NP tissue (Chapter 2) (Figure 5.2).

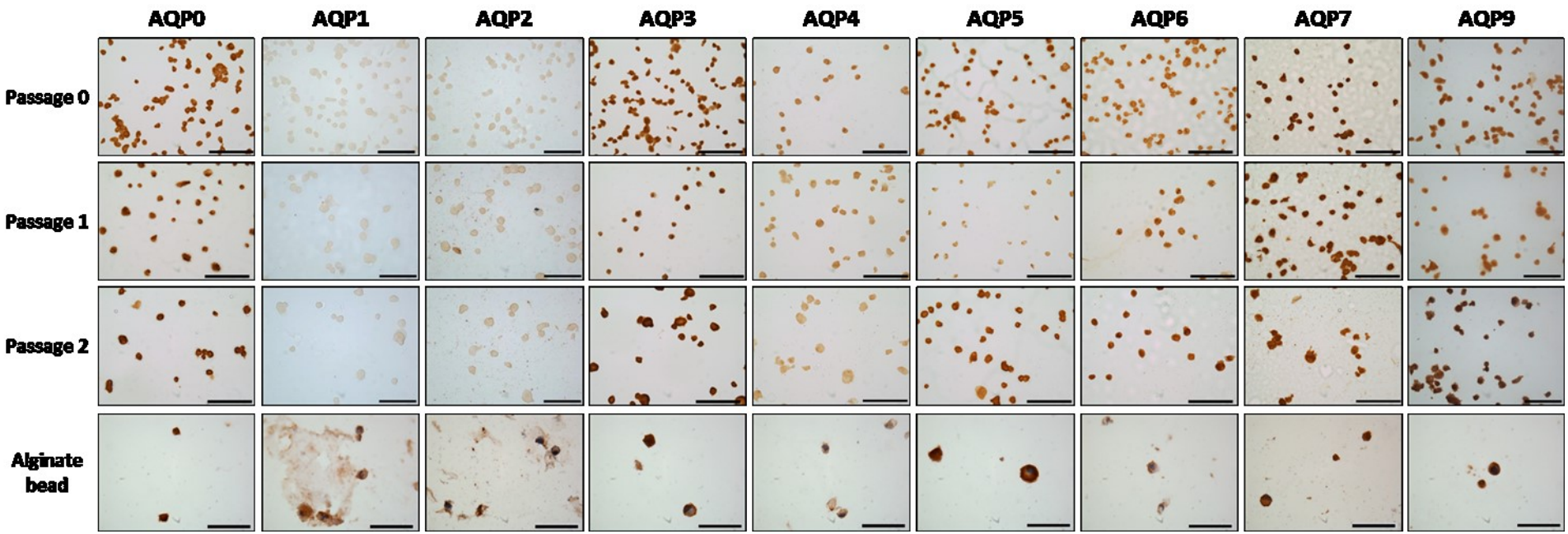

Figure 5.2 Expression of AQP proteins expressed by native human NP tissue, in cytospins of extracted and cultured human NP cells. Immunopositive cells are indicated by brown staining and nuclei are counterstained with Mayer's haematoxylin (blue). Scale bar 50µM.

5.3.2 Regulation of AQPs by cytokines in human NP cells

The gene regulation of all AQPs expressed by human NP tissue (AQP0-7 and 9) was investigated during all experiments, however, results only show AQPs that were detected by qRT-PCR, all other AQP family members were undetected.

5.3.2.1 AQP1

The relative gene expression of AQP1 was significantly down-regulated by 48h treatment with 1 and 10ng/mL IL-1β in human NP cells encapsulated in alginate beads ($p \leq 0.05$) (Figure 5.3A). The relative gene expression of AQP1 was up-regulated by 48h treatment with 10 and 100ng/mL IL-6 in human NP cells encapsulated in alginate beads ($p \leq 0.05$) (Figure 5.3B). TNF-α treatment of human NP cells did not significantly regulate the expression of AQP1 (Figure 5.3C).

5.3.2.2 AQP2

IL-1β (Figure 5.4A) or IL-6 (Figure 5.4B) treatment of alginate bead encapsulated human NP cells did not significantly regulate the gene expression of AQP2. However, the relative gene expression of AQP2 was up regulated by 48h treatment with 1 and 10ng/mL TNF-α in human NP cells ($p \leq 0.05$) (Figure 5.4C).

5.3.2.3 AQP3

The relative gene expression of AQP3, in human NP cells, was down-regulated by 48h treatment with 1ng/mL IL-1β ($p \leq 0.05$) (Figure 5.5A) but was up-regulated by 48h treatment with 10ng/mL IL-6 ($p \leq 0.05$) (Figure 5.5B). Forty-eight-hour treatment

with 1ng/mL TNF-α also up-regulated the relative gene expression of AQP3 in human NP cells ($p \leq 0.05$) (Figure 5.5C).

5.3.2.4 AQP9

The relative gene expression of AQP9 was up-regulated by 48h treatment with 1-100ng/mL IL-1β ($p \leq 0.05$) (Figure 5.6A), 10 and 100ng/mL IL-6 ($p \leq 0.05$) (Figure 5.6B) and 1-100ng/mL TNF-α ($p \leq 0.05$) (Figure 5.6C), in human NP cells.

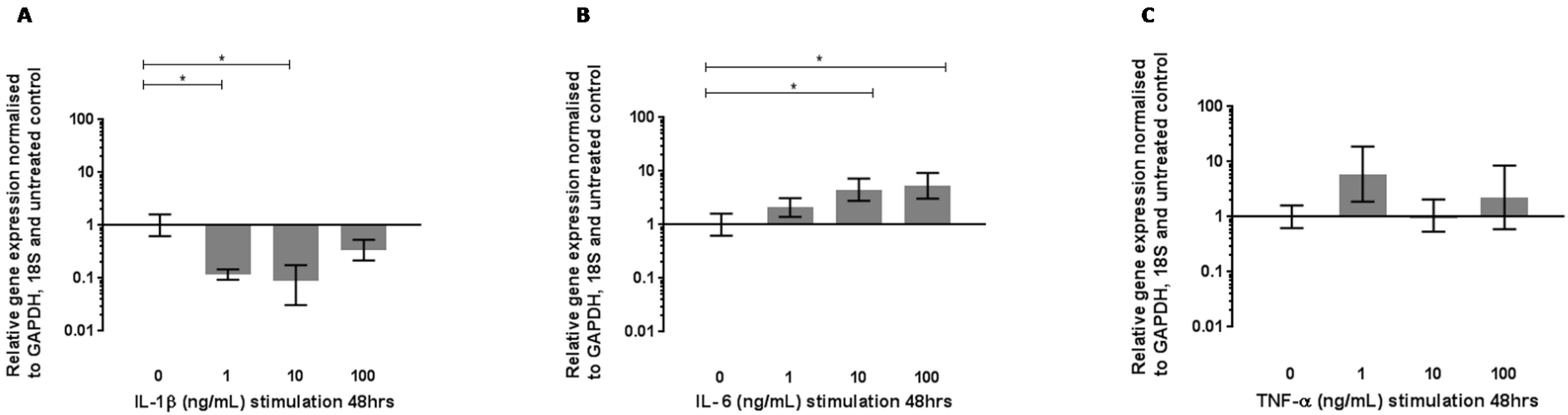

Figure 5.3 Regulation of AQP1 gene expression in 3D cultured human NP cells by catabolic cytokines. Alginate encapsulated human NP cells were treated with 0, 1, 10, and 100ng/mL IL-1β (A), IL-6 (B) and TNF-α (C) for 48h. Relative gene expression of AQP1 was determined by qRT-PCR and normalised to housekeeping genes (GAPDH and 18S) and untreated controls (0ng/mL). Statistical significance determined using Kruskal-Wallis test * = $p \leq 0.05$

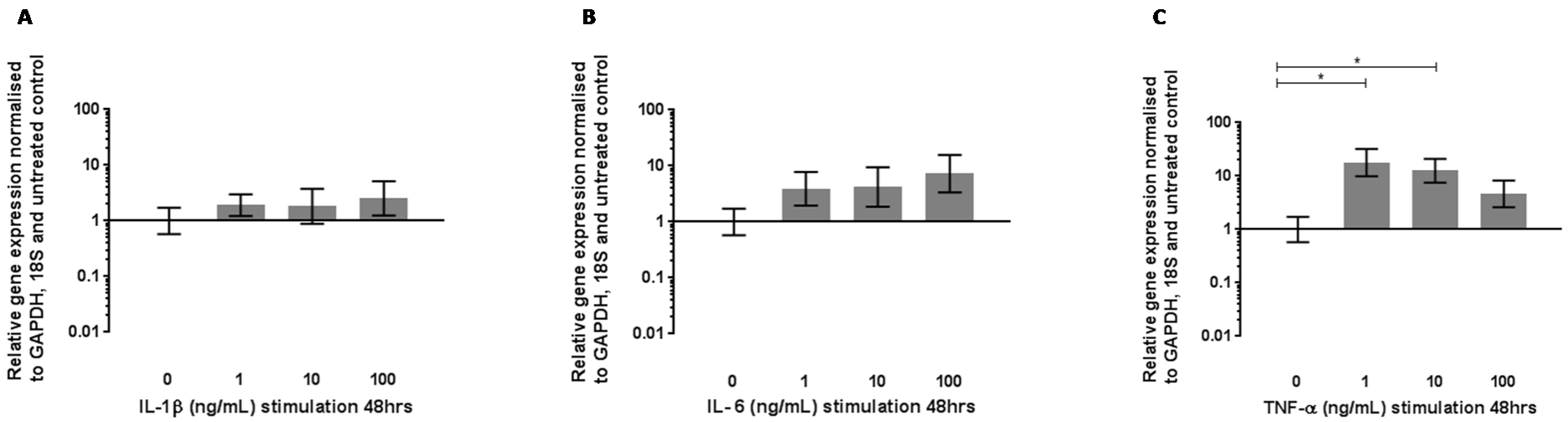

Figure 5.4 Regulation of AQP2 gene expression in 3D cultured human NP cells by catabolic cytokines. Alginate encapsulated human NP cells were treated with 0, 1, 10, and 100ng/mL IL-1β (A), IL-6 (B) and TNF-α (C) for 48h. Relative gene expression of AQP2 was determined by qRT-PCR and normalised to housekeeping genes (GAPDH and 18S) and untreated controls (0ng/mL). Statistical significance determined using Kruskal-Wallis test * = $p \leq 0.05$

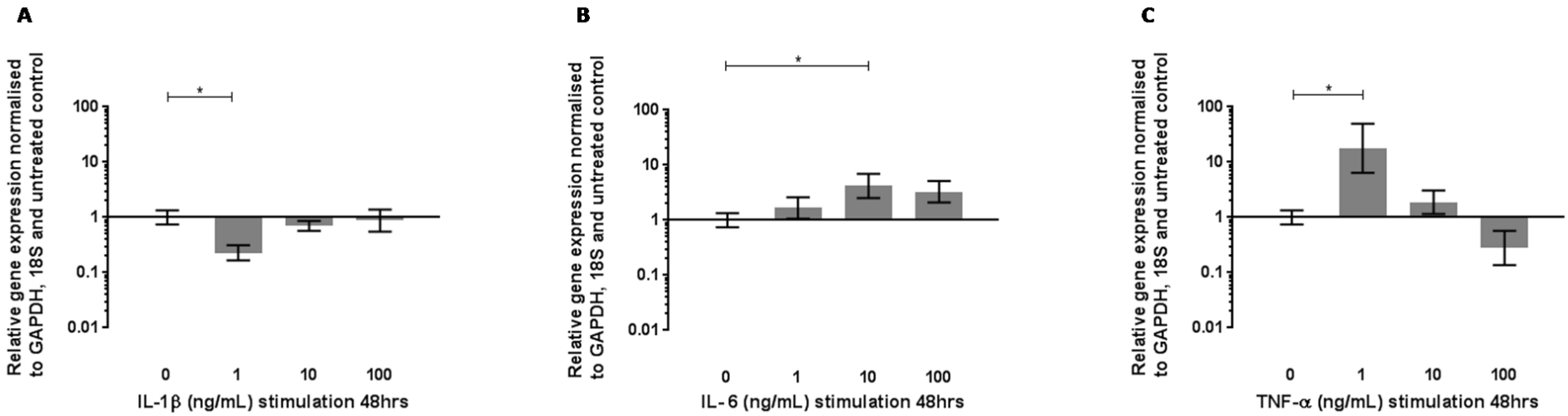

Figure 5.5 Regulation of AQP3 gene expression in 3D cultured human NP cells by catabolic cytokines. Alginate encapsulated human NP cells were treated with 0, 1, 10, and 100ng/mL IL-1β (A), IL-6 (B) and TNF-α (C) for 48h. Relative gene expression of AQP3 was determined by qRT-PCR and normalised to housekeeping genes (GAPDH and 18S) and untreated controls (0ng/mL). Statistical significance determined using Kruskal-Wallis test * = $p \leq 0.05$

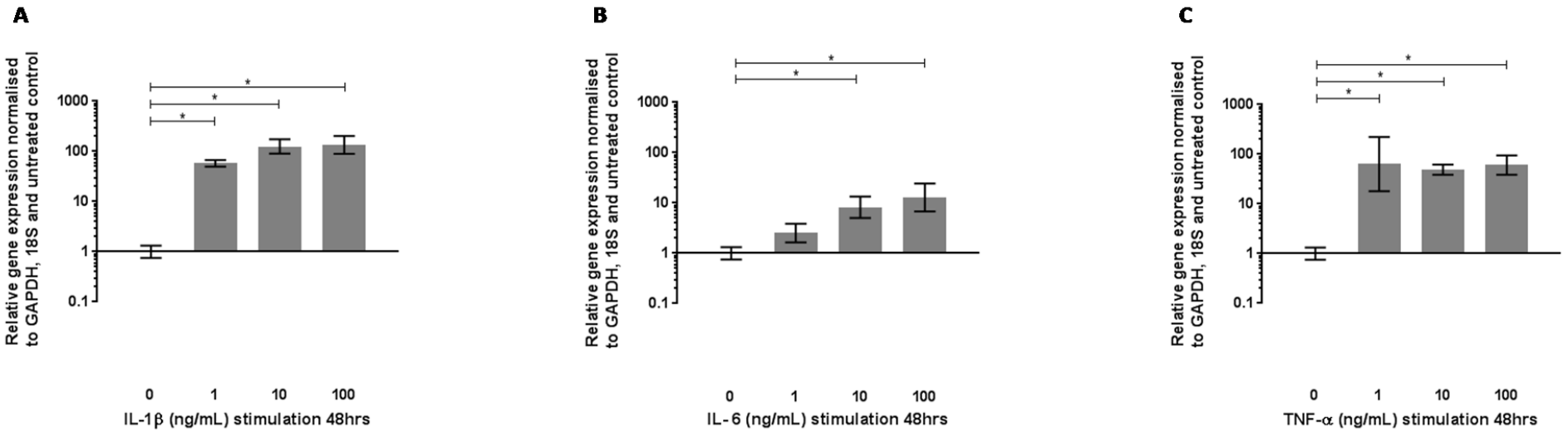

Figure 5.6 Regulation of AQP9 gene expression in 3D cultured human NP cells by catabolic cytokines. Alginate encapsulated human NP cells were treated with 0, 1, 10, and 100ng/mL IL-1β (A), IL-6 (B) and TNF-α (C) for 48h. Relative gene expression of AQP9 was determined by qRT-PCR and normalised to housekeeping genes (GAPDH and 18S) and untreated controls (0ng/mL). Statistical significance determined using Kruskal-Wallis test * = $p \leq 0.05$

5.3.3 Regulation of AQPs by pH in human NP cells

The relative gene expression of AQP5 in alginate encapsulated human NP cells was not significantly regulated by physiological changes in extracellular pH (pH7.4 - 6.5) for 48h at 21% O_2 (Figure 5.7A) or 5% O_2 (Figure 5.7B). Gene expression of AQP5 was also unchanged in 5% O_2 when compared to expression in 21% O_2 after 48h treatment in standard culture media (pH7.4) (Figure 5.7C). However, the relative gene expression of AQP5 was significantly up-regulated by 48h culture at 5% O_2, when compared to culture at 21% O_2, when extracellular pH was altered to pH7.1 ($p \leq 0.05$) (Figure 5.7D), pH6.8 ($p \leq 0.05$) (Figure 5.7E) and pH6.5 ($p \leq 0.05$) (Figure 5.7F) (NP cell viability during pH and O_2 % treatments, Appendix XIII).

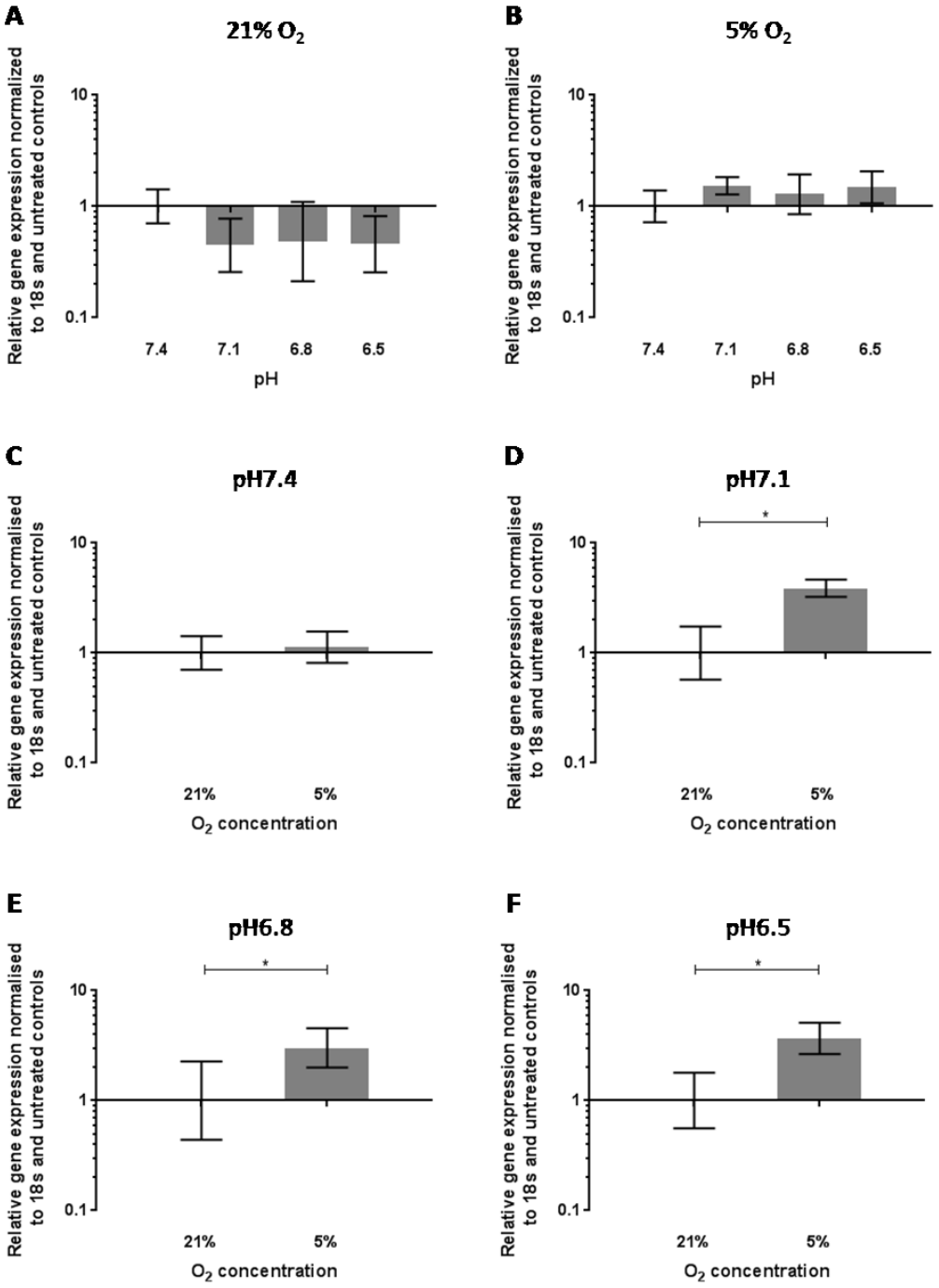

Figure 5.7 Regulation of AQP5 gene expression in 3D cultured human NP cells by pH and oxygen concentration. Alginate encapsulated human NP cells were treated with media control (pH7.4) or physiological pH (pH7.1, 6.8 and 6.5) at 21% (A) and 5% (B) O_2 for 48h. Alginate encapsulated human NP cells were treated with 21% and 5% O_2 at pH7.4 (C), 7.1 (D), pH6.8 (E) and pH6.5 (F) for 48h. Relative gene expression of AQP5 was determined by qRT-PCR, and normalised to housekeeping genes (GAPDH and 18S) and untreated controls (A & B: pH7.4, C-F: 21% O_2 concentration). Statistical significance determined using Kruskal-Wallis test * = $p \leq 0.05$.

5.3.4 Regulation of AQPs by physiological IVD conditions

The relative gene expression of AQP1 and 2 was unaltered when 3D alginate-cultured human NP cells were treated for 48h in healthy or degenerate conditions compared to standard culture controls, although an increase was seen in 5% O_2 in degenerate conditions this did not reach significance (Figure 5.8A and 5.8B). AQP5 gene expression was significantly upregulated in 3D-alginate-cultured human NP cells after 48h treatment with both healthy and degenerate conditions at 21% O_2 concentration compared to standard culture conditions, however no change was observed in these conditions under 5% O_2 ($p \leq 0.05$) (Figure 5.8C) (NP cell viability during healthy and degenerate treatments, Appendix XIV).

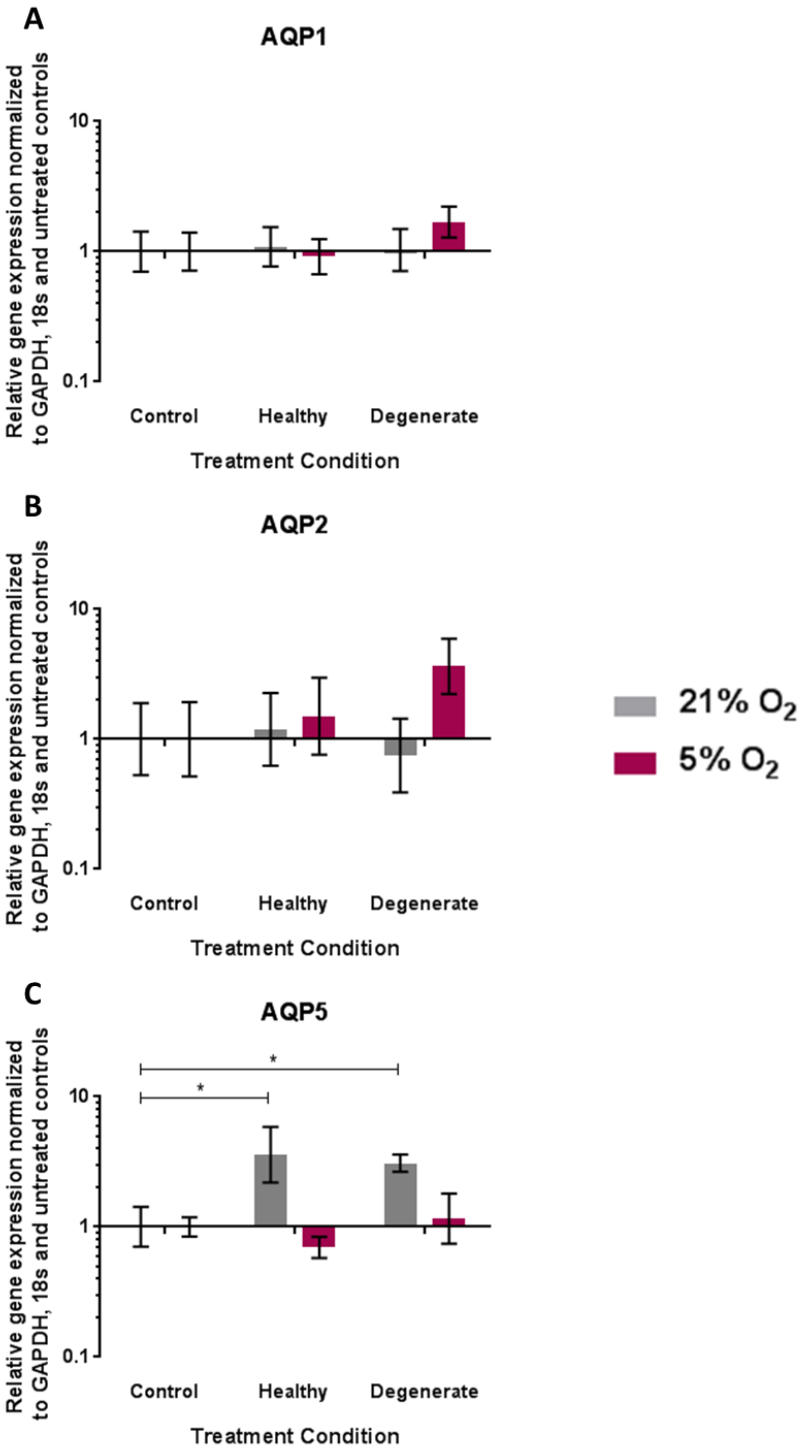

Figure 5.8 Regulation AQP gene expression in response to conditions mimicking healthy and degenerate IVD conditions. Alginate bead-encapsulated human NP cells were treated with control, healthy and degenerate conditions (Table 5.4), at 21% (grey) and 5% (magenta) O_2 concentration, for 48h. The gene regulation of (A) AQP1, (B) AQP2 and (C) AQP5 was compared to standard media controls (21% O_2). Statistical significance determined using Kruskal-Wallis test * = $p \leq 0.05$.

5.4 Discussion

NP cells have adapted to a hypoxic, hyperosmotic, acidic and mechanically stimulated environment that also has low nutrient diffusion. This environment contributes to the overall function of NP cells to maintain the integrity of the tissue (Bibby *et al.*, 2005; Tsai *et al.*, 2006; Wuertz *et al.*, 2007; Neidlinger-Wilke *et al.*, 2012). However, during degeneration the NP environment is drastically altered, causing numerous adverse cellular effects that lead to IVD degeneration. How AQPs function within NP cells is unknown, elucidating how AQPs are regulated in NP cells, possibly by environmental stimuli, may signify the specific functions of AQPs within the IVD.

5.4.1 AQP expression during culture

All AQPs that were expressed in human NP tissue (AQP0-7 and 9, Chapter 2) were also expressed in extracted NP cells. AQP protein expression was present throughout all culture conditions utilised for experiments (passage 0-2, 2w alginate bead culture). This emphasises that AQP expression remained stable throughout standard culture conditions, so the potential regulation of expression by particular treatments was able to be investigated. However, the gene expression of only certain AQP isoforms was able to be detected during qRT-PCR experiments within this chapter (AQP1-3 and 9, cytokine regulation; AQP5, pH and O_2 regulation; AQP 1, 2 and 5, combined treatment). Gene expression of all other AQPs was investigated but remained undetected. Potentially, AQP protein expression is more stable than gene expression as it was detected across all culture conditions. AQP gene expression may be more transient; gene regulation was only investigated after 48h treatment but

may be regulated and detectable by qRT-PCR at earlier or later time points. Chapter 3 identified that both AQP1 and 5 expression was upregulated by hyperosmotic treatment after 24h and also 72h. Even though the gene expression of many AQPs was undetected by qRT-PCR, their expression in human NP cells may be below detectable limits. Also, as patient-derived NP cells were used there may be variability in the AQPs that are expressed across different patients. This was also observed in Chapter 2 where AQP gene expression was investigated in patient-derived NP tissue; no AQP isoforms present were expressed in 100% of patients (102 patient samples), indicating biological variability. In contrast, AQP protein expression was observed in all patient-derived NP tissue used for IHC (Chapter 2, 30 patient samples), supporting the argument that protein expression may be more reliable when detecting AQP expression and regulation in NP cells.

5.4.2 AQP gene regulation by cytokines

Cytokines, such as IL-1β, IL-6 and TNF-α, are upregulated and trigger IVD degeneration by altering the expression of many genes (Le Maitre, Freemont and Hoyland, 2005; Le Maitre *et al.*, 2007; Le Maitre, Hoyland and Freemont, 2007a; Hoyland, Le Maitre and Freemont, 2008; Phillips *et al.*, 2015). Potential regulation of AQPs by these cytokines in NP cells may indicate that they are also dysregulated during degeneration, either as a cause or consequence.

AQP1 and 3 were both significantly down-regulated by IL-1β and up-regulated by IL-6, potentially indicating shared mechanisms of cytokine regulation, yet as both cytokines are present during IVD degeneration it is unclear if the opposite effects of singular cytokine treatments actually mimic *in vivo* regulation. TNF-α did not

significantly alter AQP1 expression in NP cells, yet a previous study has shown that AQP1 expression in NP cells is down-regulated after 10ng/mL TNF-α treatment (Maidhof, Jacobsen, Papatheodorou and Chahine, Nadeen O., 2014). However, the Maidhof *et al.*, 2014 study used juvenile bovine NP cells which may respond to TNF-α treatment differently to mature human NP cells extracted from degenerate discs, and the down-regulation in AQP1 expression was observed after 24h TNF-α treatment, whereas human NP cells were treated for 48h, indicating responses may also be time dependent.

AQP9 gene regulation by cytokines provided the clearest results. AQP9 expression was significantly up-regulated by all cytokine treatments, indicating that AQP9 expression may follow a similar pattern during *in vivo* degeneration, as all three cytokines contribute simultaneously. Whether the increase in AQP9 gene expression could be a potential cause of further degeneration or is a consequence of the cellular dysfunction observed during degeneration is unknown. However, results in Chapter 2 identified that the *in vivo* AQP9 immunopositivity was unaltered during IVD degeneration, which may indicate that the *in vitro* AQP9 gene regulation by cytokines may be irrelevant during this process. Although, immunopositivity is only a measure of the number of cells within the tissue expressing the protein of interest, not the actual levels of expression, which potentially could be altered during degeneration, thus utilising western blotting or ELISA techniques would be important to investigate to investigate changes in AQP 9 protein expression both *in vivo* and *in vitro*.

5.4.3 AQP gene regulation by pH

As the IVD is an avascular and hypoxic tissue, NP cells favour anaerobic glycolysis as their main form of metabolism, producing an acidic environment (Bibby *et al.*, 2005). NP cells have adapted several mechanisms to adapt to this environment (Silagi *et al.*, 2018a; Silagi *et al.*, 2018b), yet during degeneration the pH decreases further, as removal of waste products (lactic acid) is reduced. There is limited evidence for pH regulation of AQP expression (Table 5.3), highlighting such regulation is only observed in tissues where pH balance is essential (or because no one has investigated this in other tissues), such as the kidney (Promeneur *et al.*, 2000; Amlal, Sheriff and Soleimani, 2004) and possibly the IVD.

AQP5 gene expression was unchanged by altered pH in human NP cells cultured in 21% or 5% O_2, indicating that AQP5 expression may not be sensitive to oxygen tension or pH. However, when NP cells were cultured in physiological pH (pH7.1 - 6.5) and physioxia (5% O_2) AQP5 expression was up-regulated compared to 21% O_2 controls. This indicates that both physiological pH and oxygen tension may contribute to the correct regulation of AQP5 expression in NP cells, whereas individual treatment with either does not. This provides evidence highlighting that multiple environmental cues all provide NP cells with the correct (and incorrect, in the case of degeneration) stimuli to regulate expression and function accordingly, which will be the case *in vivo*. Hence NP cell treatment with combined treatments mimicking the healthy and degenerate IVD niche was investigated.

5.4.4 AQP gene regulation by combined healthy and degenerate IVD conditions

The regulation of AQP1, 2 and 5 gene expression by healthy and degenerate IVD conditions was unclear. The gene expression of these AQPs was largely unaffected by these conditions at 21% and 5% O_2 when compared to standard culture conditions at 21% O_2, indicating that AQPs may not be regulated within NP cells during degenerative processes and their functions may be independent of degeneration. However, only changes in oxygen tension, osmolality, pH and cytokines were used to 'mimic' the healthy and degenerate IVD niche, compared to standard culture media. This is a simplified environment and thus, full recapitulation of the degenerate and normal niche is needed to investigate this more accurately.

The pH of treatments was altered using HCl; this may be an ineffective way of altering media pH as desired alterations may be buffered out, an alternative which may be more physiologically relevant could be to use lactic acid. Furthermore, the addition of the appropriate amount of $NaHCO_3$ to media (without $NaHCO_3$), calculated using the Henderson-Hasselbalch equation, will enable the correct maintenance of the desired media pH (Esser, Thermo Scientific, 2010; Gilbert *et al.*, 2016).

The native environment of the NP is far more complicated than the treatments devised in these experiments. Treatments failed to address the mechanical forces (Neidlinger-Wilke *et al.*, 2012), low nutrient diffusion (Urban *et al.*, 1977) and diurnal patterns (McMillan, Garbutt and Adams, 1996) that NP cells are exposed to *in vivo*. Also, an increased level of calcium deposition within the endplates and IVD has been observed during degeneration (Grant *et al.*, 2016), indicating the

inclusion of increased calcium concentration may be important to mimic degenerate conditions as well. Therefore, without including all environmental factors that contribute to IVD health and degeneration, treatments aiming to mimic these complex systems will not be physiologically relevant and should be expanded on, to gain a more complete view of AQP regulation. Furthermore, these physiological conditions may affect AQPs at protein levels rather than gene expression levels, as many post-translational modifications (channel gating, phosphorylation, calcium binding cytoskeletal remodelling and protein interactions) (Yasui *et al.*, 1999; Nicchia *et al.*, 2008; Benfenati *et al.*, 2011b; Conner, Bill and Conner, 2013; Jo *et al.*, 2015; Kitchen *et al.*, 2015; Kitchen, P. *et al.*, 2015) all potentially play a significant role on the expression, regulation, trafficking and function of AQPs during IVD physiology, which should be explored further, particularly due to the issues experienced with gene expression analysis of AQPs within NP cells.

5.4.5 Conclusion

AQPs within NP cells may be regulated by many environmental cues within NP cells, such as cytokines and pH (Figure 5.9), along with (the well documented) alterations in osmolality. Yet, to date the true regulation and function of AQPs within the IVD is relatively unknown (Figure 5.9). The *in vivo* conditions of the IVD must be replicated very specifically to gather the information required to unfold the potential roles AQPs, and all other genes and proteins, may play during IVD physiology.

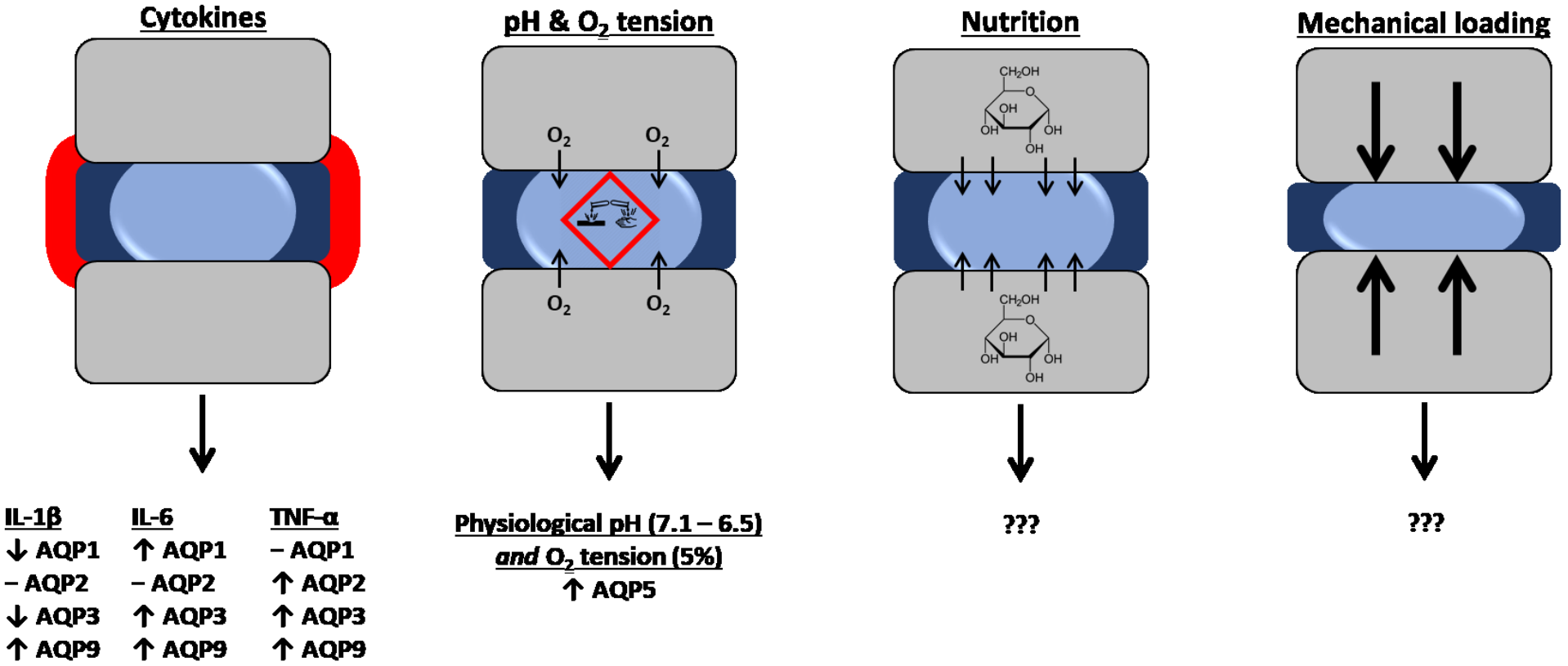

Figure 5.9. Regulation of AQP gene expression in 3D alginate cultured human NP cells. Cytokines present during IVD degeneration upregulate and downregulate AQP gene expression, depending on the individual cytokine and AQP. AQP5 is upregulated by simultaneous physiological pH and O_2 tension treatment, indicating many microenvironmental factors may influence AQP expression in human NP cells, in unison. However, there are more factors that contribute to NP cell function *in vivo* than have been investigated in this study, such as nutrition and mechanical loading. To determine how AQP expression is truly regulated in the IVD, the *in vivo* conditions must be recapitulated very precisely.

Chapter 6: General discussion and future directions

IVD degeneration-associated LBP remains a debilitating condition with no treatments currently available that are directed towards halting and reversing the degenerative cascade at a cellular level. The lack of such treatments is in part due to incomplete knowledge of the molecular mechanisms that govern IVD function in health and degeneration. Due to the unique location and role of the IVD within the spine, many factors contribute to the microenvironment that cells reside within. The survival and function of cells has been irrefutably linked to their ability to adapt to the microenvironment in which they live. During IVD degeneration the microenvironment is altered which has a detrimental effect on cell behaviour and, in part, plays a role in the dysfunction that causes cells to display a catabolic phenotype, intensifying IVD degeneration. As such, increasing the understanding of normal cellular functions, and how the IVD microenvironment contributes to this, may help elucidate mechanisms that are altered during degenerative processes. Potentially revealing novel strategies and treatments to target the cellular causes of IVD degeneration.

The overall aim of this thesis was to investigate the expression, regulation and function of AQP transmembrane water channels within the IVD and how they potentially contribute to the adaptation of cells to their environment. Chapter 2 investigated the expression of AQPs in the IVD, specifically how expression may be altered during developmental and degenerative processes. Chapter 3 presented the regulation of AQP expression by hyperosmolality, physiological to the IVD and well known to regulate AQPs in other tissues, and the control of regulation by a transcription factor (TonEBP) implicated in NP cell function. Chapter 4 demonstrated

that AQPs contribute to fundamental cellular processes such as the control of cell volume in response to altered extracellular osmolality in NP cells, and that other transmembrane channels work in unison with AQPs to facilitate this. Chapter 5 set out to further characterise that AQP expression in NP cells was also regulated by other microenvironmental factors that contribute to IVD health and degeneration. A summary of key findings from this body of work is provided below.

6.1 The expression of AQPs within the intervertebral disc

The IVD is an osmotically challenged tissue which is altered from development to maturation and further changes during degeneration. Therefore, NC and NP cells must employ several tightly regulated mechanisms to survive and function within their unique osmotic environment. Their function as transmembrane water channels, highlighted that many AQP isoforms may be expressed by these cells to enable their adaptation to the surrounding environment. In fact, results here did identify the expression of 9 different AQP isoforms (AQP0 – 7 and 9) within the developing and mature IVD, of which 5 had not previously been shown to be expressed (AQP0, 4, 6, 7 and 9). Results presented here imply that the expression of numerous AQP family members in the disc highlights the importance of maintaining intricate control over regulation of water and solute transport and cell volume in NP cells. The increased proportion of NP cells expressing AQP2 and AQP7 during degeneration may reflect consequences or potential repair mechanisms employed by the disc as NP cells lose their ability to adapt to the degenerate hypo-osmolar environment, which is identified by the loss of AQP1, AQP4 and AQP5 expression during degeneration. The expression of numerous AQPs within the disc may

highlight the importance of controlling water and solute transport in relation to maintaining NC and NP cell function. As yet the actual roles of AQPs within disc maturation and degeneration are unknown; warranting further investigation into the identification of mechanisms of regulation and functions of AQPs (determined by later chapters), to elucidate the true action of these transmembrane channel proteins on the overall behaviour and health of the disc.

6.2 The osmotic regulation of AQP1 and 5 in nucleus pulposus cells

AQP1 and 5 expression is decreased during human IVD degeneration (Johnson *et al.*, 2015). This study has identified that AQP1 and 5 are upregulated by hyperosmolality, mimicking the healthy NP, and may explain why expression is decreased during degeneration, when the osmolality is decreased. This suggests AQP1 and 5 may be part of the mechanisms that allow NP cells to adapt to their hyperosmotic environment. TonEBP has already been established as an integral part of those mechanisms; as the hyperosmotic upregulation of AQP1 and 5 is dependent on TonEBP, this implies they both participate in the osmoadaptation process and matrix synthesis. During IVD degeneration TonEBP function is uncoupled from the altered osmolality and catabolic genes are upregulated instead of the classical osmotic response genes, which may also include AQP1 and 5. As expression of these genes (and AQP1 and 5) is reduced, NP cells can no longer adapt to the altered environment and degeneration is exacerbated Therefore, AQPs may play a role in adapting NP cells to their environment and maintaining the function of NP tissue.

6.3 The regulation of cell volume and water permeability in nucleus pulposus cells

Identifying how NP cells adapt to their osmotically challenging environment is key to understanding their fundamental functions, which in turn enables their adaptation. The activity of AQP4 and TRPV4, an osmotic and mechano-sensitive Ca^{2+} channel, were identified by this thesis to contribute to the fundamental functions of NP cells when physiological extracellular osmolality levels were changed. AQP4 and TRPV4 function may be linked in NP cells in order to control the rate of cell volume regulation, water permeability and Ca^{2+} influx, which may trigger downstream mechanisms enabling the adaptation of NP cells to their osmotic environment. During IVD degeneration, this thesis identified that AQP4 expression was decreased; as a result, NP cells will not be able to respond to the hypo-osmotic environment due to impaired cell volume regulation and Ca^{2+} influx. Due to the lack of osmotic response, downstream mechanisms may not be employed by NP cells to ensure their survival and function in the increasingly degenerate environment. Further study is warranted to determine what impact AQP4 and TRPV4 expression and function have on potential downstream mechanisms such as RVD, cell survival and matrix synthesis.

6.4 Regulation of AQP expression by physiological conditions within the intervertebral disc

AQPs within NP cells may be regulated by many environmental cues within NP cells, such as cytokines and pH, along with alterations in osmolality. Yet, to date the true regulation and function of AQPs within the IVD is relatively unknown. Cytokines along with combined physiological pH and O_2 concentration regulated AQP

expression in NP cells indicating that multiple conditions control AQP expression in the IVD, and that multiple conditions may work in tandem to finely tune AQP expression. However, AQP regulation by healthy and degenerate conditions was unclear, and other factors that contribute to the IVD microenvironment, such as nutrition and mechanical loading, were not investigated. The *in vivo* conditions of the IVD must be replicated very specifically to gather the information required to unfold the potential roles AQPs, and all other genes/proteins, may play during IVD physiology.

6.5 Future directions

6.5.1 AQP membrane trafficking

The regulation of AQP expression at gene and protein level in NP cells has been investigated and linked to the potential roles AQPs play within the IVD, in this thesis. However, the function of AQPs as channels relies on their insertion into the cell membrane; which has been shown to be regulated by cellular trafficking mechanisms, such as protein kinase phosphorylation, calcium signalling and cytoskeletal rearrangement (Section 1.6).

In order to investigate if AQP (particularly 1, 4, and 5) membrane expression is regulated by physiological hyperosmolality in NP cells, the use of cell surface biotinylation can be used. This ELISA-based method biotinylates cell surface proteins after short (minutes) or longer-term (hours) osmotic treatments, and then immobilises them to avidin-coated wells. Proteins of interest can then be probed using antibodies and HRP-substrate absorbance changes detected to determine AQP

abundance at the cell membrane (Kitchen, P. *et al.*, 2015). The mechanisms that control AQP trafficking can also be determined by introducing protein kinase inhibitors or transfection of AQP phosphorylation mutants (Kuwahara *et al.*, 1995; Conner *et al.*, 2010, 2012; Kitchen, P. *et al.*, 2015), calcium inhibitors such as BAPTA-AM (Kitchen, P. *et al.*, 2015), and microtubule and actin inhibitors (Nicchia *et al.*, 2008; Conner *et al.*, 2010). If the trafficking of AQPs was determined, this would identify another level of functional regulation and control of AQPs within NP cells that investigations which this thesis has not elucidated.

6.5.2 AQP contribution to NP cell function

This thesis determined that AQP expression is altered during IVD development and degeneration, and that physiological conditions regulated their expression and function. However, it was not determined whether changes in expression were causes or consequences of the changing physiology of the IVD and what changes in AQP expression actually meant for the function of NP cells.

Performing AQP knockdown on NP cells by using siRNA or lentiviral vectors and transfection of AQP over-expression plasmids and determining the effects of AQP deletion and over-expression on matrix synthesis and cytokine, ADAMTS and MMP expression, will give an indication on how AQP expression (and changes during degeneration) may be linked to the functions of NP cells.

The effects of AQP3 expression on NP cell function has previously been investigated (Xie *et al.*, 2016). It was determined that siRNA knockdown of AQP3 in NP cells was detrimental for matrix synthesis and proliferation and ADAMTS

expression was upregulated (Xie *et al.*, 2016). This investigation shows promise that AQPs do contribute to the overall functions of NP cells and the integrity of the IVD, but as AQP3 expression is not altered during human IVD degeneration (Chapter 3), it remains to be determined what changes in AQP1, 2, 4, 5 and 7 (which showed altered expression during degeneration (Chapter 2)) actually correspond to with regards to IVD health. However, Xie *et al.*, 2016 used commercial human NP cell lines in their studies, which are reported to remain differentiated up to 15 passages and are not properly characterised as actual NP cells; vimentin and fibronectin are reported as phenotypic markers (ScienCell Research Laboratories, San Diego, CA, USA) which are not NP markers (Section 1.2.3). To accurately determine AQP function in the IVD, it would be beneficial to use NP cells extracted from tissue and used at a low passage, such as the NP cells utilised in this thesis.

6.5.3 AQP regulation by mechanical loading

Many environmental factors govern the function of NP cells. This thesis identified that physiological conditions regulate AQP expression and function in NP cells, however, not all physiological conditions were considered. Mechanical loading of the IVD, and how NP cells have adapted to this, is an essential part of how NP cells function. Yet, to date no studies have investigated how AQPs may contribute to this adaptation.

The regulation of AQP expression by mechanical loading in healthy and degenerate NP tissue explants could be investigated by using mechanical testing equipment such as the ElectroForce BioDynamic 5200 (TA Instruments) mechanical stimulation bioreactor. This system enables axial compression of tissue to simulate

the physiological loading of the IVD on *ex vivo* NP tissue explants, whilst media is perfused through a bioreactor chamber (also allowing the nutrient diffusion and osmolality to be controlled at the same time), to determine how this effects AQP expression. The potential underlying mechanisms that control AQP expression under load, could be investigated using Flexcell (Burlington, NC, USA) culture plates, for example limited studies have previously shown that AQP function may be linked to integrin-linked kinase and focal adhesion kinase (Cano-Peñalver *et al.*, 2014; Meng *et al.*, 2014; Mamuya *et al.*, 2016; Hatem-Vaquero *et al.*, 2017). This technology allows the application of loading, such as tension and compression, to cells in monolayer which will enable the use of function-modulating compounds to determine mechanisms that control AQP expression. Such experiments may be able to determine how AQPs contribute to NP cell adaptation to mechanical loading and how they may be involved in altered mechanotransduction during IVD degeneration (Le Maitre *et al.*, 2009).

6.6 Concluding remarks

The anatomy of the IVD and age-related changes has been well documented over the past few centuries. However, LBP still costs the UK £12 billion per year in the 21st century, with 40% of cases attributed to IVD degeneration. Much of the physiology contributing to the disc during health and degeneration has been elucidated in recent years. However, despite this, current treatment options only ameliorate symptoms; there are no treatments that target the underlying cellular causes to halt or reverse IVD degeneration. There is current research interest to develop therapies to combat IVD degeneration, but whether research findings will

translate into clinical use remains to be seen. It is clear however, that an increased understanding of the fundamental processes that control the physiology of the IVD is of great importance to enable the development of new therapies that take into consideration how IVD cells determine the fate of the tissue.

Together, the data presented in this thesis have contributed novel findings and increased knowledge in the field of IVD biology and spine-related research. Results have highlighted NP cells express many AQP water channels *in vivo*, whose expression may be altered between disc development and degeneration. AQP1 and 5 were found to be upregulated by TonEBP in hyperosmotic conditions, mimicking the healthy IVD, which may implicate them in the adaptation of NP cells to their environment, which is no longer achievable when AQP1 and 5 are decreased during degeneration. The importance of AQP4 and TRPV4 function in the way NP cells adapt to their osmotically fluxing environment has also been determined. Additionally, this PhD project has raised new avenues of research for future study, which have the potential to unravel the roles of AQPs in the fundamental cellular processes of IVD biology.

References

Abreu-Rodríguez, Sánchez Silva, Martins, Soveral, Toledo-Aral, López-Barneo and Echevarría (2011) 'Functional and transcriptional induction of aquaporin-1 gene by hypoxia; analysis of promoter and role of Hif-1α.', *PloS one*. Edited by M. B. Fessler, 6(12), p. e28385.

Adams, Keller and Koehl (1990) 'The mechanics of notochord elongation, straightening and stiffening in the embryo of Xenopus laevis.', *Development (Cambridge, England)*, 110(1), pp. 115–30.

Adams, May, Freeman, Morrison and Dolan (2000) 'Effects of backward bending on lumbar intervertebral discs. Relevance to physical therapy treatments for low back pain.', *Spine*, 25(4), pp. 431–7; discussion 438.

Adams and Roughley (2006) 'What is intervertebral disc degeneration, and what causes it?', *Spine*, 31(18), pp. 2151–61.

Adan, Alizada, Kiraz, Baran and Nalbant (2017) 'Flow cytometry: basic principles and applications', *Critical Reviews in Biotechnology*, 37(2), pp. 163–176.

Agrawal, Guttapalli, Narayan, Albert, Shapiro and Risbud (2007) 'Normoxic stabilization of HIF-1alpha drives glycolytic metabolism and regulates aggrecan gene expression in nucleus pulposus cells of the rat intervertebral disk.', *American journal of physiology. Cell physiology*, 293(2), pp. C621-31.

Agre, King, Yasui, Guggino, Ottersen, Fujiyoshi, Engel and Nielsen (2002) 'Aquaporin water channels--from atomic structure to clinical medicine.', *The Journal of physiology*, 542(Pt 1), pp. 3–16.

Agre, Preston, Smith, Jung, Raina, Moon, Guggino and Nielsen (1993) 'Aquaporin CHIP: the archetypal molecular water channel', *American Journal of Physiology-Renal Physiology*, 265(4), pp. F463–F476.

Aharon and Bar-Shavit (2006) 'Involvement of aquaporin 9 in osteoclast differentiation.', *The Journal of biological chemistry*, 281(28), pp. 19305–9.

van den Akker, Surtel, Cremers, Rodrigues-Pinto, Richardson, Hoyland, van Rhijn, Welting and Voncken (2014) 'Novel immortal human cell lines reveal subpopulations in the nucleus pulposus', *Arthritis Research & Therapy*, 16(3), p. R135.

Alkhatib, Ban, Williams and Serra (2018) 'IVD Development: Nucleus pulposus development and sclerotome specification.', *Current molecular biology reports*, 4(3), pp. 132–141.

Amlal, Sheriff and Soleimani (2004) 'Upregulation of collecting duct aquaporin-2 by metabolic acidosis: role of vasopressin.', *American journal of physiology. Cell physiology*, 286(5), pp. C1019-30.

Andrade, Hoogland, Garcia, Steinbusch, Daemen and Visser-Vandewalle (2013) 'Elevated IL-1β and IL-6 levels in lumbar herniated discs in patients with sciatic pain.', *European spine journal : official publication of the European Spine Society, the European Spinal Deformity Society, and the European Section of the Cervical Spine Research Society*, 22(4), pp. 714–20.

Andrade, Visser-Vandewalle, Philippens, Daemen, Steinbusch, Buurman and Hoogland (2011) 'Tumor necrosis factor-α levels correlate with postoperative pain severity in lumbar disc hernia patients: opposite clinical effects between tumor necrosis factor receptor 1 and 2.', *Pain*, 152(11), pp. 2645–52.

Andrews and Lavyne (1990) 'Retrospective analysis of microsurgical and standard lumbar discectomy.', *Spine*, 15(4), pp. 329–35.

Antoniou, Steffen, Nelson, Winterbottom, Hollander, Poole, Aebi and Alini (1996) 'The human lumbar intervertebral disc: evidence for changes in the biosynthesis and denaturation of the extracellular matrix with growth, maturation, ageing, and degeneration.', *Journal of Clinical Investigation*, 98(4), pp. 996–1003.

Arima, Yamamoto, Sobue, Umenishi, Tada, Katsuya and Asai (2003) 'Hyperosmolar mannitol simulates expression of aquaporins 4 and 9 through a p38 mitogen-activated protein kinase-dependent pathway in rat astrocytes.', *The Journal of biological chemistry*, 278(45), pp. 44525–34.

Arniges, Vázquez, Fernández-Fernández and Valverde (2004) 'Swelling-activated Ca^{2+} Entry via TRPV4 Channel Is Defective in Cystic Fibrosis Airway Epithelia', *Journal of Biological Chemistry*, 279(52), pp. 54062–54068.

Bach, Tellegen, Beukers, Miranda-Bedate, Teunissen, de Jong, de Vries, Creemers, Benz, Meij, Ito and Tryfonidou (2018) 'Biologic canine and human intervertebral disc repair by notochordal cell-derived matrix: from bench towards bedside.', *Oncotarget*, 9(41), pp. 26507–26526.

Barron, Rybchyn, Ramesh, Mason, Fiona Bonar, Stalley, Khosla, Hudson, Arthur, Kim, Clifton-Bligh and Clifton-Bligh (2017) 'Clinical, cellular, microscopic, and ultrastructural studies of a case of fibrogenesis imperfecta ossium.', *Bone research*, 5, p. 16057.

Bartels, Fairbank, Winlove and Urban (1998) 'Oxygen and lactate concentrations measured in vivo in the intervertebral discs of patients with scoliosis and back pain.', *Spine*, 23(1), pp. 1–7; discussion 8.

Battié, Videman, Gill, Moneta, Nyman, Kaprio and Koskenvuo (1991) '1991 Volvo Award in clinical sciences. Smoking and lumbar intervertebral disc degeneration: an MRI study of identical twins.', *Spine*, 16(9), pp. 1015–21.

Behind the Coulter Principle - Beckman Coulter.

Beitz, Liu, Ikeda, Guggino, Agre and Yasui (2006) 'Determinants of AQP6 trafficking to intracellular sites versus the plasma membrane in transfected mammalian cells', *Biology of the Cell*, 98(2), pp. 101–109.

Beitz, Wu, Holm, Schultz and Zeuthen (2006) 'Point mutations in the aromatic/arginine region in aquaporin 1 allow passage of urea, glycerol, ammonia, and protons', *Proceedings of the National Academy of Sciences*, 103(2), pp. 269–274.

Benfenati, Caprini, Dovizio, Mylonakou, Ferroni, Ottersen and Amiry-Moghaddam (2011a) 'An aquaporin-4/transient receptor potential vanilloid 4 (AQP4/TRPV4) complex is essential for cell-volume control in astrocytes.', *Proceedings of the National Academy of Sciences of the United States of America*, 108(6), pp. 2563–8.

Benfenati, Caprini, Dovizio, Mylonakou, Ferroni, Ottersen and Amiry-Moghaddam (2011b) 'An aquaporin-4/transient receptor potential vanilloid 4 (AQP4/TRPV4) complex is essential for cell-volume control in astrocytes.', *Proceedings of the National Academy of Sciences of the United States of America*, 108(6), pp. 2563–8.

Benfenati and Ferroni (2010) 'Water transport between CNS compartments: functional and molecular interactions between aquaporins and ion channels', *Neuroscience*, 168(4), pp. 926–940.

Bergknut, Smolders, Grinwis, Hagman, Lagerstedt, Hazewinkel, Tryfonidou and Meij (2013) 'Intervertebral disc degeneration in the dog. Part 1: Anatomy and physiology of the intervertebral disc and characteristics of intervertebral disc degeneration.', *Veterinary journal (London, England : 1997)*, 195(3), pp. 282–91.

Bibby, Jones, Ripley and Urban (2005) 'Metabolism of the intervertebral disc: effects of low levels of oxygen, glucose, and pH on rates of energy metabolism of bovine nucleus pulposus cells.', *Spine*, 30(5), pp. 487–96.

Binch, Cole, Breakwell, Michael, Chiverton, Creemers, Cross and Le Maitre (2015) 'Class 3 semaphorins expression and association with innervation and angiogenesis within the degenerate human intervertebral disc.', *Oncotarget*, 6(21), pp. 18338–54.

Binch, Cole, Breakwell, Michael, Chiverton, Cross and Le Maitre (2014) 'Expression and regulation of neurotrophic and angiogenic factors during human intervertebral disc degeneration', *Arthritis Research & Therapy*, 16(4), p. 416.

Biswas, Brako, Gu, Jiang and Lo (2014) 'Regional changes of AQP0-dependent square array junction and gap junction associated with cortical cataract formation in the Emory mutant mouse', *Experimental Eye Research*, 127, pp. 132–142.

Boesen (2013) 'Chronic elevation of IL-1β induces diuresis via a cyclooxygenase 2-mediated mechanism.', *American journal of physiology. Renal physiology*, 305(2), pp. F189-98.

Burg, Ferraris and Dmitrieva (2007) 'Cellular response to hyperosmotic stresses.', *Physiological reviews*, 87(4), pp. 1441–74.

Burg, Kwon and Kültz (1996) 'Osmotic regulation of gene expression.', *FASEB journal : official publication of the Federation of American Societies for Experimental Biology*, 10(14), pp. 1598–606.

Burke, Watson, McCormack, Dowling, Walsh and Fitzpatrick (2002) 'Intervertebral

discs which cause low back pain secrete high levels of proinflammatory mediators.', *The Journal of bone and joint surgery. British volume*, 84(2), pp. 196–201.

C, X, Z, N, H, M, G, H, Z and S (2012) 'Hypertonic saline reduces lipopolysaccharide-induced mouse brain edema through inhibiting aquaporin 4 expression', *Critical Care*, 16(5), p. R186.

Cai, Lei, Li, Chen and Li (2017) 'Aquaporin-4 Blockage by siRNA Protects Rat Articular Chondrocytes from IL-1β-induced Apoptosis by Inhibiting p38 MAPK Signal Pathway.', *Annals of clinical and laboratory science*, 47(5), pp. 563–571.

Cano-Peñalver, Griera, Serrano, Rodríguez-Puyol, Dedhar, de Frutos and Rodríguez-Puyol (2014) 'Integrin-linked kinase regulates tubular aquaporin-2 content and intracellular location: a link between the extracellular matrix and water reabsorption', *The FASEB Journal*, 28(8), pp. 3645–3659.

Cao, Quan, Jiang, Luo, Zhong and Liu (2012) '[Effect of adenovirus human bone morphogenetic protein 4 on human degenerative lumbar intervertebral disc cells].', *Zhongguo xiu fu chong jian wai ke za zhi = Zhongguo xiufu chongjian waike zazhi = Chinese journal of reparative and reconstructive surgery*, 26(12), pp. 1442–7.

Capdevila, Tabin and Johnson (1998) 'Control of Dorsoventral Somite Patterning by Wnt-1 and β-Catenin', *Developmental Biology*, 193(2), pp. 182–194.

Carette, Leclaire, Marcoux, Morin, Blaise, St.-Pierre, Truchon, Parent, Lévesque, Bergeron, Montminy and Blanchette (1997) 'Epidural Corticosteroid Injections for Sciatica Due to Herniated Nucleus Pulposus', *New England Journal of Medicine*, 336(23), pp. 1634–1640.

Caron, van der Windt, Emans, van Rhijn, Jahr and Welting (2013) 'Osmolarity determines the in vitro chondrogenic differentiation capacity of progenitor cells via nuclear factor of activated T-cells 5', *Bone*. Elsevier, 53(1), pp. 94–102.

Caterina, Schumacher, Tominaga, Rosen, Levine and Julius (1997) 'The capsaicin receptor: a heat-activated ion channel in the pain pathway.', *Nature*, 389(6653), pp. 816–24.

Chai, Jiang, Wong, Jiang, Gao, Vatcher and Hoi Yu (2013) 'AQP5 is differentially regulated in astrocytes during metabolic and traumatic injuries.', *Glia*, 61(10), pp. 1748–65.

Chan, Ferguson, Wuertz and Gantenbein-Ritter (2011) 'Biological Response of the Intervertebral Disc to Repetitive Short-Term Cyclic Torsion', *Spine*, 36(24), pp. 2021–2030.

Chastre, Jiang, Desjardins and Butterworth (2010) 'Ammonia and proinflammatory cytokines modify expression of genes coding for astrocytic proteins implicated in brain edema in acute liver failure.', *Metabolic brain disease*, 25(1), pp. 17–21.

Chen and Knutson (1988) ‘Mechanism of fluorescence concentration quenching of carboxyfluorescein in liposomes: energy transfer to nonfluorescent dimers.’, *Analytical biochemistry*, 172(1), pp. 61–77.

Chen, Yan and Setton (2006) ‘Molecular phenotypes of notochordal cells purified from immature nucleus pulposus’, *European Spine Journal*, 15(S3), pp. 303–311.

Chen, Zhou, Yan, Ma and Zheng (2015) ‘Hyperosmotic stress induces cisplatin sensitivity in ovarian cancer cells by stimulating aquaporin-5 expression.’, *Experimental and therapeutic medicine*, 10(6), pp. 2055–2062.

Chmelova, Sucha, Bochin, Vorisek, Pivonkova, Hermanova, Anderova and Vargova (2019) ‘The role of aquaporin-4 and transient receptor potential vaniloid isoform 4 channels in the development of cytotoxic edema and associated extracellular diffusion parameter changes’, *European Journal of Neuroscience*.

Choi, Chaiyamongkol, Doolittle, Johnson, Gogate, Schoepflin, Shapiro and Risbud (2018) ‘COX-2 expression mediated by calcium-TonEBP signaling axis under hyperosmotic conditions serves osmoprotective function in nucleus pulposus cells’, *Journal of Biological Chemistry*, 293(23), pp. 8969–8981.

Choi, Cohn and Harfe (2008) ‘Identification of nucleus pulposus precursor cells and notochordal remnants in the mouse: implications for disk degeneration and chordoma formation.’, *Developmental dynamics : an official publication of the American Association of Anatomists*, 237(12), pp. 3953–8.

Choi, Lee and Harfe (2012) ‘Sonic hedgehog in the notochord is sufficient for patterning of the intervertebral discs’, *Mechanisms of Development*, 129(9–12), pp. 255–262.

Chou, Atlas, Stanos and Rosenquist (2009) ‘Nonsurgical Interventional Therapies for Low Back Pain’, *Spine*, 34(10), pp. 1078–1093.

Christ, Huang and Scaal (2004) ‘Formation and differentiation of the avian sclerotome’, *Anatomy and Embryology*, 208(5), pp. 333–50.

Christ and Scaal (2008) ‘Formation and differentiation of avian somite derivatives.’, *Advances in experimental medicine and biology*, 638, pp. 1–41.

Clark, Votta, Kumar, Liedtke and Guilak (2010) ‘Chondroprotective role of the osmotically sensitive ion channel transient receptor potential vanilloid 4: age- and sex-dependent progression of osteoarthritis in Trpv4-deficient mice.’, *Arthritis and rheumatism*, 62(10), pp. 2973–83.

Clément, Rodriguez-Grande and Badaut (2018) ‘Aquaporins in brain edema’, *Journal of Neuroscience Research*.

Conner, Bill and Conner (2013) ‘An emerging consensus on aquaporin translocation as a regulatory mechanism’, *Molecular Membrane Biology*, 30(1), pp. 101–112.

Conner, Conner, Bland, Taylor, Brown, Parri and Bill (2012) 'Rapid Aquaporin Translocation Regulates Cellular Water Flow', *Journal of Biological Chemistry*, 287(14), pp. 11516–11525.

Conner, Conner, Brown and Bill (2010) 'Membrane Trafficking of Aquaporin 1 Is Mediated by Protein Kinase C via Microtubules and Regulated by Tonicity', *Biochemistry*, 49(5), pp. 821–823.

Corasanti, Gleeson and Boyer (1990) 'Effects of osmotic stresses on isolated rat hepatocytes. I. Ionic mechanisms of cell volume regulation.', *The American journal of physiology*, 258(2 Pt 1), pp. G290-8.

Cs-Szabo, Ragasa-San Juan, Turumella, Masuda, Thonar and An (2002) 'Changes in mRNA and protein levels of proteoglycans of the anulus fibrosus and nucleus pulposus during intervertebral disc degeneration.', *Spine*, 27(20), pp. 2212–9.

Day, Kitchen, Owen, Bland, Marshall, Conner, Bill and Conner (2014) 'Human aquaporins: Regulators of transcellular water flow', *Biochimica et Biophysica Acta (BBA) - General Subjects*, 1840(5), pp. 1492–1506.

Denker, Smith, Kuhajda and Agre (1988) 'Identification, purification, and partial characterization of a novel Mr 28,000 integral membrane protein from erythrocytes and renal tubules.', *The Journal of biological chemistry*, 263(30), pp. 15634–42.

van Dijk, Potier and Ito (2011) 'Culturing Bovine Nucleus Pulposus Explants by Balancing Medium Osmolarity', *Tissue Engineering Part C: Methods*, 17(11), pp. 1089–1096.

Ding, Kreipke, Speirs, Schafer, Schafer and Rafols (2009) 'Hypoxia-inducible factor-1alpha signaling in aquaporin upregulation after traumatic brain injury.', *Neuroscience letters*, 453(1), pp. 68–72.

Ding, Shao and Xiong (2013) 'Cell death in intervertebral disc degeneration', *Apoptosis*, 18(7), pp. 777–785.

Ding, Zhang, Xu, Sheng and Huang (2013) 'Propofol administration modulates AQP-4 expression and brain edema after traumatic brain injury.', *Cell biochemistry and biophysics*, 67(2), pp. 615–22.

Doege, Sasaki, Kimura and Yamada (1991) 'Complete coding sequence and deduced primary structure of the human cartilage large aggregating proteoglycan, aggrecan. Human-specific repeats, and additional alternatively spliced forms.', *The Journal of biological chemistry*, 266(2), pp. 894–902.

Dolan and Adams (2001) 'Recent advances in lumbar spinal mechanics and their significance for modelling.', *Clinical biomechanics (Bristol, Avon)*, 16 Suppl 1, pp. S8–S16.

Elliott and Setton (2000) 'A Linear Material Model for Fiber-Induced Anisotropy of the Anulus Fibrosus', *Journal of Biomechanical Engineering*. American Society of Mechanical Engineers, 122(2), p. 173.

Esensten, Tsytsykova, Lopez-Rodriguez, Ligeiro, Rao and Goldfeld 'NFAT5 binds to the TNF promoter distinctly from NFATp, c, 3 and 4, and activates TNF transcription during hypertonic stress alone'.

Esser and Thermo Scientific, *pH and Pressure in Closed Tissue Culture Vessels*.

Everaerts, Nilius and Owsianik (2010a) 'The vanilloid transient receptor potential channel TRPV4: From structure to disease', *Progress in Biophysics and Molecular Biology*, 103(1), pp. 2–17.

Everaerts, Nilius and Owsianik (2010b) 'The vanilloid transient receptor potential channel TRPV4: From structure to disease', *Progress in Biophysics and Molecular Biology*, 103(1), pp. 2–17.

Fan and Tessier-Lavigne (1994) 'Patterning of mammalian somites by surface ectoderm and notochord: evidence for sclerotome induction by a hedgehog homolog.', *Cell*, 79(7), pp. 1175–86.

Fasshauer, Klein, Lossner, Klier, Kralisch and Paschke (2003) 'Suppression of aquaporin adipose gene expression by isoproterenol, TNFalpha, and dexamethasone.', *Hormone and metabolic research = Hormon- und Stoffwechselforschung = Hormones et metabolisme*, 35(4), pp. 222–7.

Feng, Zhang, Dang, Zhang, Doleyres, Song, Chen and Ma (2017) 'Injectable nanofibrous spongy microspheres for NR4A1 plasmid DNA transfection to reverse fibrotic degeneration and support disc regeneration', *Biomaterials*, 131, pp. 86–97.

Fenton, Moeller, Nielsen, de Groot and Rützler (2010) 'A plate reader-based method for cell water permeability measurement', *American Journal of Physiology-Renal Physiology*, 298(1), pp. F224–F230.

Fischer, Kosinska-Eriksson, Aponte-Santamaría, Palmgren, Geijer, Hedfalk, Hohmann, de Groot, Neutze and Lindkvist-Petersson (2009) 'Crystal structure of a yeast aquaporin at 1.15 angstrom reveals a novel gating mechanism.', *PLoS biology*. Edited by G. A. Petsko, 7(6), p. e1000130.

Fotiadis, Suda, Tittmann, Jenö, Philippsen, Müller, Gross and Engel (2002) 'Identification and structure of a putative Ca2+-binding domain at the C terminus of AQP1.', *Journal of molecular biology*, 318(5), pp. 1381–94.

Freemont, A. J., Watkins, Le Maitre, Baird, Jeziorska, Knight, Ross, O'Brien and Hoyland (2002) 'Nerve growth factor expression and innervation of the painful intervertebral disc', *The Journal of Pathology*, 197(3), pp. 286–292.

Freemont, A J, Watkins, Le Maitre, Jeziorska and Hoyland (2002) 'Current understanding of cellular and molecular events in intervertebral disc degeneration: implications for therapy.', *The Journal of pathology*, 196(4), pp. 374–9.

FUJII, HIRAYAMA, FUKUDA, KAGEYAMA, NAITO, YOSHINO, MORIYASU, YAMAZAKI, SAKAMOTO, HAYAKAWA, TAKAHASHI, TAKAHASHI and SAWAI (2018) 'Expression and localization of aquaporins 3 and 7 in bull spermatozoa and their relevance to sperm motility after cryopreservation', *Journal of Reproduction and Development*, 64(4), pp. 327–335.

Fujita, Markova, Anderson, Chiba, Toyama, Shapiro and Risbud (2012) 'Expression of Prolyl Hydroxylases (PHDs) Is Selectively Controlled by HIF-1 and HIF-2 Proteins in Nucleus Pulposus Cells of the Intervertebral Disc', *Journal of Biological Chemistry*, 287(20), pp. 16975–16986.

Gajghate, Hiyama, Shah, Sakai, Anderson, Shapiro and Risbud (2009) 'Osmolarity and intracellular calcium regulate aquaporin2 expression through TonEBP in nucleus pulposus cells of the intervertebral disc', *Journal of Bone and Mineral Research*, 24(6), pp. 992–1001.

Gal An-Cobo, Ram Irez-Lorca and Echevarr (2016) 'Role of aquaporins in cell proliferation: What else beyond water permeability?'

Galante (1967) 'Tensile properties of the human lumbar annulus fibrosus.', *Acta orthopaedica Scandinavica*, p. Suppl 100:1-91.

Galcheva-Gargova, Dérijard, Wu and Davis (1994) 'An osmosensing signal transduction pathway in mammalian cells.', *Science (New York, N.Y.)*, 265(5173), pp. 806–8.

Galizia, Pizzoni, Fernandez, Rivarola, Capurro and Ford (2012) 'Functional interaction between AQP2 and TRPV4 in renal cells', *Journal of Cellular Biochemistry*, 113(2), pp. 580–589.

Gan, Tu, Li, Ye, Zhao, Luo, Zhang, Zhang, Zhu and Zhou (2018) 'Low Magnitude of Compression Enhances Biosynthesis of Mesenchymal Stem Cells towards Nucleus Pulposus Cells via the TRPV4-Dependent Pathway', *Stem Cells International*, 2018, pp. 1–12.

Gilbert, Hodson, Baird, Richardson and Hoyland (2016) 'Acidic pH promotes intervertebral disc degeneration: Acid-sensing ion channel-3 as a potential therapeutic target OPEN', *Nature Publishing Group*.

Gilbert, Hoyland, Freemont and Millward-Sadler (2011) 'The involvement of interleukin-1 and interleukin-4 in the response of human annulus fibrosus cells to cyclic tensile strain: an altered mechanotransduction pathway with degeneration.', *Arthritis research & therapy*, 13(1), p. R8.

Gilbert, Hoyland and Millward-Sadler (2010) 'The response of human anulus fibrosus cells to cyclic tensile strain is frequency-dependent and altered with disc degeneration.', *Arthritis and rheumatism*, 62(11), pp. 3385–94.

Gorth, Mauck, Chiaro, Mohanraj, Hebela, Dodge, Elliott and Smith (2012) 'IL-1ra delivered from poly(lactic-co-glycolic acid) microspheres attenuates IL-1β-mediated degradation of nucleus pulposus in vitro.', *Arthritis research & therapy*, 14(4), p. R179.

Gorth, Shapiro and Risbud (2019) 'Transgenic mice overexpressing human TNF-α experience early onset spontaneous intervertebral disc herniation in the absence of overt degeneration', *Cell Death & Disease*, 10(1), p. 7.

Götz, Osmers and Herken (1995) 'Localisation of extracellular matrix components in the embryonic human notochord and axial mesenchyme.', *Journal of anatomy*, 186 (Pt 1), pp. 111–21.

Grabarek (2005) 'Structure of a Trapped Intermediate of Calmodulin: Calcium Regulation of EF-hand Proteins from a New Perspective', *Journal of Molecular Biology*, 346(5), pp. 1351–1366.

Grant, Epure, Bokhari, Roughley, Antoniou and Mwale (2016) 'Human cartilaginous endplate degeneration is induced by calcium and the extracellular calcium-sensing receptor in the intervertebral disc.', *European cells & materials*, 32, pp. 137–51.

de Groot and Grubmüller (2005) 'The dynamics and energetics of water permeation and proton exclusion in aquaporins', *Current Opinion in Structural Biology*, 15(2), pp. 176–183.

Gruber and Hanley (1998) 'Analysis of aging and degeneration of the human intervertebral disc. Comparison of surgical specimens with normal controls.', *Spine*, 23(7), pp. 751–7.

Gruber, Ingram, Norton and Hanley (2007) 'Senescence in Cells of the Aging and Degenerating Intervertebral Disc', *Spine*, 32(3), pp. 321–327.

Haefeli, Kalberer, Saegesser, Nerlich, Boos and Paesold (2006) 'The course of macroscopic degeneration in the human lumbar intervertebral disc.', *Spine*, 31(14), pp. 1522–31.

Halterman, Kwon and Wamhoff (2012) 'Tonicity-independent regulation of the osmosensitive transcription factor TonEBP (NFAT5)', *American Journal of Physiology-Cell Physiology*, 302(1), pp. C1–C8.

Hamann, Kiilgaard, Litman, Alvarez-Leefmans, Winther and Zeuthen (2002) 'Measurement of Cell Volume Changes by Fluorescence Self-Quenching', *Journal of Fluorescence*. Kluwer Academic Publishers-Plenum Publishers, 12(2), pp. 139–145.

Han, Lee, Bibbs and Ulevitch (1994) 'A MAP kinase targeted by endotoxin and hyperosmolarity in mammalian cells.', *Science (New York, N.Y.)*, 265(5173), pp. 808–11.

Hartman, Patil, Tisherman, St. Croix, Niedernhofer, Robbins, Ambrosio, Van Houten, Sowa and Vo (2018) 'Age-dependent changes in intervertebral disc cell mitochondria and bioenergetics', *European Cells and Materials*, 36, pp. 171–183.

Hasler, Nunes, Bouley, Lu, Matsuzaki and Brown (2008) 'Acute hypertonicity alters aquaporin-2 trafficking and induces a MAPK-dependent accumulation at the plasma membrane of renal epithelial cells.', *The Journal of biological chemistry*, 283(39), pp. 26643–61.

Hatem-Vaquero, Griera, Giermakowska, Luengo, Calleros, Gonzalez Bosc, Rodríguez-Puyol, Rodríguez-Puyol and De Frutos (2017) 'Integrin linked kinase regulates the transcription of AQP2 by NFATC3', *Biochimica et Biophysica Acta (BBA) - Gene Regulatory Mechanisms*, 1860(9), pp. 922–935.

Hayashi, Edwards, Proescholdt, Oldfield and Merrill (2007) 'Regulation and function of aquaporin-1 in glioma cells.', *Neoplasia (New York, N.Y.)*, 9(9), pp. 777–87.

He, Wang, Yang, Peng and Li (2013) 'Normal and degenerated rabbit nucleus pulposus cells in in vitro cultures: A biological comparison', *Journal of Huazhong University of Science and Technology [Medical Sciences]*, 33(2), pp. 228–233.

Higashida, Peng, Li, Dornbos, Teng, Li, Kinni, Guthikonda and Ding (2011) 'Hypoxia-inducible factor-1α contributes to brain edema after stroke by regulating aquaporins and glycerol distribution in brain.', *Current neurovascular research*, 8(1), pp. 44–51.

Hill and Shachar-Hill 'Are Aquaporins the Missing Transmembrane Osmosensors?'

Hiyama, Gajghate, Sakai, Mochida, Shapiro and Risbud (2009) 'Activation of TonEBP by calcium controls {beta}1,3-glucuronosyltransferase-I expression, a key regulator of glycosaminoglycan synthesis in cells of the intervertebral disc.', *The Journal of biological chemistry*. American Society for Biochemistry and Molecular Biology, 284(15), pp. 9824–34.

Ho, Yeh, Sandstrom, Chorny, Harries, Robbins, Miercke and Stroud (2009) 'Crystal structure of human aquaporin 4 at 1.8 A and its mechanism of conductance', *Proceedings of the National Academy of Sciences*, 106(18), pp. 7437–7442.

Hollborn, Rehak, Iandiev, Pannicke, Ulbricht, Reichenbach, Wiedemann, Bringmann and Kohen (2012) 'Transcriptional regulation of aquaporins in the ischemic rat retina: upregulation of aquaporin-9.', *Current eye research*, 37(6), pp. 524–31.

Hollborn, Vogler, Reichenbach, Wiedemann, Bringmann and Kohen (2015) 'Regulation of the hyperosmotic induction of aquaporin 5 and VEGF in retinal pigment epithelial cells: involvement of NFAT5.', *Molecular vision*, 21, pp. 360–77.

Holm, Maroudas, Urban, Selstam and Nachemson (1981) 'Nutrition of the intervertebral disc: solute transport and metabolism.', *Connective tissue research*, 8(2), pp. 101–19.

Horie, Maeda, Yokoyama, Hisatsune, Katsuki, Miyata and Isohama (2009) 'Tumor necrosis factor-alpha decreases aquaporin-3 expression in DJM-1 keratinocytes.', *Biochemical and biophysical research communications*, 387(3), pp. 564–8.

Horner, Roberts, Bielby, Menage, Evans and Urban (2002) 'Cells from different regions of the intervertebral disc: effect of culture system on matrix expression and cell phenotype.', *Spine*, 27(10), pp. 1018–28.

Horner and Urban (2001) '2001 Volvo Award Winner in Basic Science Studies: Effect of nutrient supply on the viability of cells from the nucleus pulposus of the intervertebral disc.', *Spine*, 26(23), pp. 2543–9.

Horsefield, Nordén, Fellert, Backmark, Törnroth-Horsefield, Terwisscha van Scheltinga, Kvassman, Kjellbom, Johanson and Neutze (2008) 'High-resolution x-ray structure of human aquaporin 5.', *Proceedings of the National Academy of Sciences of the United States of America*, 105(36), pp. 13327–32.

Hoy, Smith, Cross, Sanchez-Riera, Blyth, Buchbinder, Woolf, Driscoll, Brooks and March (2015) 'Reflecting on the global burden of musculoskeletal conditions: lessons learnt from the Global Burden of Disease 2010 Study and the next steps forward', *Annals of the Rheumatic Diseases*, 74(1), pp. 4–7.

Hoyland, Le Maitre and Freemont (2008) 'Investigation of the role of IL-1 and TNF in matrix degradation in the intervertebral disc', *Rheumatology*, 47(6), pp. 809–814.

Hub and de Groot (2008) 'Mechanism of selectivity in aquaporins and aquaglyceroporins.', *Proceedings of the National Academy of Sciences of the United States of America*, 105(4), pp. 1198–203.

Hunter, Matyas and Duncan (2003a) 'The Notochordal Cell in the Nucleus Pulposus: A Review in the Context of Tissue Engineering', *Tissue Engineering*, 9(4), pp. 667–677.

Hunter, Matyas and Duncan (2003b) 'The three-dimensional architecture of the notochordal nucleus pulposus: novel observations on cell structures in the canine intervertebral disc.', *Journal of anatomy*, 202(Pt 3), pp. 279–91.

Hunter, Matyas and Duncan (2004a) 'Cytomorphology of notochordal and chondrocytic cells from the nucleus pulposus: a species comparison', *Journal of Anatomy*, 205(5), pp. 357–362.

Hunter, Matyas and Duncan (2004b) 'The functional significance of cell clusters in the notochordal nucleus pulposus: survival and signaling in the canine intervertebral disc.', *Spine*, 29(10), pp. 1099–104.

Iatridis, Kumar, Foster, Weidenbaum and Mow (1999) 'Shear mechanical properties of human lumbar annulus fibrosus', *Journal of Orthopaedic Research*, 17(5), pp. 732–737.

Inkinen, Lammi, Lehmonen, Puustjärvi, Kääpä and Tammi (1998) 'Relative increase of biglycan and decorin and altered chondroitin sulfate epitopes in the degenerating human intervertebral disc.', *The Journal of rheumatology*, 25(3), pp. 506–14.

Ishihara, Warensjo, Roberts and Urban (1997) 'Proteoglycan synthesis in the intervertebral disk nucleus: the role of extracellular osmolality', *American Journal of Physiology-Cell Physiology*, 272(5), pp. C1499–C1506.

Ito, Yamamoto, Arima, Hirate, Morishima, Umenishi, Tada, Asai, Katsuya and Sobue (2006) 'Interleukin-1beta induces the expression of aquaporin-4 through a nuclear factor-kappaB pathway in rat astrocytes.', *Journal of neurochemistry*, 99(1), pp. 107–18.

James, Abate, Abate, Abay, Abbafati, Abbasi, Abbastabar, Abd-Allah, Abdela, Abdelalim, Abdollahpour, Abdulkader, Abebe, Abera, Abil, Abraha, Abu-Raddad, Abu-Rmeileh, Accrombessi, Acharya, Murray, *et al.* (2018) 'Global, regional, and national incidence, prevalence, and years lived with disability for 354 diseases and injuries for 195 countries and territories, 1990–2017: a systematic analysis for the Global Burden of Disease Study 2017', *The Lancet*, 392(10159), pp. 1789–1858.

Janosi and Ceccarelli (2013) 'The gating mechanism of the human aquaporin 5 revealed by molecular dynamics simulations.', *PloS one*. Edited by E. Paci, 8(4), p. e59897.

Jauliac, López-Rodriguez, Shaw, Brown, Rao and Toker (2002) 'The role of NFAT transcription factors in integrin-mediated carcinoma invasion.', *Nature cell biology*, 4(7), pp. 540–4.

Jenq, Mathieson, Ihara and Ramirez (1998) 'Aquaporin-1: an osmoinducible water channel in cultured mIMCD-3 cells.', *Biochemical and biophysical research communications*, 245(3), pp. 804–9.

Jo, Ryskamp, Phuong, Verkman, Yarishkin, Macaulay and Križaj (2015) 'Cellular/Molecular TRPV4 and AQP4 Channels Synergistically Regulate Cell Volume and Calcium Homeostasis in Retinal Müller Glia'.

Johansson, Karlsson, Shukla, Chrispeels, Larsson and Kjellbom (1998) 'Water transport activity of the plasma membrane aquaporin PM28A is regulated by phosphorylation.', *The Plant cell*, 10(3), pp. 451–9.

Johnson, Doolittle, Snuggs, Shapiro, Le Maitre and Risbud (2017) 'TNF-α promotes nuclear enrichment of the transcription factor TonEBP/NFAT5 to selectively control inflammatory but not osmoregulatory responses in nucleus pulposus cells', *Journal of Biological Chemistry*, 292(42), pp. 17561–17575.

Johnson, Gogate, Day, Binch, Markova, Chiverton, Cole, Conner, Shapiro, Le Maitre and Risbud (2015) 'Aquaporin 1 and 5 expression decreases during human intervertebral disc degeneration: Novel HIF-1-mediated regulation of aquaporins in NP cells.', *Oncotarget*, 6(14), pp. 11945–58.

Johnson, Shapiro and Risbud (2014a) 'Extracellular osmolarity regulates matrix homeostasis in the intervertebral disc and articular cartilage: evolving role of TonEBP.', *Matrix biology : journal of the International Society for Matrix Biology*, 40, pp. 10–6.

Johnson, Shapiro and Risbud (2014b) 'Extracellular osmolarity regulates matrix homeostasis in the intervertebral disc and articular cartilage: Evolving role of TonEBP HHS Public Access', *Matrix Biol*, 40, pp. 10–16.

Johnson, Wootton, El Haj, Eisenstein, Curtis and Roberts (2006) 'Topographical guidance of intervertebral disc cell growth in vitro: towards the development of tissue repair strategies for the anulus fibrosus', *European Spine Journal*, 15(S3), pp. 389–396.

Kaneko, Yagui, Tanaka, Yoshihara, Ishikawa, Takahashi, Bujo, Sakurai and Saito (2008) 'Aquaporin 1 is required for hypoxia-inducible angiogenesis in human retinal vascular endothelial cells.', *Microvascular research*, 75(3), pp. 297–301.

Karppinen, Solovieva, Luoma, Raininko, Leino-Arjas and Riihimäki (2009) 'Modic changes and interleukin 1 gene locus polymorphisms in occupational cohort of middle-aged men', *European Spine Journal*, 18(12), pp. 1963–1970.

Kasimanickam, Kasimanickam, Arangasamy and Kastelic (2017) 'Associations of hypoosmotic swelling test, relative sperm volume shift, aquaporin7 mRNA abundance and bull fertility estimates', *Theriogenology*, 89, pp. 162–168.

Kauppila (1997) 'Prevalence of stenotic changes in arteries supplying the lumbar spine. A postmortem angiographic study on 140 subjects.', *Annals of the rheumatic diseases*, 56(10), pp. 591–5.

Kawedia, Yang, Sartor, Gozal, Czyzyk-Krzeska and Menon (2013) 'Hypoxia and hypoxia mimetics decrease aquaporin 5 (AQP5) expression through both hypoxia inducible factor-1α and proteasome-mediated pathways.', *PloS one*. Edited by L. Eisenberg, 8(3), p. e57541.

Kim, Ha, Lee, Nam, Woo, Lim and An (2009) 'Notochordal cells stimulate migration of cartilage end plate chondrocytes of the intervertebral disc in in vitro cell migration assays', *The Spine Journal*, 9(4), pp. 323–329.

Kino, Takatori, Manoli, Wang, Tiulpakov, Blackman, Su, Chrousos, DeCherney and Segars (2009) 'Brx mediates the response of lymphocytes to osmotic stress through the activation of NFAT5.', *Science signaling*, 2(57), p. ra5.

Kitchen and Conner (2015) 'Control of the Aquaporin-4 Channel Water Permeability by Structural Dynamics of Aromatic/Arginine Selectivity Filter Residues', *Biochemistry*, 54(45), pp. 6753–6755.

Kitchen, Conner, Bill and Conner (2016) 'Structural Determinants of Oligomerization of the Aquaporin-4 Channel', *Journal of Biological Chemistry*, 291(13), pp. 6858–6871.

Kitchen, Day, Salman, Conner, Roslyn and Conner (2015) 'Beyond water homeostasis: Diverse functional roles of mammalian aquaporins.', *Biochimica et biophysica acta*, 1850(12), pp. 2410–21.

Kitchen, P., Day, Taylor, Salman, Bill, Conner and Conner (2015) 'Identification and Molecular Mechanisms of the Rapid Tonicity-induced Relocalization of the Aquaporin 4 Channel.', *The Journal of biological chemistry*, 290(27), pp. 16873–81.

Köhler, Heyken, Heinau, Schubert, Si, Kacik, Busch, Grgic, Maier and Hoyer (2006) 'Evidence for a functional role of endothelial transient receptor potential V4 in shear stress-induced vasodilatation.', *Arteriosclerosis, thrombosis, and vascular biology*, 26(7), pp. 1495–502.

Korecki, MacLean and Iatridis (2008) 'Dynamic Compression Effects on Intervertebral Disc Mechanics and Biology', *Spine*, 33(13), pp. 1403–1409.

Kortenoeven and Fenton (2014) 'Renal aquaporins and water balance disorders', *Biochimica et Biophysica Acta (BBA) - General Subjects*, 1840(5), pp. 1533–1549.

Kraemer, Kolditz and Gowin (1985) 'Water and electrolyte content of human intervertebral discs under variable load.', *Spine*, 10(1), pp. 69–71.

Krane, Melvin, Nguyen, Richardson, Towne, Doetschman and Menon (2001a) 'Salivary acinar cells from aquaporin 5-deficient mice have decreased membrane water permeability and altered cell volume regulation.', *The Journal of biological chemistry*, 276(26), pp. 23413–20.

Krane, Melvin, Nguyen, Richardson, Towne, Doetschman and Menon (2001b) 'Salivary Acinar Cells from Aquaporin 5-deficient Mice Have Decreased Membrane Water Permeability and Altered Cell Volume Regulation', *Journal of Biological Chemistry*, 276(26), pp. 23413–23420.

Küper, Beck and Neuhofer (2012) 'NFAT5 Contributes to Osmolality-Induced MCP-1 Expression in Mesothelial Cells', *Mediators of Inflammation*. Hindawi, 2012, pp. 1–12.

Kuwahara, Fushimi, Terada, Bai, Marumo and Sasaki (1995) 'cAMP-dependent phosphorylation stimulates water permeability of aquaporin-collecting duct water channel protein expressed in Xenopus oocytes.', *The Journal of biological chemistry*, 270(18), pp. 10384–7.

Laforenza, Pellavio, Marchetti, Omes, Todaro and Gastaldi (2016) 'Aquaporin-Mediated Water and Hydrogen Peroxide Transport Is Involved in Normal Human Spermatozoa Functioning', *International Journal of Molecular Sciences*, 18(1), p. 66.

Lamandé, Yuan, Gresshoff, Rowley, Belluoccio, Kaluarachchi, Little, Botzenhart, Zerres, Amor, Cole, Savarirayan, McIntyre and Bateman (2011) 'Mutations in TRPV4 cause an inherited arthropathy of hands and feet.', *Nature genetics*, 43(11), pp. 1142–6.

Lanaspa, Miguel A, Andres-Hernando, Li, Rivard, Cicerchi, Roncal-Jimenez, Schrier and Berl (2010) 'The expression of aquaporin-1 in the medulla of the kidney is dependent on the transcription factor associated with hypertonicity, TonEBP.', *The Journal of biological chemistry*, 285(41), pp. 31694–703.

Lanaspa, Miguel A., Andres-Hernando, Li, Rivard, Cicerchi, Roncal-Jimenez, Schrier and Berl (2010) 'The Expression of Aquaporin-1 in the Medulla of the Kidney Is Dependent on the Transcription Factor Associated with Hypertonicity, TonEBP', *Journal of Biological Chemistry*, 285(41), pp. 31694–31703.

LANG, BUSCH, RITTER, VÖLKL, WALDEGGER, GULBINS and HÄUSSINGER (1998) 'Functional Significance of Cell Volume Regulatory Mechanisms', *Physiological Reviews*, 78(1), pp. 247–306.

Leggett, Maylor, Undem, Lai, Lu, Schweitzer, King, Myers, Sylvester, Sidhaye and Shimoda (2012) 'Hypoxia-induced migration in pulmonary arterial smooth muscle cells requires calcium-dependent upregulation of aquaporin 1.', *American journal of physiology. Lung cellular and molecular physiology*, 303(4), pp. L343-53.

Leitch, Agre and King (2001) 'Altered ubiquitination and stability of aquaporin-1 in hypertonic stress.', *Proceedings of the National Academy of Sciences of the United States of America*, 98(5), pp. 2894–8.

Lewis, Feetham and Barrett-Jolley (2011) 'Cell Volume Regulation in Chondrocytes', *Cellular Physiology and Biochemistry*, 28(6), pp. 1111–1122.

Li, Lang, Karfeld-Sulzer, Mader, Richards, Weber, Sammon, Sacks, Yayon, Alini and Grad (2017) 'Heterodimeric BMP-2/7 for nucleus pulposus regeneration-In vitro and ex vivo studies', *Journal of Orthopaedic Research*, 35(1), pp. 51–60.

Liebscher, Haefeli, Wuertz, Nerlich and Boos (2011) 'Age-Related Variation in Cell Density of Human Lumbar Intervertebral Disc', *Spine*, 36(2), pp. 153–159.

Liedtke, Choe, Martí-Renom, Bell, Denis, Sali, Hudspeth, Friedman and Heller (2000) 'Vanilloid receptor-related osmotically activated channel (VR-OAC), a candidate vertebrate osmoreceptor.', *Cell*, 103(3), pp. 525–35.

Liedtke and Friedman (2003) 'Abnormal osmotic regulation in trpv4-/- mice.', *Proceedings of the National Academy of Sciences of the United States of America*, 100(23), pp. 13698–703.

Litman, Søgaard and Zeuthen (2009) 'Ammonia and Urea Permeability of Mammalian Aquaporins', in *Aquaporins*. Berlin, Heidelberg: Springer Berlin Heidelberg, pp. 327–358.

Liu, Bandyopadhyay, Bandyopadhyay, Nakamoto, Singh, Liedtke, Melvin and Ambudkar (2006) 'A role for AQP5 in activation of TRPV4 by hypotonicity: concerted involvement of AQP5 and TRPV4 in regulation of cell volume recovery.', *The Journal of biological chemistry*. American Society for Biochemistry and Molecular Biology, 281(22), pp. 15485–95.

Liu, Song, Wang, Rojek, Nielsen, Agre and Carbrey (2009) 'Osteoclast differentiation and function in aquaglyceroporin AQP9-null mice.', *Biology of the cell*, 101(3), pp. 133–40.

Livak and Schmittgen (2001) ‘Analysis of relative gene expression data using real-time quantitative PCR and the 2(-Delta Delta C(T)) Method.’, *Methods (San Diego, Calif.)*, 25(4), pp. 402–8.

Loo, Zeuthen, Chandy and Wright (1996) ‘Cotransport of water by the Na+/glucose cotransporter.’, *Proceedings of the National Academy of Sciences of the United States of America*, 93(23), pp. 13367–70.

Lund and Oxland (2011) ‘Adjacent Level Disk Disease—Is it Really a Fusion Disease?’, *Orthopedic Clinics of North America*, 42(4), pp. 529–541.

Luoma, Riihimäki, Luukkonen, Raininko, Viikari-Juntura and Lamminen (2000) ‘Low back pain in relation to lumbar disc degeneration.’, *Spine*, 25(4), pp. 487–92.

MacDonald and Zaech (1982) ‘Light scatter analysis and sorting of cells activated in mixed leukocyte culture.’, *Cytometry*, 3(1), pp. 55–8.

Macey and Farmer (1970) ‘Inhibition of water and solute permeability in human red cells.’, *Biochimica et biophysica acta*, 211(1), pp. 104–6.

Macián, López-Rodríguez and Rao (2001) ‘Partners in transcription: NFAT and AP-1’, *Oncogene*, 20(19), pp. 2476–2489.

Maclean, Lee, Alini and Iatridis (2004) ‘Anabolic and catabolic mRNA levels of the intervertebral disc vary with the magnitude and frequency of in vivo dynamic compression.’, *Journal of orthopaedic research : official publication of the Orthopaedic Research Society*, 22(6), pp. 1193–200.

Maidhof, Jacobsen, Papatheodorou and Chahine.(2014) ‘Inflammation induces irreversible biophysical changes in isolated nucleus pulposus cells.’, *PloS one*. Edited by D. Kletsas, 9(6), p. e99621.

Maidhof, Jacobsen, Papatheodorou and Chahine. (2014) ‘Inflammation Induces Irreversible Biophysical Changes in Isolated Nucleus Pulposus Cells’, *PLoS ONE*. Edited by D. Kletsas, 9(6), p. e99621.

Le Maitre, Binch, Thorpe and Hughes (2015) ‘Degeneration of the intervertebral disc with new approaches for treating low back pain.’, *Journal of neurosurgical sciences*, 59(1), pp. 47–61.

Le Maitre, Frain, Millward-Sadler, Fotheringham, Freemont and Hoyland (2009) ‘Altered integrin mechanotransduction in human nucleus pulposus cells derived from degenerated discs.’, *Arthritis and rheumatism*, 60(2), pp. 460–9.

Le Maitre, Freemont and Hoyland (2004) ‘Localization of degradative enzymes and their inhibitors in the degenerate human intervertebral disc.’, *The Journal of pathology*, 204(1), pp. 47–54.

Le Maitre, Freemont and Hoyland (2005) ‘The role of interleukin-1 in the pathogenesis of human intervertebral disc degeneration.’, *Arthritis Research & Therapy*, 7(4), p. R732.

Le Maitre, Freemont and Hoyland (2007) ‘Accelerated cellular senescence in degenerate intervertebral discs: a possible role in the pathogenesis of intervertebral disc degeneration.’, *Arthritis research & therapy*, 9(3), p. R45.

Le Maitre, Freemont and Hoyland (2009) ‘Expression of cartilage-derived morphogenetic protein in human intervertebral discs and its effect on matrix synthesis in degenerate human nucleus pulposus cells’, *Arthritis Research & Therapy*, 11(5), p. R137.

Le Maitre, Hoyland and Freemont (2007a) ‘Catabolic cytokine expression in degenerate and herniated human intervertebral discs: IL-1beta and TNFalpha expression profile.’, *Arthritis research & therapy*, 9(4), p. R77.

Le Maitre, Hoyland and Freemont (2007b) ‘Interleukin-1 receptor antagonist delivered directly and by gene therapy inhibits matrix degradation in the intact degenerate human intervertebral disc: an in situ zymographic and gene therapy study’, *Arthritis Research & Therapy*, 9(4), p. R83.

Le Maitre, Pockert, Buttle, Freemont and Hoyland (2007) ‘Matrix synthesis and degradation in human intervertebral disc degeneration’, *Biochemical Society Transactions*, 35(4), pp. 652–655.

Mak, Lam, Chan, Bond Lau, Ho Tang, Ka, Yeung, Chi, Ko, Chung and Chung (2011) ‘Embryonic Lethality in Mice Lacking the Nuclear Factor of Activated T Cells 5 Protein Due to Impaired Cardiac Development and Function’.

Malko, Hutton and Fajman (2002) ‘An in vivo MRI study of the changes in volume (and fluid content) of the lumbar intervertebral disc after overnight bed rest and during an 8-hour walking protocol.’, *Journal of spinal disorders & techniques*, 15(2), pp. 157–63.

Mamuya, Cano-Peñalver, Li, Rodriguez Puyol, Rodriguez Puyol, Brown, de Frutos and Lu (2016) ‘ILK and cytoskeletal architecture: an important determinant of AQP2 recycling and subsequent entry into the exocytotic pathway’, *American Journal of Physiology-Renal Physiology*, 311(6), pp. F1346–F1357.

Maniadakis and Gray (2000) ‘The economic burden of back pain in the UK.’, *Pain*, 84(1), pp. 95–103. Available at: http://www.ncbi.nlm.nih.gov/pubmed/10601677 (Accessed: 24 February 2019).

Marlar, Jensen, Login and Nejsum (2017) ‘Aquaporin-3 in Cancer’, *International Journal of Molecular Sciences*, 18(10), p. 2106.

Maroudas (1970) ‘Distribution and diffusion of solutes in articular cartilage.’, *Biophysical journal*, 10(5), pp. 365–79.

Maroudas, Muir and Wingham (1969) ‘The correlation of fixed negative charge with glycosaminoglycan content of human articular cartilage’, *Biochimica et Biophysica Acta (BBA) - General Subjects*. Elsevier, 177(3), pp. 492–500.

Marples, Knepper, Christensen and Nielsen (1995) 'Redistribution of aquaporin-2 water channels induced by vasopressin in rat kidney inner medullary collecting duct', *American Journal of Physiology-Cell Physiology*, 269(3), pp. C655–C664.

Martin, Deyo, Mirza, Turner, Comstock, Hollingworth and Sullivan (2008) 'Expenditures and health status among adults with back and neck problems.', *JAMA*, 299(6), pp. 656–64.

Matsui, Kanamori, Ishihara, Yudoh, Naruse and Tsuji (1998) 'Familial predisposition for lumbar degenerative disc disease. A case-control study.', *Spine*, 23(9), pp. 1029–34.

Matsuzaki, Suzuki and Takata (2001) 'Hypertonicity-induced expression of aquaporin 3 in MDCK cells.', *American journal of physiology. Cell physiology*, 281(1), pp. C55-63.

Mazzaferri, Costantino and Lefrancois (2013) 'Analysis of AQP4 trafficking vesicle dynamics using a high-content approach.', *Biophysical journal*, 105(2), pp. 328–37.

McCann and Séguin (2016) 'Notochord Cells in Intervertebral Disc Development and Degeneration', *Journal of Developmental Biology*, 4(1), p. 3.

McCann, Tamplin, Rossant and Seguin (2012) 'Tracing notochord-derived cells using a Noto-cre mouse: implications for intervertebral disc development', *Disease Models & Mechanisms*, 5(1), pp. 73–82.

McConnell, Yunus, Gross, Bost, Clemens and Hughes (2002) 'Water permeability of an ovarian antral follicle is predominantly transcellular and mediated by aquaporins.', *Endocrinology*, 143(8), pp. 2905–12.

McGann, Walterson and Hogg (1988) 'Light scattering and cell volumes in osmotically stressed and frozen-thawed cells.', *Cytometry*, 9(1), pp. 33–8.

McMillan, Garbutt and Adams (1996) 'Effect of sustained loading on the water content of intervertebral discs: implications for disc metabolism.', *Annals of the rheumatic diseases*, 55(12), pp. 880–7.

Medline. Available at: https://www.medline.eu/

Mehrkens, Matta, Karim, Kim, Fehlings, Schaeren and Mark Erwin (2017) 'Notochordal cell-derived conditioned medium protects human nucleus pulposus cells from stress-induced apoptosis.', *The spine journal : official journal of the North American Spine Society*, 17(4), pp. 579–588.

Melrose, Roberts, Smith, Menage and Ghosh (2002) 'Increased nerve and blood vessel ingrowth associated with proteoglycan depletion in an ovine anular lesion model of experimental disc degeneration.', *Spine*, 27(12), pp. 1278–85

Méndez-Giménez, Ezquerro, da Silva, Soveral, Frühbeck and Rodríguez (2018) 'Pancreatic Aquaporin-7: A Novel Target for Anti-diabetic Drugs?', *Frontiers in chemistry*, 6, p. 99.

Meng, Rui, Xu, Wan, Jiang and Li (2014) 'Aqp1 Enhances Migration of Bone Marrow

Mesenchymal Stem Cells Through Regulation of FAK and β-Catenin', *Stem Cells and Development*, 23(1), pp. 66–75.

Mesbah-Benmessaoud, Benabdesselam, Hardin-Pouzet, Dorbani-Mamine and Grange-Messent (2011) 'Cellular and subcellular aquaporin-4 distribution in the mouse neurohypophysis and the effects of osmotic stimulation.', *The journal of histochemistry and cytochemistry : official journal of the Histochemistry Society*, 59(1), pp. 88–97.

Mezzasoma, Cagini, Antognelli, Puma, Pacifico and Talesa (2013) 'TNF-α regulates natriuretic peptides and aquaporins in human bronchial epithelial cells BEAS-2B.', *Mediators of inflammation*, 2013, p. 159349.

Minogue, Richardson, Zeef, Freemont and Hoyland (2010a) 'Characterization of the human nucleus pulposus cell phenotype and evaluation of novel marker gene expression to define adult stem cell differentiation', *Arthritis & Rheumatism*, 62(12), pp. 3695–3705.

Minogue, Richardson, Zeef, Freemont and Hoyland (2010b) 'Transcriptional profiling of bovine intervertebral disc cells: implications for identification of normal and degenerate human intervertebral disc cell phenotypes', *Arthritis Research & Therapy*, 12(1), p. R22.

Miyakawa, Kyoon Woo, Dahl, Handler and Moo Kwon (1999) *Tonicity-responsive enhancer binding protein, a Rel-like protein that stimulates transcription in response to hypertonicity*, *Physiology*. Available at: www.pnas.org. (Accessed: 18 January 2019).

Mobasheri, Trujillo, Bell, Carter, Clegg, Martín-Vasallo and Marples (2004) 'Aquaporin water channels AQP1 and AQP3, are expressed in equine articular chondrocytes.', *Veterinary journal (London, England : 1997)*, 168(2), pp. 143–50.

Mobasheri, Wray and Marples (2005) 'Distribution of AQP2 and AQP3 water channels in human tissue microarrays.', *Journal of molecular histology*, 36(1–2), pp. 1–14.

Moeckel, Zhang, Chen, Rossini, Zent and Pozzi (2006) 'Role of integrin alpha1beta1 in the regulation of renal medullary osmolyte concentration.', *American journal of physiology. Renal physiology*, 290(1), pp. F223-31.

Moeller and Fenton (2012) 'Cell biology of vasopressin-regulated aquaporin-2 trafficking', *Pflügers Archiv - European Journal of Physiology*, 464(2), pp. 133–144.

Mola, Nicchia, Svelto, Spray, Frigeri and Purpura (2009) 'Automated Cell-Based Assay for Screening of Aquaporin Inhibitors NIH Public Access', *Anal Chem*, 81, pp. 8219–8229.

Mola, Sparaneo, Gargano, Spray, Svelto, Frigeri, Scemes and Nicchia (2016) 'The speed of swelling kinetics modulates cell volume regulation and calcium signaling in astrocytes: A different point of view on the role of aquaporins.', *Glia*, 64(1), pp. 139–54.

Monsoro-Burq, Bontoux, Teillet and Le Douarin (1994) 'Heterogeneity in the development of the vertebra.', *Proceedings of the National Academy of Sciences of the United States of America*, 91(22), pp. 10435–9.

Moon, Hong, Shin and Jung (2006) 'Increased aquaporin-1 expression in choroid plexus epithelium after systemic hyponatremia', *Neuroscience Letters*, 395(1), pp. 1–6.

Muller, Sendler and Hildebrandt (2006) 'Downregulation of aquaporins 1 and 5 in nasal gland by osmotic stress in ducklings, Anas platyrhynchos: implications for the production of hypertonic fluid', *Journal of Experimental Biology*, 209(20), pp. 4067–4076.

Murata, Mitsuoka, Hirai, Walz, Agre, Heymann, Engel and Fujiyoshi (2000) 'Structural determinants of water permeation through aquaporin-1.', *Nature*, 407(6804), pp. 599–605.

Mwale, Roughley and Antoniou (2004) 'Distinction between the extracellular matrix of the nucleus pulposus and hyaline cartilage: a requisite for tissue engineering of intervertebral disc.', *European cells & materials*, 8, pp. 58–63; discussion 63-4.

Nagahara, Waguri-Nagaya, Yamagami, Aoyama, Tada, Inoue, Asai and Otsuka (2010) 'TNF-alpha-induced aquaporin 9 in synoviocytes from patients with OA and RA.', *Rheumatology (Oxford, England)*, 49(5), pp. 898–906.

Navaro, Bleich-Kimelman, Hazanov, Mironi-Harpaz, Shachaf, Garty, Smith, Pelled, Gazit, Seliktar and Gazit (2015) 'Matrix stiffness determines the fate of nucleus pulposus–derived stem cells', *Biomaterials*, 49, pp. 68–76.

Neidlinger-Wilke, Mietsch, Rinkler, Wilke, Ignatius and Urban (2012) 'Interactions of environmental conditions and mechanical loads have influence on matrix turnover by nucleus pulposus cells.', *Journal of orthopaedic research : official publication of the Orthopaedic Research Society*, 30(1), pp. 112–21.

Nesverova and Törnroth-Horsefield (2019) 'Phosphorylation-Dependent Regulation of Mammalian Aquaporins', *Cells*, 8(2), p. 82.

Nicchia, Rossi, Mola, Procino, Frigeri and Svelto (2008) 'Actin cytoskeleton remodeling governs aquaporin-4 localization in astrocytes', *Glia*, 56(16), pp. 1755–1766.

Nicchia, Srinivas, Li, Brosnan, Frigeri and Spray (2005) 'New possible roles for aquaporin-4 in astrocytes: cell cytoskeleton and functional relationship with connexin43.', *FASEB journal : official publication of the Federation of American Societies for Experimental Biology*, 19(12), pp. 1674–6.

Nilius, Prenen, Wissenbach, Bödding and Droogmans (2001) 'Differential activation of the volume-sensitive cation channel TRP12 (OTRPC4) and volume-regulated anion currents in HEK-293 cells.', *Pflugers Archiv : European journal of physiology*, 443(2), pp. 227–33.

Nimmagadda, Geetha-Loganathan, Scaal, Christ and Huang (2007) 'FGFs, Wnts and BMPs mediate induction of VEGFR-2 (Quek-1) expression during avian somite development.', *Developmental biology*, 305(2), pp. 421–9.

Nyblom, Frick, Wang, Ekvall, Hallgren, Hedfalk, Neutze, Tajkhorshid and Törnroth-Horsefield (2009) 'Structural and Functional Analysis of SoPIP2;1 Mutants Adds Insight into Plant Aquaporin Gating', *Journal of Molecular Biology*, 387(3), pp. 653–668.

O'Connell, Newman and Carapezza (2014) 'Effect of long-term osmotic loading culture on matrix synthesis from intervertebral disc cells.', *BioResearch open access*, 3(5), pp. 242–9.

O'conor, Leddy, Benefield, Liedtke and Guilak (no date) 'TRPV4-mediated mechanotransduction regulates the metabolic response of chondrocytes to dynamic loading'.

Ohshima and Urban (1992) 'The effect of lactate and pH on proteoglycan and protein synthesis rates in the intervertebral disc.', *Spine*, 17(9), pp. 1079–82.

Ozu, Galizia, Acuña and Amodeo (2018) 'cells Aquaporins: More Than Functional Monomers in a Tetrameric Arrangement'.

Paavola, Wilson and Center (1980) 'Histochemistry of the developing notochord, perichordal sheath and vertebrae in Danforth's short-tail (sd) and normal C57BL/6 mice.', *Journal of embryology and experimental morphology*, 55, pp. 227–45.

Palacio-Mancheno, Evashwick-Rogler, Laudier, Purmessur and Iatridis (2018) 'Hyperosmolarity induces notochordal cell differentiation with aquaporin3 upregulation and reduced N-cadherin expression.', *Journal of orthopaedic research : official publication of the Orthopaedic Research Society*, 36(2), pp. 788–798.

Papadopoulos, Saadoun and Verkman (2008) 'Aquaporins and cell migration', *Pflügers Archiv - European Journal of Physiology*, 456(4), pp. 693–700.

Parker, Mendenhall, Godil, Sivasubramanian, Cahill, Ziewacz and McGirt (2015) 'Incidence of Low Back Pain After Lumbar Discectomy for Herniated Disc and Its Effect on Patient-reported Outcomes', *Clinical Orthopaedics and Related Research®*, 473(6), pp. 1988–1999.

Patel, Sandy, Akeda, Miyamoto, Chujo, An and Masuda (2007) 'Aggrecanases and aggrecanase-generated fragments in the human intervertebral disc at early and advanced stages of disc degeneration.', *Spine*, 32(23), pp. 2596–603.

PEACOCK (1951) 'Observations on the prenatal development of the intervertebral disc in man.', *Journal of anatomy*, 85(3), pp. 260–74.

Pedersen, Braunstein, Jørgensen, Larsen, Holstein-Rathlou and Frederiksen (2007) 'Stimulation of aquaporin-5 and transepithelial water permeability in human airway epithelium by hyperosmotic stress', *Pflügers Archiv - European Journal of Physiology*, 453(6), pp. 777–785.

Peters, Wilm, Sakai, Imai, Maas and Balling (1999) 'Pax1 and Pax9 synergistically regulate vertebral column development.', *Development (Cambridge, England)*, 126(23), pp. 5399–408.

Pfander, Cramer, Schipani and Johnson (2003) 'HIF-1alpha controls extracellular matrix synthesis by epiphyseal chondrocytes.', *Journal of cell science*, 116(Pt 9), pp. 1819–26.

Phillips, Cullen, Chiverton, Michael, Cole, Breakwell, Haddock, Bunning, Cross and Le Maitre (2015) 'Potential roles of cytokines and chemokines in human intervertebral disc degeneration: interleukin-1 is a master regulator of catabolic processes', *Osteoarthritis and Cartilage*, 23(7), pp. 1165–1177.

Phillips, Jordan-Mahy, Nicklin and Le Maitre (2013) 'Interleukin-1 receptor antagonist deficient mice provide insights into pathogenesis of human intervertebral disc degeneration', *Annals of the Rheumatic Diseases*, 72(11), pp. 1860–1867.

Pockert, Richardson, Le Maitre, Lyon, Deakin, Buttle, Freemont and Hoyland (2009) 'Modified expression of the ADAMTS enzymes and tissue inhibitor of metalloproteinases 3 during human intervertebral disc degeneration.', *Arthritis and rheumatism*, 60(2), pp. 482–91.

Pritchard, Erickson and Guilak (2002) *Hyperosmotically Induced Volume Change and Calcium Signaling in Intervertebral Disk Cells: The Role of the Actin Cytoskeleton*.

Promeneur, Kwon, Yasui, Kim, Frøkiær, Knepper, Agre and Nielsen (2000) 'Regulation of AQP6 mRNA and protein expression in rats in response to altered acid-base or water balance', *American Journal of Physiology-Renal Physiology*, 279(6), pp. F1014–F1026.

Purmessur, Walter, Roughley, Laudier, Hecht and Iatridis (2013) 'A role for TNFα in intervertebral disc degeneration: a non-recoverable catabolic shift.', *Biochemical and biophysical research communications*, 433(1), pp. 151–6.

Qin, Xu, Fan, Witt and Da (2009) 'High-salt loading exacerbates increased retinal content of aquaporins AQP1 and AQP4 in rats with diabetic retinopathy', *Experimental Eye Research*, 89(5), pp. 741–747.

Rabaud, Song, Wang, Agre, Yasui and Carbrey (2009) 'Aquaporin 6 binds calmodulin in a calcium-dependent manner.', *Biochemical and biophysical research communications*, 383(1), pp. 54–7.

Rajpurohit, Risbud, Ducheyne, Vresilovic and Shapiro (2002) 'Phenotypic characteristics of the nucleus pulposus: expression of hypoxia inducing factor-1, glucose transporter-1 and MMP-2.', *Cell and tissue research*, 308(3), pp. 401–7.

Ramli, Giribabu, Karim and Salleh (2019) 'Hormonal control of vas deferens fluid volume and aquaporin expression in rats', *Journal of Molecular Histology*, 50(1), pp. 21–34.

Ran, Wang, Chen, Zeng, Zhou, Zheng, Sun, Wang, Lv, Liang, Zhang and Liu (2010) 'Aquaporin-1 expression and angiogenesis in rabbit chronic myocardial ischemia is decreased by acetazolamide', *Heart and Vessels*, 25(3), pp. 237–247.

Reichow, Clemens, Freites, Németh-Cahalan, Heyden, Tobias, Hall and Gonen (2013) 'Allosteric mechanism of water-channel gating by Ca2+–calmodulin', *Nature Structural & Molecular Biology*, 20(9), pp. 1085–1092.

Richardson, Knowles, Marples, Hoyland and Mobasheri (2008) 'Aquaporin expression in the human intervertebral disc', *Journal of Molecular Histology*, 39(3), pp. 303–309.

Richardson, Knowles, Tyler, Mobasheri and Hoyland (2008) 'Expression of glucose transporters GLUT-1, GLUT-3, GLUT-9 and HIF-1α in normal and degenerate human intervertebral disc', *Histochemistry and Cell Biology*, 129(4), pp. 503–511.

Risbud, Guttapalli, Stokes, Hawkins, Danielson, Schaer, Albert and Shapiro (2006) 'Nucleus pulposus cells express HIF-1α under normoxic culture conditions: A metabolic adaptation to the intervertebral disc microenvironment', *Journal of Cellular Biochemistry*, 98(1), pp. 152–159.

Risbud, Schaer and Shapiro (2010) 'Toward an understanding of the role of notochordal cells in the adult intervertebral disc: from discord to accord.', *Developmental dynamics : an official publication of the American Association of Anatomists*, 239(8), pp. 2141–8.

Risbud, Schoepflin, Mwale, Kandel, Grad, Iatridis, Sakai and Hoyland (2015) 'Defining the phenotype of young healthy nucleus pulposus cells: recommendations of the Spine Research Interest Group at the 2014 annual ORS meeting.', *Journal of orthopaedic research : official publication of the Orthopaedic Research Society*, 33(3), pp. 283–93.

Risbud and Shapiro (2014) 'Role of cytokines in intervertebral disc degeneration: pain and disc content', *Nature Reviews Rheumatology*, 10(1), pp. 44–56.

Roberts, Caterson, Menage, Evans, Jaffray and Eisenstein (2000) 'Matrix metalloproteinases and aggrecanase: their role in disorders of the human intervertebral disc.', *Spine*, 25(23), pp. 3005–13.

Roberts, Evans, Kletsas, Jaffray and Eisenstein (2006) 'Senescence in human intervertebral discs', *European Spine Journal*, 15(S3), pp. 312–316.

Roberts, Hollander, Caterson, Menage and Richardson (2001) 'Matrix turnover in human cartilage repair tissue in autologous chondrocyte implantation.', *Arthritis and rheumatism*, 44(11), pp. 2586–98.

Roberts, Urban, Evans and Eisenstein (1996) 'Transport properties of the human cartilage endplate in relation to its composition and calcification.', *Spine*, 21(4), pp. 415–20.

Rodrigo, Hill, Balling, Münsterberg and Imai (2003) 'Pax1 and Pax9 activate Bapx1 to induce chondrogenic differentiation in the sclerotome.', *Development (Cambridge, England)*, 130(3), pp. 473–82.

Rodrigues-Pinto, Berry, Piper-Hanley, Hanley, Richardson and Hoyland (2016) 'Spatiotemporal analysis of putative notochordal cell markers reveals CD24 and keratins 8, 18, and 19 as notochord-specific markers during early human intervertebral disc development.', *Journal of orthopaedic research : official publication of the Orthopaedic Research Society*, 34(8), pp. 1327–40.

Roos, Strait, Raphael, Blount and Kohan (2012) 'Collecting duct-specific knockout of adenylyl cyclase type VI causes a urinary concentration defect in mice', *American Journal of Physiology-Renal Physiology*, 302(1), pp. F78–F84.

Roughley (2004) 'Biology of intervertebral disc aging and degeneration: involvement of the extracellular matrix.', *Spine*, 29(23), pp. 2691–9.

Rubenwolf, Georgopoulos, Kirkwood, Baker and Southgate (2012) 'Aquaporin expression contributes to human transurothelial permeability in vitro and is modulated by NaCl.', *PloS one*. Edited by B. C. B. Ko, 7(9), p. e45339.

Rutges, Creemers, Dhert, Milz, Sakai, Mochida, Alini and Grad (2010) 'Variations in gene and protein expression in human nucleus pulposus in comparison with annulus fibrosus and cartilage cells: potential associations with aging and degeneration', *Osteoarthritis and Cartilage*, 18(3), pp. 416–423.

Rutkovskiy, Bliksøen, Hillestad, Amin, Czibik, Valen, Vaage, Amiry-Moghaddam and Stensløkken (2013) 'Aquaporin-1 in cardiac endothelial cells is downregulated in ischemia, hypoxia and cardioplegia.', *Journal of molecular and cellular cardiology*, 56, pp. 22–33.

Rutkovskiy, Mariero, Nygård, Stensløkken, Valen and Vaage (2012a) 'Transient hyperosmolality modulates expression of cardiac aquaporins.', *Biochemical and biophysical research communications*, 425(1), pp. 70–5.

Rutkovskiy, Mariero, Nygård, Stensløkken, Valen and Vaage (2012b) 'Transient hyperosmolality modulates expression of cardiac aquaporins', *Biochemical and Biophysical Research Communications*, 425(1), pp. 70–75.

Rutkovskiy, Stensløkken, Mariero, Skrbic, Amiry-Moghaddam, Hillestad, Valen, Perreault, Ottersen, Gullestad, Dahl and Vaage (2012) 'Aquaporin-4 in the heart: expression, regulation and functional role in ischemia.', *Basic research in cardiology*, 107(5), p. 280.

Sadowska, Kameda, Krupkova and Wuertz-Kozak (2018) 'Osmosensing, osmosignalling and inflammation: how intervertebral disc cells respond to altered osmolarity', *European Cells and Materials*, 36, pp. 231–250.

Sakai, Nakai, Mochida, Alini and Grad (2009) 'Differential Phenotype of Intervertebral Disc Cells', *Spine*, 34(14), pp. 1448–1456.

Samanta, Hughes, Moiseenkova-Bell and Author (2018) 'Transient Receptor Potential (TRP) Channels HHS Public Access Author manuscript', *Subcell Biochem*, 87, pp. 141–165.

Sato, Kikuchi, Asazuma, Yamada, Maeda and Fujikawa (2001) 'Glycosaminoglycan accumulation in primary culture of rabbit intervertebral disc cells.', *Spine*, 26(24), pp. 2653–60.

Sato, Yamamoto, Sakai and Mochida (2004) '[Characterization of intervertebral disc--disc cells and pericellular microenvironment].', *Clinical calcium*, 14(7), pp. 64–9.

Savage and Stroud (2007) 'Structural Basis of Aquaporin Inhibition by Mercury', *Journal of Molecular Biology*, 368(3), pp. 607–617.

Scherer, Pfisterer, Wagner, Maren, Odebeck, Cattaruzza, Hecker and Korff (no date) 'Arterial Wall Stress Controls NFAT5 Activity in Vascular Smooth Muscle Cells'.

Schey, Petrova, Gletten and Donaldson (2017) 'The Role of Aquaporins in Ocular Lens Homeostasis', *International Journal of Molecular Sciences*, 18(12), p. 2693.

Séguin, Bojarski, Pilliar, Roughley and Kandel (2006) 'Differential regulation of matrix degrading enzymes in a TNFalpha-induced model of nucleus pulposus tissue degeneration.', *Matrix biology : journal of the International Society for Matrix Biology*, 25(7), pp. 409–18.

Séguin, Chan, Dahia and Gazit (2018) 'Latest advances in intervertebral disc development and progenitor cells.', *JOR spine*, 1(3), p. e1030.

Setton and Chen (2004) 'Cell mechanics and mechanobiology in the intervertebral disc.', *Spine*, 29(23), pp. 2710–23.

Setton and Chen (2006) 'Mechanobiology of the Intervertebral Disc and Relevance to Disc Degeneration', *The Journal of Bone and Joint Surgery (American)*, 88(suppl_2), p. 52.

Shenegelegn Mern, Tschugg, Hartmann and Thomé (2017) 'Self-complementary adeno-associated virus serotype 6 mediated knockdown of ADAMTS4 induces long-term and effective enhancement of aggrecan in degenerative human nucleus pulposus cells: A new therapeutic approach for intervertebral disc disorders', *PLOS ONE*. Edited by G. D. Almeida-Porada, 12(2), p. e0172181.

Silagi, Batista, Shapiro and Risbud (2018) 'Expression of Carbonic Anhydrase III, a Nucleus Pulposus Phenotypic Marker, is Hypoxia-responsive and Confers Protection from Oxidative Stress-induced Cell Death', *Scientific Reports*, 8(1), p. 4856.

Silagi, Schoepflin, Seifert, Merceron, Schipani, Shapiro and Risbud (2018) 'Bicarbonate Recycling by HIF-1-Dependent Carbonic Anhydrase Isoforms 9 and 12 Is Critical in Maintaining Intracellular pH and Viability of Nucleus Pulposus Cells', *Journal of Bone and Mineral Research*, 33(2), pp. 338–355.

Sloot, Hoekstra and Figdor (1988) 'Osmotic response of lymphocytes measured by means of forward light scattering: Theoretical considerations', *Cytometry*, 9(6), pp. 636–641.

Smits and Lefebvre (2003) 'Sox5 and Sox6 are required for notochord extracellular matrix sheath formation, notochord cell survival and development of the nucleus pulposus of intervertebral discs.', *Development (Cambridge, England)*, 130(6), pp. 1135–48.

Smolders, Bergknut, Grinwis, Hagman, Lagerstedt, Hazewinkel, Tryfonidou and Meij (2013) 'Intervertebral disc degeneration in the dog. Part 2: Chondrodystrophic and non-chondrodystrophic breeds', *The Veterinary Journal*, 195(3), pp. 292–299.

Solenov, Watanabe, Manley and Verkman (2004) 'Sevenfold-reduced osmotic water permeability in primary astrocyte cultures from AQP-4-deficient mice, measured by a fluorescence quenching method', *Am J Physiol Cell Physiol*, 286, pp. 426–432.

Solovieva, Kouhia, Leino-Arjas, Ala-Kokko, Luoma, Raininko, Saarela and Riihimäki (2004) 'Interleukin 1 polymorphisms and intervertebral disc degeneration.', *Epidemiology (Cambridge, Mass.)*, 15(5), pp. 626–33.

Solovieva, Lohiniva, Leino-Arjas, Raininko, Luoma, Ala-Kokko and Riihimäki (2006) 'Intervertebral disc degeneration in relation to the COL9A3 and the IL-1ß gene polymorphisms', *European Spine Journal*, 15(5), pp. 613–619.

Sowa, Coelho, Vo, Pacek, Westrick and Kang (2012) 'Cells from degenerative intervertebral discs demonstrate unfavorable responses to mechanical and inflammatory stimuli: a pilot study.', *American journal of physical medicine & rehabilitation*, 91(10), pp. 846–55.

Spector, Wade, Dillow, Steplock and Weinman (2002) 'Expression, localization, and regulation of aquaporin-1 to -3 in rat urothelia.', *American journal of physiology. Renal physiology*, 282(6), pp. F1034-42.

Spillekom, Smolders, Grinwis, Arkesteijn, Ito, Meij and Tryfonidou (2014) 'Increased Osmolarity and Cell Clustering Preserve Canine Notochordal Cell Phenotype in Culture', *Tissue Engineering Part C: Methods*, 20(8), pp. 652–662.

Spring, Robichaux and Hamlin (2009) 'The role of aquaporins in excretion in insects.', *The Journal of experimental biology*, 212(Pt 3), pp. 358–62.

Stefanakis, Al-Abbasi, Harding, Pollintine, Dolan, Tarlton and Adams (2012) 'Annulus Fissures Are Mechanically and Chemically Conducive to the Ingrowth of Nerves and Blood Vessels', *Spine*, 37(22), pp. 1883–1891.

Steinberg, Ritchie, Roumeliotis, Jayasuriya, Clark, Brooks, Binch, Shah, Coyle, Pardo, Le Maitre, Ramos, Nelissen, Meulenbelt, McCaskie, Choudhary, Wilkinson and Zeggini (2017) 'Integrative epigenomics, transcriptomics and proteomics of patient chondrocytes reveal genes and pathways involved in osteoarthritis.', *Scientific reports*, 7(1), p. 8935.

Strotmann, Harteneck, Nunnenmacher, Schultz and Plant (2000) 'OTRPC4, a nonselective cation channel that confers sensitivity to extracellular osmolarity.', *Nature cell biology*, 2(10), pp. 695–702.

Studer, Vo, Sowa, Ondeck and Kang (2011) 'Human nucleus pulposus cells react to IL-6: independent actions and amplification of response to IL-1 and TNF-α.', *Spine*, 36(8), pp. 593–9.

Sugiyama, Ota, Hara and Inoue (2001) 'Osmotic stress up-regulates aquaporin-3 gene expression in cultured human keratinocytes.', *Biochimica et biophysica acta*, 1522(2), pp. 82–8.

Sui, Han, Lee, Walian and Jap (2001) 'Structural basis of water-specific transport through the AQP1 water channel', *Nature*, 414(6866), pp. 872–878.

Takahashi, Suguro, Okazima, Motegi, Okada and Kakiuchi (1996) 'Inflammatory cytokines in the herniated disc of the lumbar spine.', *Spine*, 21(2), pp. 218–24.

Takeuchi, Hayashi, Matumoto, Hashimoto, Takayama, Chinzei, Kihara, Haneda, Kirizuki, Kuroda, Tsubosaka, Nishida and Kuroda (2018) 'Downregulation of aquaporin 9 decreases catabolic factor expression through nuclear factor‑κB signaling ins chondrocytes', *International Journal of Molecular Medicine*, 42(3), pp. 1548–1558.

Tanaka and Koyama (2011) 'Endothelins decrease the expression of aquaporins and plasma membrane water permeability in cultured rat astrocytes', *Journal of Neuroscience Research*, 89(3), pp. 320–328.

Tanaka, Sakurai, Kaneko, Ogino, Yagui, Ishikawa, Ishibashi, Matsumoto, Yokote and Saito (2011) 'The Role of the Hypoxia-Inducible Factor 1 Binding Site in the Induction of Aquaporin-1 mRNA Expression by Hypoxia', *DNA and Cell Biology*, 30(8), pp. 539–544.

Tancharoen, Matsuyama, Abeyama, Matsushita, Kawahara, Sangalungkarn, Tokuda, Hashiguchi, Maruyama and Izumi (2008) 'The role of water channel aquaporin 3 in the mechanism of TNF-alpha-mediated proinflammatory events: Implication in periodontal inflammation.', *Journal of cellular physiology*, 217(2), pp. 338–49.

Taş, Caylı, Inanır, Ozyurt, Ocaklı, Karaca and Sarsılmaz (2012) 'Aquaporin-1 and aquaporin-3 expressions in the intervertebral disc of rats with aging.', *Balkan medical journal*, 29(4), pp. 349–53.

Tchekneva, Khuchua, Davis, Kadkina, Dunn, Bachman, Ishibashi, Rinchik, Harris, Dikov and Breyer (2008) 'Single amino acid substitution in aquaporin 11 causes renal failure.', *Journal of the American Society of Nephrology : JASN*, 19(10), pp. 1955–64.

Thorpe, Bach, Tryfonidou, Le Maitre, Mwale, Diwan and Ito (2018) 'Leaping the hurdles in developing regenerative treatments for the intervertebral disc from preclinical to clinical', *JOR Spine*. John Wiley & Sons, Ltd, 1(3), p. e1027.

Thorpe, Binch, Creemers, Sammon and Le Maitre (2016) 'Nucleus pulposus phenotypic markers to determine stem cell differentiation: fact or fiction?', *Oncotarget*, 7(3), pp. 2189–200.

Tian, Yuan, Fujita, Wang, Wang, Shapiro and Risbud (2013) 'Inflammatory Cytokines Associated with Degenerative Disc Disease Control Aggrecanase-1 (ADAMTS-4) Expression in Nucleus Pulposus Cells through MAPK and NF-κB', *The American Journal of Pathology*, 182(6), pp. 2310–2321.

Tie, Lu, Pan, Pan, An, Gao, Lin, Yu and Li (2012) 'Hypoxia-induced up-regulation of aquaporin-1 protein in prostate cancer cells in a p38-dependent manner.', *Cellular physiology and biochemistry : international journal of experimental cellular physiology, biochemistry, and pharmacology*, 29(1–2), pp. 269–80.

Tietz, McNiven, Splinter, Huang and LaRusso (2006) 'Cytoskeletal and motor proteins facilitate trafficking of AQP1-containing vesicles in cholangiocytes', *Biology of the Cell*, 98(1), pp. 43–52.

Tim Yoon, Su Kim, Li, Soo Park, Akamaru, Elmer and Hutton (2003) 'The Effect of Bone Morphogenetic Protein-2 on Rat Intervertebral Disc Cells in Vitro', *Spine*, 28(16), pp. 1773–1780.

Toft-Bertelsen, Larsen and Macaulay (2018) 'Sensing and regulation of cell volume - we know so much and yet understand so little: TRPV4 as a sensor of volume changes but possibly without a volume-regulatory role?', *Channels*, 12.

Tong, Briggs and McIntosh (2012) 'Water permeability of aquaporin-4 channel depends on bilayer composition, thickness, and elasticity.', *Biophysical journal*, 103(9), pp. 1899–908.

Törnroth-Horsefield, Hedfalk, Fischer, Lindkvist-Petersson and Neutze (2010) 'Structural insights into eukaryotic aquaporin regulation.', *FEBS letters*, 584(12), pp. 2580–8.

Tournaire-Roux, Sutka, Javot, Gout, Gerbeau, Luu, Bligny and Maurel (2003) 'Cytosolic pH regulates root water transport during anoxic stress through gating of aquaporins', *Nature*, 425(6956), pp. 393–397.

Trujillo, González, Marín, Martín-Vasallo, Marples and Mobasheri (2004) 'Human articular chondrocytes, synoviocytes and synovial microvessels express aquaporin water channels; upregulation of AQP1 in rheumatoid arthritis.', *Histology and histopathology*, 19(2), pp. 435–44.

Tsai, Danielson, Guttapalli, Oguz, Albert, Shapiro and Risbud (2006) 'TonEBP/OREBP is a regulator of nucleus pulposus cell function and survival in the intervertebral disc.', *The Journal of biological chemistry*. American Society for Biochemistry and Molecular Biology, 281(35), pp. 25416–24.

Ueno, Shen, Patel, Greenberg, Azhar and Kraemer (2013) 'Fat-specific protein 27 modulates nuclear factor of activated T cells 5 and the cellular response to stress.', *Journal of lipid research*. American Society for Biochemistry and Molecular Biology, 54(3), pp. 734–43.

Ulrich-Vinther, Maloney, Schwarz, Rosier and O'Keefe (2003) 'Articular cartilage biology.', *The Journal of the American Academy of Orthopaedic Surgeons*, 11(6), pp. 421–30.

Umenishi and Schrier (2003) 'Hypertonicity-induced aquaporin-1 (AQP1) expression is mediated by the activation of MAPK pathways and hypertonicity-responsive element in the AQP1 gene.', *The Journal of biological chemistry*, 278(18), pp. 15765–70.

Urban (2002) 'The role of the physicochemical environment in determining disc cell behaviour.', *Biochemical Society transactions*, 30(Pt 6), pp. 858–64.

Urban, Holm and Maroudas (1978) 'Diffusion of small solutes into the intervertebral disc: as in vivo study.', *Biorheology*, 15(3–4), pp. 203–21.

Urban, Holm, Maroudas and Nachemson (1977) 'Nutrition of the intervertebral disk. An in vivo study of solute transport.', *Clinical orthopaedics and related research*, (129), pp. 101–14.

Urban and McMullin (1985) 'Swelling pressure of the inervertebral disc: influence of proteoglycan and collagen contents.', *Biorheology*, 22(2), pp. 145–57.

Urban and McMullin (1988) 'Swelling pressure of the lumbar intervertebral discs: influence of age, spinal level, composition, and degeneration.', *Spine*, 13(2), pp. 179–87.

Urban and Roberts (2003) 'Degeneration of the intervertebral disc.', *Arthritis research & therapy*, 5(3), pp. 120–30.

Varadaraj and Kumari (2018) 'Molecular mechanism of Aquaporin 0-induced fiber cell to fiber cell adhesion in the eye lens', *Biochemical and Biophysical Research Communications*, 506(1), pp. 284–289.

Verdoucq, Grondin and Maurel (2008) 'Structure–function analysis of plant aquaporin *At* PIP2;1 gating by divalent cations and protons', *Biochemical Journal*, 415(3), pp. 409–416.

Vos, Abajobir, Abate, Abbafati, Abbas, Abd-Allah, Abdulkader, Abdulle, Abebo, Abera, Aboyans, Abu-Raddad, Ackerman, Adamu, Adetokunboh, Afarideh, Afshin, Agarwal, Aggarwal, Agrawal, Murray, *et al.* (2017) 'Global, regional, and national incidence, prevalence, and years lived with disability for 328 diseases and injuries for 195 countries, 1990–2016: a systematic analysis for the Global Burden of Disease Study 2016', *The Lancet*, 390(10100), pp. 1211–1259.

de Vries, van Doeselaar, Meij, Tryfonidou and Ito (2016) 'The Stimulatory Effect of Notochordal Cell-Conditioned Medium in a Nucleus Pulposus Explant Culture', *Tissue Engineering Part A*, 22(1–2), pp. 103–110.

Walter, Korecki, Purmessur, Roughley, Michalek and Iatridis (2011) 'Complex loading affects intervertebral disc mechanics and biology.', *Osteoarthritis and cartilage*, 19(8), pp. 1011–8.

Walter, Purmessur, Moon, Occhiogrosso, Laudier, Hecht and Iatridis (2016) 'Reduced tissue osmolarity increases TRPV4 expression and pro-inflammatory cytokines in intervertebral disc cells.', *European cells & materials*, 32, pp. 123–36.

Wang, Y., Fan, Cao, Yu, Zhang and Wang (2011) '2-Methoxyestradiol inhibits the up-regulation of AQP4 and AQP1 expression after spinal cord injury.', *Brain research*, 1370, pp. 220–6.

Wang, Jiang and Dai (2007) 'Biologic Response of the Intervertebral Disc to Static and Dynamic Compression In Vitro', *Spine*, 32(23), pp. 2521–2528.

Wang, Markova, Anderson, Zheng, Shapiro and Risbud (2011) 'TNF-α and IL-1β Promote a Disintegrin-like and Metalloprotease with Thrombospondin Type I Motif-5-mediated Aggrecan Degradation through Syndecan-4 in Intervertebral Disc', *Journal of Biological Chemistry*, 286(46), pp. 39738–39749.

Wang and Tajkhorshid (2007) 'Molecular Mechanisms of Conduction and Selectivity in Aquaporin Water Channels', *The Journal of Nutrition*, 137(6), pp. 1509S-1515S.

Wang and Zheng (2011) 'Nuclear factor kappa B pathway down-regulates aquaporin 5 in the nasal mucosa of rats with allergic rhinitis.', *European archives of oto-rhino-laryngology : official journal of the European Federation of Oto-Rhino-Laryngological Societies (EUFOS) : affiliated with the German Society for Oto-Rhino-Laryngology - Head and Neck Surgery*, 268(1), pp. 73–81.

Wang and Zhu (2011) 'Aquaporin-1: a potential membrane channel for facilitating the adaptability of rabbit nucleus pulposus cells to an extracellular matrix environment.', *Journal of orthopaedic science : official journal of the Japanese Orthopaedic Association*, 16(3), pp. 304–12.

Wehner, Sauer, Kinne, Beetz, Giffey, Rosin-Steiner and Schlitz (1995) *Hypertonic Stress Increases the Na + Conductance of Rat Hepatocytes in Primary Culture*, *THE JOURNAL OF GENERAL PHYSIOLOGY*.

Weiler, Nerlich, Bachmeier and Boos (2005) 'Expression and distribution of tumor necrosis factor alpha in human lumbar intervertebral discs: a study in surgical specimen and autopsy controls.', *Spine*, 30(1), pp. 44–53; discussion 54.

Wilke, Neef, Caimi, Hoogland and Claes (1999) 'New in vivo measurements of pressures in the intervertebral disc in daily life.', *Spine*, 24(8), pp. 755–62.

Willermain, Janssens, Arsenijevic, Piens, Bolaky, Caspers, Perret and Delporte (2014) 'Osmotic stress decreases aquaporin-4 expression in the human retinal pigment epithelial cell line, ARPE-19.', *International journal of molecular medicine*, 34(2), pp. 533–8.

Wilting, Kurz, Brand-Saberi, Steding, Yang, Hasselhorn, Epperlein and Christ (1994) 'Kinetics and differentiation of somite cells forming the vertebral column: studies on human and chick embryos.', *Anatomy and embryology*, 190(6), pp. 573–81.

Wu, Gao, Brown, Heller and O'Neil (2007) 'Dual role of the TRPV4 channel as a sensor of flow and osmolality in renal epithelial cells.', *American journal of physiology. Renal physiology*, 293(5), pp. F1699-713.

Wu, Morrison and Schweitzer (2006) 'Edematous Schmorl's nodes on thoracolumbar MR imaging: characteristic patterns and changes over time.', *Skeletal radiology*, 35(4), pp. 212–9.

Wu, Steinbronn, Alsterfjord, Zeuthen and Beitz (2009) 'Concerted action of two cation filters in the aquaporin water channel', *The EMBO Journal*, 28(15), pp. 2188–2194.

Wuertz, Godburn, MacLean, Barbir, Stinnett Donnelly, Roughley, Alini and Iatridis (2009) 'In vivo remodeling of intervertebral discs in response to short- and long-term dynamic compression', *Journal of Orthopaedic Research*, 27(9), pp. 1235–1242.

Wuertz, Urban, Klasen, Ignatius, Wilke, Claes and Neidlinger-Wilke (2007) 'Influence of extracellular osmolarity and mechanical stimulation on gene expression of intervertebral disc cells.', *Journal of orthopaedic research : official publication of the Orthopaedic Research Society*, 25(11), pp. 1513–22.

Xie, Jing, Xia, Wang, You and Yan (2016) 'Aquaporin 3 protects against lumbar intervertebral disc degeneration via the Wnt/β-catenin pathway.', *International journal of molecular medicine*, 37(3), pp. 859–64.

Yamada, Placzek, Tanaka, Dodd and Jessell (1991) 'Control of cell pattern in the developing nervous system: polarizing activity of the floor plate and notochord.', *Cell*, 64(3), pp. 635–47.

Yamamura, Motegi, Kani, Takano, Momota, Aota, Yamanoi and Azuma (2012) 'TNF-α inhibits aquaporin 5 expression in human salivary gland acinar cells via suppression of histone H4 acetylation', *Journal of Cellular and Molecular Medicine*, 16(8), pp. 1766–1775.

Yáñez, Gil-Longo and Campos-Toimil (2012) 'Calcium Binding Proteins', in *Advances*

in experimental medicine and biology, pp. 461–482.

Yang, Leung, Luk, Chan and Cheung (2009) 'Injury-induced sequential transformation of notochordal nucleus pulposus to chondrogenic and fibrocartilaginous phenotype in the mouse.', *The Journal of pathology*, 218(1), pp. 113–21.

Yang and Verkman (1997) 'Water and glycerol permeabilities of aquaporins 1-5 and MIP determined quantitatively by expression of epitope-tagged constructs in Xenopus oocytes.', *The Journal of biological chemistry*, 272(26), pp. 16140–6.

Yasui, Hazama, Kwon, Nielsen, Guggino and Agre (1999) 'Rapid gating and anion permeability of an intracellular aquaporin', *Nature*, 402(6758), pp. 184–187.

Yurinskaya, Aksenov, Moshkov, Model, Goryachaya and Vereninov (2017) 'A comparative study of U937 cell size changes during apoptosis initiation by flow cytometry, light scattering, water assay and electronic sizing', *Apoptosis*, 22(10), pp. 1287–1295.

Zeidel, Ambudkar, Smith and Agre (1992) 'Reconstitution of functional water channels in liposomes containing purified red cell CHIP28 protein.', *Biochemistry*, 31(33), pp. 7436–40.

Zhang, H. Z., Kim, Lim and Bae (2013) 'Time-dependent expression patterns of cardiac aquaporins following myocardial infarction.', *Journal of Korean medical science*, 28(3), pp. 402–8.

Zhang, J., Xiong, Lu, Wang, Zhang, Fang, Song and Jiang (2013) 'AQP1 expression alterations affect morphology and water transport in Schwann cells and hypoxia-induced up-regulation of AQP1 occurs in a HIF-1α-dependent manner.', *Neuroscience*, 252, pp. 68–79.

Zhao, Zhang, Jiang, Li, Jiang and Dai (2011) 'ADAMTS-5 and intervertebral disc degeneration: the results of tissue immunohistochemistry and in vitro cell culture.', *Journal of orthopaedic research : official publication of the Orthopaedic Research Society*, 29(5), pp. 718–25.

Zhou, Ann, Li, Kim, Lin, Minoo, Crandall and Borok (2007) 'Hypertonic induction of aquaporin-5: novel role of hypoxia-inducible factor-1α', *American Journal of Physiology-Cell Physiology*, 292(4), pp. C1280–C1290.

Zou, Vetreno and Crews (2012) 'ATP-P2X7 receptor signaling controls basal and TNFα-stimulated glial cell proliferation.', *Glia*, 60(4), pp. 661–73.

Appendices

NHS

National Research Ethics Service

Sheffield Local Research Ethics Committee
1st Floor Vickers Corridor
Northern General Hospital
Herries Road
Sheffield
S5 7AU

Telephone: 0114 271 4011
Facsimile: 0114 256 2489

14 April 2009

Dr Christine L Le Maitre
Senior Lecturer in Molecular and Cell Biology
Sheffield Hallam University
Biomedical Research Centre
Owen Building
Howard Street
S1 1WB

Dear Dr Le Maitre

Full title of study: **Role of cytokines and chemokines in the pathogenesis of low back pain and methods of modulating their response.**
REC reference number: **09/H1308/70**

The Research Ethics Committee reviewed the above application at the meeting held on 06 April 2009. Thank you for attending to discuss the study.

Ethical opinion

The members of the Committee present gave a favourable ethical opinion of the above research on the basis described in the application form, protocol and supporting documentation, subject to the conditions specified below.

Ethical review of research sites

The favourable opinion applies to all NHS sites taking part in the study, subject to management permission being obtained from the NHS/HSC R&D office prior to the start of the study (see "Conditions of the favourable opinion" below).

Conditions of the favourable opinion

The favourable opinion is subject to the following conditions being met prior to the start of the study.

Management permission or approval must be obtained from each host organisation prior to the start of the study at the site concerned.

For NHS research sites only, management permission for research ("R&D approval") should be obtained from the relevant care organisation(s) in accordance with NHS research governance arrangements. Guidance on applying for NHS permission for research is available in the Integrated Research Application System or at http://www.rdforum.nhs.uk.

Where the only involvement of the NHS organisation is as a Participant Identification Centre, management permission for research is not required but the R&D office should be notified of the study. Guidance should be sought from the R&D office where necessary.

Sponsors are not required to notify the Committee of approvals from host organisations.

Other conditions of approval:

Favourable opinion with conditions as follows:

1 Provide a copy of the tissue transfer agreement.

2 The consent form – include the standard regulatory authorities reference (See guides). This statement is necessary as it ensures that relevant bodies e.g. R & D Departments can monitor the project.

3 Ensure that all modified documents are referenced with an up to date version number and date e.g. version 2 dated 2 April 2009.

It is the responsibility of the sponsor to ensure that all the conditions are complied with before the start of the study or its initiation at a particular site (as applicable

Approved documents

The documents reviewed and approved at the meeting were:

Document	Version	Date
Disc Material Details	1	10 March 2009
Participant Consent Form	1	
Participant Information Sheet	1	10 March 2009
Statistician Comments		
Peer Review		22 January 2009
Letter from Sponsor		11 March 2009
Summary/Synopsis	1	10 March 2009
Covering Letter		10 March 2009
Protocol	1	10 March 2009
Investigator CV		
Application		10 March 2008

Membership of the Committee

The members of the Ethics Committee who were present at the meeting are listed on the attached sheet.

Statement of compliance

The Committee is constituted in accordance with the Governance Arrangements for Research Ethics Committees (July 2001) and complies fully with the Standard Operating Procedures for Research Ethics Committees in the UK.

After ethical review

Now that you have completed the application process please visit the National Research

This Research Ethics Committee is an advisory committee to Yorkshire and The Humber Strategic Health Authority

The National Research Ethics Service (NRES) represents the NRES directorate within The National Patient Safety Agency and Research Ethics Committees in England

Appendix I. Sheffield Research Ethics Committee approval letter

	Reference	Source		IVD Level	Intact IVD?	Average Grade	Classification	DE	IHC
HD	1	Surgical	42	L4/L5	No	3	ND	X	
HD	2	Surgical	40	L5/S1	Yes	3.9	I	X	
HD	3	Surgical	25	L4/L5	Yes	4.8	MD	X	
HD	5	Surgical	33	L5/S1	Yes	9	SD	X	
HD	9	Surgical	32	L5/S1	Yes	5	MD	X	
HD	16	Surgical				7	SD	X	
HD	17	Surgical	45	L5/S1	Yes	4	ND	X	
HD	23	Surgical				7.8	SD	X	
HD	24	Surgical				2	ND	X	
HD	25	Surgical	20	L4/L5	No	2	ND	X	
HD	26	Surgical	40	L5/S1	No	5	MD	X	
HD	31	PM	45	L3/L4	Yes	1	ND	X	
HD	33	Surgical	48	L4/L5	No	8	SD	X	
HD	34	Surgical	26	L5/S1	No	12	I	X	
HD	36	Surgical	33	L5/S1	Yes	9	I	X	
HD	40	PM	74	L2/L3	Yes	11	SD		X
HD	44	Surgical	42	L5/S1	Yes	2	ND	X	
HD	45	Surgical	36	L5/S1	Yes	8	SD	X	
HD	53	Surgical	38	L5/S1	No	7	SD	X	
HD	54	Surgical	28	L4/L5	Yes	6	MD	X	
HD	56	Surgical	43	L5/S1	No	8	I	X	
HD	57	Surgical	44	L5/S1	Yes	9	SD	X	
HD	58	Surgical	28	L5/S1	No	8	SD	X	
HD	59	Surgical	35	L5/S1	Yes	6	MD	X	
HD	61	Surgical	43	L5/S1	No	7	SD	X	
HD	63	Surgical	42	L5/S1	No	5	MD	X	
HD	65	Surgical	43	L4/L5	No	10	I	X	X
HD	66	Surgical	62	L3/L4	Yes	10	I	X	
HD	71	Surgical	42	L5/S1	Yes	3	ND		X
HD	75	Surgical	40	L3/L4	Yes	11	SD	X	

	Reference	Source		IVD Level	Intact IVD?	Average Grade	Classification	DE	IHC
HD	79	Surgical	45	L4/L5	No	2.6	ND	X	
HD	85	Surgical	85	L2/L3	No	8	I	X	
HD	86	Surgical	40	L5/S1	No	9	I	X	
HD	89	Surgical	21	L5/S1	No	4	ND		X
HD	92	Surgical	38	L5/S1		7	SD	X	
HD	93	Surgical	38	L5/S1		12	SD	X	
HD	94	Surgical	66	L5/S1	Yes	10	SD	X	
HD	97	Surgical	46	L5/S1	No	10	SD	X	
HD	98	Surgical	65	L3/L4	Yes	11	SD	X	X
HD	103	Surgical	45	C5/C6	No	9.5	SD		X
HD	145	Surgical	38	L4/L5	No	11	I	X	X
HD	146	Surgical	47	L5/S1		7	SD	X	
HD	148	Surgical	70	C5/C6		8.5	SD	X	
HD	151	Surgical	47	L5/S1		8.5	SD	X	
HD	153	Surgical	30	L5/S1	No	5	MD	X	
HD	154	Surgical	52	L4/L5	No	11	SD	X	X
HD	156	Surgical	24	L4/L5	Yes	3	ND	X	
HD	157	Surgical	31	L5/S1	No	5	I	X	
HD	158	Surgical	38	L4/L5	No	7	I		X
HD	159	Surgical	39	L4/L5	No	9	I	X	X
HD	160	Surgical	26	C3/C5					
HD	166	Surgical	33	L4/L5	Yes	8	SD	X	
HD	170	Surgical		L5/S1	No	10	SD	X	
HD	174	Surgical	29	L5/S1	Yes	6	I	X	
HD	175	Surgical	37	L5/S1	Yes	7	SD	X	
HD	184	Surgical	49	L4/L5		5	I	X	
HD	192	Surgical	29	L5/S1	No	8	SD	X	
HD	194	Surgical	35	L4/L5	No	11	SD	X	
HD	195	Surgical	38	C6/C7	No	9	SD	X	
HD	197	Surgical	42	L4/L5	No	8	SD	X	
HD	203	Surgical	45	L5/S1	Yes	4	ND		X
HD	207	Surgical	38	L5/S1	No	8	SD	X	

	Reference	Source		IVD Level	Intact IVD?	Average Grade	Classification	DE	IHC
HD	219	Surgical	54	L5/S1	No	11	I	X	X
HD	225	Surgical	36	L5/S1	Yes	10	SD	X	
HD	228	Surgical				7	I	X	
HD	229	Surgical	56	L5	Yes	6	MD	X	X
HD	231	Surgical	56	L4/L5	No	5	MD	X	
HD	232	Surgical	58	L5/S1	No	8	SD	X	
HD	233	Surgical	44	L5/S1	Yes	10	SD	X	X
HD	234	Surgical	54	L5/S1	Yes	9	SD	X	X
HD	243	Surgical	28	L4/L5	Yes	6	I	X	
HD	246	Surgical	40	L5/S1	Yes	7	I	X	
HD	253	Surgical	63	C5/C6	Yes	4	I	X	
HD	254	Surgical	47	L4/L5	No	6	I	X	X
HD	257	Surgical	46	L5/S1	No	3	I	X	X
HD	264	Surgical	65	C3/C5	Yes	6	MD		X
HD	266	Surgical	27	L5/S1	No	4	ND		X
HD	270	Surgical	45	L5/S1	No	6	MD		X
HD	276	Surgical	71	C5/C6		6	MD	X	
HD	281	Surgical	27	L4/L5	Yes	3	ND	X	
HD	282	Surgical	21	L5/S1	No	4	ND		X
HD	287	Surgical	46	L5/S1	Yes	5	MD	X	
HD	292	Surgical	23	L2/L3	Yes	4	ND	X	
HD	309	Surgical	52	L2/L3	No	7	SD	X	
HD	310	Surgical	37	L4/L5	Yes	5	I	X	X
HD	319	Surgical	47	L5/S1	No	5	MD	X	X
HD	320	Surgical	68	L4/L5	No	4	I	X	
HD	321	Surgical	22	L4/L5	Yes	4	ND	X	
HD	328	Surgical	38	L5/S1		6	I	X	
HD	329	Surgical	48	L5/S1	Yes	5	I	X	
HD	330	Surgical	32	L5/S1	Yes	5.5	MD		X
HD	332	Surgical	24	L5/S1	No	10	I	X	
HD	339	Surgical		L5/S1	No	7	SD	X	
HD	342	Surgical	18	L4/L5	Yes	6	I	X	

	Reference	Source		IVD Level	Intact IVD?	Average Grade	Classification	DE	IHC
HD	346	Surgical	46	C5/C6	Yes	6	MD		X
HD	350	Surgical	38	L4/L5	Yes	9	SD	X	
HD	352	Surgical	82	L4/L5	No	8	SD	X	
HD	355	Surgical	33	L4/L5	No	5	I	X	
HD	356	Surgical	26	L5/S1	Yes	4	ND	X	
HD	357	Surgical	53	L4/L5	Yes	4	I	X	
HD	359	Surgical	40	L5/S1	No	4	ND		X
HD	360	Surgical	50	C6		5.5	MD		X
HD	369	Surgical	50	L5/S1	Yes	7	SD	X	
HD	370	Surgical	50	L5/S1	Yes	8	SD	X	X
HD	372	Surgical	49	L4/L5	No	7	I	X	
HD	374	Surgical	37	L4/L5	Yes	4	ND	X	
HD	375	Surgical	41	L5/S1	No	6	MD		X
HD	378	PM	33	L4/L5	Yes	2	ND	X	
HD	379	PM	33	L3/L4	Yes	5	MD	X	
HD	380	PM	33	L2/L3	Yes	4	ND	X	X
HD	388	Surgical	54	C6/C7	Yes	6	MD	X	
HD	396	Surgical	44	L4/L5	Yes	9	SD	X	
HD	397	Surgical	20	L4/L5	No	3	ND	X	
HD	480	Surgical			No	5	MD		
HD	482	Surgical			No	7	SD		
HD	521	Surgical	42	L5/S1	No	5	MD		
HD	538	Surgical	43	L3/L4	No	6	MD		
HD	540	Surgical	45	L4/L5	No	8	SD		
HD	545	Surgical	38	L4/L5	No	4	ND		

Appendix II. Human patient details. Samples were separated into different grades, 0-4 (Non-degenerate, ND), 4.1-6.9 (Moderately-degenerate, MD) and 7-12 (severely-degenerate, SD). X indicates samples used for direct extraction (DE) of RNA and RT-qPCR and immunohistochemistry (IHC).

Pathology number (Sample No.)	Breed	Disc level	Thompson grade	Age (month)	NC/C	Dog no.
7	Mongrel	T12-T13	1	16	0	6
23	kerry beagle	T12-T13	1	36	0	15
22	kerry beagle	L7-S1	1	36	0	14
25	kerry beagle	L5-L6	1	96	0	16
24	kerry beagle	L4-L5	1	36	0	15
8	Mongrel	T13-L1	1	16	0	6
1	Mongrel	L4-L5	1	17	0	2
21	Flatcoated retriever	T11/T12	1	7	1	11
2	Beagle	L7-S1	2	25	1	3
9	Mongrel	L4-L5	2	16	0	6
6	Beagle	L6-L7	2	28	1	5
10	Foxhound	L4-L5	2	84	0	7
5	Beagle	L3-L4	2	25	1	4
11	Foxhound	L5-L6	2	84	0	7
3	Beagle	L3-L4	2	25	1	3
27	Beagle	L7-S1	3	117	1	18
26	Beagle	L6-L7	3	117	1	18
12	Foxhound	T13-L1	3	84	0	7
14	Foxhound	T12-T13	3	120	0	8
17	Foxhound	L2-L3	3	120	0	8
4	Beagle	T13-L1	3	25	1	3
15	Foxhound	T13-L1	3	120	0	8
36	Bouvier	L7-S1	3	142	ND	17
13	Foxhound	L7-S1	4	84	0	7
29	Beagle	L2-L3	4	120	1	19
18	Foxhound	L7-S1	4	108	0	9
32	Beagle	T13-L1	4	120	1	19
30	Beagle	L7-S1	4	120	1	19
28	Beagle	L1-L2	4	120	1	19
34	Beagle	L5-L6	5	120	1	19
33	Beagle	T11-T12	5	120	1	19
31	Beagle	T12-T13	5	120	1	19
19	Welsh Ter	L7/S1	5	192	1	12
20	Welsh Ter	L1/L2	5	192	1	12
35	Beagle	L4-L5	5	120	1	19

Appendix III. Canine sample details. Non-chondrodystrophic (NC)=0. Chondrodystrophic (C)=1. Not determined (ND).

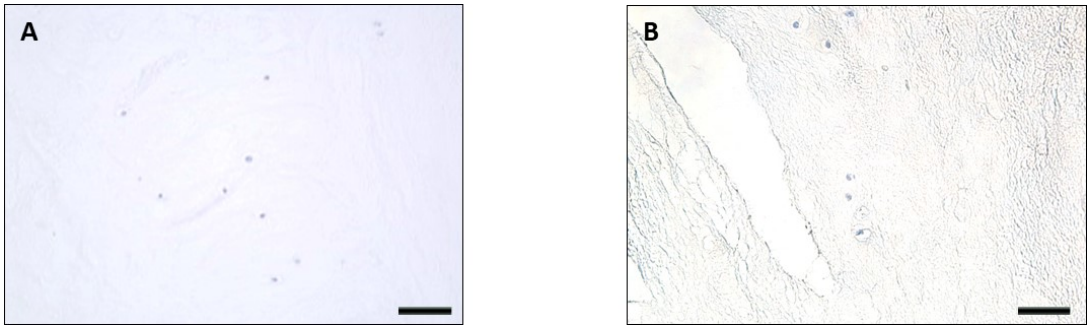

Appendix IV. IHC of (A) Rabbit and (B) mouse IgG controls of human NP tissue used in AQP protein expression experiments. Scale bar 50µm.

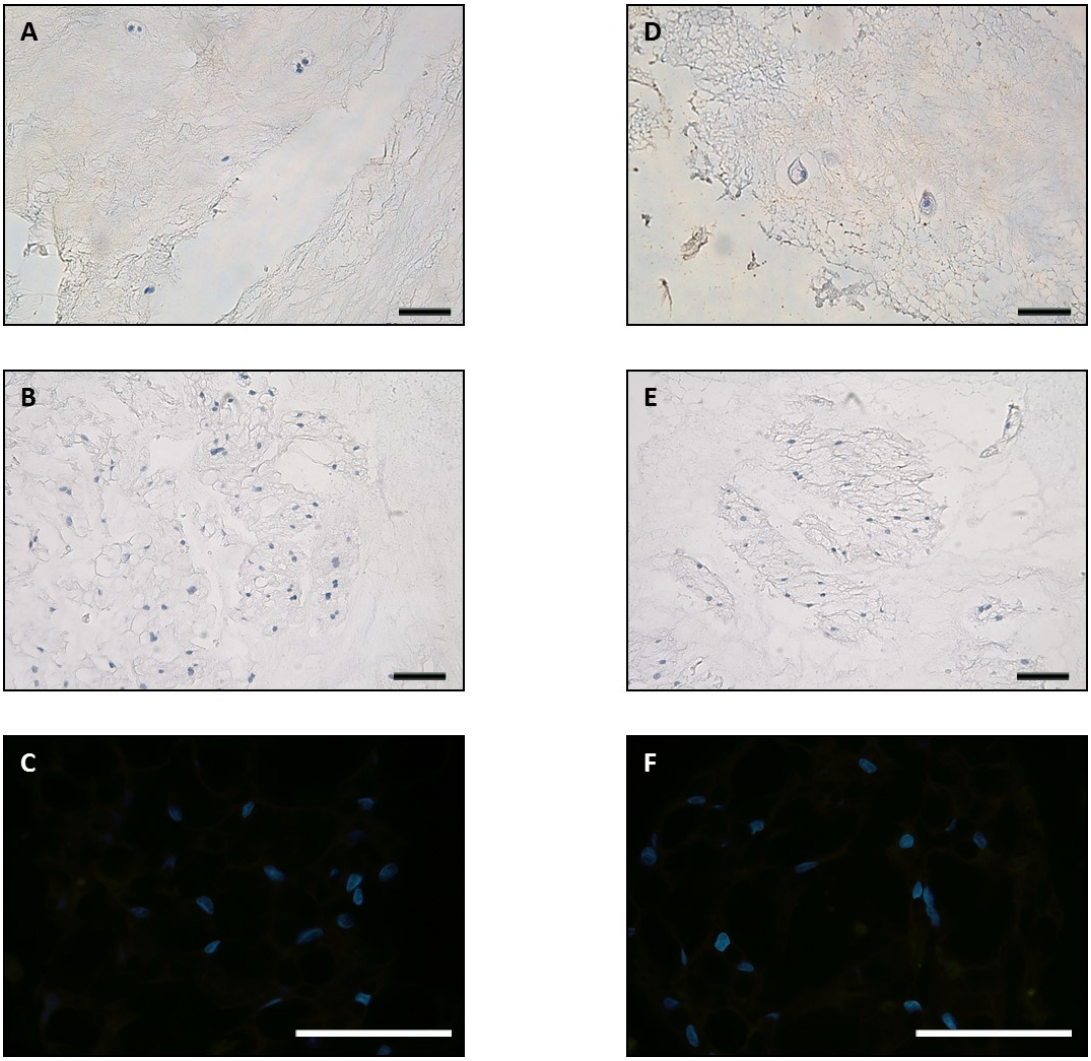

Appendix V. IHC of rabbit IgG controls of (A) NP cells and (B) NC cell clusters in canine IVD tissue and (C) sections of NC cells in alginate beads used for IF. IHC of mouse IgG controls of (D) NP cells and (E) NC cell clusters in canine IVD tissue and (F) sections of NC cells in alginate beads used for IF. IHC scale bar 50µm. IF scale bar 20µm.

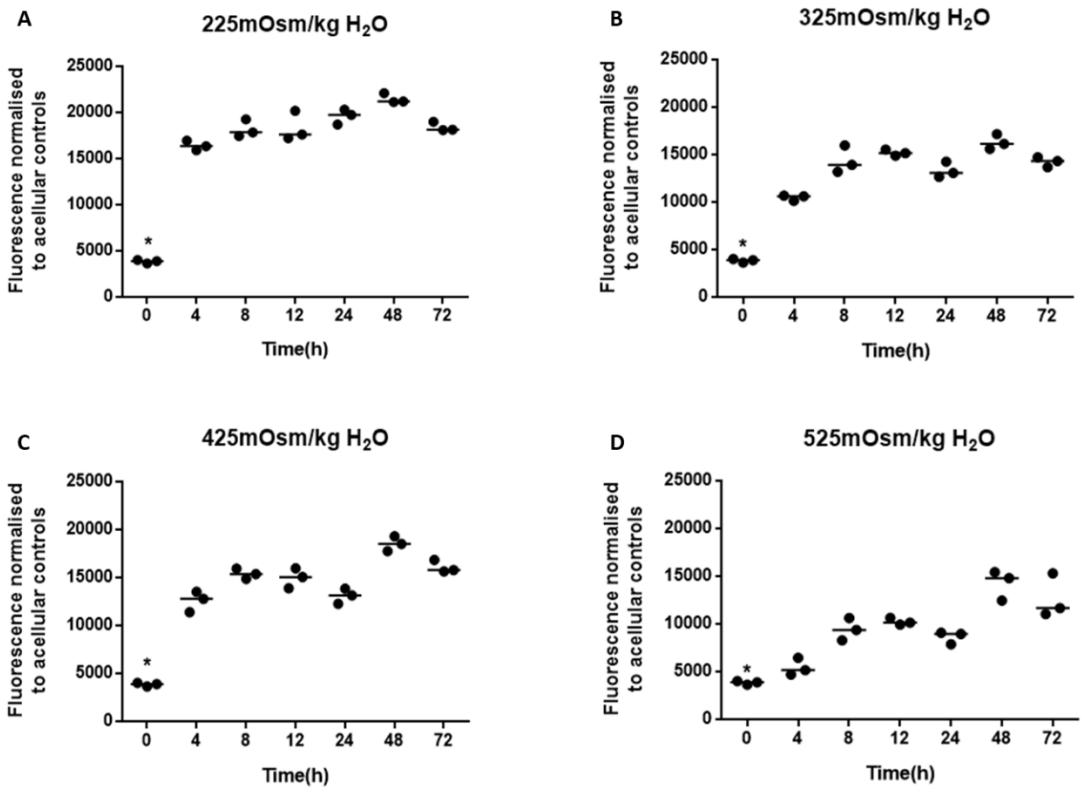

Appendix VI. NP cell viability in response to altered osmolality treatment. NP cells were treated with (A)225, (B) 325, (C) 425 or (D) 535mOsm/kg media for 0 – 72h and metabolic activity was measured using the resazurin reduction assay. Resazurin sodium salt (Sigma-Aldrich) stock solution (3mg/mL, prepared in DMEM) was diluted 1:100 and was incubated on cells for 2h at 37°C 5% CO_2 (v/v) before absorbance was read at excitation: 560nm, emission 590nm. Fluorescence values normalised to acellular controls. Significance determined by Kruskal-Wallis *$p \leq 0.05$.

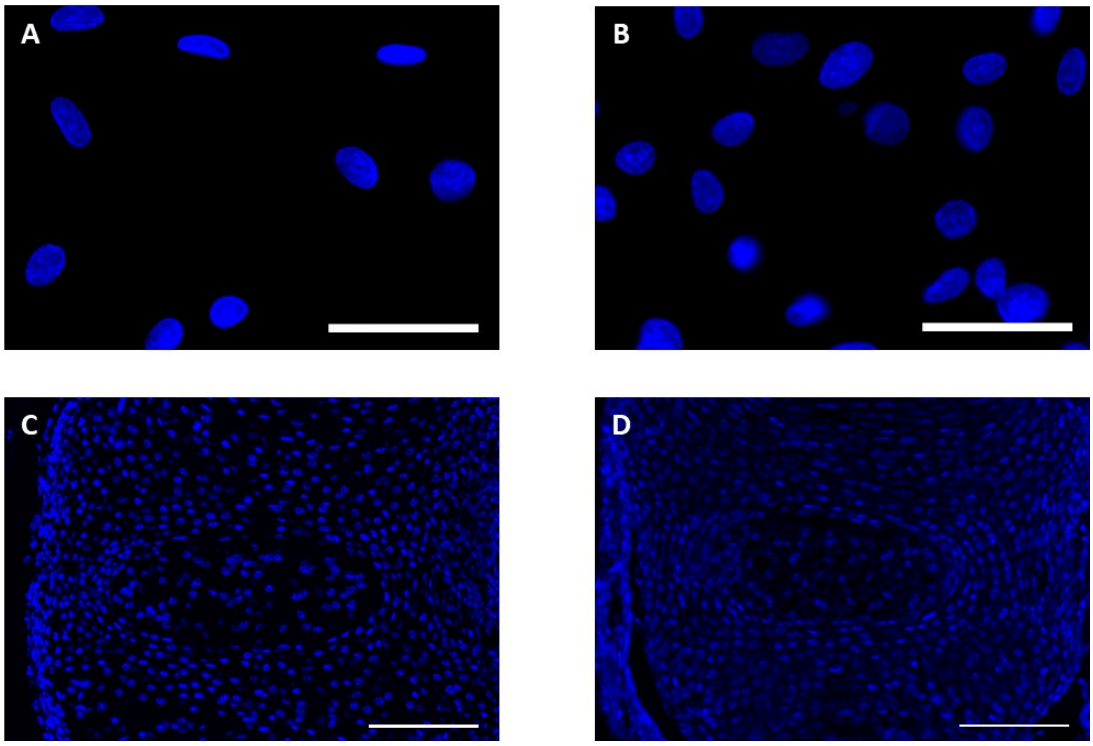

Appendix VII. (A) Rat NP cell fluorescent ICC and (B) mouse IVD IHC Secondary antibody only controls for AQP1. (C) Rat NP cell fluorescent ICC and (D) mouse IVD IHC Secondary antibody only controls for AQP5. ICC scale bar 20µm. IHC scale bar 100µm.

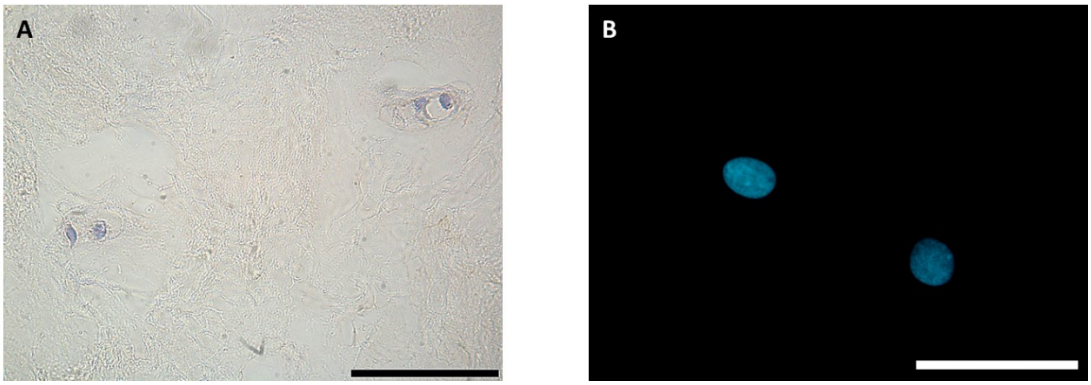

Appendix VIII. (A) Rabbit IgG control of human NP tissue from TonEBP IHC experiments. Scale bar 20µm. (B) Rabbit IgG control of human NP cells from TRPV4 immunofluorescence experiments. Scale bar 20µm.

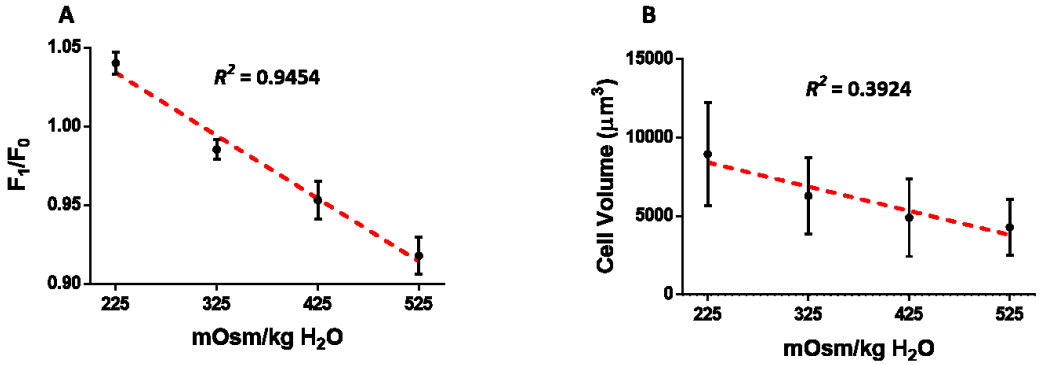

Appendix IX. Calcein fluorescence and cell volume correlation with osmolality in human NP cells. (A) Relative fluorescence (F_1/F_0) of calcein depends linearly on extracellular osmolality. (B) NP cell volume is not linearly correlated to extracellular osmolality; therefore, cell volume cannot be deduced directly from calcein fluorescence. Similar findings were observed by Fenton *et al.*, 2010 when developing this method. Average results for calcein F_1/F_0 and NP cell volume were plotted with standard deviation. Linear regression analysis was plotted as a red-dashed line.

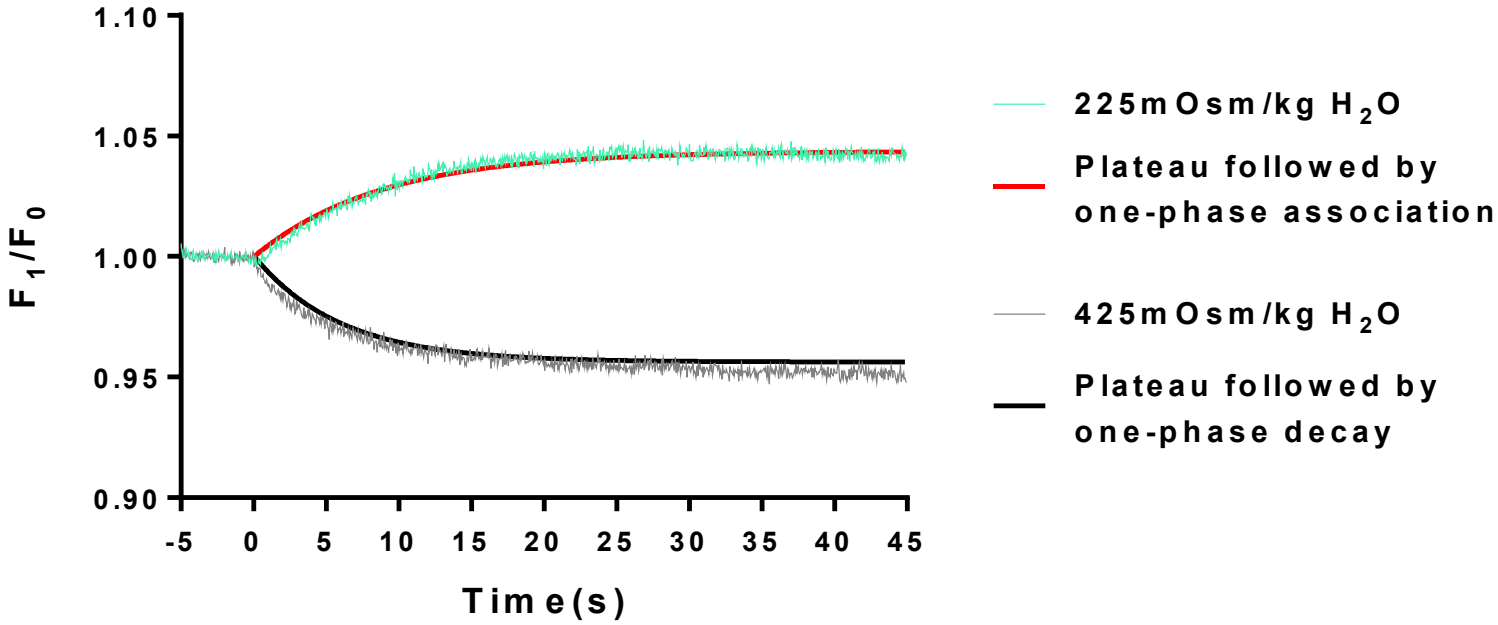

Appendix X. Example of non-linear regression curve fitting to determine rate of cell volume change in response to extracellular osmolality changes. The change in intracellular calcein F_1/F_0 is plotted when NP cells are exposed to altered osmolality. To determine the rate of change in calcein F_1/F_0, plateau followed by one-phase association (increase in F_1/F_0) or decay (decrease in F_1/F_0) curves were fitted to data using GraphPad Prism v7.03 software. The average baseline value of Y (Y0) before experimental intervention (X0) was constrained to 1; X0 was constrained to 0.05s (the first fluorescence reading after injection).

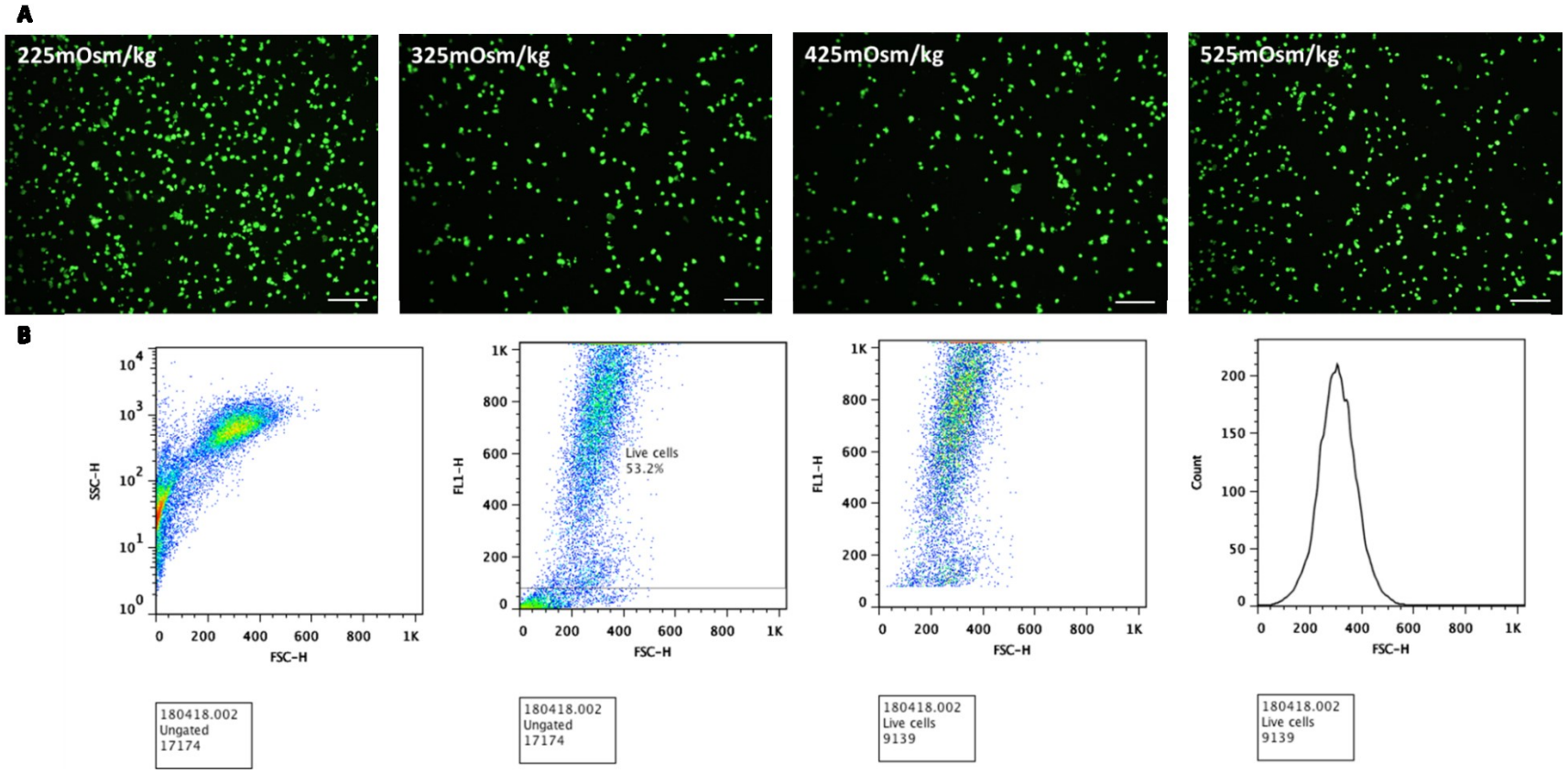

Appendix XI. (A) Fluorescent images of CFSE-labelled human NP cells exposed to altered extracellular osmolality used for ImageJ cell size determination. Scale bar 20µm. (B) Flow cytometry gating strategy to determine changes in forward scatter (FSC) of CFSE-labelled human NP cells in response to altered extracellular osmolality.

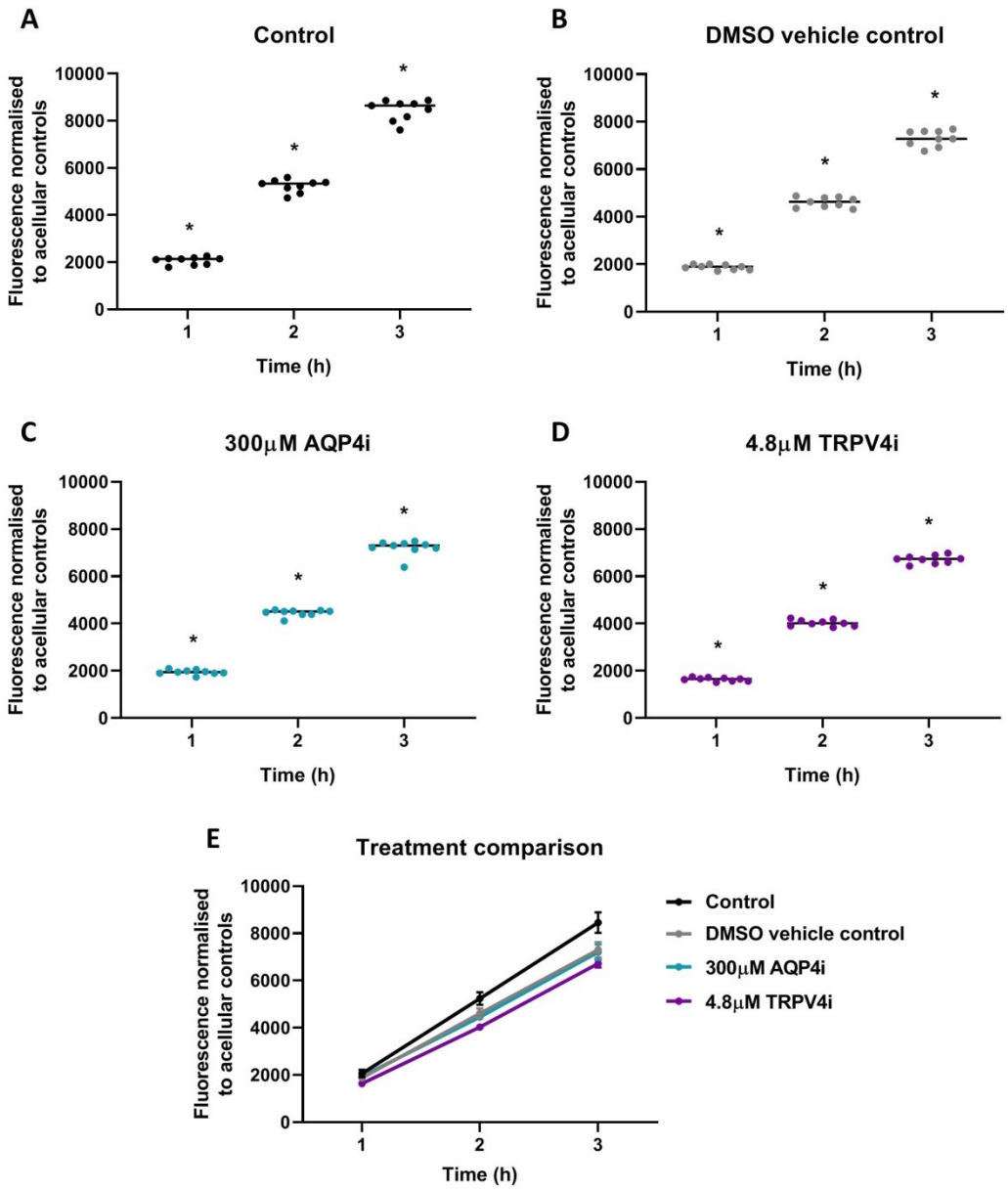

Appendix XII. NP cell viability in response to AQP4 and TRPV4 channel inhibition. NP cells were treated with (A) no treatment control (B) DMSO vehicle control (C) 300μM AQP4i or (D) 4.8μM TRPV4i for 1 − 3h and metabolic activity was measured using the resazurin reduction assay. Resazurin sodium salt (Sigma-Aldrich) stock solution (3mg/mL, prepared in DMEM) was diluted 1:100 and was incubated on cells for 2h (prior to treatment) at 37°C 5% CO_2 (v/v) before absorbance was read at excitation: 560nm, emission 590nm. Fluorescence values normalised to acellular controls. Significance determined by Kruskal-Wallis *$p \leq 0.05$.

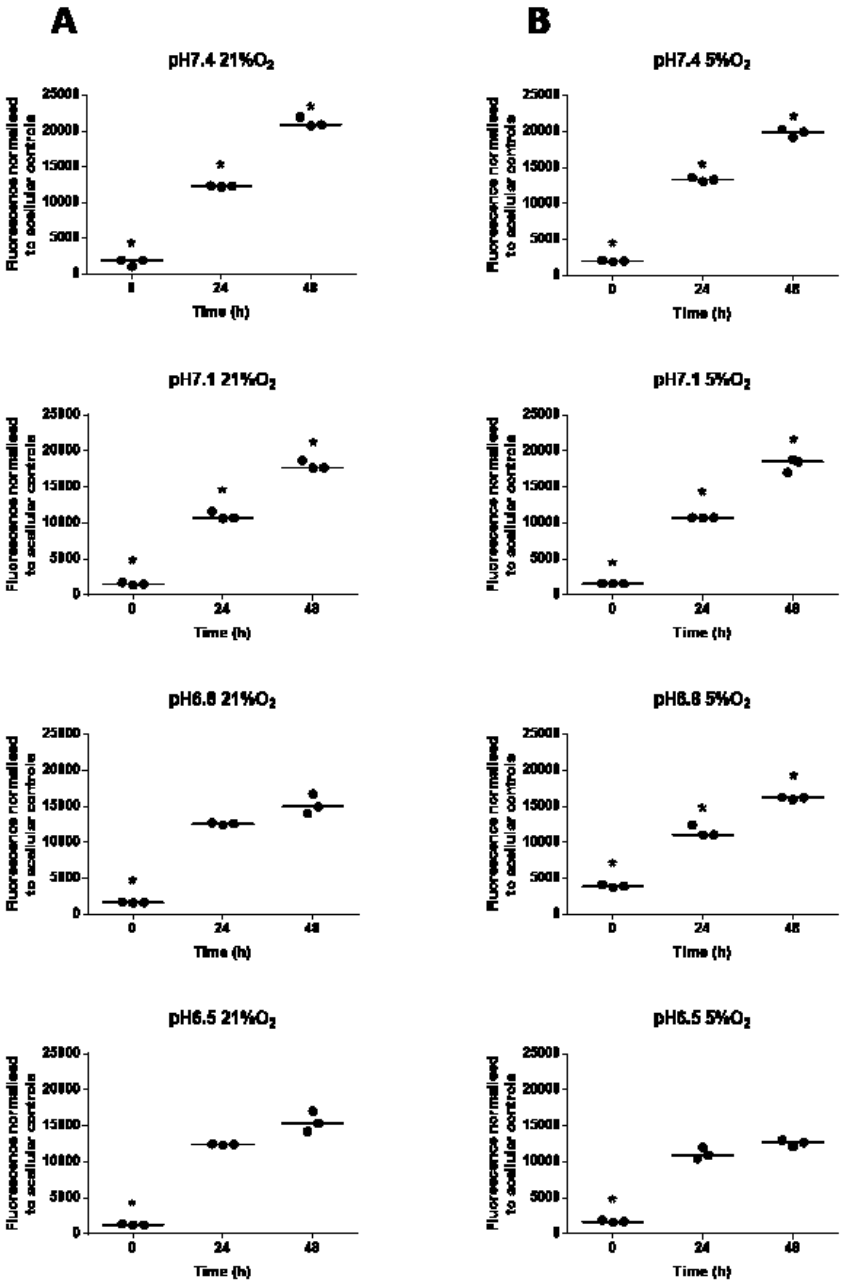

Appendix XIII. NP cell viability in response to altered pH and O_2 % treatment. NP cells (in alginate beads) were treated with altered pH (7.4 – 6.5) at (A) 21% O_2 and (B) 5% O_2 for 0 – 48h and metabolic activity was measured using the resazurin reduction assay. Resazurin sodium salt (Sigma-Aldrich) stock solution (3mg/mL, prepared in DMEM) was diluted 1:100 and was incubated on cells for 4h at 37°C 5% CO_2 (v/v) before absorbance was read at excitation: 560nm, emission 590nm. Fluorescence values normalised to acellular controls. Significance determined by Kruskal-Wallis *$p \leq 0.05$.

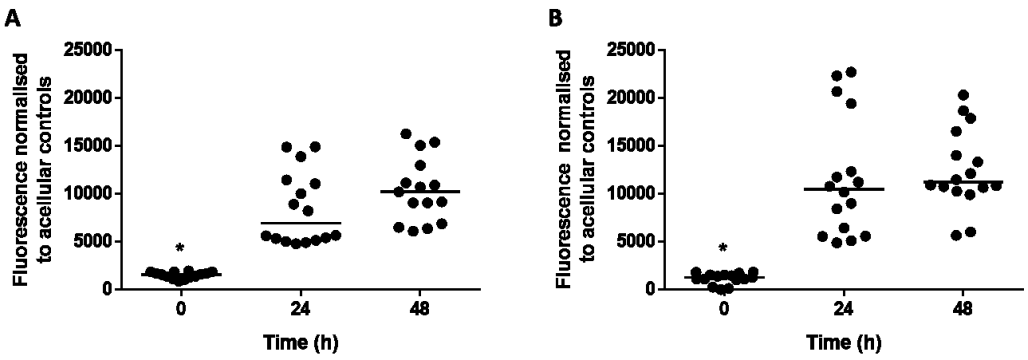

Appendix XIV. NP cell viability in response to healthy and degenerate treatment. NP cells (in alginate beads) were treated with combined (A) healthy or (B) degenerate IVD conditions for 0 – 48h and metabolic activity was measured using the resazurin reduction assay. Resazurin sodium salt (Sigma-Aldrich) stock solution (3mg/mL, prepared in DMEM) was diluted 1:100 and was incubated on cells for 4h at 37°C 5% (v/v) before absorbance read at excitation: 560nm, emission 590nm. Fluorescence values normalised to acellular controls. Significance determined by Kruskal-Wallis *$p \leq 0.05$.